POSTER ID	First Name	Middle Initial	Last Name	IC	Scientific Focus Area	Title	Abstract	Co-Authors	YEAR	PostCat
2023-001	Olena		Kamenyeva	NIAID	Immunology	Through the Looking Glass: Imaging Animal Models of Infection	The mammalian immune system is a network of organs that detects and eliminates infection. Pathogens, in return, undergo and escape immune surveillance by recruiting numerous strategies engaging highly dynamic and interactive processes. While in vitro and in vivo experiments provide strong evidence for how pathogens interact with and evade the immune system, visualizing these in both space and time allows for better understanding infection spread and outcome. Intravaital microscopy (IVM) allows imaging live animals at their cellular level during ongoing physiological processes. However, some compartments of immune system such as the lung are difficult to access optically. Live microscopy of tissues and organ explants provides access to the regions of interest and allows immunostaining. In an ideal biomedical study, both techniques become indispensable, together. We recruit both approaches using confocal DIVE (Deep In Vivo Explorer) and Stellaris 8 microscopes each equipped with dual MP lasers, and image multiple animal models of infection. In addition to lymph nodes, we have established imaging of the liver, spleen, brain, and lung from model animals. By employing both in vivo an ex vivo microscopy, we visualize in detail infection spread and immune responses to viruses, bacteria, and pathogenic protozoa. We have performed high speed and high-resolution imaging of Staphylococcus aureus, Mycobacterium tuberculosis, Leishmania major, Vaccinia virus, SIV and SARS-CoV-2 viruses among other infections, for up to continuous 6 hours and over the course of days. This reveals new potential targets for therapeutical intervention and effective vaccine development in patients suffering from infectious diseases.	O Kamenyeva, J Kabat, OM Schwartz	2023	IMMUNO
2023-002	Kianoush		Jeiran	NHLBI	Computational Biology	A New Structural Model of Apolipoprotein B100 Based on Computational Modeling and Cross Linking	ApoB-100 is a member of a large lipid transfer protein superfamily and is one of the main apolipoproteins found on low-density lipoprotein (LDL) and very low-density lipoprotein (VLDL) particles. Despite its clinical significance for the development of cardiovascular disease, there is limited information on apoB-100 structure. We have developed a novel method based on the “divide and conquer” algorithm, using PSIPRED software, by dividing apoB-100 into five subunits and 11 domains. Models of each domain were prepared using I-TASSER, DEMO, RoseTTAFold, Phyre2, and MODELLER. Subsequently, we used disuccinimidyl sulfoxide (DSSO), a new mass spectrometry cleavable cross-linker, and the known position of disulfide bonds to experimentally validate each model. We obtained 65 unique DSSO cross-links, of which 87.5% were within a 26 Å threshold in the final model. We also evaluated the positions of cysteine residues involved in the eight known disulfide bonds in apoB-100, and each pair was measured within the expected 5.6 Å constraint. Finally, multiple domains were combined by applying constraints based on detected long-range DSSO cross-links to generate five subunits, which were subsequently merged to achieve an uninterrupted architecture for apoB-100 around a lipoprotein particle. Moreover, the dynamics of apoB-100 during particle size transitions was examined by comparing VLDL and LDL computational models and using experimental cross-linking data. In addition, the proposed model of receptor-ligand binding of apoB-100 provides new insights into some of its functions.	K Jeiran, SM Gordon, DO Sviridov, AM Aponte, A Haymond, G Piszczek, D Lucero, EB Neufeld, II Vaisman, L Liotta, A Baranova, AT Remaley	2023	COMPBIO
2023-003	Riley	D	Metcalfe	NCI	Structural Biology	Structure and regulation of full-length human leucine-rich repeat kinase 1	The two human leucine-rich repeat kinases (LRRKs), LRRK1 and LRRK2 are large and unusually complex multi-domain kinases which serve to regulate fundamental cellular processes. Near-uniquely, the LRRKs contain both a kinase domain and Ras-like GTPase domain in the same polypeptide chain, along with several scaffolding domains. Both LRRKs are implicated in human disease. Specifically, LRRK1 is implicated in bone development, with mutations in LRRK1 causing a bone disease, osteosclerotic metaphyseal dysplasia (OSMD), while mutations in LRRK2 are associated with Parkinson’s disease. Despite their biological significance, both LRRKs have proved to be challenging structural targets, due to their size (~250 kDa), heterogeneity, flexibility, and low recombinant expression levels. Recent experimental structures of LRRK2 in a variety of states have begun to provide structural detail into this family of proteins, however the structure and exact molecular mechanisms regulating the activity of LRRK1 remain unclear. Here, we report a cryo-EM structure of the LRRK1 monomer, and a lower-resolution cryo-EM map of the LRRK1 dimer. The monomer structure, in which the kinase is in an inactive conformation, reveals key interdomain interfaces which serve to control kinase activity through linking the kinase domain and the Ras-like GTPase domain, which we have further validated experimentally. LRRK1 is structurally distinct compared to LRRK2, particularly in the position of the leucine-rich repeats relative to the kinase domain. Overall, our results provide new structural insights into the human LRRKs for understanding the physiology and pathology of these proteins. A preprint is available describing these results: doi.org/10.1101/2022.12.21.521433.	RD Metcalfe, JA Martinez Fiesco, P Zhang	2023	STRUCTBIO
2023-004	Julia		Segal	NCI	Clinical Research	A phase I study of autologous activated NK cells ± rhIL15 in children and young adults with refractory solid tumors	Patients with high-risk pediatric solid tumors experience poor outcomes and require improved treatments. NK cell immunotherapies hold promise for potential anti-tumor activity; however, clinical translation faces challenges. In this single-institution Phase I trial (NCT01875601), we enrolled children and young adults with refractory solid tumors, to evaluate the manufacturing feasibility and safety of infusing activated NK cells. Using a 3+3 dose escalation design, NK cells were administered after lymphodepleting cyclophosphamide. Artificial antigen-presenting cells (aAPC) expressing human 4-1BBL and human IL-15Rα were used to expand autologous NK cells ex vivo. Three dose levels (DL) of NK cells were explored for Cohort A. Cohort B evaluated administration of NK cells followed by a ten-day rhIL-15 infusion. Sixteen patients enrolled, with a median age of 16.1 years. The average ex vivo NK cell expansion was 19.4 fold. Expansion was insufficient to achieve the top DL. Following administration, partial responses per RECIST criteria were observed in 3 patients, two in DL1 of Cohort A, and one in DL1 of Cohort B. The remaining 13 patients had stable disease. Symptoms of cytokine release syndrome occurred in 2/12 patients in Cohort A, one being a dose limiting toxicity. Four patients received rhIL-15 with one dose limiting toxicity related to pericardial tamponade and capillary leak syndrome, prior to pause of enrollment for supply issues. Harvesting, expanding, and administering 1x107 cells/kg of aAPC-activated autologous NK cells is feasible and safe. Anti-tumor activity was observed following administration of aAPC-activated autologous NK cells with three partial responses. Correlative studies are underway.	JE Segal, S Kaczanowska, D Bernstein, N Zhang, A Dinh, R Somerville, S Highfill, D Stroncek, KC Conlon, TA Waldmann, R Nguyen, MS Merchant, CL Mackall, RN Kaplan	2023	CLINICAL
2023-005	Angelica		Medina Farias	NCATS	Microbiology and Infectious Diseases	Developing human spheroid models as high-throughput compatible screening platforms for therapeutics against emerging and re-emerging viruses with pandemic potential.	Patients with high-risk pediatric solid tumors experience poor outcomes and require improved treatments. NK cell immunotherapies hold promise for potential anti-tumor activity; however, clinical translation faces challenges. In this single-institution Phase I trial (NCT01875601), we enrolled children and young adults with refractory solid tumors, to evaluate the manufacturing feasibility and safety of infusing activated NK cells. Using a 3+3 dose escalation design, NK cells were administered after lymphodepleting cyclophosphamide. Artificial antigen-presenting cells (aAPC) expressing human 4-1BBL and human IL-15Rα were used to expand autologous NK cells ex vivo. Three dose levels (DL) of NK cells were explored for Cohort A. Cohort B evaluated administration of NK cells followed by a ten-day rhIL-15 infusion. Sixteen patients enrolled, with a median age of 16.1 years. The average ex vivo NK cell expansion was 19.4 fold. Expansion was insufficient to achieve the top DL. Following administration, partial responses per RECIST criteria were observed in 3 patients, two in DL1 of Cohort A, and one in DL1 of Cohort B. The remaining 13 patients had stable disease. Symptoms of cytokine release syndrome occurred in 2/12 patients in Cohort A, one being a dose limiting toxicity. Four patients received rhIL-15 with one dose limiting toxicity related to pericardial tamponade and capillary leak syndrome, prior to pause of enrollment for supply issues. Harvesting, expanding, and administering 1x107 cells/kg of aAPC-activated autologous NK cells is feasible and safe. Anti-tumor activity was observed following administration of aAPC-activated autologous NK cells with three partial responses. Correlative studies are underway.	A Medina Farias, S Cotsmire, J Zhang, S Ogden, M Ferrer, E Lee	2023	MICROBIO

2023-006	Nathan	P	Manes	NIAID	Systems Biology	EnsMOD: A software program for omics sample outlier detection	Detection of omics sample outliers is important for preventing erroneous biological conclusions, developing robust experimental protocols, and discovering rare biological states. Two recent publications describe robust algorithms for detecting transcriptomic sample outliers, but neither algorithm had been incorporated into a software tool for scientists. Here we describe Ensemble Methods for Outlier Detection (EnsMOD) which incorporates both algorithms. EnsMOD calculates how closely the quantitation variation follows a normal distribution, plots the density curves of each sample to visualize anomalies, performs hierarchical cluster analyses to calculate how closely the samples cluster with each other, and performs robust principal component analyses to statistically test if any sample is an outlier. The probabilistic threshold parameters can be easily adjusted to tighten or loosen the outlier detection stringency. EnsMOD can be used to analyze any omics dataset with normally distributed variance. Here it was used to analyze a simulated proteomics dataset, a multiomic (proteome and transcriptome) dataset, a single-cell proteomics dataset, and a phosphoproteomics dataset. EnsMOD successfully identified all of the simulated outliers, and subsequent removal of a detected outlier improved data quality for downstream statistical analyses.	NP Manes, J Song, A Nita-Lazar	2023	SYSBIO
2023-007	Masato		Ooka	NCATS	Chemical Biology	Lestaurtinib Induces DNA Damage that is Related to Estrogen Receptor Activation	Numerous environmental chemicals pose potential risks to human health due to their ability to disrupt endocrine systems. As recent research indicated that estradiol induces DNA damage by activating estrogen receptors (ER), it is possible that environmental chemicals that act as hormones in the human body may also damage DNA. Additionally, BRCA1, whose mutations have been associated with breast cancer, is responsible for repairing estrogen-induced DNA damage. Therefore, ER-related DNA damage is of great concern to people with BRCA1 mutations. In this study, we developed a high-content imaging assay measuring γH2AX, a biomarker for DNA damage, and used this assay to test a subset of 907 compounds using breast cancer cells. From the screening, we identified 128 compounds that induced γH2AX. To examine which chemicals' genotoxicity depended on ERα, we tested the effect of an ER inhibitor, tamoxifen, on genotoxicity. Tamoxifen treatment suppressed the induction of γH2AX by four compounds, indicating that these compounds induced γH2AX through ERα activation. These four compounds were further studied to assess their ERα activating capability and their induction of c-MYC, a target gene of ER signaling. Only lestaurtinib, a tyrosine kinase inhibitor, activated ERα, which was confirmed by both an ERα reporter gene assay and molecular docking analysis. Lestaurtinib also increased c-MYC expression. These data suggest lestaurtinib induces DNA damage through ERα activation. We established a high-throughput screening method with follow-up assays for DNA damage-related compound screening and identified a novel compound, lestaurtinib, that potentially promotes breast cancer by activating ER and inducing DNA damage.	M Ooka, S Yang, L Zhang, R Huang, K Hirota, S Takeda, M Xia	2023	CHEMBIO
2023-009	Adam		Yasgar	NCATS	Chemical Biology	Quantitative Bioactivity Signatures of Dietary Supplements and Natural Products	Dietary supplements and natural products are often marketed as safe and effective alternatives to conventional drugs, but their safety and efficacy are not well regulated. To address the lack of scientific data in these areas, we assembled a collection of Dietary Supplements and Natural Products (DSNP), as well as Traditional Chinese Medicinal (TCM) plant extracts. These collections were then profiled in a series of in vitro high-throughput screening assays, including a liver cytochrome p450 enzyme panel, CAR/PXR signaling pathways, and P-glycoprotein (P-gp) transporter assay activities. This pipeline facilitated the interrogation of natural product–drug interaction (NaPDI) through prominent metabolizing pathways. In addition, we compared the activity profiles of the DSNP/TCM substances with those of an approved drug collection (the NCATS Pharmaceutical Collection or NPC). Many of the approved drugs have well-annotated mechanisms of action (MOAs), while the MOAs for most of the DSNP and TCM samples remain unknown. Based on the premise that compounds with similar activity profiles tend to share similar targets or MOA, we clustered the library activity profiles to identify overlap with the NPC to predict the MOAs of the DSNP/TCM substances. Our results suggest that many of these substances may have significant bioactivity and potential toxicity, and they provide a starting point for further research on their clinical relevance.	AS Yasgar, D Bougie, RT Eastman, R Huang, M Itkin, J Kouznetsova, C Lynch, C McKnight, M Miller, DK Ngan, T Peryea, P Shah, P Shinn, M Xia, X Xu, AV Zakharov, A Simeonov	2023	CHEMBIO
2023-010	Rani		Richardson	NIDA	Neuroscience	β1 adrenergic receptors interact with the ghrelin system to mediate binge drinking in a mouse model of AUD	Alcohol use disorder (AUD) and binge drinking are highly prevalent public health issues. Studies show that the stomach-derived peptide ghrelin is implicated in alcohol-related outcomes. Ghrelin receptors (GHSR) are expressed in the brain and periphery. We previously found that intraperitoneal and intracerebroventricular administration of GHSR antagonists reduced intake in the Drinking-in-the-Dark mouse model of binge drinking, whereas sequestering circulating ghrelin did not. We hypothesize that central GHSRs drive binge drinking independently of peripheral ghrelin. To investigate this hypothesis, we targeted β-1 adrenergic receptors (β1ARs), which are required for stress and fasting-induced ghrelin release. The involvement of β1AR has not been addressed in a model of alcohol binge drinking; within the context of ghrelin-alcohol signaling; through the lens of central vs. peripheral signaling; or in subjects of both sexes. We hypothesized that β1AR blockade would not effect alcohol drinking. We administered two β1AR blockers intraperitoneally: atenolol (AT, peripherally restricted) and metoprolol (MT, brain permeable). MT but not AT decreased alcohol intake. Co-administration of AT or MT with JMV2959 (GHSR antagonist) or with PF-5190457 (inverse agonist) decreased intake. MT and JMV2929 had an additive effect. Finally, blood measurements indicate that AT and MT decrease blood ghrelin levels. No sex differences were observed. These results suggest that central but not peripheral β1ARs drive binge-like alcohol drinking. Also, β1AR blockade blocks ghrelin secretion and depletes ghrelin levels. Finally, blockade of β1AR does not prevent GHSR antagonists from decreasing drinking. β1ARs and GHSRs represent possible targets for therapeutic intervention for AUD, including potential additive effects.	RS Richardson, GF Koob, LF Vendruscolo, L Leggio	2023	NEURO
2023-011	Santosh		Kumar	NIDDK	Neuroscience	Anatomical and functional communication between vagal sensory neurons and pancreatic islet β-cells in mice	Brain and the gastrointestinal tract communicate via complex bidirectional processes. This higher order communication includes, but is not limited to, the parasympathetic (via the vagus nerve) and the sympathetic (via the prevertebral ganglia) arms of the autonomic nervous system. The role of the autonomic nervous system in metabolism and associated disorders is poorly understood due to insufficient understanding of the neural pathways that communicate with internal organs. Vagal sensory neurons (VSNs) are known to innervate the brain and the peripheral organs. However, the anatomical and functional details of these communications are unclear and, hence, are the focus of my research. My preliminary experiments using monosynaptic tracing in combination with RNAscope methods suggest the existence of molecularly diverse types of VSNs innervating pancreatic islet β-cells in mice. More specifically, I find that the VSNs anatomically connected to insulin producing β-cells express cocaine- and amphetamine-regulated transcript (CART). Further, I observed that CART-positive axons densely innervate the pancreatic islets. The preliminary results on the functional aspects of this vagal CART neuron – islet β-cell circuit suggest a role in glucose homeostasis and food intake that depend on the metabolic state of the mice. Specifically, via chemogenetics approaches in combination with automated glucose telemetry, I find that activation of vagal CART neurons modifies blood glucose levels. Further, optogenetics stimulation of vagal CART neuron terminals in the brainstem alter food consumption. Delineating the vagal sensory complex-endocrine pancreas communications will unravel a central–peripheral neuronal circuitry vital to glucose homeostasis and metabolic disorders.	S Kumar, SG Rane	2023	NEURO
2023-012	Hannah		Goldbach	NIMH	Neuroscience	Circuits underlying striatal dopamine signaling during visual learning	The primary input area of the basal ganglia, the striatum, plays a role in integrating signals from the cortex, midbrain, and thalamus to make associations between stimuli, actions, and rewards. The canonical view was that midbrain activity drove all dopamine signals in the striatum. However, recent findings have forced the field to reconsider this viewpoint: cortical and thalamic inputs to the striatum can also produce local dopamine signals indirectly through striatal cholinergic interneurons. Here, we aimed to determine how cholinergic-evoked dopamine may be involved in visual learning. This would reveal a novel mechanism for learning specific associations and would be consistent with recent evidence linking corticostriatal circuits to visual learning. We used fiber photometry to measure striatal dopamine while animals learned a unilateral orientation-change detection task requiring them to report a visual stimulus change. While all mice had dopamine responses to the stimulus onset, only expertly performing mice developed a dopamine response to the stimulus change. We then used ex vivo voltammetry to measure evoked dopamine transients in trained animals. We found striking differences in the cholinergic-evoked component of the overall dopamine transient, dependent on visual task training. Interestingly, we found no primary sensory area connected strongly with cholinergic interneurons, leading to an inability to evoke dopamine signals. However, frontal cortical inputs are reliably connected directly to cholinergic interneurons, suggesting that these inputs could serve as potential mediators of dopamine signaling. These findings provide surprising information regarding corticostriatal connectivity and the neural circuits involved in visual learning and sensory perception.	HC Goldbach, ES Swanson, ME Authement, K Elliott, HB Kwon, S Preuss, CA Mejias-Aponte, CR Gerfen, C Quaia, VA Alvarez, RJ Krauzlis	2023	NEURO
2023-013	Abhishek		Basu	NIAAA	Molecular Pharmacology	Inhalation Delivery of MRI-1867 (zevaquenabant) As A Novel and Effective Therapeutic Modality in Pulmonary Fibrosis	Idiopathic pulmonary fibrosis (IPF) is a progressive interstitial lung disease and requires long-term treatment. Recent research has identified cannabinoid receptor 1 (CB1R) as a potential target for treating IPF. Following this line, we have developed MRI-1867 (zevaquenabant) as a dual CB1R/iNOS inhibitor that can be administered systemically to effectively reduce experimental pulmonary fibrosis in mice. Our research has shown that CB1R is expressed in alveolar macrophages (AMs) and epithelial cells in the fibrotic environment of the lungs, indicating that these cells may contribute to the progression of PF. We hypothesized that delivering MRI-1867 through inhalation could provide high exposure to these target cells and limit distribution to other tissues, improving safety. During trials, we found that MRI-1867 at a dose of 0.5 mg/kg b.w. in mice can achieve the same concentration in the lungs as the therapeutic intraperitoneal (I.P.) dose of 10 mg/kg b.w. Further studies showed that administering MRI-1867 through pulmonary delivery at the O.P. dose of 0.5 mg/kg b.w. had comparable antifibrotic efficacy to the established I.P. dose of 10 mg/kg b.w. in a murine PF model. MRI-1867 treatment reduced monocyte-derived AMs and inflammatory cytokines and chemokines in the lungs, and restored several pathways involved in fibrosis initiation and modification, fibroblast proliferation, and inflammation. Overall, inhalation delivery of MRI-1867 is a promising treatment for PF and offers a more targeted therapeutic modality that could potentially increase safety during prolonged therapy. At present, clinical trials are in progress to validate the inhalation-based formulation of MRI-1867 for humans.	A Basu, M Arif, K M Wolf, M Behee, C N Zawatsky, N Johnson, L Pommerolle, J Harvey-White, M R Iyer, R Cinar	2023	PHARMA
2023-014	Evan	S	Swanson	NIMH	Neuroscience	Partial D2 receptor deletion causes a sex-dependent reduction of striatal dopamine signals	Dopamine signaling in the striatum is a crucial component of drug reinforcement that, when dysregulated, is thought to increase the risk for substance use disorders. In particular, low availability of the dopamine D2 receptor (D2R) has traditionally been linked to the development of substance use disorders in humans. Yet the mechanisms by which low levels of striatal D2Rs generate vulnerability are not fully understood. Here, we directly manipulate the levels of striatal D2Rs in transgenic mice to explore the impact on dopamine signals in the striatum. These mice have a ~25-30% reduction in D2-like agonist binding throughout the striatum, compared to littermate controls that are bred alongside these animals from the cross between Adora2a-cre x Drd2loxP/wt mice. Using fast-scan cyclic voltammetry, we recorded ex vivo electrically-evoked dopamine signals in the dorsomedial striatum (DMS) of male and female mice of both genotypes. Relative to controls, we find that the magnitude of dopamine transmission in mice expressing partial D2R deletion is significantly reduced at baseline, and the extent of this reduction differs between sexes. Later, we block nicotinic acetylcholine receptors, GABAA and GABAB receptors, and kappa opioid receptors with a variety of drug antagonists while recording dopamine signals. In so doing, we aim next to identify systems that regulate the mechanism of D2R modulation of dopamine signaling in the striatum. This work will facilitate our understanding of the role of D2Rs in drug reinforcement and may shed light on the mechanism by which only certain individuals develop substance use disorders.	ES Swanson, VA Alvarez	2023	NEURO
2023-015	Jeehye		Shin	NCI	Stem Cell Biology	Smurf ubiquitin ligases regulate development processes in embryonic stem cells	Smurfs are HECT domain containing E3 ubiquitin ligases that have Smurf1 and 2 in mammals. They are originally found to be negative regulators of TGFb/BMP signaling, and which have been shown to play key roles in many biological processes. Mouse lacking Smurf1 and Smurf2 are embryonic lethal, and they displayed gastrulation defects. To understand the role of Smurfs in early embryonic development, we established ESC lines using E3.5 blastocytes for WT, SF1KO, SF2KO, and SF1/2KO (DKO) from mouse. We found that Smurf-deletion had no effect on ESC morphology, alkaline phosphatase staining, or pluripotent marker expression as assessed by RT-qPCR or immunofluorescence. Moreover, WT and Smurf-deficient ESCs supported teratoma formation to a similar degree in vivo, confirming that Smurf1 and Smurf2 are not required for maintaining pluripotent potential of ESCs. However, when these ESCs formed embryoid body (EB), we observed that the size of DKO EBs were considerably smaller than that of WT, SF1KO or SF2KO EBs. H&E staining revealed that the DKO EBs were less differentiated than that of WT EBs. Further RNAseq and RT-qPCR assays revealed that depletion of both Smurf1 and Smurf2 causes the developmental delay and arrests cells at the gastrulation stage. These observations were also confirmed using monolayer neuronal differentiation assay. Besides higher level of Smad-dependent TGFb signaling in DKO EBs or differentiated cells, several other developmental signaling pathways were also affected by Smurf DKO. These results indicating that Smurfs regulate developmental process in embryonic stem cells by affecting multiple signaling pathways, including TGFb signaling.	JH Shin, X Xu, T Chen, Y Tang, Y Du, C Liu, Y Zhang	2023	STEMCELL
2023-016	Ewa		Szczesna	NINDS	Molecular Biology and Biochemistry	Combinatorial readout of the tubulin code by katanin	Cells functionalize microtubules with spatiotemporally complex patterns of posttranslational modifications. How effectors interpret this tubulin modification code is largely unknown. Here, we show that katanin, a microtubule severing AAA ATPase mutated in microcephaly and critical for cell division, axonal elongation and cilia biogenesis, responds precisely, differentially and combinatorially to three chemically distinct modifications: glycylation, glutamylation, and tyrosination, but is insensitive to tubulin acetylation. Glutamylation and glycylation act as antagonistic rheostats with glycylation being protective of microtubules. Katanin exhibits graded and divergent responses to glutamylation on the α- and β-tubulin tails, and these act combinatorially. The structure of the katanin hexamer central pore constrains the polyglutamate chain patterns on β-tails that can productively be recognized. In contrast, elements distal to the katanin AAA core sense α-tubulin tyrosination, and detyrosination downregulates severing. The multivalent microtubule recognition that enables katanin to read multiple tubulin modification inputs explains in vivo observations and illustrates how effectors can integrate tubulin code signals to produce diverse functional outcomes.	E Szczesna, EA Zehr, SW Cummings, A Szyk, KK Mahalingan, Y Li, A Roll-Mecak	2023	MOLBIO

2023-017	Javan	O	Okendo	NHGRI	Computational Biology	The reference genome of the paradise fish (Macropodus opercularis)	Over the decades, a small number of model species, each representative of a larger taxa, have dominated the field of biological research. Amongst fishes, zebrafish (Danio rerio) has gained popularity over most other species and while their value as a model is well documented, their usefulness is limited in certain fields of research such as behavior. By embracing other, less conventional experimental organisms, opportunities arise to gain broader insights into evolution and development, as well as studying behavioral aspects not available in current popular model systems. The anabantoid paradise fish (Macropodus opercularis), an "air-breather" species from Southeast Asia, has a highly complex behavioral repertoire and has been the subject of many ethological investigations, but lacks genomic resources. Here we report the draft genome of Macropodus opercularis. The final assembly consisted of ~485 Mb on 162 contigs. Within the assembled genome we were able to identify and annotate 20,157 protein coding genes and assigned ~90% of them to orthogroups. Completeness analysis showed that 98.5% of the Actinopterygii core gene set (ODB10) was present as a complete ortholog in our draft genome with a further 1.2 % being present in a fragmented form. Additionally, we cloned multiple genes important during early development and using newly developed in situ hybridization protocols, we show that they have conserved expression patterns.This annotated and validated paradise fish genome will be essential to establish this species as a model for future comparative neurogenetic, genomic, evolutionary, and ethological studies.	JO Okendo, E Fodor, S Korens, A Rhie, M Varga, SM Burgess	2023	COMPBIO
2023-018	Tanmay		Mondal	NICHD	Chemical Biology	Mechanistic dissection of substrate selectivity of protein palmitoyltransferases	Protein palmitoylation is the most prevalent form among all forms of protein lipidation and recognition of its importance in cellular physiology has been emerging in recent years. Approximately 6000 proteins are known to be targets of protein palmitoylation, which is catalyzed by 23 members of the zDHHC family of integral membrane enzymes and plays critical roles in numerous pathologies such as neurodegenerative diseases, cancer. Many substrates can be palmitoylated by more than one zDHHC enzymes in cell-based experiments, raising the question whether there are any substrate-selective interactions for each zDHHC-substrate pair at all. However, the role of complex cellular factors cannot be eliminated in these experiments and therefore there is a dire need for biochemical reconstitution experiments to study protein palmitoylation. I have developed an in vitro reconstitution assay for palmitoylation of several substrates using purified zDHHC enzymes and synthesized peptide fragments of the substrates. Remarkably, all the zDHHC enzymes showed distinct preferred activity for substrates over non-substrates. This is the first in vitro reconstitution of substrate discrimination of any zDHHC enzyme with a biochemical assay. Using this assay, I examined how nearby residues around the target cysteine on the substrate impact substrate palmitoylation, yet another completely unexplored aspect of protein palmitoylation. This work also builds the groundwork for future structural studies to understand the atomic basis of substrate palmitoylation by zDHHC enzymes.	T Mondal, A Banerjee	2023	CHEMBIO
2023-019	Lanqi		Gong	NCI	Cancer Biology	Single-cell spatial characterization of microenvironmental impacts on clinical discrepancies between adult and pediatric nasopharyngeal carcinoma patients	Background Nasopharyngeal carcinoma (NPC) is an EBV-related and highly inflamed malignancy of strategic importance in Asia and Africa. Only 0.1-1% of NPC incidences are diagnosed in children which exhibits superior prognosis and immunotherapy outcomes. Microenvironmental characteristics might contribute to such discrepancies between adult/pediatric NPC. Thus, we apply scRNA-seq and Visium spatial RNA-seq to pediatric NPC with paired blood, and incorporate our data with multi-central NPC cohorts. We report low lipid metabolism, weak tumor-T cell interactions, and enriched T memory stem cells (Tscm) collectively result in long-lasting immunity in pediatric NPC and as therapeutic vulnerabilities. Method and results We established a systematic NPC scRNA-seq and spatial-seq cohort containing 503,021 cells from 69 samples, and 15,222 spatial spots from 11 samples. We developed a personalized computational framework to characterize spatial co-localization and enriched signaling. We unveiled that fatty acid (FA)/cholesterol metabolism was elevated in adult NPC, and such metabolic aberrance was validated by lipid staining and blood tests. Strong co-localizations and interactions between NPC cells and Tregs/exhausted T cells were found in adult NPC. We identified novel Tscm populations in pediatric NPC, with resilience to immunosuppressive cues, and had an impact on long-term immunity and immunotherapeutic outcomes. Conclusion We demonstrate that higher immunosuppression and exhaustion caused by lipid metabolism and tumor-intrinsic interactions, and a lower Tscm pool, are the vital drivers of clinical discrepancies in adult/pediatric NPC patients. Pre-treatment screening of Tscm abundance in NPC patients might help stratify immunotherapy responders, and targeting metabolic and interacting vulnerabilities might benefit NPC patients.	L Gong, Y Zhang, G Guan, B Ru, J Peng	2023	CANCER
2023-020	Markus	D	Hoffmann	NIDDK	Systems Biology	circRNA-sponging: a pipeline for extensive analysis of circRNA expression and their role in miRNA sponging	Motivation: Circular RNAs (circRNAs) are long non-coding RNAs (lncRNAs) often associated with diseases and considered potential biomarkers for diagnosis and treatment. Among other functions, circRNAs have been shown to act as microRNA (miRNA) sponges, preventing the role of miRNAs that repress their targets. However, there is no pipeline to systematically assess the sponging potential of circRNAs. Results: We developed circRNA-sponging, a nextflow pipeline that (1) identifies circRNAs via backsplicing junctions detected in RNA-seq data, (2) quantifies their expression values in relation to their linear counterparts spliced from the same gene, (3) performs differential expression analysis, (4) identifies and quantifies miRNA expression from miRNA-sequencing (miRNA-seq) data, (5) predicts miRNA binding sites on circRNAs, (6) systematically investigates potential circRNA-miRNA sponging events, (7) creates a network of competing endogenous RNAs, and (8) identifies potential circRNA biomarkers. We showed the functionality of the circRNA-sponging pipeline using RNA sequencing data from brain tissues, where we identified two distinct types of circRNAs characterized by a specific ratio of the number of the binding site to the length of the transcript. The circRNA-sponging pipeline is the first end-to-end pipeline to identify circRNAs and their sponging systematically with raw total RNA-seq and miRNA-seq files, allowing us to better indicate the functional impact of circRNAs as a routine aspect in transcriptomic research. Availability https://github.com/biomedbigdata/circRNA-sponging	MD Hoffmann, L Schwartz, OA Ciora, N Trummer, LL Willruth, J Jankowski, HK Lee, J Baumbach, P Furth, L Hennighausen, M List	2023	SYSBIO
2023-021	Alfonso	S	Gozalo	NIAID	Microbiology and Infectious Diseases	Intra-abdominal helminthiasis in a Patas monkey.	Several pyriform-shaped, white-cream masses, measuring approximately 2.5-3 mm long by 1 mm at its widest point, firm to touch, with cuticular folds, and an invagination on one end were found encysted in the serosal surface of the gastrointestinal tract during surgery in a wild-caught adult female Patas monkey (Erythrocebus patas). Microscopic examination revealed the masses were parasites with no digestive tract, a thin cuticle, thick hypodermis with lacunar channels, and an inverted proboscis with hooks, all characteristics of Acanthocephala. Acanthocephalans are cylindrical pseudocoelomates with an armed, retractable proboscis, no digestive tract, and shed embryonated eggs which are ingested by the intermediate host (usually a beetle, cockroach, or beetle larvae, depending on the species). The definitive host becomes infected after ingesting the intermediate host containing the cystacanth. Acanthocephaliasis is sporadically reported in humans associated to ingestion of the infected intermediate or paratenic host. Clinical signs range from asymptomatic to severe gastrointestinal signs including intestinal perforation. The parasite location in our case was unusual and this is most likely due to Patas monkeys not being the natural final host. The monkey most likely ingested the intermediate host of either the pig, raccoon, or rodent acanthocephalan, with the parasites migrating out of the gastrointestinal tract to encyst in the abdominal cavity waiting for the final host. Acanthocephalan intermediate hosts are ubiquitous in nature and can be found in man-made infrastructures potentially being ingested by captive nonhuman primates. Rigorous pest control programs are essential to prevent infection and persistence in captive nonhuman primate colonies.	AS Gozalo, WR Elkins	2023	MICROBIO
2023-022	David		Adzrago	NIMHD	Health Disparities	Mental health and physical activity in children with and without ADHD: The intersection of physical activity and parental nativity	Background: Physical activity has been shown to improve mental health in individuals with attention-deficit/hyperactivity disorder (ADHD) with minimal side effects, unlike traditional pharmacotherapy that can result in drug interactions with increased side effects. However, the influence of physical activity on mental health among children with ADHD is understudied. We examined the relationship between current anxiety/depression and past-week physical activity and parental nativity among U.S. children with and without ADHD. We also analyzed whether parental nativity moderates the relationship between anxiety/depression and physical activity. Methods: Data on children aged 6-17 years (n= 22,626) were derived from the 2016 to 2021 National Health Interview Surveys, cross-sectional surveys. We performed multivariable logistic regression analyses to assess the study objectives. Results: Among children without ADHD, those who engaged in physical activity (versus did not) for 1 to 3 days, 4 to 6 days, and daily were less likely to experience anxiety/depression. The odds were also lower for children whose parents were immigrants compared to children whose parents were non-immigrants. For children with ADHD, engaging in physical activity for 1 to 3 days was associated with lower odds of anxiety/depression. Children whose parents were immigrants were less likely to experience anxiety/depression. Parental nativity significantly moderated the association between anxiety/depression among children with and without ADHD. Conclusions: Physical activity reduced the risks of experiencing anxiety/depression among children, especially in children with ADHD and those whose parents were immigrants. Incorporating personalized physical activity in ADHD and anxiety/depression management can improve mental illness and ADHD symptoms among children.	D Adzrago, F Williams	2023	HEALTH
2023-023	Elissa		Moller	NICHD	Structural Biology	Chemically Stabilizing the fully open conformation of the bacterial mechanosensitive channel MscS	Structure determination for membrane proteins remains not only technically challenging but is further complicated by potentially non-native conformations resulting from removal of stabilizing lipids. This is especially applicable to mechanosensitive channels that gate in response to subtle changes in membrane tension, such as MscS. Cryo-EM structures of MscS fall into two categories depending on the method of solubilization: (1) nonconductive (lipid-reconstituted or mixed micelles) characterized by kinked pore-lining helices and splayed lipid-facing helices, or (2) semi-open (pure detergent or short-chain lipids) satisfying ~70% of experimental conductance. However, MscS has 3 functional states: open, closed, and inactivated. In patch-clamp, the closed to open transition occurs in response to abruptly applied membrane tensions of 7-9 mN/m, opening a 1.6 nm pore resulting in an 18 nm2 in-plane expansion. But under slowly applied moderate tensions of 5-6 mN/m, MscS transitions from closed to a nonconductive and tension insensitive inactivated state, producing an 8 nm2 expansion. We attempt to relate these functional states with existing MscS structures and hypothesize that MscS bears internal stress that is finely balanced by lateral pressure from lipids. This imparts the discrete tension sensitivities for the opening and inactivation transitions which leads to the two observed structural categories. Using MD simulations, we generated models for the missing states based on experimental conductance and in-plane area expansion and aim to capture these conformations through stabilizing mutations using cryo-EM. We present the first attempt to chemically stabilize the fully open state of MscS in cryo-EM, resulting in a 2.6 Å map.	E Moller, M Britt, A Anishkin, I Rowe, F Zhou, S Sukharev, D Matthies	2023	STRUCTBIO
2023-024	Andrea	J	Luker	NIAID	Immunology	Attenuated germinal center (GC) reactions in Sphingosine-1-Phosphate Receptor 4 (S1PR4) knockout mice still produce high-affinity antibodies despite severe deficiencies	Sphingosine-1-Phosphate (S1P) is a lipid that exists in strict biological gradients to direct vital homeostatic functions such as lymphocyte re-circulation. In addition, S1P supports processes during immune activation, such as retention of germinal center (GC) B cells. While these examples are controlled through other well-studied members of the S1P receptor (S1PR1-5) family, little is known about the role of S1PR4 in immunity. In a TH1 footpad immunization model, S1PR4-/- mice developed attenuated immune responses that lacked the robust proliferative burst of B cells, which is characteristic of the peak of a GC reaction. Flow cytometric analysis revealed key populations, including T follicular helper (TFH) and GC B cells, were strikingly diminished in KO mice. Interestingly, at later time-points the GC B cell population ultimately achieved comparable levels to WT despite initial deficiencies and without the recovery of TFH cell numbers. Because GC reactions are considered the main mechanism underlying antigen (ag)-specific antibody production, we evaluated the humoral response and found similar levels of total and ag-specific IgG isotypes. This was unexpected because KO GC B cells had developed among fewer TFH cells to facilitate affinity maturation and isotype switching. While histological analysis confirmed the phenotypic findings, it also provided important insight into the lymphoid architecture. In particular, we noticed abnormal localization of CD31+ endothelium within KO follicular B cell areas, rather than within the T cell cortex. Through on-going studies, we are working to tie these inappropriate vascular entry points to the deficient immune response observed in S1PR4-/- mice.	AJ Luker, AM Wukitch, AA Olivera	2023	IMMUNO
2023-025	Marissa	E	Davies	NCATS	Chemical Biology	High-throughput characterization of isozyme-specific Aldehyde Dehydrogenase (ALDH) inhibitors	Aldehyde Dehydrogenases (ALDH) are a family of 19 enzymes that catalyze oxidation of aldehydes to carboxylic acids using NAD(P)+ and have been implicated in several human diseases including cancer. High ALDH activity was shown to sustain cancer stem cell growth and self-renewal, and induce chemotherapy resistance. Hence, development of ALDH inhibitors may provide a promising avenue to treat cancer. However, it remains challenging to dissect the functional role and pathological contribution of individual ALDH isozymes as different tumor types express different levels of each isozyme. Isozyme-selective inhibitors may help overcome this hurdle as well as prevent any toxicity from non-specific ALDH inhibition. Our objective is to identify isozyme-selective inhibitors for ALDH isozymes and expand the chemical probe toolbox for ALDHs to aid in studying ALDHs and developing therapeutics. To this end, we have implemented high-throughput small molecule screening and optimization of lead molecules as well as in silico strategies. Here, we describe a suite of high-throughput assays including biochemical, activity-based, functional, and target-engagement assays to characterize inhibitors. Our focus is the 1A subfamily, ALDH2, and ALDH3A1 due to commercial availability for recombinant proteins, specific antibodies, and cell lines expressing individual isozymes. Thus far, we have identified selective inhibitors for the 1A subfamily, ALDH2, and ALDH3A1 for further study.	ME Davies, S-M Yang, S-I Son, D Talley, G Bantukallu, S Jain, A Zakharov, A Simeonov, A Yasgar, N Martinez	2023	CHEMBIO
2023-026	Steven	M	Ferguson	OD	Research Support Services	Careers for NIH scientists in technology transfer & business development	What is technology transfer / business development and what are the career opportunities in the field? What are the skills required and how does one acquire them? How can an intramural scientist start a non-traditional career such as this? These are the questions to be answered in this presentation from two former NCI bench scientists. In terms of background, the field of technology transfer itself is still relatively new and can trace its origins and rapid growth to the economic developments legislation of the early 1980s, a time when the US was looking to enhance its global competitiveness. The need for translating the ideas that have originated from academic labs into useful products (and the people to handle these tasks) is still with us and has only grown since then. The technology transfer profession employs more than 10,000 professionals in the US with a fairly large number practicing their trade in the greater Washington, DC area. Career information is available from the sites of number of professional organizations such as www.autm.net , www.federallabs.org or www.lesi.org.	JW Thomas, SM Ferguson	2023	RSCHSUPP

2023-027	Steven	M	Ferguson	OD	Research Support Services	NIH scientists and the Federal Laboratory Consortium for Technology Transfer (FLC)	The Federal Laboratory Consortium for Technology Transfer (FLC) is the nationwide network of federal laboratories (including NIH) that provides the forum to develop strategies and opportunities for linking laboratory mission technologies and expertise with the marketplace. Today, approximately 300 federal laboratories and centers and their parent departments and agencies are FLC members. The Consortium creates an environment that adds value to and supports the technology transfer efforts of its members and potential partners. The FLC develops and tests transfer methods, addresses barriers to the process, provides training, highlights grass-roots transfer efforts, and emphasizes national initiatives where technology transfer has a role. For the public and private sectors, the FLC brings laboratories together with potential users of government-developed technologies. This is in part accomplished by the FLC's Technology Locator network and regional and national meetings. In consonance with the Federal Technology Transfer Act of 1986 and related federal policy, the mission of the FLC is to promote and facilitate the rapid movement of federal laboratory research results and technologies into the mainstream of the U.S. economy. NIH staff members serve as both agency and laboratory FLC representatives as well as in national and regional FLC organization positions.	TL Kirby, SM Ferguson, WA Hastings, PR Zielinski, VL Popov	2023	RSCHSUPP
2023-028	Satheesh	k	Sengodan	NCI	Genetics and Genomics	MLH1 Mitigates Replicative Stress and Promotes Synthetic Viability of BRCA2-deficient cells	Loss of BRCA2 (BReast CAncer 2) is lethal for normal cells. Yet, it remains poorly understood how in BRCA2 mutation carriers, cells undergoing loss of heterozygosity overcome the lethality and undergo tissue-specific neoplastic transformation. Here, we have identified mismatch-repair gene, MLH1 as a novel genetic interactor of BRCA2 whose over-expression supports the viability of Brca2-null cells. Mechanistically, we show that MLH1 interacts with Flap endonuclease 1 (FEN1) and competes to process the RNA flaps of Okazaki fragments. Together, they restrain DNA2 nuclease activity on the reversed forks of lagging strands, leading to replication-fork (RFs) stability in BRCA2-deficient cells. In these cells, MLH1 also attenuates R-loops allowing stable RFs to progress, altogether suppressing the genomic instability. We demonstrate the significance of their genetic interaction by the lethality of Brca2-mutant mice and inhibition of Brca2-deficient tumor growth in mice by Mlh1 loss. Furthermore, we describe that estrogen induces MLH1 expression through estrogen receptor alpha (ER), which may explain why the majority of BRCA2 mutation carriers develop ER positive breast cancer. Taken together, our findings reveal a novel role of MLH1 in relieving replicative stress and how it may contribute to the establishment of BRCA2-deficient breast tumors.	SK Sengodan, X Hu, V Peddibhotla, E Sterneck, S De, SK Sharan	2023	GEN
2023-029	Shuai		Xie	NCI	Epidemiology	Occupational exposure to organic solvents and risk of bladder cancer	Background: Bladder cancer has been linked to several occupations that involve the use of solvents, including those used in the dry-cleaning industry. Objectives: we evaluated exposure to solvents and risk of bladder cancer in 1182 incident cases and 1408 controls from a population-based study. Methods: Exposure to 21 specific solvents was quantitatively assessed using a job-exposure matrix (CANJEM). Exposure to benzene, toluene and xylene often co-occur. Therefore, we created two additional sets of metrics for combined benzene, toluene and xylene (BTX) exposure: 1) CANJEM-based BTX metrics and 2) hybrid BTX metrics, using a novel approach that integrates the CANJEM-based BTX metrics together with lifetime occupational histories and exposure-oriented modules that captured within-job, respondent-specific details about tasks and chemicals. Adjusted odds ratios (ORs) and 95% confidence intervals (95% CI) were estimated using logistic regression. Results: Bladder cancer risks were increased among those ever exposed to benzene (OR=1.63, 95%CI: 1.14-2.32), toluene (OR=1.60, 95%CI: 1.06-2.43), and xylene (OR=1.67, 95%CI: 1.13-2.48) individually. We further observed a statistically significant exposure-response relationship for cumulative BTX exposure, with a stronger association using the novel hybrid BTX metrics (OR_Q1 vs. Unexposed=1.26, 95% CI: 0.83-1.90; OR_Q2 vs. Unexposed=1.52, 95% CI: 1.00-2.31; OR_Q3 vs.Unexposed=1.88, 95% CI: 1.24- 2.85; and OR_Q4 vs. Unexposed=2.23, 95% CI: 1.35- 3.69) (p-trend=0.001) than using CANJEM-based metrics (p-trend=0.02). Significance: The integration of occupational exposure data from personal interviews with the use of CANJEM likely decreased misclassification of exposure, improving our ability to identify an exposure-response between BTX and bladder cancer risk.	S Xie, MC Friesen, D Baris, M Schwenn, N Rothman, A Johnson, MR Karagas, DT Silverman, S Koutros	2023	EPIG
2023-030	Tongyi		Dou	NHLBI	Structural Biology	The substrate and inhibitor binding mechanism of polyspecific transporter OAT1 revealed by high-resolution cryo-EM	Organic anion transporters (OATs) of the SLC22 family play critical roles in the transport of organic anions, including metabolites and therapeutic drugs, and in the transporter-mediated drug-drug interactions. Likely, OATs mediate the elimination of metabolic waste products and xenobiotics through the kidney, while OATs accumulating toxic compounds can also result in kidney failure. Moreover, OATs are important drug targets, as their inhibition can modulate the elimination or retention of substrates linked to diseases or treatments. Despite extensive research on OATs, the molecular basis of substrate and inhibitor binding has been hindered by the lack of structural information. Here, we report the cryo-electron microscopy structures of rat OAT1 (Rn-SLC22A6) and its complexes with substrate para-aminohippuric acid and inhibitor probenecid (a drug used in the treatment of chronic gout) at 2.1, 2.8, and 2.9 Å resolution, respectively. Our findings reveal a highly conserved mechanism for substrate and inhibitor binding in the SLC22 transporters, wherein four aromatic residues form a cage to accommodate the polyspecific binding of diverse compounds.	T Dou, T Lian, S Shu, Y He, J Jiang	2023	STRUCTBIO
2023-031	Jorge		Gomez DEza	NICHD	Neuroscience	DLK-dependent mitochondrial fission drives axon degeneration and neuronal cell death	Currently there are no effective treatments for an array of neurodegenerative disorders to a large part because cell-based models fail to recapitulate disease. Here we developed a robust human iPSCbased model where laser axotomy causes retrograde axon degeneration leading to neuronal cell death. Time-lapse confocal imaging revealed that damage triggers a wave of mitochondrial fission proceeding from the site of injury to the soma. We demonstrated that mitochondrial fission and resultant cell death is entirely dependent on phosphorylation of dynamin related protein 1 (DRP1) by dual leucine zipper kinase (DLK). Importantly, we show that CRISPR mediated Drp1 depletion protected mouse retinal ganglion neurons from mitochondrial fission and degeneration after optic nerve crush. Our results provide a powerful platform for studying degeneration of human neurons, pinpoint key early events in damage related neural death and new focus for therapeutic intervention	J Gomez-Deza, M Nebiyou, MR Alkaslasi, P Somasundaran, AL Slavutsky, ME Ward, TA Watkins, CE Le Pichon	2023	NEURO
2023-032	Apostolos		Manolopoulos	NIA	Clinical Research	Brain effects of 5-2 calorie restriction in a randomized controlled clinical trial	Insulin Resistance (IR) is implicated in brain aging and Alzheimer's disease (AD) pathogenesis. An extensive animal literature suggests pro-cognitive and beneficial systemic and brain effects of intermittent calorie restriction (CR). We conducted a Randomized Controlled Trial of 5-2 CR (2 days 480 Kcal/day; 5 non-restricted days) compared to low-intensity "healthy living" (HL) diet by USDA recommendations for 8 weeks, in 40 overweight cognitively intact individuals > 55 years old with peripheral IR. After 8 weeks, both diets decreased BMI, weight and waist circumference suggesting high compliance. 5-2 CR but not HL diet increased blood beta-hydroxybutyrate and acetoacetate suggesting increased ketogenesis and decreased HOMA2-IR indicating IR alleviation. 5-2 CR but not HL diet improved executive function and cued memory. 5-2 CR but not HL diet decreased sedentary behavior by actigraphy. Moreover, 5-2 CR but not HL diet decreased brain glucose by magnetic resonance spectroscopy (MRS) indicating increased glucose metabolism. Both diets decreased equally regional BrainAGE (brain-age-gap on structural magnetic resonance imaging (MRI)) in the anterior cingulate cortex. Many effects varied by APOE e4 genotype. However, in cerebrospinal fluid (CSF) and neuron-derived extracellular vesicles (NDEVs), no changes were observed for Abeta42, Abeta40, total Tau and P181-Tau with either diet, and no change in neuronal IR, as assessed by NDEV-associated P-S312-insulin receptor substrate (IRS)-1. Overall, both diets had beneficial systemic and brain effects, with 5-2 CR showing additional positive effects on IR, ketogenesis, cognition, and brain glucose metabolism, potentially contributing to healthier brain aging. However, no biomarker evidence emerged indicating AD cascade modulation.	A Manolopoulos, F Delgado-Peraza, M Mustapic, K.A Pucha, M.P Mattson, D Kapogiannis	2023	CLINICAL
2023-033	Jessie	L	Ellis	NIAID	Microbiology and Infectious Diseases	Metabolic adaptation of Bordetella hinzii in an immunocompromised host	Bordetella hinzii is an emerging zoonotic pathogen. We recently characterized a series of B. hinzii isolates collected from the bloodstream and gastrointestinal tract of an IL12-RB1-deficient patient over 45 months. Genomic analysis revealed isolates derived from a clonal lineage that underwent extensive within-host diversification. Notably, 20/24 isolates shared a substitution in DNA polymerase III (DnaQ E9G) conferring a DNA proofreading defect resulting in hypermutation, potentially accelerating within-host adaptive evolution. In this work, we study genomic and phenotypic features of metabolic reprogramming that occurred during host adaptation. Using phenotypic microarrays, we assessed the capacity of each isolate to metabolize hundreds of substrates. Hierarchical clustering analysis grouped isolates into two clusters based on utilization of nitrogen sources, with one cluster demonstrating significantly greater utilization of 173/368 nitrogen sources (Bonferroni-corrected p<0.05). To investigate specific metabolic alterations, the four DnaQ wildtype isolates were cultured in defined Stainer-Scholte media. Interestingly, only one isolate demonstrated growth. Comparative genomics analysis revealed that growth-impaired isolates had mutations in metE encoding a methionine synthase, or pheA encoding a chorismate mutase/prephenate dehydratase involved in phenylalanine biosynthesis. Supplementation with L-Met or L-Phe, respectively, rescued growth in a concentration-dependent manner. Our work demonstrates the evolution of specific auxotrophies in these isolates during the course of infection. Future work will involve 1) complementation of wildtype genes into isolates to validate the genetic basis of these auxotrophies, and 2) competition assays to understand the fitness consequences of these mutations, which occurred in isolates that rose to dominance at defined times in the infection course.	JL Ellis, S Ghosh, JP Dekker	2023	MICROBIO
2023-034	Shreya		Ghosh	NIDDK	Structural Biology	Quantitative NMR analysis of the mechanism and kinetics of chaperone Hsp104 action on amyloid-β42 aggregation and fibril formation	Hsp104 is a unique disaggregase chaperone found in yeast, yet has been shown to function synergistically with mammalian chaperones, without displaying any overt toxicity and in turn, conferring increased stress tolerance. Additionally, Hsp104 is also the sole known chaperone to dissociate mature amyloid fibrils and help them convert back to native polypeptides. While the ability of Hsp104 to prevent and disaggregate fibrils is common knowledge, yet the pathway, mechanism, and kinetics associated with the activity still remains unanswered. To this end, I have used a combination of several biophysical techniques to probe the mechanism by which Hsp104 prevents fibrilization of amyloid β-42, which plays a central role in the onset and progression of Alzheimer's disease. Using a combination of Thioflavin T assays, nuclear magnetic resonance spectroscopic techniques, electron and atomic force microscopic techniques, we observe that Aβ42 aggregation occurs by a branching mechanism: an irreversible on-pathway leading to mature fibrils that entails primary and secondary nucleation and saturating elongation; and a reversible off-pathway to form nonfibrillar oligomers. Hsp104 binds reversibly with nanomolar affinity to sparsely populated Aβ42 nuclei, generated by primary and secondary nucleation, present in nanomolar concentrations, thereby completely inhibiting on-pathway fibril formation at substoichiometric ratios of Hsp104 to Aβ42 monomers. Hsp104 also impacts off-pathway oligomerization but to a much smaller degree, increasing the rate of off-pathway oligomerization.	S Ghosh, v Tugarinov, G M Clore	2023	STRUCTBIO
2023-035	Abraham	G	Moller	NIAID	Microbiology and Infectious Diseases	Evolution of the Opportunistic Pathogen Burkholderia vietnamiensis in an Immunocompromised Host	Burkholderia vietnamiensis is an opportunistic pathogen within the Burkholderia cepacia complex responsible for infections in certain immunocompromised human hosts. In this work, we analyze the evolution of B. vietnamiensis in a patient with IL-12 receptor b1 deficiency presenting with persistent bloodstream infection for more than 7 months. Bacterial isolates were collected nearly daily over the period of bacteremia (n=183 isolates), providing unprecedented temporal sampling of the underlying population. All isolates were sequenced with Illumina technology, and 24 isolates underwent PacBio long read sequencing to generate highly contiguous assemblies. A composite reference assembly was then constructed from nonredundant complete PacBio contigs derived from individual assemblies and annotated. Single nucleotide variants (SNVs) in individual short read datasets and structural variants in long-read assemblies were identified against this reference. A maximum-likelihood phylogeny computed from the identified SNVs (n=440) revealed a complex underlying population structure with successive bifurcations and distinct clades. Surprisingly, isolates cultured in the first two weeks were distributed broadly throughout the tree, suggesting that this diverse population was present when sampling began. Analysis identified a nonredundant set of 386 insertions relative to the composite reference genome, encoding at least five distinct insertion sequence (IS) elements that were either present in all isolates (ancestral) or only in a subset (differential). We hypothesize that differential IS presence resulted from active IS mobility and that IS insertional mutagenesis contributed to adaptive evolution in the host. Future work will include validation of IS mobility and characterization of transcriptional and fitness consequences of the identified insertions.	AG Moller, AP Launay, S Das, SM Holland, JP Dekker	2023	MICROBIO
2023-036	Soma		Ghosh	NIAID	Microbiology and Infectious Diseases	Transcriptional and epigenomic landscape of Bordetella hinzii human host adaptation	Bordetella hinzii is an emerging zoonotic pathogen that infects immunocompromised human hosts. Previous work in the lab reported genomic analysis of 25 isolates cultured over a period of 45 months from a patient with germline IL-12Rβ1 deficiency and persistent blood and GI tract infection with B. hinzii. These isolates demonstrated striking phenotypic diversity and were shown to have descended from a clonal lineage with extensive genomic diversification due to an inactivating E9G substitution in the DNA polymerase III ε- proofreading subunit (DnaQ) resulting in proofreading-deficient hypermutation. In this work, we evaluate the transcriptional and epigenomic landscape of these isolates to understand how mutations selected during infection reprogramed gene expression. Our study reveals four main observations. 1) Genes involved in flagellar biosynthesis appeared to be convergently downregulated in the DnaQ E9G lineages and a DnaQ WT isolate, suggesting a potential evolutionary tradeoff between motility and host immune escape. 2) Two isolates that shared a stop gain mutation in a Type III specific methyltransferase exhibited loss of methylation in a type III motif. Loss of methylation at this motif, present 2282 times throughout the genome, represents a global change in epigenetic state, with predicted global transcriptional changes and potential fitness consequences, to be tested. 3) Each isolate displayed unique transcriptional pattern, but shared general functional patterns as classified by gene ontology. 4) A putative phage, phiEt88, demonstrated variable expression across isolates. Overall, our study demonstrates that remarkable transcriptional diversity evolved during host adaptation with evidence of potential convergent evolution.	S Ghosh, C.J Wu, A.J Moller, A Launay, J.H Youn, P.P Khil, J.P Dekker	2023	MICROBIO
2023-037	David		Peeney	NCI	Molecular Biology and Biochemistry	Mapping the interactome of matrisome targets using extracellular proximity labeling (ePL)	Classical methods to investigate protein-protein interactions (PPIs) are generally performed in non-living systems, yet in recent years new technologies utilizing proximity labeling (PL) have given researchers the tools to explore PPIs in living systems. PL has distinct advantages over traditional protein interactome studies, such as the ability to identify weak and transient interactions in vitro and in vivo. Most PL studies are performed on targets within or on the cell membrane. We describe a method to investigate PPIs within the extracellular compartment, using both BioID2 and TurboID, that we term extracellular PL (ePL). To demonstrate the utility of this modified technique, we investigate the interactome of the widely expressed matrisome protein TIMP2 using carboxyl- and amino-terminal fusion peptides of TIMP2 with BioID2 and TurboID. Expanding on this pipeline, we have started to screen the interactomes of new matrisome targets in simple 2D and complex 3D culture conditions. We describe the TIMP2 interactome in unique tissue compartments. We also illustrate how the TIMP2 interactome changes in the presence of different stimuli, in different cell lines, and with different reaction kinetics (BioID2 vs. TurboID); demonstrating the power of this technique versus classical PPI methods. Furthermore, we expand this method to interrogate the interactomes of new matrisome targets such as TIMP3 and Thrombospondin-1. We propose that the screening of matrisome PPIs in disease models using ePL will reveal new therapeutic targets for further comprehensive studies. Knowledge of disease specific PPIs may also garner understanding of patient-specific therapeutic resistance to conventional and next-generation therapies.	D Peeney, S Gurung, J Rich, S Coates-Park, Y Liu, C Richie, L Jenkins, WG Stetler-Stevenson	2023	MOLBIO

2023-038	Abhinav		Sur	NICHD	Developmental Biology	Single-cell analysis of shared signatures and transcriptional diversity during zebrafish development	During development, animals generate distinct cell populations with specific identities, functions, and morphologies. To profile the molecular cell types during vertebrate development, we mapped transcriptionally distinct populations across 489,686 cells from 62 stages during wild-type zebrafish embryogenesis and early larval development (3–120 hours post-fertilization). By analyzing these data together and per tissue, we generated a detailed catalog of >300 cell states in zebrafish development and characterized the developmental trajectory of transcriptional changes that occur during the differentiation of several cell types. Cross-tissue comparisons revealed the limited catalog of gene expression programs reused across multiple tissues and their cell-type-specific adaptations. Focused analyses of non-skeletal muscle and the endoderm identified transcriptional profiles of understudied cell types and subpopulations, including the pneumatic duct, individual intestinal smooth muscle layers, spatially distinct pericyte populations and homologs of recently discovered human best4+ enterocytes that are potentially linked to human disease. Their developmental origins and specification programs remain unexplored, so we used trajectory analysis to identify the cascade of gene expression events leading to these cells and predict candidate regulators that govern their specification. To enable additional discoveries, we have made this comprehensive transcriptional atlas of early zebrafish development available through our website, Daniocell. Funding: NIH Intramural ZIAHD008997 to JAF.	A Sur, Y Wang, P Capar, G Margolin, JA Farrell	2023	DEVBIO
2023-039	Ian		Trees	NICHD	Epidemiology	Prenatal exposure to particulate matter and birthweight in the Upstate KIDS cohort	This study explores how prenatal exposure to particulate matter (PM) at different time windows during pregnancy impacts birthweight. We included 4,959 mother-infant pairs from the Upstate KIDS cohort born in New York State. Air pollution data were gathered from the EPA's Community Multiscale Air Quality model and matched to home addresses at the census tract level. Birthweight and gestational age were gathered from vital records. We ran multiple linear regressions adjusting for maternal socio-demographics, traffic-related pollutants (O3, NO, and SO2), infant sex, plurality, and seasonality. Participants were exposed to relatively low levels of PM during pregnancy (median PM2.5: 8.81 µg/m3, median PM10: 12.19 µg/m3). Nevertheless, higher PM exposure across virtually all windows of pregnancy was associated with lower birthweight in unadjusted models (Model 1). After controlling for traffic co-pollutants (Model 2), PM2.5 and PM10 exposure around birth remained associated with lower birthweight, as did PM10 around the 1st trimester. However, further accounting for maternal and infant characteristics (Model 3) attenuated associations for the latter, while PM exposure around birth remained associated with lower birthweight (PM2.5: -42.89g; 95% CI: -69.22, -16.56; PM10: -35.40g; -61.67, -9.13). Prenatal exposure to PM may impact birthweight depending on other pollutants and specific windows of exposure. Prenatal exposure to PM during specific pregnancy windows, particularly later in pregnancy, requires further research. In addition, studies using more precise exposure assessment methods and looking at non-linear pollution interactions are required.	A Saha, IR Trees, DL Putnick, PK Clayton, R Sundaram, P Mendola, EM Bell, EH Yeung	2023	EPIG
2023-040	Jordan	E	Jarvis	NIAMS	ACI/IRS	Developing nanoparticles to repurpose disulfiram as a treatment for skin cancers	Merkel cell carcinoma (MCC) and acral lentiginous melanoma (ALM) are rare and aggressive skin cancers often treated with immunotherapy. Unfortunately, immunotherapy is not effective or appropriate for all patients, therefore new therapeutic options are needed. Using a high-throughput drug screen, we identified the aldehyde dehydrogenase inhibitor disulfiram (DSF) as an agent that selectively reduced MCC viability. DSF is known to kill other cancer lines and complexing it with copper (Cu) increases its anti-cancer activity. We discovered that combined DSF/Cu decreased the viability of MCC and ALM cell lines in vitro. However, DSF has poor pharmacokinetics and biodistribution in mice, hindering in vivo testing. To improve the in vivo stability and biodistribution of DSF, we created two nanoparticle (NP) formulations of DSF/Cu, a metal-organic framework (MOF) NP and a poly(lactic-co-glycolic acid) (PLGA) NP. MOF NP decreased cell viability in four MCC cell lines. PLGA NP decreased cell viability in four MCC and three ALM cell lines. As PLGA NP are more potent than MOF NP, we are testing these in xenograft mouse models of MCC and ALM. PLGA NP also reduced the viability of mouse melanoma B16F10 cells in vitro, which allows us to test the combined effect of NP plus immunotherapy in a mouse cancer model. Overall, we successfully developed a DSF/Cu PLGA NP formulation capable of decreasing cell viability in MCC, ALM, and mouse melanoma. Ongoing in vivo studies will test the utility of PLGA NP for treatment of these skin cancers.	J Jarvis, D Reed, S Vilasi, T Gelb, A Lin, T Kellenberger, D Urban, M Hall, I Brownell, N Hill	2023	ACI/IRS
2023-041	Matthew	W	Anderson	NIAID	Microbiology and Infectious Diseases	Development of a lipid-based method for fluorescent labeling of Coxiella burnetii	As the etiologic agent of Q fever, Coxiella burnetii is a Gram-negative bacterium with significant scientific and clinical relevance. Currently, Q-Vax is the only commercially available preventative vaccine, however due to severe local and systemic reactions, it is only approved in Australia. These adverse reactions are collectively referred to as post-vaccination hypersensitivity (PVH) responses and are a form of granulatomous type IV delayed hypersensitivity resulting in leukocyte localization and subsequent severe inflammation and abscess formation. Although the PVH response is somewhat understood from the host perspective, the mechanisms of vaccine and pathogen dissemination are poorly understood, which in turn, contributes to the elusivity of reaching a full understanding of mechanisms underlying vaccine efficacy and post-vaccination hypersensitivity reactions. Given the lack of knowledge regarding both infection and vaccination dissemination kinetics as well as the difficulties associated with tracking the bacteria within host tissues, we are developing a method for the labeling of C. burnetii with fluorescent lipid dyes for use in future dissemination studies. Labeled C. burnetii exhibits detectable levels of fluorescence that appear to be long lasting and are unaffected by fixation methods. Completion of this project should allow for the tracking and visualization of C. burnetii dissemination within in vivo animal models for the first time in an easy and efficient manner. Insights into dissemination patterns will be essential to better understand Q fever pathogenesis and inform therapeutic and countermeasure development, especially with regards to the development of an improved vaccine candidate with decreased risk for severe PVH reactions.	MW Anderson, CL Richards, PS Binette, CM Long	2023	MICROBIO
2023-042	Eun-Jeong		Yu	NHGRI	Cancer Biology	Functional characterization of ALK5 (TGFBR1) mutations in endometrial cancer	ALK5 (TGFBR1) is a transmembrane receptor serine/threonine kinase that transduces TGF-β(Transforming Growth Factor β) signaling to activate SMAD2/3-dependent and -independent pathways. The purpose of this study is to determine the functional effects of ALK5 mutations in endometrial cancer (EC). Using nine in silico algorithms, we found that 79% (23 of 39) of ALK5 kinase domain mutations in EC are predicted to impact protein function. To test these predictions experimentally, constructs expressing wildtype-, constitutively active-, kinase-dead-, or mutant-ALK5, including ALK5-A230V, were transfected into NIH3T3 cells, which have low endogenous ALK5 levels. Following TGF-β stimulation, we observed that transient exogenous expression of ALK5-A230V, located in the ATP-binding pocket, delayed SMAD2/3 signal transduction and altered SMAD-independent signaling. We further showed that the ALK5-A230V mutant has reduced protein stability via a ubiquitin-dependent protein degradation mechanism. Our structural modeling predicts that SB431542, a small molecule ATP-competitive inhibitor of ALK5 will bind to the ALK5-A230V mutant with less affinity than to wildtype ALK5. We, therefore, examined the inhibitory effect of SB431542 on wildtype- and mutant-ALK5 activity using a Smad-binding element (SBE) luciferase reporter assay in combination with TGF-β stimulation. SBE luciferase activity in ALK5-A230V-transfected cells was inhibited less by SB431542 than in wildtype-ALK5 transfected cells indicating that ALK5-A230V is less sensitive to SB431542 than wildtype ALK5, potentially due to the changes in affinity. Our findings are novel and show that the ALK5-A230V mutant is a partial loss-of-function mutant that attenuates TGF-β signal transduction and has reduced sensitivity to an ALK5 small molecule inhibitor.	E Yu, DW Bell	2023	CANCER
2023-043	Noa		Reuveni	NIAAA	ACI/IRS	Establishing a Vaporized Delta-9-Tetrahydrocannabinol Self-Administration Model in Mice	Cannabis is the most widely abused illicit drug. With recent trends of cannabis medicalization and recreational legalization, we expect high prevalence of cannabis use to continue or even increase. Delta-9-tetrahydrocannabinol (THC), the main psychoactive compound in cannabis, is typically administered to animals through forceful routes of administration (e.g., injections) which differ from cannabis users willingly choosing to inhale cannabis. Therefore, it is important to develop a translationally relevant model of vaporized THC self-administration in mice to investigate the neural circuits underlying volitional cannabis use such as in cannabis use disorder. Rats have been reported to self-administer vaporized cannabis extracts, but anecdotal reports suggest mice are resistant to this procedure, and our pilot studies showed similar trends. However, a recent study demonstrated that mice self-administer vapor mixed with a green apple chemical flavorant commonly found in electronic cigarettes in the absence of nicotine. Therefore, by utilizing 1 % green apple flavored vapor to train mice to acquire vapor self-administration, we hope to facilitate THC vapor self-administration. In a cohort of animals trained to lever-press to earn green apple flavored vapor, we found, indeed, mice would increase responding to earn "puffs" of this vapor. We are currently performing studies to "fade out" the green apple flavorant and "fade in" THC.	N Reuveni, A Kesner	2023	ACI/IRS
2023-044	Shreeta		Chakraborty	NICHD	Genetics and Genomics	Enhancer-promoter interactions can bypass CTCF-mediated boundaries and contribute to phenotypic robustness	Transcriptional control by distal regulatory elements called enhancers is an integral feature of gene regulation. CTCF-mediated chromatin loops play a crucial role in facilitating interactions between distal genomic regions. However, the in vivo significance of this model is poorly understood. To explore how enhancer-promoter interactions arise and assess the impact of disrupting 3D chromatin structure on gene expression, we generated an allelic series of mouse mutants that perturb the structure of the Sox2 locus. We show that in the epiblast and in neuronal tissues, CTCF-mediated loops are neither required for the interaction of the Sox2 promoter with distal enhancers, nor for its expression. Insertion of various combinations of CTCF motifs between Sox2 and its distal enhancers generated ectopic loops with varying degrees of insulation that directly correlated with reduced transcriptional output. Yet mutants exhibiting strongest insulation, with six CTCF motifs in divergent orientation, could not fully abolish activation by enhancers, and failed to disrupt implantation and neurogenesis. In contrast, cells of the anterior foregut were more susceptible to chromatin structure disruption with no detectable SOX2 expression in mutants with the strongest CTCF-mediated boundaries. These animals phenocopied loss of SOX2 in the anterior foregut, failed to separate trachea from esophagus and died perinatally. We propose that baseline transcription and enhancer density may influence the tissue-specific ability of distal enhancers to overcome physical barriers and maintain faithful gene expression during embryonic development. Our work suggests that enhancer-promoter interactions that can overcome chromosomal structural perturbations, play an essential role in maintaining phenotypic robustness.	S Chakraborty, N Kopitchinski, Z Zuo, A Eraso, P Awasthi, R Chari, A Mitra, IC Tobias, SD Moorthy, R Dale, J Mitchell, TJ Petros, PP Rocha	2023	GEN
2023-045	Yuta		Koui	NHLBI	Neuroscience	Imaging neuropathic pain and abnormal neuro-vascular branching in obese and type 2 diabetes mouse model	At least 50% of diabetic patients develop nerve dysfunction in the skin, leading to severe burning or shooting pain called small fiber neuropathy. In addition to functional abnormalities, patients with small fiber neuropathy develop degeneration of axon terminals and vascular abnormalities in the skin. Although the symptoms of diabetic small fiber neuropathy are well characterized, the mechanism of etiology and therapeutic strategies remain elusive. We have developed an in vivo live calcium imaging of sensory nerves in the ear skin of the diet-induced obesity (DIO) mice to visualize pain reactions in response to capsaicin stimulation. The DIO skin at 22 weeks-of-age shows abnormal sensory hypersensitivity characterized as a pain reaction, while exhibiting no severe sensory axon terminal degeneration or vascular abnormalities. At 30 weeks-of-age, the DIO skin shows a significant reduction of sensory axon terminals, indicating that sensory axons undergo severe degeneration, as well as an increased expression of the vascular leakage marker PLVAP in capillary endothelial cells. These results suggest that sensory nerve hypersensitivity develops prior to sensory degeneration and vascular abnormalities in the DIO skin. At mechanistic level, the enhanced expression of nerve growth factor (NGF) is observed in the DIO skin. Short-term treatment of the DIO skin with anti-NGF neutralized antibody or Wortmannin as a selective inhibitor of phosphatidylinositol 3-kinase (PI3K) results in suppression of hypersensitivity. Taken together, a modulation of local NGF-TrkA-PI3K signaling could be an effective therapeutic strategy for diabetic small fiber neuropathy.	Y Koui, S Song, Y Mukoyama	2023	NEURO
2023-046	Maria	A	Aronova	NIBIB	Structural Biology	Deep learning analysis of 3D electron microscopy data reveals quantitative differences in platelet and organelle Packing in COVID-19 patient derived platelets.	It has been shown that COVID-19 patients can exhibit a range of symptoms, one of which is microclotting in the pulmonary vasculature, a prominent contributor to respiratory deficits. Clotting is a complex process, which involves both circulating proteins and platelets, anucleated cells in the blood. When clotting occurs, it can be suggestive of an increased level of platelet activation. Thus, we reasoned that parts of the platelet involved in the release of platelet contents during clotting would lose their content and appear as expanded, empty "ghosts". To test this, we drew blood from three severely ill COVID-19 patients and compared the platelets within the blood draws to those from three healthy volunteers. We used 3D high-resolution focused ion beam scanning electron microscopy (FIB-SEM) and employed deep learning computational methods to evaluate nearly 600 individual platelets and 30,000 organelles such as a-granules and mitochondria from both, the healthy donors and severely ill COVID-19 patients. We found that COVID-19 patient platelets were 35% smaller in volume, with most of the difference in organelle packing density being due to decreased platelet size, rather than differences in organelle count or their volume. There was little to no 3D ultrastructural evidence for differential activation of the COVID-19 patients' platelets. Though limited by sample size, our studies suggest that factors outside of the platelets themselves are likely responsible for such COVID-19 complications as microclotting. In addition, our studies show how deep learning 3D methodology can become the gold standard for 3D ultrastructural studies.	MA Aronova, SS Matharu, CS Nordmann, KR Ottman, R Akkem, K Campbell, G Sievert, J Sturgill, JZ Porterfield, S Joshi, HR Alfar, C Peng, ID Pokrovskaya, JA Kamykowski, JP Wood, B Garvy, SW Whiteheart, RD Leapman, B Storrie	2023	STRUCTBIO
2023-047	Jinchutha		Duangdara	NCI	Cell Biology	CAR T cells targeting mesothelin for treating intrahepatic cholangiocarcinoma	In the US and the rest of the world, intrahepatic cholangiocarcinoma (iCCA) is a major type of liver cancer. iCCA is one of the most common cancers in Thailand, where there is an endemic of the liver fluke. We previously reported that mesothelin (MSLN) was highly expressed in over 30% of iCCA and suggested that MSLN might be a promising therapeutic target in iCCA. The MSLN CAR T cells have been developed against several MSLN-expressing solid tumors. However, this strategy has not been extensively evaluated for treating iCCA. The present study aims to evaluate the anti-tumor effect of MSLN CAR T cells based on the humanized rabbit antibodies with various specificities and affinities in iCCA models. We developed MSLN CAR T cells against membrane-proximal epitope (hYP218), membrane-middle epitope (hYP223), membrane-distal epitope (HN1 and hYP158), and membrane-conformation epitope (hYP3). Their anti-tumor activity was evaluated in vitro using MSLN-positive iCCA cell lines. Among CAR T cell constructs, hYP218 CAR T cells targeting membrane-proximal epitope are the most effective against CCA cell lines. A single intravenous injection of hYP218 CAR T cells eliminated tumors in mice within two weeks. In conclusion, the current results demonstrate that MSLN CAR T cells targeting membrane-proximal epitope are very effective against iCCA. Ongoing studies are to establish iCCA tumor models in mice for testing the efficacy of CAR T cells in vivo.	J Duangdara, S Lin, J Hong, D Li, K Wongprasert, M Ho	2023	CELLBIO

2023-048	Chandra Mani		Kafle	NHGRI	Cancer Biology	Investigation of the mechanism of PADI2-regulation by the FBXW7 tumor suppressor	Introduction: Serous endometrial cancer (SEC) is an aggressive form of cancer that frequently exhibits recurrent somatic mutations in FBXW7 at residues 465, 479, and 505. FBXW7 is a tumor suppressor that is part of a Skp-Cullin-F-box containing (SCF) complex that targets various oncoproteins for proteasome-mediated degradation. FBXW7 interacts with the Cdc4 phosphodegron (CPD) motif(s) within the target proteins. We previously reported upregulation of Peptidyl arginine deiminase 2 (PADI2) in FBXW7-mutant cell lines compared to the isogenic FBXW7-wildtype SEC cells. Purpose: Here we investigate the mechanism of PADI2-regulation by FBXW7. Methods: We searched for the CPD motif in the PADI2 protein sequence. We employed biochemical analyses to study transiently transfected HEK293 and CRISPR-Cas9 knock-in FBXW7-mutant and isogenic FBXW7-wildtype SEC cells. Results: We identified three putative CPD motifs in PADI2 leading us to hypothesize that wildtype FBXW7 binds PADI2, and thus targets PADI2 for degradation via a proteasome-dependent mechanism. We have shown that FBXW7 interacts with PADI2, in presence of a proteasome inhibitor, in transiently transfected HEK293 cells. Additionally, we have shown that mutation of the putative CPD domains of PADI2 abrogates the PADI2-FBXW7 interaction. We are currently testing whether the recurrent somatic mutations of R465, R479 and R505 in FBXW7 affect binding to PADI2. Conclusions: Our interim findings implicate PADI2 as a novel target of the FBXW7 tumor suppressor. Because PADI2 is upregulated in FBXW7-mutated EC cells, we will conduct future studies to determine whether FBXW7-mutated EC cells exhibit increased sensitivity to PADI2 inhibitors.	CM Kafle, DW Bell	2023	CANCER
2023-049	Christina	M	Fitzsimmons	NCI	RNA Biology	Rewiring of RNA methylation by the oncometabolite fumarate in renal cell carcinoma	Metabolic reprogramming is a hallmark of cancer that facilitates changes in many adaptive biological processes. Mutations in the tricarboxylic acid (TCA) cycle enzyme fumarate hydratase (FH) lead to fumarate accumulation and cause hereditary leiomyomatosis and renal cell cancer (HLRCC). HLRCC is a rare, inherited disease characterized by the development of non-cancerous smooth muscle tumors of the uterus and skin, and an increased risk of a highly metastatic and aggressive form of kidney cancer. Fumarate has been shown to inhibit 2-oxyglutarate-dependent dioxygenases (2OGDDs) involved in the hydroxylation of HIF1a, as well as in DNA and histone demethylation. However, the link between fumarate accumulation and changes in RNA post-transcriptional modifications has not been defined. Here, we determine the consequences of fumarate accumulation on the activity of different members of the 2OGDD family targeting RNA modifications. By evaluating multiple RNA modifications in patient-derived HLRCC cell lines, we show that mutation of FH selectively alters the activity of demethylases acting upon N6-methyladenosine (m6A), while the demethylase acting upon N1-methyladenosine (m1A) and 5-formylcytosine (f5C) in mitochondrial RNA are unaffected. The observation that metabolites modulate specific subsets of RNA-modifying enzymes offers new insights into the intersection between metabolism and the epitranscriptome.	CM Fitzsimmons, MD Mandler, JC Lunger, D Chan, SS Maligireddy, AC Schmiechen, S Thallalla Gmage, C Link, LM Jenkins, DR Crooks, JL Meier, WM Linehan, PJ Batista	2023	RNA
2023-050	Huan		Mo	NHGRI	Genetics and Genomics	Investigation of pathogenic and truncated variants of RUNX1 and DDX41 in all of us	Myeloid neoplasms associated with germline disposition can be caused by inherited variants involving multiple genes such as RUNX1, DDX41, CEBPA, GATA2, ETV6, TP53, ANKRD26s. Inherited pathogenic/likely pathogenic (P/LP) variants of RUNX1 lead to familial platelet disorder with predisposition to myeloid malignancy (FPDMM), and those of DDX41 lead to late onset MDS/AML. However, previous generated data has mostly focused on clinically ascertained probands and their families and thus may be subjected to ascertainment biases. Here, we used a genotype-first strategy to investigate the natural behaviors of the pathogenic and likely pathogenic (P/LP) variants involving RUNX1 and DDX41 in a phenotypically unselected population on the All of Us Research Platform. In RUNX1, we identified ?20 individuals who carry P/LP variants, all located in the RUNT domain. Phenotypes included undiagnosed persistent thrombocytopenia, myeloid neoplasm, and absence of significant hematological diseases in different carrying individuals. In DDX41, we identified 33 individuals with P/LP variants with a median age of 53 years. The prevalence of cytopenia was similar to non-carriers (anemia 65.2% in carriers compared to 54.5% in non-carriers; thrombocytopenia 5.8% compared to 20%, neutropenia 33% compared to 28.7%; all statistically non-significant). However, we observed that among the < 20 male carriers with CBC data, 75% of them had documented anemia with first onset at ages of 49-64 years old. There were no diagnosed myeloid neoplasms among the carriers, which might be due to the younger ages of the All of Us participants.	H Mo, TC Tran, A Awan, TM Ferrara, C Wilcozewski, T Clesson, R kanagal-Shamanna, JC Denny	2023	GEN
2023-051	Toluleke	O	Famuyiwa	NCI	Virology	HIV -1 Antisense RNA is Detected in Infected Cells In Vivo	Natural antisense transcripts (NATs), which are transcribed from the opposite strand of protein-coding genes, regulate gene expression through epigenetic, post-transcriptional, and/or post-translational modifications. The human immunodeficiency virus type I (HIV-1) has been shown to express one or more NATs from a promoter within the 3' long terminal repeat. HIV-1 antisense transcripts (Ast) are capable of inducing proviral latency in in vitro cell culture. Our studies will identify and quantify HIV-1 Ast in vivo. We developed and optimized a digital PCR-based assay to measure levels of Ast in small pools of infected cells using the ACH2 cell line. ACH2 cells each carry a single copy of an integrated HIV- 1 provirus that expresses sense and antisense RNA at low levels. In 6 experimental replicates of 50 ACH2 cells, our digital PCR approach detected HIV-1 Ast in an average of 36% of the cells (range 22%-70%), consistent with previous studies. We next applied our new assay to PBMC collected from a donor with HIV- 1 and on antiretroviral therapy. Testing 2 pools of aliquots of about 22 infected PBMC from this donor, we found that up to 54% of the infected cells contain HIV-1 Ast. These data demonstrate that Ast is expressed in people living with HIV-1 and lead to the question of whether HIV-1 Ast expression can contribute to viral latency and persistence during treatment. In our future studies, we will investigate varying levels of plasma viremia in a cohort of 50 people living with HIV-1.	TF Famuyiwa, AA Capoferri, SH Pathak, R Sklutuis, SG Deeks, JW Rausch, JL Groebner, MF Kearney	2023	VIROL
2023-052	Ting-Yi		Lin	NEI	Genetics and Genomics	Genetic and epigenetic insights into aging of the human retina	Aging is a major contributing risk factor for age-related diseases. The complex interplay of genetics, environment, and stochasticity alters local accessibility and regulation of genetic information, resulting in transcriptomic dysregulations. Although GWAS of age-related diseases have suggested genes and pathways contributing to pathophysiology, the effects of aging in these study designs are challenging to account for and are often forgone when using age as a covariate. QTL are genomic regions statistically correlated with traits (e.g., GE/mCpGs) and are largely non-coding regulatory sites that mediate changes in gene expression. We hypothesize that aging-associated gene expression changes are determined, at least in part, by genetic variations and epigenetic changes resulting from environmental factors and lifestyle. We present a novel framework to study the effect of aging in age-related diseases by longitudinally characterizing the physiologic aging of the retina by integrating diverse "omics" datasets across the lifespan. First, we modeled GE changes across age with linear and non-linear regression to identify age-related differential GE. Secondly, we will establish retinal QTLs (eQTL, mQTL) to study natural genetic variations' impact on expression and methylation. With the QTLs, we (1) dissect genetic variation in GE/mCpGs with QTLs accounting for aging and natural variability of genetic polymorphism on GE/mCpGs; (2) explore GE/mCpGs effect on aging by analyzing the differential GE and methylated regions by comparing across the lifespan; and (3) distinguish the role of epigenetics in transcriptome by integrating the GE and mCpGs associated with aging with eQTM to capture the dynamics of epigenetic in the transcriptome.	TY Lin, J Advani, M English, DA Ferrington, AV Segre, A Swaroop	2023	GEN
2023-053	Reza		Amanipour	NIDCD	Neuroscience	Estrogen Receptor-2 Agonists for Protection Against Noise-Induced Hidden Hearing Loss in Female Mice	One of the most common forms of hearing loss in adults is noise-induced hidden hearing loss (NIHHL). A noise exposure that only causes a temporary threshold shift (TTS) can nevertheless result in permanent damage to ribbon synapses between inner hair cells (IHCs) and spiral ganglion neurons (SGNs). Work from our laboratory shows that female mice are less susceptible to NIHL, and that this protection is due to endogenous 17β-estradiol. Additionally, this protective effect is partially mediated through estrogen receptor β (ESR2). In this study we investigate whether augmentation of ESR2 signaling via administration of DPN (diarylpropionitrile, an ESR2 specific agonist) or 17β-estradiol (E2) can protect female mice against NIHHL. Female B6CBAF1/J mice at 8 weeks, were implanted with pellets containing DPN, E2, or a placebo. Baseline auditory brainstem response (ABR) and distortion product otoacoustic emission (DPOAE) thresholds were recorded at 9 weeks of age. At 10 weeks, mice were exposed to noise (8-16 kHz, 93- or 97-dB SPL, for 2-hours). ABRs and DPOAEs were re-evaluated at 1-day, 1-week, and 6-weeks after noise exposure. Comparison of ABR and DPOAE threshold shifts between treated and placebo animals revealed lower threshold shifts for the E2- and DPN-treated mice. Histologically, treatment with E2 and DPN resulted in significantly higher survival of IHC synapses 6-weeks after noise exposure at 24 kHz frequency. These results show that augmentation of ESR2-mediated signaling ameliorates NIHHL in intact female mice. This study indicates that ESR2 specific agonists, are promising candidates for future clinical trials for hearing preservation in females.	R Amanipour, B Shuster, B Milon, R Hertzano	2023	NEURO
2023-054	Soniya		Chatterjee	NCI	Chromosome Biology	TZAP mediated BTR localization to telomeres	Maintenance of telomere length is a critical process required to ensure genome stability. This process involves the balancing between process that result in telomere shortening and telomere lengthening. Excessive shortening results in replicative senescence whereas unregulated lengthening allows for unlimited cell proliferation and increase risk of cancer development. A critical factor involved in telomere length homeostasis is TZAP (telomeric zinc finger–associated protein). This protein binds specifically to telomeric repeat but shows preferential binding to long telomeres. Upon binding TZAP triggers rapid telomere deletion characterized by generation of extra-chromosomal telomeric DNA (ECTR) circles. The TZAP-mediated generation of ECTR is dependent on a protein complex called Bloom (BLM)-Topoisomerase III α-RMI1-RMI2 (BTR). However, the specific nature of the relationship between TZAP and BTR is not fully understood. Here we show that BLM is recruited to telomeres directly by TZAP through its two putative SIM domains, since alterations in these domains significantly decreases the localization. Additionally, we demonstrate that TZAP can recruit BLM to telomeres independently of PML (promyelocytic leukemia protein), a known recruiter of BLM. These results contribute to our understanding of the complex relationship between TZAP and BTR in telomere biology.	S Chatterjee, JSZ Li, MN Boddy, EL Denchi	2023	CHROM
2023-056	Domenico		D'Atri	NCI	Cancer Biology	Synthetic Bacillus subtilis inspired spores: A new approach for cancer treatment	Delivery of cancer therapeutics to non-specific sites decreases treatment efficacy while increasing toxicity. In ovarian cancer, overexpression of the cell surface marker HER2, which several therapeutics target, relates to poor prognosis. We recently reported the assembly of biocompatible bacterial spore-like particles, termed "SSHELs." Here, we modify SSHELs with an affibody directed against HER2 and load them with the chemotherapeutic agent doxorubicin. Drug-loaded SSHELs reduce tumor growth and increase survival with lower toxicity in a mouse tumor xenograft model compared with free drug and with liposomal doxorubicin by preferentially accumulating in the tumor mass. Target cells actively internalize and then traffic bound SSHELs to acidic compartments, whereupon the cargo is released to the cytosol in a pH-dependent manner. We propose that SSHELs represent a versatile strategy for targeted drug delivery, especially in cancer settings.	D D'Atri, MS Kong, MT Bilotta, F Machinandiarena, K Tanner, D Fitzgerald, KS Ramamurthi	2023	CANCER
2023-057	Brice		Wilson	NCI	Molecular Pharmacology	Natural products as a source of chemical diversity in cyclic-AMP-dependent Protein Kinase A (PKA) inhibitor discovery	cAMP dependent protein kinase A (PKA) enzymatic activity is a central cellular signaling node underlying many fundamental physiological processes. PKA dysregulation is associated with a number of human diseases including Cushing's syndrome, Carney Complex disorders, and certain cancers. This cohort of PKA dependent diseases includes fibrolamellar hepatocellular carcinoma (FLHCC), a rare largely incurable liver cancer uniquely driven by the overexpression of an oncogenic fusion between an HSP40 family member, DNAJB1, and the catalytic domain of PKA alpha, PRKACA. This fusion protein (J-PKAcα) is enzymatically active and drives FLHCC tumor growth, making it an attractive target for inhibitor discovery. We implemented a high throughput screening campaign of >140,000 fractionated natural products extracts to discover pharmacophores evaluated for J-PKAcα inhibition, fusion specificity, direct binding, intracellular activity, and x-ray crystallography. This screen revealed several previously unreported PKA inhibitors which may form the foundation of future medicinal chemistry efforts to optimize these scaffolds for translational applications.	BA Wilson, L Du, DS Sendadeera, D Wang, RW Fuller, T Grkovic, R Shah, N Li, JA Martinez Fiesco, P Zhang, BR O'Keefe	2023	PHARMA
2023-058	Veronique		Bolduc	NINDS	RNA Biology	A humanized knock-in COL6A1 mouse recapitulates a splicing defect correctable with exon skipping	Splice-modulating antisense oligonucleotides have recently entered the clinical space as a viable therapeutic strategy for personalized medicine. Our goal is to develop a splice-modulating therapy to skip a pathogenic pseudoexon in the collagen 6 alpha 1 (COL6A1) gene, associated with a severe form of collagen VI-related muscular dystrophy. The pseudoexon insertion is driven by an unexpectedly common deep-intronic variant (c.930+189C>T) in intron 11 of COL6A1, that our group recently identified. We previously showed in cultured primary fibroblasts that phosphorodiamidate morpholino (PMO) antisense oligonucleotides efficiently skip the pseudoexon and restore COL6A1 expression. Here, we aim at creating a preclinical mouse model to test our exon-skipping therapy in vivo. Modeling splicing defects caused by deep-intronic variants, however, is complicated by the poor degree of conservation of intronic sequences between human and mouse. To address this challenge, we knocked in 1.9 kb of the human COL6A1 genomic sequence into the corresponding mouse locus, encompassing human exons 9-14 and their corresponding human introns. We generated one humanized knock-in (KI) mouse line that carries the reference C nucleotide (Col6a1HumC/HumC) at the c.930+189 position in intron 11, and one line that carries the pathogenic variant T nucleotide (Col6a1HumC/HumT, and Col6a1HumT/HumT). Using long-read sequencing, we validated that the human exons are properly spliced into the Col6a1 transcripts, including the 72-nt pseudoexon in Col6a1HumC/HumT, and Col6a1HumT/HumT. Males and females show grip strength deficit as early as one month of age. The Col6a1 humanized KI mouse represents an invaluable tool to assess the potential of human-ready exon-skipping antisense oligonucleotides.	V Bolduc, F Guirguis, A Brull, J Cheng, L Garrett, CG Bönnemann	2023	RNA
2023-059	Nadia		Said	NIDA	Neuroscience	A putative role of the neuroimmune system in heroin withdrawal	Over the last two decades, opioid overdose has become the third leading cause of accidental deaths in the United States. Recent evidence suggests that glial activation and the related neuroimmune signals may be involved in the dependence-inducing properties of opioids. Therefore, the main purpose of this study is to investigate the role of neuroimmune systems in opioid withdrawal-related behavior in rats. We first measured hyperalgesia and the aversive effects of heroin withdrawal in adult male and femaleWistar rats. Hyperalgesia was assessed using von Frey and Hargreaves tests, for mechanical and thermal sensitivity, respectively, after two weeks of repeated heroin administration. We also investigated the heroin withdrawal-induced conditioned place aversion (CPA) and naloxone-precipitated somatic withdrawal. Then, we quantified 17 cytokines and chemokines in whole brains of both saline- and heroin-treated rats by a FirePlex immunoassay. The data showed that two chemokines (CCL2 and CXCL1) and a cytokine (IL-10) were significantly upregulated in male rats that received heroin but not in females. Based on these results, we investigated whether an acute injection of a CCL2 antagonist could reverse the heroin-induced hyperalgesia, CPA and somatic withdrawal symptoms in heroin-dependent male and female Wistar rats. Results showed that the antagonist significantly reversed mechanical and thermal hyperalgesia, and attenuated CPA and somatic withdrawal symptoms in males and females. In summary, our findings suggest a sex-dependent proinflammatory effect of heroin withdrawal in the rat brain. Our data also shows that CCL2 may contribute to motivational and somatic signs of opioid withdrawal in adult Wistar rats.	N SAID, H Mills, LF Vendruscolo, GF Koob	2023	NEURO

2023-060	Khalid		Garman	NIAMS	Molecular Pharmacology	Dinaciclib inhibits mRNA processing in Merkel cell Carcinoma: a novel therapeutic with a unique mechanism of action	Merkel cell carcinoma (MCC) is a rare, aggressive neuroendocrine skin cancer with a high fatality rate. Currently, immune check point inhibitors (ICI) are the first line of treatment for metastatic MCC, but over 50% of patients do not achieve durable responses. To identify novel treatments for MCC, we screened 4,000 compounds for their ability to reduce MCC viability. Using the Area Under the Dose-Response Curve, we identified dinaciclib, a CDK 1/2/5/9 inhibitor as efficacious against multiple MCC cell lines. In vitro studies demonstrated that dinaciclib induced MCC cell death accompanied by reduction in cell size, diminished S-phase, DNA damage, and apoptosis. Further mechanistic studies using RNA-seq and phosphoproteomics surprisingly revealed that the immediate effects of dinaciclib treatment in MCC cells included inhibition of mRNA splicing, resulting in an accumulation of retained intron transcripts. This rapid inhibition of RNA processing may account for the increased activity of dinaciclib over other CDK inhibitors. In vivo, dinaciclib was able to reduce tumor growth in a pre-clinical xenograft model of MCC. Overall, our studies identified dinaciclib as a promising novel treatment for metastatic MCC and support a clinical trial of this agent in patients whose MCC has progressed despite ICI therapy.	K Garman, T Gelb, D Anastasakis, S Davies, A Polash, D Urban, M Hall, M Hafner, I Brownell	2023	PHARMA
2023-061	Shuaizhang		Li	NCATS	Chemical Biology	Discovery of protease inhibitors for potential antivirals against Chikungunya Virus	Chikungunya virus (CHIKV) is a mosquito-borne RNA virus that belongs to the family Togaviridae, genus Alphavirus, which has emerged as one of the most important global arboviral threats over the last decade. However, there is no available antiviral drugs or licensed vaccine for CHKIV. CHIKV nsP2 protease play an important role in processing of viral nonstructural polypeptide precursor to release enzymes required for viral replication, thus making it a promising drug target. The objective of the current study was to identify small molecules that inhibit nsP2 activity. We developed a fluorescence resonance energy transfer (FRET)-based high-throughput screening (HTS) assay using a fluorogenic peptide substrate encompassing one of the endogenous cleavage sites and purified rCHIKV nsP2pro. The assay was minimized into 1536-well plate format with Z' value >0.8 and CV <10%. Using this assay, we then interrogated NCATS-sourced small moleculelibraries including 9866(8500 unique) compounds . From the screenings, 250 compounds were selected for follow-up validation and counter-screenings. Specifically,Full-length nsP2 and an additional peptide were employed for follow-up validations, and FRET-based assays for Papain and NS3-4A proteases were utilized ascounter screening assays. Novel compounds were identified to be potential nsP2 inhibitors andmolecular docking analyses were performed to explain the binding mode of selected compounds. These hits constitute good candidates for testing in cell-based live-virus assay.	SZ Li, X Hu, L Ye, YM Ahn, S Messing, D Esposito, NJ Martinez	2023	CHEMBIO
2023-062	Kaitlyn	N	Sadtler	NIBIB	Biomedical Engineering and Biophysics	The CD103-XCR1 axis mediates the recruitment of immunoregulatory dendritic cells after traumatic injury	After an injury, the body must establish a delicate balance between immune activation, to fight off infection and clear debris, while preventing immune reactivity to the body's own tissue to promote optimal healing and long-term survival. During wounding and surgical material implantation for tissue reconstruction, there is a disturbance in homeostasis and release of self-antigen. Regulation between tolerance and auto-inflammation in this process is not well understood. Here, we analyzed antigen-presenting cells in muscle injury and found that pro-regenerative biomaterials enrich a novel Batf3-dependent CD103+XCR1+CD206+CD301b+ dendritic cell population associated with cross-presentation and self-tolerance. Up-regulation of E-Cadherin (the ligand for CD103) and XCL-1 in injured tissue suggests a mechanism for cell recruitment to trauma. Muscle injury recruited NK cells that produced Xcl1 when stimulated with fragmented extracellular matrix. Without cross-presenting cells T cell activation increases, pro-regenerative macrophage polarization decreases, and there are alterations in myogenesis, adipogenesis, fibrosis, and increased muscle calcification. While this pathway has been described in cancer, this is the first time it has been implicated in wound healing. These data represent a new fundamental mechanism of immune regulation that has not previously been linked to trauma and material implantation, resulting in downstream effects on tissue regeneration, having implications for both short- and long-term injury recovery.	R Lokwani, A Josyula, TB Ngo, S DeStefano, D Fertil, M Faust, KM Adusei, M Bhuiyan, A Lin, M Karkanitsa, E Maclean, P Fathi, Y Su, J Liu, HD Vishwasrao, K Sadtler	2023	BIOENG
2023-063	Jennifer		Zink	NCI	Social and Behavioral Sciences	A longitudinal compositional analysis of leisure screen time and body mass index in the ABCD Study	Background: Youth use different screen types (e.g., streaming, gaming) that may be uniquely related to body mass index (BMI). Time spent on screens is interconnected with other activities, such as physical activity and sleep, that affect BMI. Compositional data analysis (CoDA) models the association between interconnected behaviors and health outcomes. We used CoDA to examine how different screen types and other interconnected behaviors relate to BMI one year later. Methods: Baseline and one-year follow-up data were from the Adolescent Brain Cognitive Development Study (N=5,165, mean [SD] baseline age=10.0 [0.6] years, 49% female, 48% non-White). Participants reported baseline screen time (streaming, gaming, and socializing), physical activity, and sleep. Sex-stratified linear regressions estimated the association between baseline relative proportion of time spent in each behavior and follow-up BMI z-score, adjusted for baseline BMI z-score, participant characteristics, and depressive/anxiety symptoms. Results: Mean time (min/day) spent in different activities was 152.0 streaming, 72.7 gaming, 46.8 socializing, 29.7 physical activity, 534.9 sleep and 603.9 other. In males, a greater proportion of time spent in baseline socializing via screens, relative to time spent in the remaining behaviors, was related to a higher follow-up BMI z-score (β [95% CI] = 0.05 [0.02 to 0.08]). No other significant associations were observed. Conclusions: CoDA can advance our understanding of the distinct BMI implications of different screen types, independent of other relevant behaviors. Further investigation of possible biological and behavioral mechanisms underlying the observed sex differences in the association between screen time and BMI is warranted.	J Zink, R Booker, DL Wolff-Hughes, N Allen, SJ Alexandria, MR Carnethon, D Berrigan	2023	SOCIAL
2023-064	Yukiko		Yano	NCI	ACI/IRS	The human oral microbiome and mortality in three prospective cohort studies	Poor oral health (e.g., periodontal disease) has been associated with mortality and various chronic diseases, suggesting the oral microbiome impacts systemic. We analyzed associations between the oral microbiome and overall mortality risk using data from three large, prospective cohorts in the United States. Our analysis included a reference sub-cohort (N=3,499) that had been randomly selected by strata of age, sex, and smoking status from the NIH-AARP Diet and Health Study, Agricultural Health Study, and the Prostate, Lung, Colorectum, and Ovarian Cancer Screening Trial cohorts. Over a median follow-up of 16 years, a total of 1,236 deaths occurred. DNA was extracted from oral wash samples, the 16S rRNA gene V4 region was amplified and sequenced, and bioinformatic processing was performed using QIIME 2. Cox proportional hazards models were used to calculate hazard ratios (HRs) and 95% confidence intervals (CIs). Higher alpha diversity was associated with lower mortality risk. For example, every standard deviation increase in observed amplicon sequence variants was associated with lower mortality risk with a HR of 0.89 (95% CI: 0.83-0.96). Multiple genera of the Clostridiales order were inversely associated with mortality risk. For example, the presence of the Eubacterium nodatum group was associated with 0.70 times the risk of mortality (95% CI: 0.61-0.82) compared with those without this bacterium. Higher relative abundances of a few genera (e.g., Lactobacillus and Scardovia) were associated with an increased risk of mortality. Results from this large prospective investigation suggest that multiple characteristics of the oral microbiome are associated with mortality risk.	Y Yano, E Vogtmann, X Hua, V Purandare, Y Wan, S Li, CL Dagnall, K Jones, BD Hicks, A Hutchinson, JG Caporaso, LB Freeman, DP Sandler, LM Liao, WY Huang, ND Freedman, R Sinha, MH Gail, J Shi, CC Abnet	2023	ACI/IRS
2023-065	Joydeep		Aoun	NIDCR	Cell Biology	PtdSer Scramblase TMEM16F (Anoctamin 6): Indispensable for Regulated Exocytosis and Epithelial Fluid Secretion	Regulated exocytosis is a fundamental polarized cellular activity that orchestrates the release of neurotransmitters and exocrine glands secretory granules (Zymogens) at the apical pole in response to a stimulus. Phospholipids have established roles in membranes trafficking, with PtdSer externalization has roles in cell-cell fusion, synaptic exocytosis and endocytosis, and in several cell death modalities and viral entry. However, the role and mechanisms of PtdSer regulation, particularly in epithelial exocytosis and epithelial fluid and electrolyte secretion, are not well understood. We discovered that both activities of TMEM16F (ANO6), Ca2+ activated Cl- channel function and PtdSer scrambling are required epithelial fluid and electrolyte secretion and for regulated exocytosis, respectively. Exocytosis by pancreatic acinar cells is triggered by Ca2+, whereas exocytosis by salivary glands acinar cells is primarily mediated by cAMP but Ca2+ and cAMP synergize to mediate the physiological response. Exocytosis and fluid secretion by the Pancreas and Salivary Gland are markedly reduced in ANO6-/- mice, which we traced to impaired receptor stimulated PtdSer scrambling and Cl- channel function by ANO6 in isolated acinar cells, respectively. Impaired exocytosis occurred in the face of minimally altered receptor stimulated second messenger generation and likely involved both second messenger detection by the exocytotic apparatus. Impaired fluid secretion is being traced to the role of ANO6 in the synergistic cAMP/Ca2+ component of fluid secretion.	J Aoun, M Ahuja, WY Lin, C Zheng, S Muallem	2023	CELLBIO
2023-066	Parinaz		Fathi	NIBIB	ACI/IRS	Unit for NanoEngineering and MicroPhysiological Systems (UNEMPS)	The NIBIB Unit for NanoEngineering and MicroPhysiological Systems (UNEMPS) is part of the Section on Immunoengineering. The goal of UNEMPS research is to integrate biomedical engineering and mechanical engineering with basic mechanistic biology to understand and develop therapies for autoimmune diseases and cancer. UNEMPS research focus areas include: 1) Developing organ-on-a-chip models of immune-related conditions, and 2) Evaluating the role of biological nanoparticles in autoimmune diseases and cancer. Current UNEMPS research focuses on thyroid immunity, specifically modelling the thyroid tissue microenvironment and evaluating the potential role of bacterial extracellular vesicles (EVs) in inducing thyroid autoimmunity. In this poster, two ongoing UNEMPS research projects will be presented. The first project is the development of a thyroid organoid-on-a-chip model incorporating thyroid follicular organoids with thyroid microvasculature to model healthy and diseased thyroid tissue. The second project is the evaluation of bacterial extracellular vesicle molecular mimicry in inducing immune responses against thyroid proteins. Additionally, data on the storage stability of gram-positive and gram-negative bacterial extracellular vesicles will be presented.	A Rama Varma, K Sadtler, P Fathi	2023	ACI/IRS
2023-067	Anagha		Rama Varma	NIBIB	ACI/IRS	Development of a Microfluidic Thyroid-on-a-Chip Model to Study Fluidic Effects on Cellular Behavior	Thyroid disorders, including autoimmune disorders and cancer, are complex conditions with far-reaching effects. Many studies have attempted to further elucidate the development and progression of these conditions through the use of animal and cell culture models. However, newer modeling techniques such as organ-on-a-chip devices provide the potential for higher accuracy in modeling organ physiology as well as personalized modeling. We are developing a vascularized organ-on-a-chip model of the thyroid for use in studying thyroid autoimmune diseases and cancer. We have induced the formation of thyroid microvasculature by culturing primary human thyroid microvascular endothelial cells (HTMECs) on basement membrane extract. Furthermore, through a similar procedure, we have established a protocol for the formation of thyroid follicle-like organoids from immortalized human thyroid epithelial cells (huThyrECs). We intend next to explore the results of co-culturing the HTMECs and huThyrECs, in hopes of obtaining organoids interconnected by tubular networks. Our goal is to develop a microchannel device into which we can seed the HTMECs and huThyrECs in order to obtain a vascularized structure replete with thyroid follicles which reflects the native structure of the human thyroid. We will then evaluate the effects of flow on the behavior of the cells and characterize the architecture and microenvironment present in the chip. Following development and optimization of the chip, the device may prove valuable as a tool to model the diseased state of the thyroid under autoimmune or cancerous conditions.	A Rama Varma, K Sadtler, P Fathi	2023	ACI/IRS
2023-068	Young-Kwon		Park	NIDDK	Cell Biology	ISWI Chromatin Remodeling Complex Is Essential for Adipogenesis and Myogenesis	Chromatin remodeling complexes are required for many distinct nuclear processes during replication and transcriptional regulation. The imitation SWI (ISWI) is an ATP-dependent chromatin remodeling complex and is represented by enzymatic subunits Snf2h (Smarca5) and Snf2l (Smarca1). Although studies have shown that Snf2h is essential for early mouse development and survival, it has remained unclear whether Snf2h plays a role in the development of adipose tissue and muscle. By crossing Snf2l-/-;Snf2hf/f mice with Myf5-Cre, which is selectively expressed in precursor cells giving rise to brown adipose tissue (BAT) and skeletal muscle, we demonstrate that Snf2h, but not Snf2l, is essential for adipose tissue and muscle development in mice. We find deletion of ISWI blocks adipogenesis and myogenesis as well as cell type-specific gene expression in isolated cells from BAT and muscle. Mechanistically, ISWI is required for lineage determining transcription factors (LDTFs) binding on enhancers and LDTF-induced activation of enhancers. Furthermore, we show that Snf2h co-localized with CTCF and the genomic binding of CTCF is globally decreased without change of the protein levels in ISWI KO cells. Our findings suggest an important role of ISWI complex in adipose tissue and muscle development. Collectively, this study shows that ISWI is critical for cell differentiation through correct genomic binding of LDFTs.	YK Park, JE Lee, K Ge	2023	CELLBIO
2023-069	Chris		Gunter	NHGRI	Social and Behavioral Sciences	NIH Science of Science Communication SIG	In July 2022, we created and held the first meeting for the NIH Science of Science Communication Interest Group (ScioSciComm-SIG) to respond to an NIH-wide interest in focusing specifically on the scientific design and evaluation of science communication. Our SIG holds seminars and journal clubs highlighting both measures of effectiveness and methods to increase general success or target efforts to respond to specific goals. As of July 2023, we have nearly 600 interested members and have held monthly meetings in response to the most-requested topics from our members. In order, these included communicating scientific uncertainty, strategies to combat misinformation in public health, science in the news (focused on retractions), the future of preprints and pre-publication peer review, and community-based public health communication. NIH researchers have used findings shared in these seminars directly in their public communication projects and institutional activities. More importantly, this SIG forms a nucleus of parties at NIH who want to establish best, evidence-based practices for science communication in almost all fields of biomedicine. In a few short months, this has already built networks and connections throughout the NIH campus and beyond. We serve as a resource for NIH staff to address the challenges of not just putting scientific information out to the public, but also understanding the underlying body of literature from psychology, sociology, and political science that provide a theoretical foundation for scientific communications. The NIH ScioSciComm-SIG is a nascent, valuable opportunity to address the challenges of theory meeting real-world experience in this area.	C Gunter, E Bizzell, N Sugden, M Zaringhalam, A Hilliard	2023	SOCIAL

2023-070	HeungSun		Kwon	NIDDK	Chromosome Biology	LDB1-mediated regulation of gene expression and chromatin structure in development	The Lim domain binding protein 1 (LDB1) is essential for cell identity determination and cell-specific gene expression regulation through promoter-enhancer looping. In erythropoiesis, the activation of the β-globin gene relies on the LDB1 complex, which enables interaction with the distant locus control region (LCR) enhancer. However, the precise mechanisms by which LDB1 contributes to gene regulation and chromatin structure modification during erythrocyte development stages are not well understood. Using CRISPR/Cas9 gene editing, we generated LDB1-deleted mouse embryonic stem cells (ESCs) to investigate LDB1's role in erythropoiesis. LDB1 deletion impaired embryoid body formation and hindered erythrocyte differentiation in ESCs. Knocking out LDB1 significantly reduced the levels of key transcription factors involved in stem cell regulation, including Sox2, Oct4, and KLF4, and revealed an interaction between LDB1 and KLF4. LDB1 deficiency also affected erythrocyte differentiation after ESCs transitioned to embryoid bodies, as indicated by decreased expression of Ter119 and CD71 markers. Additionally, ATAC-sequencing and CUT&TAG analysis showed reduced accessibility and H3K27ac modification at the Sox2 locus following LDB1 deletion. Transcriptomic analysis revealed upregulated expression of Lin28b, a gene typically suppressed during erythroid progenitor differentiation and loss of self-renewal capacity. Moreover, reduced transcription of let-7 microRNA, a Lin28 target, mirrored effects observed with Lin28b overexpression in hematopoietic stem cells. These findings highlight the critical role of LDB1 in maintaining both ESC stemness and promoting differentiation through its influence on gene expression and genome organization. LDB1 may also mediate developmentally timed changes in hematopoietic stem cell self-renewal capacity by regulating Lin28.	HS kwon, JH Kim, A Dean	2023	CHROM
2023-071	Mackenzie	R	Zendt	NIAID	ACI/IRS	Post-vaccination SARS-CoV-2 infections and immune response in people with immune disorders	While some immune-deficient persons (IDP) face higher risk for severe SARS-CoV-2 infection than the general population, little is known about their immune response to post-vaccination infections. A cohort of 217 IDP and 54 healthy volunteers (HV) were followed from April 2021 to April 2023. Blood was collected at baseline, 1-, and 6-months post vaccination. Anti-spike IgG response was assessed by ELISA. SARS-CoV-2 infection was actively monitored for 6 months post-vaccination; participants could self-report at any point. Thirty-six percent of IDP and 46% of healthy volunteers experienced a post-vaccination SARS-CoV-2 infection (p=0.21). Infections occurred from September 3, 2021 to March 25, 2023 and were primarily of the Omicron lineage. Clinical symptoms, severity, and time from last vaccination to infection (IDP: 140 days, HV: 161 days, p=0.28) did not significantly differ between groups. While ~50% of both groups received ≥3 doses, IDP received more doses pre-infection than HV. Of the 84 (39%) IDP and 19 (35%) HV who received a bivalent booster, 9 (11%) IDP and 2 (11%) HV later experienced an infection (p=1). Among the 50 IDP who received Evusheld, only 9 (18%) experienced an infection after its receipt. Infection increased anti-spike IgG relative to infection-naïve participants 6 months post-dose 3 (IDP and HV) and post-dose 4 only (IDP) (Figure). IDP experienced post-vaccination infections at a similar rate as HV, mostly during the Omicron period. Less than half of IDP have received a bivalent booster. Additional doses, especially the bivalent dose, enhances the immune response in this population.	MR Zendt, FB Carrillo, R Subramanian, V Callier, A Ortega-Villa, EE Ricotta	2023	ACI/IRS
2023-072	Ruchi		Komal	NIMH	Neuroscience	Molecular features of SCN neuron subtypes across time	All organisms have evolved intrinsic biological rhythms to anticipate cyclic changes in their environment. In mammals, daily rhythmic changes in metabolism, physiology, and behavior are driven by intrinsic oscillatory mechanisms generated by the central clock located in the suprachiasmatic nucleus (SCN). To understand how an external cue shifts the central clock, we compared intrinsic gene expression in SCN neurons across the day to the change in gene expression induced by light using single nucleus RNA-sequencing. We find that the same light stimulus delivered in the early versus late night leads to divergent changes in gene expression in the mouse SCN. Changes in gene expression were not limited to clock/circadian genes in SCN neurons. Unexpectedly, the expression of genes involved in synaptic assembly and transmission also changed in response to light at night, suggesting that SCN neuron connectivity is plastic and involved in shifting the circadian clock. By measuring SCN gene expression at high depth across different times of day, we provide new insights into SCN neuron complexity and its responsiveness to light. This study is also crucial to understanding the mechanisms underlying the disruptive effects of light, such as those observed in shift work, trans meridian travel and seasonal affective disorder.	R Komal, M Thomsen, S Hattar	2023	NEURO
2023-073	Nick		Williams	NLM	Social and Behavioral Sciences	Considering birth cohort when evaluating endemic HIV in the United States, age-period-cohort findings from CMS beneficiaries, 1999-2020	Introduction: There is high agreement that HIV+ cases are 'surviving' to later ages. Counterfactually, age at HIV diagnosis has increased since peak AIDS death in 1995-1996. Cases observed later in life may not be survivors infected young, but cases who were infected later in life. An 'at-scale' case by case assessment of HIV from at scale, real-world data is lacking for the United States. Methods: This study collected a 100% sample of Medicare and Medicaid claims from 1999 through 2020. Every claim with a declared HIV diagnosis (B20, 042, Z21) and said HIV status was attributed to the individual referenced. Date of birth and date of death was integrated with HIV status for a CMS wide HIV+ case index. Age-period-cohort disambiguation was performed for attributed mortality and case observation by study year. Results: CMS data found 283,688,152 cases, of which 1,543,041 were HIV+. 48,598,568 decedents were identified, with 363,425 being HIV+. There is birth cohort variation in eligibility for mortality. These mortality seasons have 'years old at observation' eligibility requirements that some birth cohorts have yet to reach because they are 'too young' in the final study year. Conclusions: Applying population survival outcomes to cases too young to die of a given illness is a prime example of APC confounding. Cases born after 1980 could experience mortality later in life similar to cases born in 1960, given additional study time.	ND Williams	2023	SOCIAL
2023-074	My-Asia		Chaplin	CC	Health Disparities	Increasing Blood Diversity: How Blood Center Websites Tackle Critical Blood Shortages for Sickle Cell Patients through Recruitment of African-American Donors	Sickle cell disease (SCD) is a life-threatening condition that affects 1/500 African-Americans. Patients with SCD rely on transfusions from closely-matched healthy blood donors of similar ethnicity; however, African Americans are under-represented among blood donors due to multiple complex factors including mistrust of medical systems. Blood center websites are a "virtual interface" with the community that may convey the need for African-American persons to donate blood for SCD patients. We selected 12 blood systems or centers in 3 categories (large blood systems, regional systems, and hospital-based blood centers). A popular search engine was mined using the name of each blood center and the keywords "sickle cell disease" and "African-American" to identify websites. An inductive approach was used to analyze commonalities, differences, patterns, and themes in the study findings. Only 5/12 websites explained the role of red blood cell antigens in providing matched blood for SCD patients. 83% of evaluated websites included testimonials from patients, 42% included interviews from medical professionals, and 58% included a specific "call to action", inviting African-Americans to donate blood for patients with SCD. Hospital-based blood centers were least likely (43.8%). Most blood center websites specified the need for matched blood donors for SCD patients and utilized images of African-Americans. Few websites explained the role of RBC antigens in identifying matched donors. Several websites lacked a specific call to action for African-Americans to donate blood. Few blood centers addressed the difference between sickle cell disease and trait, and very few informed sickle cell trait patients of their eligibility.	MAC Chaplin, K West-Mitchell, S Hughes	2023	HEALTH
2023-075	Bingning		Xie	NIDDK	Chromosome Biology	Non-coding function of super enhancer derived mRNA in modulating neighboring gene expression and TAD interaction	Super enhancers are important regulators of gene expression that often overlap with protein-coding genes. However, it is unclear whether the overlapping protein-coding genes and the mRNA derived from them contribute to enhancer activity. Using an erythroid-specific super enhancer that overlaps the CPOX gene as a model, we found that CPOX mRNA has a non-coding function in regulating neighboring protein-coding genes, eRNA expression and TAD interactions. Depletion of CPOX mRNA leads to accumulation of H3K27me3 and release of p300 from the CPOX locus, activating intra-TAD enhancer and gene expression. Additionally, we identified a transcription start site-transcription termination site (TSS-TTS) interaction between the TAD boundary genes CPOX and DCBLD2 that is facilitated by a novel type of repressive loop anchored by p300 and PRC2/H3K27me3. Our results uncover a regulatory role for mRNA transcribed within a super enhancer context and provide insights into head-to-tail inter-gene interaction in the regulation of gene expression.	B Xie, A Dean	2023	CHROM
2023-076	Ian		Adoremos	NIMH	Neuroscience	Investigating Cellular Composition of the Subgenual Anterior Cingulate Cortex in Bipolar Disorder, Schzophrenia and Major Depressive Disorder (ASHG)	Using various RNA sequencing data sources, this study investigates the cellular composition of the subgenual anterior cingulate cortex (sgACC) in schizophrenia (SCZ), bipolar disorder (BD), and major depressive disorder (MDD) to identify specific cell types potentially implicated these psychiatric conditions. We employed cellular deconvolution, a computational method to estimate cell type-specific proportions from transcriptomic data. Postmortem sgACC samples from 185 donors (55 controls, 44 SCZ, 35 BD, 51 MDD) underwent RNA sequencing. Single-cell RNA sequencing data from five sgACC and dorsolateral prefrontal cortex control samples were used as a reference dataset for deconvolution. Bisque deconvolution software was implemented, due to its ability to manage heterogeneous and noisy biological data. After cell type fractions were acquired, ANOVA was implemented to identify, for each cell type, whether diagnosis impacts proportion estimates, subsequent pairwise t-tests to identify key differences in cell type proportions across each diagnostic group, and Tukey's tests to adjust p values for multiple comparisons. Oligodendrocyte precursor cells showed the most significant impact, with ANOVA results ($p < 0.001$, $F = 6.43$), a significant t-test for SCZ ($t = 3.00$, $p = 0.003$), and Tukey's test (p-adjusted= 0.03). Inhibitory neurons also showed significant ANOVA results ($p = 0.009$, $F = 3.99$), suggesting reduced neurons in SCZ individuals. Astrocytes showed a marginally significant ANOVA result ($p = 0.05$, $F = 2.65$), with SCZ individuals having higher proportions. Tukey's tests showed no deviation for inhibitory neurons (p-adjusted= 0.14) and astrocytes (p-adjusted = 0.24) in SCZ individuals from controls.	I.P Adoremos, N. Akula, A. Schulmann, F.J McMahon, S. Marenco, P. Auluck	2023	NEURO
2023-077	Nicole		Nguyen	NIDDK	Developmental Biology	Regulation of Ldb1-dependent erythroid genes by Sp1 and Sp3	Gene expression during erythropoiesis is closely regulated by transcription factors (TFs), often through protein complexes that bind to DNA. One example is the LIM domain binding 1 (Ldb1) complex that includes DNA binding proteins Gata1 and Tal1, bridge protein Lmo2, and chromatin looping factor Ldb1. The Ldb1 complex binds to erythroid enhancers and a subset of erythroid gene promoters, mediating enhancer-promoter proximity to activate transcription via Ldb1 homodimerization. However, many erythroid Ldb1-dependent gene promoters are not occupied by Ldb1, suggesting that other TFs may orchestrate their interaction with Ldb1 enhancers. Specificity proteins 1 and 3 (Sp1/3) are ubiquitous TFs that regulate erythroid gene promoters and interact with other proteins involved in erythroid differentiation, including Gata1. We deleted Sp1/3 using CRISPR-Cas9 genome editing in MEL cells. RNA-seq demonstrated that Sp1/3 KO dysregulated genes (DEGs) were more abundant in uninduced than induced MEL cells. ChIP-seq revealed candidate genes whose promoters exhibited Sp1/3 occupancy and were Sp1/3 KO DEGs. We integrated these results with Ldb1 enhancer-dependent genes, confirming cooperation between Ldb1 and Sp1/3 in long-distance gene regulation. We determined that full-length Ldb1 interacts with Sp1/3 in MEL cells, which contain Gata1, and HEK293 cells, which do not, suggesting that Ldb1 and Sp1/3 interact directly. We also determined that aa200-285 of Ldb1, including OID and LCCD domains, interact with Sp1/3. We will assess the mechanism of Sp1/3 in regulating Ldb1 enhancer-dependent genes by analyzing which Sp1/3 domains interact with Ldb1. This investigation provides deeper insight into transcriptomic changes during erythroid differentiation dependent on Ldb1.	N Nguyen, J Kim, A Dean	2023	DEVBIO
2023-078	Cristina		Antich Acedo	NCATS	Biomedical Engineering and Biophysics	A high throughput 3D bioprinted human placenta as a novel predictive platform to study drug safety and pathological conditions during pregnancy	During pregnancy, fetal exposure to xenobiotics, such as medications or infective agents, can lead to adverse gestational complications and long-term health consequences. Unfortunately, due to the limited ability to monitor the human maternofetal interface and the lack of physiologically relevant in vitro models, the underlying mechanisms behind gestational pathology and the downstream effects in placenta and fetus remains poorly understood. Therefore, we developed a novel biomimetic in vitro 3D human placenta (hPB) model at different stages of pregnancy in a high throughput format using 3D bioprinting technology, to study placenta physiology, pathology, and pharmacology. Primary trophoblasts and vasculature-derived cells were resuspended in ECM-like solutions and bioprinted on a 96-well transwell plate, recreating the placental villi. Bioprinted constructs were then exposed to Forskolin treatment at different oxygen pressure conditions for 6 days to enable tissue differentiation and recreation of progressive stages of development. The anatomical resemblance to human placenta was confirmed by immunostaining assays. High levels of syncytialization markers and CK7 indicated the formation of a bilayer trophoblastic barrier, whereas the expression of CD31 and Vimentin indicated the development of subjacent vascularized stroma. The functionality of hPB was validated by transepithelial electrical resistance and paracellular transport measurements, including nutrients and non-permeable metabolites. Other function like hormone production was also demonstrated by ELISA assays. This new platform will provide a powerful tool for understanding the relationships between prenatal exposure to xenobiotics and developmental outcomes, and will ultimately serve as the foundation for establishing global public health guidelines to prevent pregnancy complications.	C. Antich, MJ. Song, M. Ferrer	2023	BIOENG
2023-079	Michael		Reidy	NIDDK	Molecular Biology and Biochemistry	The role of ATP in Hsp90 function	Hsp90 is an abundant, highly conserved molecular chaperone that is essential for eukaryotic life. It is a target for cancer therapy and is implicated the in progression of several neurodegenerative diseases. We recently showed that ATP hydrolysis is dispensable for Hsp90 function in vivo. These and other findings disagree with the current model of Hsp90 as an active machine that uses the energy from ATP hydrolysis to remodel client proteins. Here, we present findings that expand upon our recent work, and we propose a novel theory on the role of ATP in Hsp90 function.	M Reidy, C Katz, K Garzillo, D Masison	2023	MOLBIO

2023-080	Yong-Mo		Ahn	NCATS	Microbiology and Infectious Diseases	Identification of Broad-Spectrum Inhibitors against Flaviviral NS2B-NS3 Proteases	Flaviviruses, such as Dengue, West Nile, Yellow Fever, and Zika viruses, are mosquito-borne arboviruses with the potential to cause virus-induced diseases, including encephalitis and hemorrhagic fever, throughout the world. Despite the emergent spread of this public health threat, there are currently no drugs available for their treatment. Flaviviruses share epidemiological, structural, and ecologic features, and often different viruses can co-infect the same host. The identification of broad-spectrum inhibitors against flaviviruses is highly desirable, and therefore, targeting flaviviral NS2B-NS3 proteases, which are essential for viral replication, has become an attractive goal for antiviral drug development. In this study, we designed and performed ultra-high-throughput screening (uHTS) to identify broad-spectrum inhibitory agents against four recombinant NS2B-NS3 viral proteases from multiple flaviviruses, including Dengue, West Nile, Yellow Fever, and Zika. To search for effective inhibitors, a total of 12,000 compounds from structurally diverse molecular libraries, as well as libraries of approved drugs and pharmacologically active compounds, were screened using fluorescence-based enzymatic assays in the automated 1536-well plate format. From the uHTS data, we identified 81 hits as broad-spectrum inhibitors, and an AI-driven QSAR model was employed to efficiently optimize these hits for lead development. The candidate inhibitors were further validated in viral infection assays.	Y Ahn, A Medina, S Pal, AV Zakharov, EM Lee, NJ Martinez	2023	MICROBIO
2023-081	Marco	T	Egle	NINDS	Neuroscience	Association between retinal microvascular changes and late brain amyloid-β deposition: The ARIC-PET study	BACKGROUND: Abnormalities in the retinal microvasculature may be an easily obtainable and low-cost risk indicator associated with AD (Alzheimer's disease) pathogenesis. OBJECTIVE: This study aimed to test the association of retinal microvascular abnormalities in mid and late life and late life cerebral amyloid burden. METHODS: Participants from the ARIC-PET (Atherosclerosis Risk in Communities-Positron Emission Tomography) study with a valid retinal measure (N= 285) were included. The associations between mid- and late-life retinal signs with greater late-life amyloid-β (Aβ) by florbetapir PET were tested using logistic regression models. It was also assessed whether a newly created retinal score, incorporating multiple markers of abnormal retinovascular, was associated with greater Aβ burden. RESULTS: Retinopathy in midlife (OR (95% CI) = 0.36 (0.08, 1.40)) or late life (OR (95% CI) = 2.87 (0.84, 11.5)) was not significantly associated with greater late-life Aβ burden in nondemented adults. A high retinal score in late life, indicating a higher burden of retinal abnormalities, was however significantly associated with greater Aβ burden adjusting for demographic and genetic confounders (OR (95% CI)= 3.58 (1.09, 14.2)). CONCLUSION: The newly created retinal score may serve as a risk indicator for greater Aβ burden in the general population. Well-powered future studies with a greater number of retinal features and other microvascular signs are needed to test these findings.	MT Egle, JA Deal, KA Walker, DF Wong, AR Sharrett, RF Gottesman	2023	NEURO
2023-082	Shaza		Khan	NHLBI	Systems Biology	Replacing the Brattleboro Rat: Generation of an Inducible Avp Knockout Mouse Line Using CRISPR/Cas9 and Cre/LoxP	Arginine vasopressin (AVP) is a nonapeptide hormone coded by the AVP gene, synthesized in the hypothalamus and secreted by the posterior pituitary. Previous studies of roles of AVP have been largely dependent on the use of Brattleboro rats, which manifest a spontaneous mutation in the Avp gene and lack circulating AVP. Despite their utility, Brattleboro rats were difficult to breed, and commercial breeders have ceased production. Therefore, the main goal of this project is to create an experimental Avp knockout mouse model that could be used in renal and neuroendocrine research. A mixture of CRISPR elements, including sgRNAs, Cas9 mRNA, ssODN, and loxP sites was injected into C57BL/6 embryos. Successful insertion of the loxP sites was confirmed by PCR using primers flanking the targeted regions. For additional confirmation, sequencing analysis was performed. Mice harboring the floxed allele were mated to mice that globally express a tamoxifen-inducible Cre recombinase. The resultant inducible Avp knockout mice (flox/flox;Cre/wt) show no signs of polydipsia or polyuria prior to induction, indicating that the floxed gene maintains its wild-type function. The administration of an exogenous inducer like tamoxifen to (8-10) week-old mice, induced Cre mediated recombination that resulted in a decrease in urine osmolality. Sanger sequencing demonstrated the expected 1245 bp deletion at the Avp locus. Immunoblotting of AQP2 in the inner medulla showed a significant decrease in AQP2 abundance. This inducible Avp knockout mouse model provides researchers with a valuable tool to investigate the consequences of Avp gene deletion in a controlled and inducible manner.	SF Khan, L Chen, CL Chou, SJ Khundmiri, MA Knepper	2023	SYSBIO
2023-083	Yen-Ting		Tung	NCATS	Biomedical Engineering and Biophysics	Developing a perfusable 3D brain model in a multi-well chip system based on the in-vitro differentiation of the iPSC- derived radial glia cells.	Among the various 3D tissue/organ model developed in the past decade, the 3D brain model is one of the most challenging tissue models to engineer because of the physiological complexity and long maturation time for neural cells to be functional and the unique blood-characteristics of the blood-brain-barrier (BBB). Neural organoids are stem cell derived complex tissues models used to study brain development, but most lack of vascular system and immune cells. Based on our previous work developing a bioprinted 3D neurovasculature tissue model, we identified the Notch and Wnt signaling pathways as active during neurovascular formation. We hypothesized that activation of these pathways involved in neurogenesis would create an in-situ environment permissive of neuronal differentiation within a perfusable vascular network. We use iPSC-derived radial glia cells, which can differentiate into neuronal cells, astrocytes, and oligodendrocytes, and mixed them with primary human microvascular endothelial cell, primary human astrocyte, and primary human pericytes, in a fibrinogen-based hydrogel of a microfluidics channel of a 64-chips Mimetas Organograft plate. A perfusable microvascular network formed after 5 days of culture, and TUJ1 positive neuronal cells differentiated from iPSC radial glia cells were observed after two weeks. Weak signal for mature neuronal maturation cell marker, MAP2, and oligodendrocyte cell marker, Oligo2, was detected at day 21, indicating maturation of a neural tissue model. Functional assays on vascular permeability and neural activity are being conducted to demonstrate high physiological relevance of this tissue model and the potential application in biomedical/pharmacological studies.	YT Tung, O Jung, V Jovanovic, C Tristan, MJ Song, M Ferrer	2023	BIOENG
2023-084	Kalinga Pavan	T	Silva	NCI	Microbiology and Infectious Diseases	Efflux pump gene amplifications bypass necessity of multiple target mutations for resistance against dual-targeting antibiotic	Antibiotics that have multiple cellular targets theoretically reduce the frequency of resistance evolution, but adaptive trajectories and resistance mechanisms against such antibiotics are understudied. Here we investigate these in methicillin resistant Staphylococcus aureus (MRSA) using experimental evolution upon exposure to delafloxacin (DLX), a novel fluoroquinolone that targets both DNA gyrase and topoisomerase IV. We show that selection for coding sequence mutations and genomic amplifications of the gene encoding a poorly characterized efflux pump, SdrM, leads to high DLX resistance, circumventing the requirement for mutations in both target enzymes. In the evolved populations, sdrM overexpression due to genomic amplifications containing sdrM and two adjacent genes encoding efflux pumps results in high DLX resistance, while the adjacent hitchhiking efflux pumps contribute to streptomycin cross-resistance. Further, lack of sdrM necessitates mutations in both target enzymes to evolve DLX resistance, and sdrM thus increases the frequency of resistance evolution. Finally, sdrM mutations and amplifications are similarly selected in two diverse clinical isolates, indicating the generality of this DLX resistance mechanism. Our study highlights that instead of reduced rates of resistance, evolution of resistance to multitargeting antibiotics can involve alternate high-frequency evolutionary paths, that may cause unexpected alterations of the fitness landscape, including antibiotic cross-resistance.	KPT Silva, G Sundar, A Khare	2023	MICROBIO
2023-085	Monika		Rajput	NCATS	Virology	3D Perfusable vascularized model to study flavivirus recombinant NS1 induced endothelial dysfunction	Flaviviruses are a family of positive, single stranded RNA viruses, infect approximately 400 million people worldwide each year. Certain Flaviviruses, such as Japanese encephalitis virus, West Nile virus, and dengue virus can lead to severe disease involving but not limited to endothelial dysfunction and vascular damage. While it is known that dengue virus non-structural protein 1 (NS1) is secreted and circulated in blood stream during infection and its amount is linked to disease severity, the role of other related flavivirus NS1s are less well-defined. In addition, there is no current 3D model which fully recapitulate flavivirus NS1 pathogenesis to understand the pathophysiology for personalized medicine. In this study, we aimed to model diverse flavivirus induced pathogenesis using a hydrogel based vascularized model to develop potential therapeutics. We first developed a reproducible, perfusable vascular-on-chip model by combining different cell types in a fibrinogen hydrogel. We then tested effect of recombinant NS1 protein from JEV, WNV, or DENV in a dose and time dependent manner on the vascular-on-chip system and documented vascular damage by different assay read outs. Our findings reveal that flavivirus NS1 alters the permeability and morphometric parameters of vascular network in a time and dose-dependent manner, and this leads to differential disruption of endothelial glycocalyx layer components such as sialic acid and heparan sulfate and upregulation of vascular damage related genes. The results suggests that the vascular-on-chip model may recapitulate tissue- and flavivirus specific pathogenesis of vascular dysfunction. In addition, this model may provide potential targets for antiviral therapies.	M Rajput, A.M Farias, S Cotsmire, Y.T Tung, M.J Song, M Ferrer, E Lee	2023	VIROL
2023-086	Xue Zhi		Zhao	NCI	Chemical Biology	Application of Oxime Diversification to Develop Multidentate Tyrosyl-DNA Phosphodiesterase 1 (TDP1) Inhibitors by Optimizing Interactions with the Catalytic Pocket and the DNA and Protein Substrate Binding Sites	Tyrosyl-DNA phosphodiesterase 1 (TDP1) is a phospholipase D (PLD) family member that can downregulate the anticancer effects of inhibitors of the type I topoisomerase (TOP1) by hydrolyzing the 3'-phosphodiester bond between DNA and the TOP1 catalytic residue Y723. This ester bond results in a stalled covalent intermediate, which is central to the mechanism of action of TOP1 inhibitors. Thus, TDP1 antagonists are being pursued by several laboratories as potency-enhancers of TOP1 inhibitors. However, the open and extended nature of the substrate-binding regions of TDP1 have made the development of inhibitors extremely challenging. In our current work, we have applied an oxime-based click protocol to the imidazopyridine platforms of our recently identified small molecule microarray (SMM)-derived TDP1 in order to extend them into the DNA and TOP1 peptide substrate-binding channels. By reacting the aminooxy-containing precursors with approximately 250 aldehydes in microtiter format, we screened a library of 500 oximes for their in vitro TDP1 inhibitory potencies in a florescence-based catalytic assay. Select hits identified by this process were further converted to their triazole- and ether-based isosteres. We obtained crystal structures of two of the resulting inhibitors bound to the TDP1 catalytic domain. In this way, we identified TDP1 inhibitors that bind in a tridentate fashion, with a central component situated within the catalytic pocket and extensions that project into both the DNA and TOP1 peptide substrate-binding regions. The trivalent nature of these interactions could serve as a basis for further development of multivalent inhibitors.	XZ Zhao, W Wang, GT Lountos, E Kiselev, JE Tropea, D Needle, Y Pommier, TR Burke, Jr.	2023	CHEMBIO
2023-087	Abeni		Kazi	NCI	Genetics and Genomics	Relevance of Histone H3-H4 Balance in Promoting/Preventing Mislocalization of Cse4 to Ectopic Sites	Mislocalization of Cse4 (CENP-A in mammals) leads to increased chromosome loss in budding yeast, human cells and xenograft mouse models. Overexpression and mislocalization of CENP-A to non-centromeric regions is observed in many cancers. This project analyzes the role of Cse4 and histone H4 interaction in the mislocalization of Cse4 to non-centromeric regions.	AZ Kazi, K Ohkuni, M Basrai	2023	GEN
2023-088	Zhaoyi		Peng	NICHD	Cell Biology	Protein arginine methyltransferase 1 regulates adult intestinal epithelial cell proliferation and differentiation.	The adult intestinal epithelium is a complex, self-renewing tissue composed of specialized cell types with diverse functions. Intestinal stem cells (ISCs) at the base of crypts divide and differentiate into absorptive and secretory cells. Enteroendocrine cells (EEC), one type of secretory cells, are the most abundant hormone-producing cells in mammals and involved in the control of energy homeostasis. Many studies investigated the mechanisms that control cell fate determination; however, regulation of EEC development and function is still unclear. Here, we found that Protein arginine methyltransferase 1(PRMT1) is highly expressed in the proliferating transit-amplifying (TA) cells and ISCs of adult mouse intestinal crypts. By using tamoxifen-induced intestinal epithelial cell-specific deletion of PRMT1 in adult mice, we observed the number of EEC dramatically increased. Transcription analyses showed all top enriched upregulated pathways of PRMT1-deficient small intestine were associated with EEC functions and gene expression of Enteroendocrine-specific hormone and transcription factors were upregulated. Concomitantly, Neurogenin 3-expressing progenitor cells accumulated in the mutant small intestine. Furthermore, mutant mice showed elongated crypts in the small intestine, while increased cell proliferation in TA cells. Additionally, inducible PRMT1 deletion led to increased cell death, which compensated for increased cell proliferation in the crypts to maintain overall intestinal morphology and intestinal homeostasis. Together, our results revealed that the loss of PRMT1 in the adult intestinal epithelium altered TA cell proliferation and EEC differentiation, which probably via enhancement of Neurogenin 3-mediated commitment to the EEC lineage.	ZY Peng, LY BAO, BY SHI, YB SHI	2023	CELLBIO
2023-089	Sarah	C	Ogden	NCATS	Virology	Development of High Throughput Screening and High Content Platforms for La Crosse Encephalitis Virus	The recent global pandemic has highlighted the pressing need for antiviral drug discovery tools in the effort to prevent future burdens on healthcare infrastructure and human health. Multiple RNA virus families have been identified as those presenting pandemic potential, including members of the order Bunyavirales. This negative-sense RNA virus order contains major human pathogens such Rift Valley Fever Virus, California-group Encephalitis viruses, and rodent borne Hantaviruses. Of these viruses, La Crosse Encephalitis virus (LACV) is known to cause pediatric encephalitis with typically only palliative care options available as therapeutic treatment, emphasizing the need for relevant model systems and antiviral therapeutics. Previous efforts have established a high-throughput screening (HTS) platform for anti-viral compounds using a cytoprotective assay. Here, we share work expanding this model and additionally developing a 1536-well, high content screening (HCS) platform based on direct detection of LACV glycoprotein in infected cell cultures for anti-viral screening. We observed a differential effect of several known anti-LACV compounds in indirect (e.g. cytoprotective assays) vs direct (e.g. IFA-based assay). We further examined the relationship between cytoprotective and direct viral antigen-based assay readouts by comparing the efficacy of established anti-virals and then directly compared the two assays by screening a library of 752 anti-infective compounds with both the HTS and HCS platforms, and report that a combination of these two assays provide orthogonal coverage to best determine lead anti-viral compounds.	SC Ogden, A Medina, N Ibrahim, EM Lee	2023	VIROL
2023-090	Binta		Jalloh	NCI	Cell Biology	Dynamics of Transcription Factors in live Saccharomyces cerevisiae investigated by Single Molecule Tracking Microscopy	Single Molecule Tracking (SMT) allows for the biophysical characterization of protein dynamics in in vivo by providing direct information on the behavior of individual molecules. Saccharomyces cerevisiae or budding yeast, a unicellular eukaryote with a small and completely sequenced genome and the awesome powers of yeast genetics, is an attractive model organism for SMT. We used a custom-built Highly Inclined Laminated Optical (HILO) sheet illumination for SMT analysis of yeast transcription factors Ace1p and HSF1, RNA polymerase II, and histone H3 in live cells. For quantification, we applied to single molecule tracks pEM analysis which is an algorithm that determines the distinct mobility states of the molecules. We compared parameters of biophysical dynamics for each protein. Preliminary data reveal distinct mobility states for yeast Histone H3 protein compared to RNA Pol II, Transcription Factor Ace1p, and Heat Shock Factor 1 proteins in the presence and absence of heat shock conditions. The results presented here provides a foundation for characterizing dynamics of other factors involved in transcription initiation and elongation.	B Jalloh, DA Ball, TS Karpova	2023	CELLBIO

2023-091	Sashary		Ramos	NHLBI	Biomedical Engineering and Biophysics	Subcellular water mapping by Raman spectral imaging	Water is essential in maintaining cellular activity, from mediating reactions to promoting the shuttling of macromolecules. Bulk water, made up of free-moving water molecules that can make hydrogen bonds with each other, has been very well studied, and the properties associated with the bulk are well-defined. However, intracellular water is within a very crowded and confined environment and, thus, cannot be adequately described as bulk water. Intracellular water is expected to exhibit more order or structure due to a spatially constrained milieu. Herein, we apply Raman spectral imaging to characterize water throughout a cell, generating subcellular hydration maps based on the bend-libration band of water. Because this is a label-free approach relying on intrinsic molecular vibrational signatures, we also obtained spatial-chemical information on other biomacromolecules (e.g., nucleotides, lipids, and proteins) at each location. Our results show that distinctive water structures are found in subcellular compartments, such as nucleoli and lipid droplets, based on their unique vibrational signatures. This work provides direct and conclusive spectroscopic evidence that intracellular water is chemically distinct from bulk water, emphasizing the importance of the cellular hydration environment in modulating behaviors of molecular biological systems.	S Ramos, J A Shadish, J C Lee	2023	BIOENG
2023-092	Miao		Xu	NCATS	Microbiology and Infectious Diseases	A high throughput screening assay for inhibitors of SARS-CoV-2 pseudotypedparticle entry	High throughput screening assays are needed for lead discovery and optimization of small molecule SARS-CoV-2 inhibitors. In this work, we have applied viral pseudotypingto establish a cell-based SARS-CoV-2 entry assay that can be used in biosafety level 2 (BSL-2) laboratories. The pseudotypedparticles (PPs) contain SARS-CoV-2 spike in a membrane enveloping both the murine leukemia virus (MLV) gag-pol polyprotein and luciferase reporter RNA. Upon addition of PPs to HEK293-ACE2 cells, the SARS-CoV-2 spike protein binds to the ACE2 receptor on the cell surface, resulting in priming by host proteases to trigger endocytosis of these particles and membrane fusion between the particle envelope and the cell membrane. The internalized luciferase reporter gene is then expressed in cells, resulting in a luminescent readout as a surrogate for spike-mediated entry into cells. From a screening of 5,158 approved drugs and clinically trialed drug candidates, 7 active compounds were identified that inhibited the SARS-CoV-2-S PP entry. Of these compounds, six compounds were active against live SARS-CoV-2 virus in a cytopathic effect assay. Our results demonstrated the utility of this assay in the discovery and development of SARS-CoV-2 entry inhibitors as well as the mechanistic study of anti-SARS-CoV-2 compounds. Additionally, particles pseudotypedwith spike proteins from SARS-CoV-2 B.1.1.7 and B.1.351 variants were prepared and used to evaluate the therapeutic effects of viral entry inhibitors.	M Xu, M Shen, C Klumpp-Thomas, S Michael, M Itkin, Z Itkin, W Zheng, CZ Chen	2023	MICROBIO
2023-093	Nicola		Sugden	NHGRI	Social and Behavioral Sciences	"Whether we look to young children, to savages, or in a lesser degree to idiots...": evolutionary hierarchies of childhood, race, and (dis)ability in early anglophone psychology	Psychological thought in late nineteenth and early twentieth century Britain and America was greatly influenced by evolutionary thought, and depended upon racialized hierarchies of age, "primitivity", and animality. Such hierarchies did not simply embody generalized racist and ableist prejudices of the time or exist as subjective inconsistencies interfering with objective scientific inquiries. Rather, they – and the categories and categorization they depended upon – were central to the development of psychological science. Children were central to psychology and its narrative project of modernity (with its evolutionary underpinnings), in their unique casting as beings who in the course of their development elided an epistemic gap, both by recapitulating the evolution of the human mind, and through their malleability in response to education and training. Such discussions around children and their character also hinted at barely-disguised fear that progress and civilization were merely veneers, and that primal sexuality, criminality, animality and atavism truly existed outside of the fiction, memoir and popular writing of the period. The conceptual and practical interdependency of evolutionary hierarchies were laid bare in psychological discussions of communication, which placed written English and its systems of grammar and syntax at the peak of a ladder extending down past spoken English, less "perfect" spoken languages, written symbols, mere sounds, and signed language. Critical exploration of such texts establishes the fundamental significance of the developing child as the lynchpin of this framework.	N Sugden, C R Donohue	2023	SOCIAL
2023-094	Srikanya		Kundu	NCATS	Neuroscience	Fluorescent biosensor-based functional validation of biofabricated 3D human iPSC-derived neuronal models for drug screening	More than 90% of the drugs entered clinical trials fail because of lack of efficacy or unexpected toxicity. This high failure rate partly attributed to the use of in vitro cellular assays and animal models that do not reproduce human physiology and pathology during preclinical drug development. We develop 3D organotypic cellular models that capture native-like physiological features of tissues and serve as assay platforms for diseases and predictive therapeutics development and to study neurological and neurodegenerative diseases. We used fibrinogen gel with gelatin and laminin, a 3D extracellular matrix that enables the co-culture of human iPSC derived neurons and astrocytes to autonomously form neuronal networks and spontaneous synaptic connections with a native-like neuronal density thus mimicking the dynamics of human functional brain circuitry. For the functional assays, we performed double AAV-transfections of ChrimsonR-opsin with combination of different biosensors, GCaMP6f, dLight1.2 and iGluSnFr, for real time calcium flux measurement, released neurotransmitter like dopamine, glutamate assessment, respectively. The measurements of different biosensors from the functional 3D model, were modulated by optogenetics stimulation, and perturbed by pharmacological agents in a manner to be expected from in vivo data. This model can be produced in a 384/96-well platform for therapeutic screening. The fibrinogen-gel used here is compatible with extrusion-based bioprinting, should enable the biofabrication of spatially defined functional neuronal circuits. Furthermore, the approach allows for gradual inclusion of additional physiological complexity, including vasculature, additional cells like microglia in flexible 3D bioprinted patterns to mimicking various human brain region selective circuitry.	S Kundu, MJ Song, M Ferrer	2023	NEURO
2023-095	Jie		Dong	NIA	Neuroscience	Striatal Compartmental Control of Movement through Dopamine Inhibition	The direct pathway spiny projection neurons (dSPNs), primarily located in the matrix compartment of the dorsal striatum, have been extensively studied for their role in promoting locomotion. However, the contribution of the minority dSPNs in the complementary patch (or striosome) compartment to locomotion remains unclear. In this study, we employed a newly developed knock-in patch mouse strain to investigate the function of patch dSPNs using optogenetic stimulation. Surprisingly, we found that activation of patch dSPNs led to locomotion suppression, in contrast to the effects of matrix dSPNs. Previous research has indicated that patch dSPNs preferentially project to ventral nigral dopaminergic neurons (DANs) and exert robust and prolonged GABAergic inhibition through GABAb receptors. To gain insight into the underlying mechanism of patch-mediated locomotion inhibition, we employed CRISPR/SaCas9-mediated gene targeting to genetically knock down GABAb receptors specifically in DANs. Strikingly, this manipulation completely abolished the locomotion inhibition caused by the activation of patch dSPNs. These intriguing findings unveil a surprising two-level compartmental control mechanism of locomotion. We demonstrate that patch dSPNs exert regulatory control over matrix dSPNs and locomotion by inhibiting the activity of nigral DANs. Our results provide compelling evidence for the intricate interplay between patch and matrix compartments in governing locomotor behavior through the modulation of dopaminergic signaling.	J Dong, B Sullivan, LP Wang, L Chang, LX Sun, JH Ding, C Gerfen, HB Cai	2023	NEURO
2023-096	Jonathan	R	Shin	NIAID	Virology	Tracking replicating HPV genomes in proliferating keratinocytes	Human papillomavirus genomes replicate and partition as minichromosomes alongside host chromatin during persistent infection. We have previously shown that plasmids containing the HPV18 replication origin and viral transcriptional enhancer element can replicate stably in keratinocytes in the presence of the HPV18 genome. These small replicons express the neomycin resistance gene in both bacteria and eukaryotic cells and have minimal prokaryotic elements that could induce innate immunity. Additionally, the replicons are reliant on the presence of the viral genome for their own persistence. Here, we use the replicons as vectors to express different fluorescent proteins that are detectable solely in the company of the viral genome. To generate an optimal expression cassette, we have identified enhancers, promoters and polyadenylation sites that function well in keratinocytes, and have selected fluorescent proteins that are detectable in proliferating living cells. This molecular tool allows us to indirectly monitor the presence of the virus in live cells and can inform on models of papillomavirus extrachromosomal genome maintenance, tethering, and amplification.	JR Shin, AA McBride	2023	VIROL
2023-098	Nancy		Wu	NHLBI	Biomedical Engineering and Biophysics	Developing an in vitro Next Generation Sequencing Based Approach to Map Single-Stranded DNA cleavage by Topoisomerases	Topoisomerases are enzymes critical to cell survival that regulate the topology of DNA. To control DNA topology, they induce transient breaks in the double helix. If these breaks become permanent, they are highly toxic to cells, making topoisomerases a well-established target for anticancer and antimicrobial drugs. There are two functional classes of topoisomerases, Type I and Type II, which are mechanistically differentiated by whether they generate single-stranded breaks (SSBs) or double-stranded breaks (DSBs), respectively. Whereas the magnitude of topoisomerase cleavage has been well-studied, technical limitations have made it difficult to determine the location of cleavage sites with nucleotide resolution. Recently, our lab developed an in vitro technique, Simplified High Accuracy eNd sequencing (SHAN-seq) to elucidate sequence-specific double-stranded cleavage by type II topoisomerases. However, type I topoisomerases and type II topoisomerases (when treated with certain drugs) nick DNA, creating single-stranded breaks, that are not currently captured by SHAN-seq. Hence, we have extended SHAN-seq to capture the location of single-stranded breaks. We validated this method using nicking enzymes with well-defined sites on a plasmid. This work enables the full mapping of the cleavage sequence preferences for both type I and II topoisomerases and how the cleavage location and extent vary with DNA topology and topoisomerase inhibitors, which have important implications for DNA repair and determining the effects of anticancer and antimicrobial drugs.	N Wu, IL Morgan, KC Neuman	2023	BIOENG
2023-099	Kruthika		Doreswamy	CC	Clinical Research	Spinal Bulbar Muscular Atrophy (SBMA): A cross-sectional analysis of wearable sensors during the 6-minute walk test (6MWT) and timed up and go (TUG)	Spinal bulbar muscular atrophy (SBMA) is a rare, X-linked inherited neuromuscular disease that affects males, resulting in muscle weakness. The 6-minute walk test (6MWT) and timed up and go (TUG) are used to assess motor capacity in people with SBMA. Wearable sensors could be used in future therapeutic SBMA trials to objectively analyze gait and balance. This study aims to describe the wearable sensors' ability to measure motor capacity from the baseline instrumented-6MWT (i-6MWT) and -TUG (i-TUG) in individuals with SBMA. This study had 18 male participants with a mean age of 61.8 ± 6.68 years — 4 healthy controls (H), 5 with SBMA who did not use assistive devices (S), and 8 with SBMA who used assistive devices (SD). All 18 individuals participated in the i-6MWT. For the i-6MWT, the distance (m) walked ranged from: (H) 477-653, (S) 400-584, and (SD) 236-373. Cadence (steps/min) ranged from: published norms (N) 103-133, (H) 109 – 140, (S) 103-133, and (SD) 74.8-119. Gait speed (m/s) ranged from: (N) 1.04-1.64, (H) 1.22-1.67, (S) 1.05-1.56, and (SD) 0.60-0.99. Only participants with SBMA completed the i-TUG. i-TUG duration (s) ranged from: published norms (N) 6.28-11.6, (S) 5.09-8.98, and (SD) 8.91-27.9. Turn velocity ranged from: (N) 158 – 322, (S) 188 – 305, and (SD) 85.4-239. Longitudinal studies examining the i-6MWT and i-TUG in larger sample sizes are needed to validate the use of wearable sensors as an effective outcome measure for SBMA clinical trials.	K Doreswamy, G Norato, A Kokkinis, A Alqahtani, G Joe, C Grunseich, M Jain	2023	CLINICAL
2023-100	Meagan	D	Marks	NIAAA	ACI/IRS	Elucidating the role of medial septum glutamate neurons in reward-seeking behaviors	A hallmark of many psychiatric illnesses, including substance use disorders, is maladaptation in reward seeking. One of the first brain regions implicated in reward via electrical self-stimulation in rats is the Medial Septum (MS). The MS is known to be involved in navigation, learning, and theta rhythmicity in the hippocampus. However, recent studies found that optogenetic excitation of MS glutamate neurons (MSGLU) is reinforcing while another study found that general excitation of the MS enhances strategy switching in rats, a form of cognitive flexibility. How MSGLU neuronal activity correlates to reward seeking behaviors remains unknown. Therefore, chemogenetics, both excitatory and inhibitory, and fiber photometry were used to probe and visualize MSGLU activity during reward seeking paradigms in mice including the operant behaviors: fixed ratio 1 (FR1), progressive ratio (PR), and lever reversal. Inhibiting MSGLU activity seemed to decrease reward seeking during FR1 as well as increase consumption of the reward. However, enhancing MSGLU activity tended to enhance PR breakpoint ass well as improve reversal learning. Fiber photometry showed decreases in MSGLU signaling during reward consumption and lever pressing. MSGLU activity appears to track aspects of goal-related information and stimuli. While there is still more to learn about MSGLU signaling during reward seeking, these neurons as well as other neurons within the MS may be a therapeutic target for substance abuse and other psychiatric illnesses.	MD Marks, S Ramos-Maciel, N Westcott, AJ Kesner	2023	ACI/IRS
2023-101	Jee-Youn		Kang	NCI	Chromosome Biology	Cohesin mediated 3D genome structure defines Neuroblastoma cell subtypes and their plasticity.	Neuroblastoma is highly heterogenous marked by distinct epigenetic profiles with distinct 3D genome organization. In addition to its role in DNA replication/damage, Cohesin mediates the looping structure between promoters and enhancers to regulate gene expression. Our study aims to evaluate the role of cohesin in control of cell-type specific super-enhancer networks in neuroblastoma. Data mining using R2 database, Cohesin was significantly over-expressed in NB tumors compared to neural crest cells or adrenal gland and were significantly associated with poor event-free/overall survival. Studies evaluating H3K27Ac have shown distinct super-enhancer landscapes between MES/ADRN cell types. Our Cohesin ChIP-seq data show cohesin binding pattern between these two cell subtypes is very distinct, with cell type specific enhancers and promoters bound by cohesin subunits. Homer de novo motif scan of cohesin binding site in MES cell line identified well known MES specific CRC TF as highest ranked motif, whereas Homer de novo motif scan of cohesin binding site in ADRN cell line identified well known ADRN specific CRC TF as highest ranked motif. We identified that MES specific genes were differentially expressed after RAD21 knockdown in MES cells. These results indicate the possibility of cohesin bound at cell type specific enhancer-promoter regions regulating its target genes through enhancer/promoter looping. In this study we are defining the molecular mechanisms underlying regulation of 3D genome structure neuroblastoma, which is crucial for understanding how neuroblastoma cell types acquire and stabilize their cellular identity and the basic mechanisms involved in cell state changes during therapeutic interventions and differentiation.	JY Kang, Z Liu, M Sun, CJ Thiele	2023	CHROM
2023-102	Quinlin	M	Hanson	NCATS	Chemical Biology	A dual-activity ExoN/MTase platform for SARS-CoV2 NSP14 drug development	SARS-CoV-2 carries one of the largest RNA genomes (~30 kilobases) among all RNA virus families. The nonstructural protein 14 (NSP14) is a dual-function exonuclease (ExoN)/methyltransferase (MTase) protein responsible for preservation of the viral genome. NSP14 requires the accessory protein NSP10 for ExoN activity, but not for MTase activity. While the ExoN activity allows SARS-CoV-2 to edit faulty replication, the MTase activity performs the final step of viral RNA capping to prevent viral genome degradation by host cells. Both enzymatic domains are essential for successful viral replication, making NSP14 an appealing drug target. Our goal is to identify small molecules capable of impairing NSP14 activity. To this end, we developed high-throughput assays to measure both MTase and ExoN activity and interrogated these assays against a collection of ~20K approved, investigational, and pharmacologically active compounds. Our screened identified compounds active against the MTase activity of NSP14, compounds active against the ExoN activity, and compounds active against both domains. Hits were further validated using counter assays to parse out false positives. Selected hits were subsequently validated for target engagement using an activity-agnostic nano-differential scanning fluorimetry (nano-DSF) assay. Together, these assays constitute a platform amenable for NSP14 drug development, which can be deployed for screening larger and chemically diverse small molecule libraries to develop novel small molecule inhibitors of NSP14.	QM Hanson, AV Zakharov, S Pal, K Recabo, S Messing, D Esposito, NJ Martinez	2023	CHEMBIO

2023-103	Amanda		Henning	CC	Cancer Biology	Peripheral B cells from HCV-associated B cell non-Hodgkin's lymphoma patients display clonal expansion and an anergic-like transcriptional profile	Chronic hepatitis C virus (HCV) infection remains a global health issue, with its role in B cell lymphoproliferative disorders, including B cell non-Hodgkin's lymphoma (BNHL), of increasing concern. Epidemiological and clinical evidence strongly support a causal role of chronic HCV infection in BNHL pathogenesis; however, the molecular mechanisms underlying this association are poorly understood. To help elucidate this relationship, we performed RNA-sequencing on peripheral B cells collected from chronic HCV-infected patients with or without BNHL, as well as BNHL-only patients and healthy controls. In peripheral B cells from HCV-associated BNHL patients, we observed enrichment of a transcriptional signature associated with B cell anergy. This included overexpression of inhibitory receptors, pro-apoptotic genes, and BCR signaling inhibitors, as well as enrichment of anergic-like gene sets. BCR repertoire analysis of our RNA-seq data identified significant clonal expansion in peripheral B cells from HCV-associated BNHL patients, and we identified 7 expanded clonotypes corresponding to 6 Ig variable gene loci. Expanded clones included Ig genes whose encoded BCRs have been associated with viral- and non-viral-related lymphoma, autoimmunity, and autoreactivity. We also observed strong positive correlation between differentially expressed epigenetic regulatory genes and degree of clonal expansion, suggesting epigenetic regulation may be involved in B cell anergy. Studies are underway to further interrogate peripheral clonal expansion via BCR-sequencing and to investigate the BCR repertoire and transcriptome in matched lymphoma tissues. We believe these results have implications for HCV-associated BNHL treatment and monitoring and suggest dysregulation of the anergic state may play a role in HCV-associated lymphoprogression.	AN Henning, HJ Alter, N Dashdorj, V De Giorgi	2023	CANCER
2023-104	Jessica	C	Hargarten	NIAID	Clinical Research	Characterization of MTOR signaling pathway variants in previously healthy patients with non-HIV cryptococcosis.	Globally, Cryptococcus is an opportunistic fungal pathogen which causes major morbidity and mortality in a range of patient populations from the immunosuppressed to the previously healthy (PH) without obvious immune dysfunction. Cryptococcal infections in the PH are characterized by worse prognosis with mortality rate upwards of 30-50% despite antifungal therapy. Little is known about the molecular mechanisms driving the immune defects that lead to cryptococcosis in the PH. Our long-term goal is to identify and validate the major genetic and immunological defects leading to cryptococcosis susceptibility in the PH to inform human pathobiology and personalized patient care. Whole exome sequencing analysis on the largest cohort of PH patients identified rare alleles predicted to have deleterious functional consequences (CADD >30). Pathway analysis identified an enrichment in MTOR signaling (p-value =2.12E-06) defects. mTOR pathway activation is known to be critical for optimal T cell responses to fungal infections. In the present study, cryptococcosis patient MTOR variants were associated with loss of function defects in T cells. Ongoing genetic correction studies aim to functionally validate MTOR variants using patient cells. We next characterized the immunologic consequence of MTOR deficiency on susceptibility to Cryptococcus using established murine models of cryptococcosis. Mice deficient in appropriate mTOR signaling display increased susceptibility with dysregulation of effector T cell responses at the site of infection. These data suggest that appropriate MTOR signaling (particularly in CD4 T cells) is necessary for protection against infection. Ongoing experiments will further determine the mechanism by which MTOR signaling is required during cryptococcosis.	JC Hargarten, MJ Vaughan, OCR Dean, S Paul, J Lacks, PR Williamson	2023	CLINICAL
2023-105	Robert	W	Robey	NCI	Cell Biology	The methyltransferases METTL7A and METTL7B confer resistance to thiol-based histone deacetylase inhibitors	Histone deacetylase inhibitors (HDACis) are part of a growing class of epigenetic therapies used for the treatment of cancer. Although HDACis are effective in the treatment of T-cell lymphomas, treatment of solid tumors with this class of drugs has not been successful. Overexpression of the multidrug resistance protein P-glycoprotein (P-gp), encoded by ABCB1, is known to confer resistance to the HDACi romidepsin in vitro, yet increased ABCB1 expression has not been associated with resistance in patients, suggesting that other mechanisms of resistance arise in the clinic. To identify alternative mechanisms of resistance to romidepsin, we selected MCF-7 breast cancer cells with romidepsin in the presence of the P-gp inhibitor verapamil to reduce the likelihood of P-gp-mediated resistance. The resulting cell line, MCF-7 DpVp300, does not express P-gp and was found to be selectively resistant to romidepsin but not to other HDACis such as belinostat, panobinostat, or vorinostat. RNA sequencing analysis revealed upregulation of the mRNA coding for the putative methyltransferase, METTL7A, whose paralog, METTL7B, was previously shown to methylate thiol groups on hydrogen sulfide and captopril. As romidepsin has a thiol as the zinc-binding moiety, we hypothesized that METTL7A could inactivate romidepsin and other thiol-based HDACis via methylation of the thiol group. We demonstrate that expression of METTL7A or METTL7B confers resistance to thiol-based HDACis and that both enzymes are capable of methylating thiol-containing HDACis. We thus propose that METTL7A and METTL7B confer resistance to thiol-based HDACis by methylating and inactivating the zinc-binding thiol.	RW Robey, CM Fitzsimmons, WM Guiblet, WJE Frye, JM González Dalmasy, L Wang, DA Russell, AJ Perciaccante, CC Lipsey, AV Mitchell, SS Maligireddy, D Butcher, EF Edmondson, LM Jenkins, AD Piscopio, RA Totah, SE Bates, HE Arda, MM Gottesman, PJ Batista	2023	CELLBIO
2023-106	Meghan	C	Nelson	NHGRI	Clinical Research	Validation of Calcinosis Durometer Measurements in Juvenile and Adult Dermatomyositis	Objective: Dermatomyositis (DM) and juvenile dermatomyositis (JDM) are idiopathic inflammatory myopathies affecting multiple organs, including skeletal muscle and skin. Calcinosis, a known complication of DM/JDM, is associated with significant morbidity. Tools to assess calcinosis in DM/JDM patients have been inadequately validated. The goal of this study was to determine the reliability of durometer measurements of calcinosis in JDM and DM patients. Methods: Calcinosis firmness was measured using handheld digital durometer with a continuous scale across 3 institutions. Five investigators examined DM/JDM calcinosis lesions by durometry, optimally recording three readings per site, as well as control readings unaffected by calcinosis in similar anatomic areas. Intra-rater and inter-rater intraclass correlations were evaluated. Results: We enrolled 57 patients and gathered 709 durometric measurements of both calcinosis and control lesions (443 calcinosis; 266 control) over eleven anatomic regions by durometry. Intra-rater intraclass correlation was high with repeat measurements, including at control and calcinosis sites, indicating good intra-rater reliability. Inter-rater reliability was moderate to good over repeat measurements in the upper neck/clavicle, forearms, upper arms, back/torso, posterior calf, and elbows, with the exception of the thigh and anterior calf, which were below the threshold of acceptability. Durometry readings of calcinosis lesions were statistically higher than control lesions in the following locations: upper neck/clavicle, upper arms/forearms, elbows, hand/wrists, buttocks, thigh, calf and foot. Calcinosis lesions overall were harder compared to control lesions. Conclusion: Our study identifies durometry as a reliable tool in assessing targeted lesions of calcinosis lesions in DM/JDM patients.	M Nelson, L Rider, H Kim, S Gillespie, V Do, J Fuller, K Rouster-Stevens, A Schiffenbauer	2023	CLINICAL
2023-107	Dinusha		Rajapakse Todd	NEI	Cell Biology	A lasered human amelotin transgenic mouse model displays progressive outer retinal pathology and hydroxyapatite deposition similar to geographic atrophy	Geographic atrophy (GA) is a common form of age-related macular degeneration and is characterized by death of photoreceptors, which precedes the loss of retinal pigment epithelial (RPE) cells. Vision loss due to GA has no effective treatment, reflecting the complexity of the disease and lack of suitable animal models. Early signs of GA are "soft" drusen, extracellular accumulations of lipids, proteins, and mineralized calcium phosphate, hydroxyapatite (HAP), along Bruch' membrane. We discovered that amelotin (AMTN) an extracellular protein involved in formation of dental enamel, is induced in RPE in GA and is associated with HAP mineralization of drusen. Healthy RPE does not express AMTN. We have created a transgenic (Tg) mouse model in which constitutive expression of human AMTN is targeted to RPE using a construct based on the mouse gene for RPE65, a cell-specific protein. Human AMTN is expressed specifically in RPE and, by itself creates some abnormalities relevant to AMD pathology. To induce a calcium flux, retinas of Tg mice were lasered at adjacent sites using a slit lamp system with an OcuLight GLx ophthalmic laser 100µm spots, 0.1 sec duration at ±120 mW of power. This injury resulted in deposits containing HAP, reminiscent of GA drusen, 2-weeks post-laser. While wild type littermates had normal wound repair, fluorescent imaging and optical coherence tomography showed progressive obliteration of photoreceptors within lesions, but an unaffected inner retina. We further observed microglial recruitment and functional retinal deficits. We propose this mouse model as an attractive tool for GA studies and drug-discovery.	D Rajapakse Todd, J Fan, D Daily, L Dong, K Peterson, R Fariss, G Wistow	2023	CELLBIO
2023-108	Valentina		Ottaviani	NIDCR	Immunology	Dissecting the role of TGF-b in the skin	The skin is the outermost barrier in the body. The only point of entrance for all the skin-sitting pathogens and commensals are the hair follicles, which can be defined as the most immunologically active sites of the skin. So, tight regulation is needed at these sites and it is achieved through immune cells and non-hematopoietic cells, like keratinocytes and fibroblasts. Example of immune cells are regulatory T cells, which are not only activated by, but also produce large amounts of TGF-β, a multifunctional cytokine, present in the body in 3 isoforms (TGF-β1,2 and 3). These isoforms are fundamental for skin development during organogenesis and additional findings report about their role in driving cell localization in the skin as well as involvement in tissue repair. Though, little is known about their immunological role in the skin. Upon generating a working protocol to separate skin layers and isolate cells from them, we were able to start to define the cell composition of each layer both at steady state and during inflammation. Moreover, we could detect the three TGF-β isoforms in each layer at both gene and protein level further discriminating between hematopoietic and non-hematopoietic sources. Finally, the importance of TGF-β in the skin was confirmed by experiments on TGF-β receptor I depleted mice. For the future, we are planning on defining exactly which cells secrete and respond to TGF-β and confirm these findings by generating conditional KO mice. Additionally, the role of TGF-β will be assessed in world-wide skin diseases.	T Gauthier, W Jin, YJ Lim, Na Liu, T Maruyama, L Patiño, R Kazmi, G Cvijetic, N Joller, WJ Chen	2023	IMMUNO
2023-109	Grozdan		Cvijetic	NIDCR	Immunology	Notch2 deficiency generates functionally impaired cDCs and macrophages that correlates with intestinal dysbiosis and low-grade inflammation	Myeloid cells including conventional dendritic cells (cDCs) and macrophages are key responders at epithelial barriers, regulating immunity to microbial pathogens and commensals. Equipped with innate receptors, DCs and macrophages sample and monitor the environment, maintaining homeostasis. Upon detection of danger signals they become activated, secrete inflammatory cytokines, and promote T cell activation. Myeloid cells at barrier tissues may therefore be critical players controlling the balance between tolerance and immunity. Within CD11c expressing cells, Notch2 deficiency impairs type 2 dendritic cells (cDC2), resulting in increased susceptibility to C. rodentium as previously shown. In these mice we observed defects also within several macrophage subsets. Besides the reported TH17 defect, linked to the lack of ESAM+cDC2, dysfunctional macrophages may also be involved in the observed compromised barrier function. The lack of Notch2 within the myeloid compartment was accompanied by intestinal dysbiosis and low-grade inflammation. The microbial imbalance and increased CFUs could be transferred by co-housing. The dysbiosis led to increased susceptibility to DSS-induced colitis in Notch2 deficient mice. These results suggest that expression of Notch2 in either one or more myeloid subsets are responsible for the maintenance of a healthy commensal community or that they control immunity to specific opportunistic pathogens. Among the dysregulated pathways, we have focused our attention on innate immune mechanisms and identified several candidate genes that may play a fundamental role in regulating bacterial growth. Collectively, we hypothesize that Notch2 deficiency alters the functional properties of intestinal cDCs and macrophages, ultimately leading to dysbiosis and low-grade inflammation.	G Cvijetic, M Mitrovic, P Fernandes Rodrigues, IO Conway, E Reinoso Jacome, B Mendoza-Bonilla, J Shi, A du Halgouet, V Ottaviani, R Tussiwand	2023	IMMUNO
2023-110	Yasemin		Cole	NCI	Cancer Biology	Developmental insights into PPGL syndromes	Pheochromocytoma and paraganglioma (PPGL) are rare neuroendocrine tumors derived from the neural crest (NC) that can present as early as the first decade of life. Genetic variants in genes such as the succinate dehydrogenase complex subunits (SDHx) and hypoxia-inducible factor 2-alpha (HIF2A) can lead to the activation of hypoxia-inducible pathways, leading to vasculogenesis and tumorigenesis. We previously discovered a sporadic neoplastic syndrome characterized by paraganglioma and developmental malformations due to mosaic gain-of-function variants in mosaic HIF2A mutations. We believe the dysregulated response to oxygen tension in developing NC, such as through pseudohypoxia signaling driven by genetic variants, leads to the co-occurrence of developmental malformations and tumors. To better understand the implications of SDHB variants on NC and PPGL development, we evaluated a transgenic "two hit" SDHB mouse model, that we developed to recapitulate the associated human PPGL syndrome, using high-resolution ex vivo imaging and subsequent immunohistochemistry (IHC) and ddPCR of affected tissues. These studies demonstrated the adrenal glands had features suggesting abnormal development such as significantly enlarged adrenal medullas and abnormal intra-adrenal features including medullary tails and vascular defects compared to wild-type (WT) adrenals. We observed islands of medullary cells with a poorly demarcated border between the medulla and cortex, using histology and IHC, suggesting improper development. To fully understand the role of sdhb in developmental processes in the neural crest, we are extending our studies to include both embryos and early postnatal timepoints. These results suggest a role of Sdhb in adrenal embryonic and PPGL development.	Y Cole, J Rosenblum, H Wang, I Indig, T D, J Munasignhe, D Donahue, A Sowalsky, S Trostel, K Pacak, Z Zhuang	2023	CANCER
2023-112	Wei-Lun		Huang	NICHD	Clinical Research	A Novel Algorithm to Optimize View Quality for Multi-View Capture	The depth of field of a camera is a limiting factor for acquiring sharp visual information. Extending depth of field is a technique to acquire multiple images at a single camera pose with different focus distances for an all-in- focus image of a static object. However, an efficient way to arrange focus distances to optimize view quality for multi- view capture remains a challenge. In this paper, we propose a novel algorithm to derive focus distances for each camera given the 3D shape of the target object and a set of camera poses. We assign every point sampled on the 3D shape uniquely to a camera and then solve an optimal focus distance for each camera given the associated point set. We validate the algorithm in simulation under different optimization objectives and camera configurations. We demonstrate the effectiveness of the algorithm for focus arrangement. The algorithm can be used in total body photography, archaeology, and other close-range photogrammetry applications that require visual details and are limited to the depth of field.	WL Huang	2023	CLINICAL
2023-113	Andy	A	Cole	NINDS	Neuroscience	EM tomography reveals the organization and associations of transsynaptic complexes underpinning the coordination between the three synaptic compartments in cultured rat hippocampal synapses	The synapse is a complex ballet with the players, their roles, and their associations largely hidden by scale. To understand the synapse, the composition and distribution of components in each compartment has largely been analyzed and contextualized separately. Recently, advances in 3D light and electron microscopy techniques have revealed coordination between the presynaptic, postsynaptic, and cleft compartments. It is now clear that certain proteins align across the synapse and within the cleft. Here, 3D renderings visualize electron dense material from electron tomographic reconstructions of high-pressure frozen and freeze-substituted dissociated hippocampal rat neuronal cultures. In these renderings, nearly all cleft-spanning structures connect with a structure in either the pre- or postsynaptic compartment. More than half of all the abundant cleft-spanning structures connect to intracellular structures in both. These full transsynaptic assemblies can link with one another through shared intracellular structures. The resulting large clusters of intracellular structures grouped by linked transsynaptic assemblies are common around vesicles near the active zone membrane and align with groups of large structures with scaffolding morphology in the postsynaptic compartment. Here, we enumerate different types of assemblies, describe their associations, and map their distribution within the synapse. In our interpretation, the intracellular portion of linked assemblies form domains. The cleft components physically link these pre- and postsynaptic domains into nanocolumns. The mechanical forces underpinning this alignment may influence synaptic functions like endo- and exocytosis.	AA Cole, TS Reese	2023	NEURO

2023-114	Monica	A	Diaz	NIAID	Research Support Services	Overview of the national biosafety and biocontainment training program	The National Biosafety and Biocontainment Training Program (NBBTP)/Intramural Research Training Award (IRTA) is a two-year NIH fellowship designed to train fellows as emerging biosafety and biocontainment professionals. As part of this fellowship, trainees learn how to perform risk assessments for biological research; about the design, operation, principles and practices of high containment (BSL-3 and BSL-4); the role of safety specialists (i.e. performing annual laboratory safety surveys, laboratory protocol reviews, and injury investigations); and how to review recombinant and pathogen registrations and lead the Institutional Biosafety Committee (IBC). In addition, fellows participate in various trainings in occupational and laboratory safety and attend regional and national conferences on biosafety, biosecurity, and occupational health and safety. Developmental assignments are also an integral part of the NBBTP fellowship, where fellows consult for an outside institution and develop biosafety-related deliverables for that institution. NBBTP fellows also spearhead applied biosafety research projects at NIH as a capstone for their two-year tenure at NIH. Following successful completion of the NBBTP program, alumni are employed within the spectrum of the biosafety field, including industry, government, academia, and consulting, where they serve as leaders in biosafety, biosecurity, and biocontainment. It is the goal of the NBBTP fellowship to provide highly trained professionals to meet the growing needs of the biological and biomedical research community.	SM Boada, M Boes, MA Diaz, RD Johnston, N Rose, D Newcomer, A Clarkson, J McCormick-Ell	2023	RSCHSUPP
2023-115	Yi Wei		Lim	NCATS	Biomedical Engineering and Biophysics	Biofabrication of immunocompetent 3D skin tissue equivalents to model skin wound healing and fibrosis.	Wound healing is a dynamic and tightly coordinated process to maintain the structural and functional integrities of the skin. Injury to the skin initiates a cascade of events including inflammation, proliferation, and tissue remodeling. Dysregulation in these mechanisms can lead to the formation of non-healing chronic wounds, affecting around 5.7 million people in the United States alone. Therefore, there is an urgent need to understand the pathophysiology of wound healing to develop effective therapies. Macrophages are key immune regulators that play distinct roles to ensure proper wound healing and tissue regeneration. Throughout these tightly regulated processes, M1 (pro-inflammatory) and M2 (anti-inflammatory) macrophages secrete cytokines and chemokines that modulate fibroblast proliferation, activation, as well as collagen production. Our group has previously developed three-dimensional (3D) skin tissue equivalents that closely mimic human skin tissue and model inflammatory skin diseases. Here, we introduced human macrophages derived from peripheral monocytes into our 3D skin tissue model to generate an immune-competent skin tissue. The addition of macrophages into our 3D skin tissue upregulates the production of cytokines and chemokines that carries immunomodulatory effects on other cell types in the skin and modulate tissue remodeling. Furthermore, we validate that macrophages incorporated into the dermis can respond to bacterial and viral stimuli. Lastly, the introduction of M2 macrophages in our 3D skin tissue increases collagen deposition in the skin dermis layer upon TGFβ1 treatment, mimicking a skin fibrosis phenotype. This immunocompetent 3D skin model will be a powerful platform for pre-clinical testing for immune-modulated skin diseases.	YW Lim, H Zarkoob, MJ Song, M Ferrer	2023	BIOENG
2023-116	Rand Gabriel	M	Buenaventura	NCI	Cancer Biology	PAEP functions as an immune modulator to regulate tumor metastasis	Most cancer-related deaths are associated with the complex phenotypic behavior of metastasis. While it has been established that the tumor microenvironment can affect how cancer grows and spreads, the molecular mechanism by which the metastatic tumors survive and escape from immune attack in the tumor microenvironment remains unclear. To study the molecular mechanism of interaction between metastatic tumors and the immune system in metastasis, we established immune-resistant metastatic models. We identified that PAEP, a progestogen-associated endometrial protein, is significantly upregulated in immune-resistant metastatic tumors compared with non-immune-resistant tumors. PAEP is a glycoprotein that inhibits cell immune function and plays an essential role in the pregnancy process. To examine the function of PAEP in tumor metastasis, we first introduced PAEP into non-immune resistant and poorly metastatic melanoma and rhabdomyosarcoma (RMS) cells. We found that overexpression of PAEP significantly promotes tumor metastatic potential of both melanoma and RMS cells in immunocompetent mice. Interestingly, there was no difference in metastasis between the control and overexpression groups in immunodeficient mice. These data suggest that PAEP may mediate tumor metastasis relating to host immunity. To further confirm the function of PAEP in tumor metastasis, we used CRISPR/Cas9 technology to knockout endogenous PAEP and will test the metastatic potential in different hosts. We will also investigate the molecular mechanisms using RNA sequencing and Digital Spatial Profiling to analyze the metastatic samples. Our study will uncover a new mechanism for how tumors survive in the microenvironment and identify a novel target for the treatment of metastatic diseases.	RGM Buenaventura, W Chen, G Merlino, Y Yu	2023	CANCER
2023-117	Ulisse		Bocchero	NEI	Neuroscience	Selective Knockout Of Glutamic Acid-Rich Protein 2 (GARP2) Significantly alters Cellular Dark Noise in Rod Photoreceptors	GARP2, a glutamic-acid-rich protein found exclusively in rod photoreceptors, was suggested to function as a structural protein, a calcium-binding protein, a modulator of the cGMP phosphodiesterase enzyme (PDE6), and a gating inhibitor of the rod cGMP-gated cation channel, regulating visual phototransduction. GARP2 is a splice variant of the Cngb1 gene, which in the rods photoreceptor encodes the β-subunit of the cyclic nucleotide-gated cation channel and another glutamic acid-rich protein, GARP1. Mutations in Cngb1 cause retinitis pigmentosa (RP45), and β-subunit knockout mice are being studied as models of this disease. We previously showed that overexpression of GARP2 in rods accelerates phototransduction gain and slows the recovery of the light response. In this study, using ZFN-mediated gene editing, we have selectively eliminated GARP2 expression (GARP2 KO) to determine its essential functions in mouse rods. The absence of GARP2 caused perturbations of retinal structure in old KO mice. Indeed, the electroretinogram in these mice revealed functional deficits, namely a reduction in a- and b-wave amplitudes. Interestingly, single-cell patch-clamp recordings showed a significant reduction in rod photoreceptor dark noise in 3 and 6 months old KO mice, consistent with a previously proposed role for GARP2 in binding to PDE6 and stabilizing its basal activity. We suggest a role for the GARP 2-PDE6 interaction in stabilizing the PDE6 enzyme and controlling the turnover rate of cGMP in darkness, influencing the level of dark noise and the signal and noise properties of rod photoreceptors.	U Bocchero, DA Stacks, MN Nguyen, SJ Pittler, J Pahlberg	2023	NEURO
2023-119	Katherine		Kim	NIMH	Neuroscience	Hierarchical-Bayesian estimation of the Drift Diffusion model (HDDM) to study a large high-risk cohort during adolescent development	During adolescent development, decision-making processes also improve, influenced by both the child's internal and external environment. The Brazilian High-Risk Cohort (BHRC) for Psychiatric Disorders is a large longitudinal cohort that has consistently collected data from over 2500 children and adolescents since 2010, including demographic characteristics, responses to cognitive behavioral tasks, and questionnaires representative of their mental health difficulties. These variables were utilized in the context of implementing the Drift Diffusion Model (DDM) and the Hierarchical Drift Diffusion Model (HDDM) to extract parameters regarding differences in the decision-making process in populations that have and have not been clinically diagnosed with any psychiatric disorder. While the DDM does not find any statistically significant differences in the decision-making process between these two populations, the HDDM does, suggesting both the benefit of hierarchical estimation when working with small numbers of trials and a potential mechanism for the performance differences in the diagnosed and non-diagnosed adolescent groups.	K Kim, S Haller, M Brotman, Z Laky	2023	NEURO
2023-120	Madeline		Wong	NCI	Research Support Services	Empowering your Research with Services from the CCR Genomics Core	CCR Genomics Core under the Office of Science Technology Resource (OSTR) at the National Cancer Institute provides investigators with access to genomic technologies and Next-Generation Sequencing (NGS) with rapid turnaround on smaller-scale projects or projects that are not ready for production. The Core has an open-door policy operating more like a "boutique" and is unique in granting user-accessible instrumentation. Additional resources include training, consultation services, bioinformatics support, and secure data delivery/management. The Core supports 7 different platforms with 17 instruments supporting most of the CCR laboratories at the NIH Bethesda campus and multiple NIH institutes. Core instrumentation and services include [Sanger Sequencing (2 ABI 3500xL Genetic Analyzers), Illumina Next-Generation Sequencing (1-iSeq, 1-MiSeq, 1- NextSeq550 3- NextSeq2000), Nanopore Sequencing (Oxford Nanopore MinION & Mk1C), Digital Gene Expression (Nanostring nCounter Analysis System), Droplet Digital PCR (Bio-Rad QX200 Droplet Digital PCR System), DNA/RNA & Library QC (Agilent TapeStation 4150 & 4200, Fragment Analyzer, QuantStudio RT-PCR system, Pippin HT) and Digital Spatial Profiling (NanoString GeoMx DSP). This platform combines spatial and molecular profiling technologies by generating digital whole transcriptomes and profiling data. The technology is offered in collaboration with the Collaborative Protein Technology Resource (CPTR). In addition, the CCR Genomics Core functions as a support lab, containing instruments for various applications for use by CCR investigators. Analytical software for the various technologies is also made available. To learn more about our services visit us in Bldg. 41/Room D310 or our website at https://ostr.ccr.cancer.gov/resources/ccr-genomics-core/.	S Shema, Q Wei, D Tillo, M Wong, EA Conner	2023	RSCHSUPP
2023-121	Ryo		Sato	NHLBI	Cell Biology	Neuronal β-III Tubulin (Tuj1) diminishes the severity of pulmonary fibrosis	Idiopathic pulmonary fibrosis (IPF) is a devastating disease that requires an improved understanding of the pathological mechanisms for the development of novel therapies. In this study, we identified neuronal ß-III tubulin (Tuj1), a pan-neuronal marker, as a potential biomarker in pulmonary fibrosis and discovered Tuj1-expressing pericytes suppressing the severity of lung fibrosis. A series of spatial and temporal imaging and scRNA-seq analysis of bleomycin-induced fibrotic lung revealed the emergence of Tuj1-expressing pericytes in response to lung fibrosis in mice. Tuj1-expressing pericytes were also found in human IPF tissues. Our lineage-tracing experiments using the pericyte-specific CreER mice (PDGFRß-CreER or NG2-CreER) and Cre-dependent reporter mice (Rosa-LSL-YFP) supported the observation that Tuj1-expressing cells are derived from pericytes. Moreover, the combination of inflammatory and fibrotic signals such as TGF-ß1, TNFα, and IFNγ can induce Tuj1 expression in pericytes. To investigate the role of Tuj1 (gene name: Tubb3) in lung fibrogenesis, we examined what happens to fibrosis in Tubb3 knockout mice with the bleomycin administration. Interestingly, Tubb3 knockout mice exhibited enhanced lung fibrosis, accompanied by increased numbers of fibrotic fibroblasts and pro-fibrotic macrophages, without any significant neuronal abnormalities. These findings suggest that Tuj1-expressing pericytes may serve as a negative regulator in the fibrotic lung. Taken together, these studies provide a potential clue for developing a novel therapeutic strategy targeting the Tuj1-expressing pericytes in the fibrotic lung vasculature.	R Sato, K Imamura, T Tsukui, Y Tomita, K Fujino, T Ikeda, C Combs, M Murgai, M Suzuki, T Sakagami, D Sheppard, Y Mukouyama	2023	CELLBIO
2023-122	Ayaka		Hara	NCI	Immunology	The structure-function relationships of sulfatide analogs for the activity of human iNKT cells	Invariant natural killer T (iNKT) cells are an unconventional T cell subset expressing a semi-invariant T cell receptor (TCR) that recognizes lipid antigens presented by the monomorphic MHC I-like molecule CD1d. Studies of α-galactosylceramide (α-GalCer) analogs, prototype iNKT cell antigens, have shown that differences in the structures of glycolipid antigens can significantly alter the activities of iNKT cells. However, recent studies suggested that structure-function relationships provided by analysis of iNKT cell recognition of α-GalCer analogs are not necessarily applicable to other glycolipid antigens. This study investigates the structure-function relationships of a self-glycolipid antigen, sulfatide, for the activation of human iNKT cells. Eight new sulfatide analogs with structures similar to 7DW8-5, a glycolipid 100-fold more potent in stimulating iNKT cells than α-GalCer, have been synthesized. First, we examined the recognition of the sulfatide analogs by the TCR of iNKT cells by creating CD1d-tetramers loaded with sulfatide analogs and used them to stain iNKT cells. The results showed that the staining properties of CD1d-tetramers differ depending on the acyl chain structure of the sulfatide analog loaded. Next, we will examine the stimulatory properties of the analogs against a human iNKT cell line in vitro. Once we have identified analogs that can stimulate human iNKT cell lines, we plan to test their antigenicity using ex vivo human iNKT cells. The information obtained from this study could help design new agonistic lipid antigens for human iNKT cells, creating a potential therapeutic strategy to augment an anti-cancer immune response.	A Hara, J DiSapio, M Coombs, G Khayrullina, V Joshi, M Watowich, M Watanabe, K Smith, J Gumperz, M Gilbert, A Howell, M Terabe	2023	IMMUNO
2023-123	Nairith		Kalale	NIMH	Genetics and Genomics	Mental health disorders arising from mutations on the 16p chromosome region	Mental health disorders arising from mutations on the 16p chromosome region	N A Kalale	2023	GEN
2023-124	Hallie	F	Gaitsch	NINDS	Neuroscience	Characterizing oligodendrocyte lineage cell dynamics during remyelination	Remyelination is a regenerative process resulting from successful differentiation of oligodendrocyte progenitor cells (OPC) into myelinating oligodendrocytes that can repair demyelinated lesions. Remyelination failure leaves denuded axons vulnerable to damage and contributes to clinical progression of demyelinating diseases such as multiple sclerosis. While several potential remyelinating agents have proceeded to clinical trials, methods for accurately and non-invasively assessing changes in remyelination status remain limited. A better understanding of remyelination-associated glial cell turnover dynamics may aid in the discovery of relevant biomarkers to meet this clinical need. In this study, a toxin-induced model of demyelination was used to profile oligodendrocyte cell death and OPC proliferation dynamics over the course of remyelination, from initial demyelinating injury to near-complete myelin regeneration. Eight-week-old Sprague Dawley rats (n = 24) were injected bilaterally with ethidium bromide targeting the caudal cerebellar peduncles. Perfusion and brain dissection were performed at 2-, 5-, 10-, 14-, and 21-days post-lesion (4-5 animals/timepoint). Unlesioned age-/sex-matched controls were used (n = 5). Fixed, frozen tissue was cryosectioned and co-labeled with antibody markers for cell identity (PDGFRα – OPC; Olig2 – oligodendrocyte lineage; GFAP – astrocytes; Iba1 – microglia/macrophages), proliferation (Ki67), and apoptosis/DNA damage (TUNEL assay). Remyelinating lesions were characterized by widespread DNA fragmentation and proliferation as compared to control tissue, indicating a high degree of cell turnover during regeneration. These results provide the foundation for future investigation of the role of cell death in brain regeneration as well as biomarkers that may be used to track that process, such as cell-free DNA.	H Gaitsch, P Assinck, P Dimas, L Morcom, C Zhao, DH Rowitch, DS Reich, RJM Franklin	2023	NEURO
2023-125	Kingsley	A	Garrett	NIBIB	Biomedical Engineering and Biophysics	Engineered in vitro carotid artery flow model of endothelial dysfunction in Sickle cell disease	Sickle cell disease (SCD) is a genetic condition characterized by abnormal hemoglobin production that causes sickle shaped red blood cells to disturb blood flow and hinder oxygen delivery. Various vascular complications such as stroke, pose a significant health risk, especially among pediatric sickle cell disease patients. The MATRICES Lab is utilizing microfabricated devices to investigate the interactions between endothelial cells and blood cells under flow conditions to identify mechanisms to prevent stroke in children affected by SCD by understanding factors that contribute to endothelial dysfunction and vascular remodeling in large arteries. Sickle cell disease (SCD) is a genetic condition characterized by abnormal hemoglobin production that causes sickle shaped red blood cells to disturb blood flow and hinder oxygen delivery. Various vascular complications such as stroke, pose a significant health risk, especially among pediatric sickle cell disease patients. The microfabricated blood vessel model was formed with fibrin gel incorporating dye-quenched collagen that allows for the visualization, tracking, and analysis of cellular behavior under a microscope through the fluorescent signal that DQ emits upon cleavage or degradation of the gel.	HS Lee, MO Platt	2023	BIOENG
2023-126	Samuel	R	LaMunion	NIDDK	Epidemiology	Characterizing ActiGraph's idle sleep mode	Idle sleep mode (ISM) is an optional battery-conserving feature for ActiGraph accelerometers that may have implications for data handling when data are collected with ISM enabled. There is limited documentation of the properties and characteristics of ISM, however, it is generally believed to engage during nonwear, periods of inactivity, and sleep. Here we characterize the features of ISM using 1) a controlled experiment of one week of continuous, simultaneous wear of two ActiGraph wGT3X-BT devices, with and without ISM enabled, and 2) during a seven-day assessment in a nationally representative sample of 13,649 participants (6-80 y) in the United States. In the controlled experiment, we found ISM engaged 38.9% ± 3.0% of the day (Mean ± SD) during 411.1 ± 93.2 unique events·day-1 with a 16.7 ± 3.5 second median duration. There were fewer (75.6 ± 14.0 events) but longer (117.2 ± 62.2 seconds) events in the early morning (00:00-05:59) and more frequent (146.4 ± 63.6 events) but shorter (9.7 ± 2.9 seconds) events in the afternoon (12:00-17:59). In the national sample, daily ISM engagement was (Mean ± SE) 43.6% ± 0.2% with the highest engagement during the early morning (78.4% ± 0.2%) and lowest during the afternoon (20.4% ± 0.3%). ISM engages during a substantial portion of the day, which is greater during, but not limited to, periods of low movement, such as plausible sleep or probable nonwear. Additional research is needed to better inform future study designs and analyses and interpretations of data previously collected with ISM enabled.	SR LaMunion, RJ Brychta, A Ishihara, KY Chen	2023	EPIG

2023-128	Sara		Gonzalez-Hernandez	NHLBI	Developmental Biology	Prox1 Misexpression Disrupts the Blood-Brain Barrier Integrity and Lymphatic Avascularity in the Central Nervous System	Idle sleep mode (ISM) is an optional battery-conserving feature for ActiGraph accelerometers that may have implications for data handling when data are collected with ISM enabled. There is limited documentation of the properties and characteristics of ISM, however, it is generally believed to engage during nonwear, periods of inactivity, and sleep. Here we characterize the features of ISM using 1) a controlled experiment of one week of continuous, simultaneous wear of two ActiGraph wGT3X-BT devices, with and without ISM enabled, and 2) during a seven-day assessment in a nationally representative sample of 13,649 participants (6-80 y) in the United States. In the controlled experiment, we found ISM engaged 38.9% ± 3.0% of the day (Mean ± SD) during 411.1 ± 93.2 unique events·day-1 with a 16.7 ± 3.5 second median duration. There were fewer (75.6 ± 14.0 events) but longer (117.2 ± 62.2 seconds) events in the early morning (00:00-05:59) and more frequent (146.4 ± 63.6 events) but shorter (9.7 ± 2.9 seconds) events in the afternoon (12:00-17:59). In the national sample, daily ISM engagement was (Mean ± SE) 43.6% ± 0.2% with the highest engagement during the early morning (78.4% ± 0.2%) and lowest during the afternoon (20.4% ± 0.3%). ISM engages during a substantial portion of the day, which is greater during, but not limited to, periods of low movement, such as plausible sleep or probable nonwear. Additional research is needed to better inform future study designs and analyses and interpretations of data previously collected with ISM enabled.	S Gonzalez-Hernandez, YS Mukouyama	2023	DEVBIO
2023-129	Heather		Kalish	NIBIB	Immunology	Microanalytical immunochemistry- what we do and how can we help?	Clinical samples often contain a wealth of information in a very small sample volume and at very low concentrations. The analysis of these samples must be rapid and highly sensitive. Our unit uses a variety of techniques to isolate, identify and quantitate proteins, cytokines, peptides, antibodies and other biological molecules of interest. MALDI-TOF imaging isolates and identifies proteins, peptides or lipids while providing spatial resolution. Using multiplex assays from Quansys™ and Meso Scale Design™, our unit has been able to rapidly analyze small sample volumes for numerous analytes with detection levels in the picogram range. ICP-OES spectroscopy enables us to provide quantitative measurements of trace metals. These powerful techniques allow for faster analysis of critical samples and ultimately lend themselves to comprehensive analysis of clinical samples.	S Porche, JC Nelson, H Kalish	2023	IMMUNO
2023-130	Joshua		Rich	NCI	Cell Biology	New frontiers in extracellular proximity labeling: Novel matrisome targets, diverse cell types, and 3-D culture conditions	The matrisome encompasses the genes and proteins that embody extracellular matrix (ECM) and ECM-associated proteins. Investigation of protein-protein interactions (PPIs) between matrisome targets is a promising direction to improve understanding of ECM diseases and therapeutic opportunities. Proximity labeling, a powerful technique for investigating protein interactomes based on enzyme-fusion constructs and affinity chromatography, has considerable potential in detailing proximal interactors of the matrisome. We have successfully developed an extracellular proximity labeling (ePL) approach based on fusion constructs containing the biotinylation enzymes BioID2 and TurboID. We have combined this approach with mass spectrometry to gain new insights into the interactome of the matrisome protein tissue inhibitor of metalloproteinase 2 (TIMP2), an endogenous metalloproteinase inhibitor found to have therapeutic potential. We have now expanded this approach to other matrisome protein targets, including tissue inhibitor of metalloproteinase 3 (TIMP3) and thrombospondin-1 (THBS-1). TIMP3 has been shown to possess anti-tumor properties, with loss of TIMP3 function associated with poor prognosis in multiple cancers. THBS-1 is a larger (129 kDa) matrisome protein that is relatively promiscuous with diverse functions in the tumor microenvironment. The role of THBS-1 in cancer is nuanced and appears to manifest in context-dependent pro- and anti-tumorigenic effects. Experiments to expand ePL to novel gene transfer techniques (transient transfection), cell lines, and culture conditions (suspension cell models, spheroids, 3-D cocultures) are currently underway. We show that ePL is a suitable method for studying PPIs in new protein targets and experimental conditions and expect to continue applying the technique broadly to additional matrisome targets.	JA Rich, SI Coates-Park, S Gurung, Y Liu, A Govil, S Kaur, D Roberts, W Stetler-Stevenson, D Peeney	2023	CELLBIO
2023-131	Patrick	H	Hallaert	NIAMS	Developmental Biology	GFI1 controls Merkel cell survival through a dependence receptor pathway	Merkel cells (MCs) are touch sensors found in mammalian skin that bear both neuronal and epithelial features. Understanding their differentiation is crucial for modeling normal skin lineage commitment and elucidating the pathogenic mechanisms underlying Merkel cell carcinoma (MCC). Single-cell RNAseq revealed that the transcriptional repressor Gfi1 was increasingly expressed as MCs differentiated. We also found that MCs specifically expressed GFI1 in mouse skin. Gfi1 knockout mice produced a normal complement of MCs that were abnormally dendritic and rapidly underwent postnatal apoptosis. This dendritic morphology was consistent with our finding that genes involved in CNS development and neuronal differentiation were highly differentially expressed in GFI1-deficient neonatal MCs. Surprisingly, GFI1-deficient MCs also showed upregulation of the neuronal axon guidance receptor Dcc. This dependence receptor promotes cell survival when bound to its ligand, NTN1, and triggers apoptosis in its absence. Ntn1 was downregulated in our analysis. Knockout of Dcc significantly abrogated GFI1-deficient MC loss, demonstrating that suppression of dependence receptor signaling is an essential role of GFI1 in MC survival. Our findings also extended to MCC cell lines and tumors, where RNAseq verified the presence of GFI1 expression. Furthermore, CRISPR/Cas9-mediated GFI1 knockout killed MCC cells and ChIP-seq revealed that GFI1 bound the DCC gene locus, suggesting that GFI1 directly regulates DCC expression. Together, our findings shed light on the transcriptional regulation of MC differentiation and maintenance, and revealed functional parallels present in MCC pathogenesis.	P Hallaert, L Miao, M Martin, L Collado, S Barkdull, A Coxon, B Gryder, I Brownell	2023	DEVBIO
2023-132	Xiukun		Wang	NIEHS	Stem Cell Biology	Genome-wide CRISPR/Cas9 screening in mouse primordial germ cell specification	The germ cell lineage ensures the transmission of heritable genetic and epigenetic information to the next generation. In mammals, the pluripotent epiblast cells in the post-implantation embryos give rise to both the somatic and germ cell lineages during subsequent development. Under inductive cell interactions, a small number of epiblast cells adopt the fate of the primordial germ cells (PGCs) and become the multipotent precursor of germ cells. However, the underlying mechanism is not fully understood. Fortunately, the epiblast to PGC specification can be recapitulated in vitro using embryonic stem cells (ESCs), albeit with low efficiency. The specification of PGCs is accompanied by the induction of key germ-cell genes, repression of the nascent somatic program, and widespread epigenetic remodeling. Here, we carried out a CRISPR/Cas9-mediated genome-wide genetic screen in PGC-like cells (PGCLCs) in vitro differentiation system and identified several key factors that are epigenetic barriers to PGC specification. Phenotypically, when the knockout of these genes or the use of chemical inhibitors against them, it promoted PGCLCs differentiation significantly up to ~20% in vitro. Consistently, the transcriptional analysis showed the germ cell maker genes are highly activated in the knockout PGCLCs. We are currently using genomic approaches including RNA-seq and CUT&TAG to dissect the underlying mechanism. Further, we are generating knockout mouse models or embryo aggregation to test whether the deletion can promote PGC specification in vivo. Together, our study uncovered epigenetic barriers in PGC cell fate specification and illustrated the power of genetic screens in the study of cell fate transitions.	XK Wang, SR Malki, B Bennett, G Hu	2023	STEMCELL
2023-133	Shriniwas		Patwardhan	CC	Neuroscience	Ultrasound imaging as a tool to track joint kinematics across persons with varying muscle sizes	Sonomyography measures muscle deformation with ultrasound. The extracted signals can be used to proportionally control a device. Although point-to-point reaching movements in healthy individuals are known to follow a minimum jerk trajectory, it is unknown if muscle activation follows a similar control policy. To test this, we performed an experiment (10 subjects) in which seven virtual targets (five trials each) were presented on a screen. Subjects were asked to acquire these virtual targets by flexing/extending their wrist, that in turn drove a virtual cursor left/right based on the extent of flexion/extension measured by sonomyography. To assess potential feasibility in individuals with neurological disorders that result in reduced muscle volume, we examined how differences in muscle size affect the control relationships and the ability of ultrasound to capture them. Muscle thickness was defined as the distance between the superficial adipose tissue-muscle interface and the muscle-bone interface. Velocity profiles derived from imaging muscle activation during target acquisition followed a minimum jerk trajectory. Average muscle thickness across subjects was 3.35±0.44 cm. Target acquisition results showed very low average standard deviation in position traces across trials (4.4%). These current results show that sonomyography can track muscle kinematics to reveal the common minimum jerk trajectory control policy in real-time across a group with varying muscle thickness. These findings support the use of sonomyograpy to characterize muscle contraction trajectories in individuals with upper-neuromotor pathology, such as stroke or cerebral palsy, which could reveal whether their isolated muscle contractions follow similar control policies.	SM Patwardhan, JS Schofield, WMJ Joiner, TC Bulea, S Sikdar	2023	NEURO
2023-134	Yan		Zhuang	CC	Biomedical Engineering and Biophysics	Evaluating the Segment Anything Model for MRI Organ Segmentation Using a Simulated Interactive Setup	Segment Anything Model (SAM) is a recently released deep learning foundation model for image segmentation. We evaluated the multi-organ segmentation capabilities of the SAM as an interactive semi-automated annotation tool for magnetic resonance (MR) images. The evaluation utilized a simulated interactive annotation setup in a publicly available multi-organ MRI dataset (AMOS22). The initial prompt given to SAM was the ground truth bounding box with added random jitter. SAM then outputted an initial segmentation mask. In subsequent iterations, SAM took point-based prompts, as well as all previous prompts and the current segmentation mask, to generate the next refined segmentation mask. This procedure was repeated for 10 iterations to produce the final segmentation. The segmentation results of target 15 organs were evaluated against the ground truth masks using the Dice similarity coefficient (DSC) on 2D slices. The mean±std DSC for 15 organs after the initial bounding box prompt was 0.777±0.049. The final mean±std DSC after 10 iterative steps was 0.901±0.056. The best three organs were the right kidney (0.954±0.034), left kidney (0.951±0.028), and spleen (0.949±0.051). The worst three organs were right adrenal gland (0.807±0.113), prostate/uterus (0.819±0.246), and duodenum (0.825±0.156). The mean DSCs increased monotonically with the number of prompts, implying better segmentation results. Experimental results demonstrated that after 10 iterations, the SAM model was able to provide reasonable segmentation results for most of the organs in the MRI images, indicating that the SAM model can potentially reduce radiologists' annotation burden for segmenting MR images to just a few mouse clicks.	Y Zhuang, B Hou, P Mukherjee, RM Summers	2023	BIOENG
2023-135	Gregory		Tawa	NCATS	Computational Biology	Canine models for characterization, diagnosis, and treatment of human cancers using comparative canine-human multi-omics.	Most cancer modeling experiments are performed on rodents. While rodent models have been invaluable for investigating cancer mechanisms, they have not always been representative of the disease in humans. The use of companion animals to understand human tumor biology stems from decades of scientific observation that pet dogs spontaneously develop malignancies that share characteristics with human cancers. In this context, we developed an experimental/bioinformatics pipeline that generates and analyzes multi-disease, multi-species, next-generation sequencing data, identifies relevant disease genes common to the species analyzed and based on these common genes enumerates potential drug targets and therapeutic drug combinations. Validation of candidate genes is conducted using proteomics experiments to ensure that they express as proteins in tissue and existing drugs are identified that are known to modulate protein expression opposite to that exhibited in the disease. Drug combinations are derived such that each drug modulates different proteins to maximize synergy. Matrix screens are performed on canine cell lines and combinations that show significant efficacy and synergy are selected for further study in mouse PDX models with the eventual goal of translating these combinations into in vivo canine and human studies. Using this strategy, we found 68 protein targets and 6 drug combinations exhibiting synergy for canine osteosarcoma. Mouse PDX experiments at NCI are ongoing to evaluate these six drug combinations in vivo. This work exemplifies an approach that further establishes the relevance of canine to human cancer and provide opportunities to explore cancer mechanisms and treatments in both species.	G Tawa, A Leblanc, D Gerhold, J Braisted, G Grewal, G Sittampalam, C Mazcko, M Breen, D Thamm	2023	COMPBIO
2023-136	Michaella		Bono	NEI	Neuroscience	Exploring the impact of CD8+ T cell development on memory decline in Alzheimer's disease-like mouse models	Alzheimer's Disease (AD) is a prevalent cause of dementia, affecting approximately 6.7 million individuals aged 65 and above in the United States, with no effective cure currently available. While our understanding of the immune system's role in central nervous system diseases is advancing, the involvement of lymphocytes, specifically CD8+ T cells, remains incompletely understood. In our recent investigation, we utilized immunohistochemical and flow cytometry techniques to examine mouse models of Alzheimer's Disease, namely the 5xFAD and APPSAA models known for their formation of amyloid beta plaques, a hallmark of AD in humans. Through our study, we observed a significant increase in CD8+ T lymphocytes, a population of cytotoxic immune cells, in aged and AD-like mice. Moreover, we demonstrated that inhibiting the development of CD8+ T cells in these mice, achieved by deleting beta-2 microglobulin (B2m), led to improved memory and reduced plaque load. To gain a deeper understanding of the specific contributions of CD8+ T cells in AD pathology, we are currently utilizing a depletion antibody to target and eliminate CD8+ T cells in AD-like mice. Our hypothesis suggests that this intervention may provide a means to rescue or prolong memory in these mice, potentially unveiling novel therapeutic avenues for AD. By further exploring the impact of CD8+ T cells on AD progression, we aim to enhance our comprehension of the disease mechanisms and identify potential targets for therapeutic intervention.	M Bono, A Behensky, J Gopalakrishnan, N Fernando, HY Shih	2023	NEURO
2023-137	Mathew	J	Koretsky	NIA	Genetics and Genomics	Genetic risk factor clustering within and across neurodegenerative diseases	Overlapping symptoms and co-pathologies are common in closely related neurodegenerative diseases (NDDs). Investigating genetic risk variants across these NDDs can give further insight into disease manifestations. In this study we have leveraged genome-wide single nucleotide polymorphisms and genome-wide association study summary statistics to cluster patients based on their genetic status across identified risk variants for five NDDs (Alzheimer's disease, Parkinson's disease, amyotrophic lateral sclerosis, Lewy body dementia and frontotemporal dementia). The multi-disease and disease-specific clustering results presented here provide evidence that NDDs have more overlapping genetic etiology than previously expected and how neurodegeneration should be viewed as a spectrum of symptomology. These clustering analyses also show potential subsets of patients with these diseases that are significantly depleted for any known common genetic risk factors suggesting environmental or other factors at work. Establishing that NDDs with overlapping pathologies share genetic risk loci, future research into how these variants might have different effects on downstream protein expression, pathology and NDD manifestation in general is important for refining and treating NDDs.	MJ Koretsky, C Alvarado, MB Makarious, D Vitale, K Levine, S Bandres-Ciga, A Dadu, SW Scholz, L Sargent, F Faghri, H Iwaki, C Blauwendraat, A Singleton, M Nalls, H Leonard	2023	GEN
2023-138	Mina		Peyton	NIAID	Epidemiology	Using real-world data from the All of Us Research Program and UK Biobank to investigate the impact of Tuberculosis	Real-world data (RWD), defined as data routinely collected from various sources related to patient health status and/or the delivery of health care, has experienced significant growth. RWD is generated from a wide range of technology-driven services and devices. Moreover, coordinated efforts and programs, such as the All of Us Research Program (AoU) and UK Biobank (UKB) have contributed to this data amplification. Both programs provide robust health datasets to support researchers in advancing biomedical and public health research. With increased RWD, we questioned whether data repositories like AoU and UKB could be utilized to investigate the impact of tuberculosis (TB). We hypothesize that they could serve as reference data for comparison with selectively collected data, including the NIAID TB Portals (TBP). TBP, an international program comprised of drug-resistant TB data from developing countries, requires a reference dataset for certain comparative analyses. Building reference control cohorts from AoU and/or UKB for comparison with TBP (e.g., case-cohort analysis) has the potential to highlight important aspects of TB treatment and healthcare utilization. To create an initial TB reference cohort from these sources, we employed the WHO TB case definition (TB bacteriologically confirmed) as well as an adapted TB case definition (SNOMED TB code on two distinct days). We identified 33 and 1,542 TB cases, respectively, within AoU. In the UKB, we identified 2,740 TB cases using the WHO TB case definition. While both countries have low TB incidence rates, we found a sufficient number of TB cases for use as a reference set.	MP Peyton, G Rosenfeld, A Gabrielian, M Harris, Z Yaniv, A Rosenfeld, D Hurt	2023	EPIG

2023-140	Kevin		Hsu	NCI	Immunology	Understanding NKT cells through sulfatide analogues	The goal of this research is to further investigate NKT cell activation using sulfatide analogues. NKT cells have been shown to play a significant role in mediating inflammatory immune responses and because of this, there has been strong interest in pharmacologically regulating this compartment to fight cancer. NKT cells recognize lipids that are loaded on CD1d molecules on the surface of cells, and it has been shown that structural modifications of these lipids directly affect NKT cell activation and polarization. Our work is focused on the impact of modifications of sulfatide, which is a glycolipid that can be loaded onto CD1d which is known to activate sulfatide-reactive (generally type II) NKT cells when presented by CD1d monomers on plastic. We have numerous sulfatide analogues with modifications (based on previous work with alpha-galactosylceramide analogues) on the acyl chain, sphingosine chain, and changes of beta-anomeric to alpha-anomeric. These analogues have been screened with NKT cell hybridomas, DN32 and XV19, to assess their effect on activation of type I and type II NKT cells, respectively. We observed that alterations in the sphingosine or acyl chain in sulfatides do not always mimic the effects on activity of similar changes in alpha-galactosylceramide analogues and that numerous sulfatide analogues can activate DN32 (not sulfatide-reactive) when presented on CD1d monomer or bone marrow-derived dendritic cells. Our results provide further insight into NKT cell activation and have identified sulfatide analogues that may be applicable to cancer therapy by activating type I NKT cells.	KS Hsu, PB Olkhanud, IK Luvaga, E Kanyo, SK Richardson, N Sassu, A Howell, JA Berzofsky	2023	IMMUNO
2023-141	Juhyun		Kim	NIDDK	Molecular Biology and Biochemistry	Myb is regulated by -81 enhancer eRNA transcript Myrlin through recruitment of MLL1 complex	The Myb proto-oncogene encodes the transcription factor c-MYB, which is critical for the proliferation and differentiation of hematopoietic stem and progenitor cells. Distant enhancers of Myb expression have been characterized but the regulation of Myb during hematopoiesis is still incompletely understood. Here we identified a novel nuclear Myb enhancer long intergenic non-coding RNA (Myrlin) that originates from the -81 kb murine Myb enhancer within the Myb – Hbs1l intergenic region. Myrlin and Myb are coordinately regulated in a developmental stage-specific fashion during maturation of erythroid progenitors and upon differentiation of MEL cells. CRISPR/Cas9 genome editing of the Myrlin transcription start site at the -81kb enhancer reduced both Myrlin and Myb expression. The deletion of Myrlin TSS reduces the occupancy of LDB1, which mediates chromatin looping, and compromises long-range contacts between the Myb promoter and enhancer and RNA Pol II occupancy decreases across the Myb locus. In contrast, silencing of Myrlin using CRISPRi similarly reduced both Myrlin and Myb expression but left the Myb enhancer hub undisturbed, separating chromatin looping from transcription activation of Myb. In unedited cells, we found that Myrlin interacts with MLL1 complex, a transcriptional coactivator that plays an essential role in regulating gene expression during hematopoiesis. Myrlin CRISPRi compromised MLL1 occupancy in the Myb locus and decreased CDK9 and RNA Pol II binding. Myrlin CRISPRi further resulted in pausing of RNA Pol II in the Myb first exon/intron. These data suggest that Myrlin directly participates in activating Myb transcription by recruiting MLL1.	J Kim, LF Diaz, A Dean	2023	MOLBIO
2023-142	Angelina		Angelova	NIAID	Computational Biology	WGSA2 – An assembly-based shotgun metagenomics data analysis pipeline, implemented online in Nephele, a microbiome analysis cloud platform	Widespread interest in microbiome exploration has resulted in the development of various powerful computational tools and pipelines online, which can save the researcher from the burden of bioinformatics processing of their metagenomics data. Among these, some can extract taxonomic and functional information directly from shotgun metagenomic short reads (e.g. MetaPhlAn). However, more comprehensive analysis require longer contiguous sequences (e.g. KEGG tools, BLASTp). Unfortunately, there is a scarcity of online tools that provide researchers with computational resources and a command line-free experience to assemble short-read metagenomic datasets for deeper exploration. To bridge this computational gap, we have designed, developed, and integrated a command line-free Whole Metagenome Sequencing Assembly-based pipeline – WGSA2, into our cloud-based microbiome analysis platform, Nephele (https://nephele.niaid.nih.gov/). The WGSA2 pipeline processes shotgun datasets from complex microbial communities and diverse habitats (both host-associated and environmental) producing visualizations and summarized output based on functional and taxonomic annotation and binning of assemblies. The pipeline provides a user-friendly experience, that omits computational demands and experience, allows for processing customizations including a choice of databases (e.g. RefSeq, MGBC, KEGG, MetaCyc) and for efficient acquisition of biological detail. Overall, the WGSA2 pipeline allows users to gain an understanding of their metagenomic dataset as well as easy access to an assembly-based sequence and analysis of their dataset.	AG Angelova, D Doan, P Subramanian, M Quiñones, L Kim, M Dolan	2023	COMPBIO
2023-143	Darian		Williams	NCATS	Molecular Pharmacology	Development of a First-in-class High Throughput Screening Assay Based on Chromatin Accessibility	Chromatin dysregulation has been implicated in the development of a wide range of diseases, including cancer, where genetic alterations in chromatin regulatory factors and aberrant activity of transcriptional regulators alters chromatin states. Mutations in many chromatin-associated proteins have been recognized as driver mutations across multiple diverse tumors. As appreciation of the importance of chromatin dysregulation in cancers has grown, chromatin regulatory proteins have emerged as promising targets for therapeutic discovery. To identify small-molecule regulators that can reverse chromatin alterations in cancer, we are developing a target agnostic small molecule screening technology that exploits tumor-specific chromatin accessibility states as a relevant and direct functional readout for identifying novel therapeutics. Towards this goal, we have developed a high-throughput version of the Assay for Transpose-Accessible Chromatin with sequencing (ATAC-seq), termed HT-ATAC-seq (high-throughput ATAC-seq). As a proof-of-concept, we are assaying chromatin accessibility in models of Ewing sarcoma, a highly aggressive pediatric cancer with ~50% mortality. Using this cancer model, we have developed a nuclei preparation method that can reproducibly isolate nuclei from cells from each well across an entire 384-well plate for subsequent ATAC-seq. From a small-molecule library pilot screen of 331 annotated modulators of the epigenome, we identified several previously established regulators of chromatin structure in Ewing sarcoma, including the HDAC inhibitor Panobinostat, as well as several novel chromatin regulators. This assay not only shows promise for identifying modulators of chromatin state in Ewing sarcoma, but we anticipate the assay platform could be implemented in other cancers or diseases with altered chromatin states.	D Williams, A McFadden, T Sanchez, AJ Hepperla, M Henderson, G Stott, I Davis, S Pattenden	2023	PHARMA
2023-144	Mousumi		Sahu	NIAMS	Computational Biology	Activated B cells exhibit altered metabolic programs in Systemic sclerosis skin	Background Systemic sclerosis (SSc) is a rare, chronic disease characterized by autoimmunity, vasculopathy and fibrosis. Here, we examine mitochondrial (mt) gene expression in SSc skin single cell RNA sequencing data and identify activated B cells as the major cell type. Materials and methods We analyzed skin single cell RNA expression profiles of 10 healthy individuals and 27 SSc patients using Seurat and identified different skin cell-types. We interrogated expression of 14 protein-coding mt genes. Differentially expressed genes were used to identify pathways/processes dysregulated in SSc. Metabolic gene expressions were imputed in each cell and were used to estimate cell-wise fluxome. Results and discussion We identified up-regulation of 10 mt-genes (p<0.05, Log2FC = +/- 0.25) in SSc B cell as compared to healthy individuals. These genes included ATP synthase (MT-ATP6), Cytochrome c oxidase (MT-CO1, MT-CO2, MT-CO3) and NADH dehydrogenase (MT-ND1, MT-ND2, MT-ND3, MT-ND4, MT-ND4L and MT-ND5). MT-ND3 was found to have a higher expression in different SSc skin cell-types as compared to controls. Pathway enrichment analysis identified major pathways involved in fulfilling metabolic/energy needs of SSc B cells. Up-regulation of B cell receptor signaling pathway was also seen in these SSc B cells. Sub-clustering of B cell identified increased number of activated B cells in SSc with higher mt-gene expression. This metabolically activated B cells seen in SSc, had an increased class-II HLA gene expression as well. Activated B cells were found to have high Deoxycytidine yield which could be potential target in SSc.	M Sahu, R Lafyatis, P Gourh	2023	COMPBIO
2023-145	Mohammad		Moniruzzaman	NIMHD	Epidemiology	Neighborhood-level racial residential segregation and sedentary behavior in US adults	Introduction and Objective: Sedentary behavior (SB) is highly prevalent in United States (US) adults, spending an average of 9.5 hours/day sedentary, resulting in several negative health outcomes. Racial residential segregation may affect SB. We investigated whether neighborhood-level racial residential segregation is associated with sedentary time in a nationwide sample of US adults. Methods: We analyzed data from 2637 US adults aged 20–75 years (mean age [45.1 years], Female [50.6%] from the population-based AmeriSpeak panel who completed the Activities Completed over Time in 24-hours (ACT24) previous-day recall in 2019. Total daily SB (hours/day) was assessed via ACT24 recalls. We quantified segregation using isolation index (range 0 to 1) at the county level for three racial/ethnic groups: Black, Hispanic, and Asian adults (ref White). A higher index value indicates higher segregation. We performed a weighted linear regression model to assess the relationship of isolation index with time spent in SB, adjusting for age, sex, marital status, education, occupation, household income, regions, and body mass index. Findings: Counties with higher Black isolation were significantly associated with increased time spent in SB (β = 0.85, 95% confidence interval [0.28, 1.41], p = 0.004). We found similar results for Hispanic adults (β = 0.68, [0.08, 1.27], p = 0.027) and Asian adults with stronger association (β = 1.55, [0.45, 2.66], p = 0.007). Conclusions: Those Black, Hispanic, and Asian adults residing in a racially segregated neighborhood from White adults were associated with longer sedentary time in this nationwide sample of US adults.	M Moniruzzaman, Y Deng, S Islam, K Jones, D Berrigan, CE Matthews, K Tamura	2023	EPIG
2023-146	Emma		(Chang)-Rabley	NIAID	ACI/IRS	Towards standardized data collection methods for early epidemics: a scoping review	Well-designed observational studies have a tremendous capability to improve early epidemic response because of the speed at which they can be initiated, lack of experimental interventions, and potential to contribute large amounts of pooled data. Currently, no widely standardized protocol exists for nonrandomized observational data collection during early epidemics. This lack of consistency leads to variable data that often influences larger clinical trials or public health policy. Standardized data collection methods would improve our understanding of early epidemics, empowering public health officials and communities to respond more effectively and fairly. To do this, we first need to understand the current landscape of data collection in observational studies early in epidemics, including specifics about study design and the quality and timing of reported evidence. We will do this by conducting a scoping literature review to map and characterize observational data collection methods that have been employed during outbreaks of SARS-CoV-1, H1N1, Zika virus, and Ebola declared by the WHO between 2000-2019. Specifically, we will evaluate all peer-reviewed literature published in the first 12 months from an outbreak's start date (as defined by the WHO Emergency Disease Outbreak Network), as well as grey literature from reputable targeted sources. We will then attempt to quantify the policy and community impact of the methods and their limitations, and identify potential areas for improvement. Our aim is to comprehensively understand how data was collected, its quality, and its impact in the early phase of these selected epidemics.	EH (Chang)-Rabley, EE Ricotta	2023	ACI/IRS
2023-147	Mary	B	Makarious	NIA	Genetics and Genomics	Genome-wide association identifies novel etiological insights associated with Parkinson's Disease in African and African admixed populations	Aim: This research aims to conduct a comprehensive genome-wide study of Parkinson's disease (PD) in African and African admixed populations to elucidate ancestry-specific risk, genetic variations, and reveal novel disease mechanisms. Background: Genetic understanding across varied populations can shed light on complex traits like PD. However, the majority of PD genetics knowledge comes from European, Asian, and Latin American populations, leaving a significant knowledge gap concerning African and African admixed ancestries. Materials & Methods: We performed an extensive genome-wide assessment of PD in a large cohort comprising 197,918 individuals. The cohort included 1,488 PD cases and 196,430 controls, all of African and African admixed ancestry. Factors like ancestry-specific risk, differential haplotype structure, coding, structural genetic variation, and polygenic risk profiling were investigated. Results: A novel PD risk factor at the GBA1 locus, specifically the intronic rs3115534-G variant, was discovered. This risk factor, influencing age at onset, is rare in non-African/African admixed populations. Unlike previous GBA1 associated risk variants, this new signal likely mediates PD risk via expression quantitative trait locus (eQTL) mechanisms, indicating a unique functional mechanism. Discussion: This research identifies a novel GBA1 genetic risk factor in African and African admixed populations, contrasting prior studies on Northern European populations. The findings underscore the necessity for equitable inclusion in PD clinical trials, highlighting the importance of understanding ancestry-specific genetic risk. The inclusion of underrepresented groups offers fresh avenues towards RNA-based therapies aimed at reducing lifetime PD risk, crucial as the field progresses towards precision medicine in PD clinical trials.	MB Makarious, M Rizig, S Bandres-Ciga, O Ojo, P Wild Crea, O Okunoye, Nigeria Parkinson Disease Research Network International Parkinson's Disease Genomics Consortium - Africa (IPDGC Africa), Black and African American Connections to Parkinson's Disease (BLAAC PD) Study Group 23andMe Research Team, M Nalls, C Blauwendraat, H Houlden, A Singleton, N Okubadejo, on behalf of the Global Parkinson's Genetics Program	2023	GEN
2023-149	Said		Briseno Gonzalez	NIAID	Microbiology and Infectious Diseases	Roseomonas mucosa protects human keratinocytes from cell death and boosts hBD-3 production in an in vitro model of Staphylococcus aureus infection	Dysbiosis of the skin microbiota has often been associated with inflammatory skin conditions, such as atopic dermatitis. Given that keratinocytes represent the major cell type which constitutes the epidermis, they are excellent targets for the analysis of host-microbe interactions which occur on the skin. In this study, we analyzed the potential mechanisms of action by which R. mucosa, a skin commensal isolated from a healthy volunteer, protects human primary keratinocytes during infection with S. aureus. Keratinocyte monolayers were co-cultured with S. aureus and R. mucosa, and antimicrobial peptide (AMP) production and cell death were measured. S. aureus alone induced significant cell death as expected. However, co-culture with both R. mucosa and S. aureus had significantly reduced apoptotic and dead cell populations. Additionally, keratinocytes co-cultured with R. mucosa and S. aureus had significantly higher production of the AMP hBD-3, compared to keratinocytes incubated with either species alone; this trend was not observed for other AMPs such as hBD-2, S100A7, S100A9, nor S100A8. Overall, the skin commensal, R. mucosa, appears to provide protection for keratinocytes by boosting AMP production in the presence of pathogens and by ameliorating cell death caused by S. aureus-induced inflammation. The intracellular signaling mechanisms behind these protective effects mediated by R. mucosa will be further investigated.	S Briseno Gonzalez, P Gough	2023	MICROBIO

2023-150	Sarah		Porche	NIBIB	Immunology	Applications of MALDI-TOF mass spectrometry for biomolecule and tissue analysis	Matrix-assisted laser desorption/ionization time-of-flight (MALDI-TOF) mass spectrometry (MS) is a versatile analytical technique that can be adapted to target a diverse range of biomolecules. Here, the use of MALDI-TOF MS as a tool for targeted immunochemical profiling, as well as bottom-up spatial analysis of analytes, is discussed. Our unit, in collaboration with the Laboratory of Immunoregulation at NIAID, uses MALDI-TOF MS to profile IgG3 glycosylation in HIV-infected chronically viremic and healthy individuals. Following chemical glycosylation and spotting onto a target plate, the mass distribution of four major glycoforms is analyzed with MALDI-TOF MS. The resulting glycosylation patterns are then compared. Alternatively, through a non-targeted, bottom-up approach, MALDI-TOF can be adapted for tissue imaging to achieve comprehensive spatial analysis of histological samples. During the MALDI imaging process, tissue slides are subjected to a series of washes and coated with specialized matrices to favor lipid, peptide, or protein expression. Following imaging, our unit uses statistical analysis software to generate heat maps and segmentation of the tissue. Based on these results, droplet probe extraction is used to isolate analytes from regions of interest. Liquid chromatography-mass spectrometry (LCMS) is used to further break down analytes into their fragment ions and provide identification of unknown species from proteomic and lipidomic databases. Through these methods, MALDI-TOF MS can quickly provide valuable analytical insight for various sample types and targets.	S Porche, JC Nelson, S Moir, H Kalish	2023	IMMUNO
2023-151	Tzu-Hsiang		Huang	NINDS	Neuroscience	Interrogating neurodegeneration-linked CHCHD2 and CHCHD10 and their mitochondrial interaction network	Dominant mutations in the paralogs CHCHD2 (C2) and CHCHD10 (C10) cause neurodegenerative disease. These nuclear-encoded small mitochondrial proteins localize to the intermembrane space side of mitochondrial cristae. Their functions are crucial for maintaining cristae structure and oxidative phosphorylation (OXPHOS). However, the detailed molecular mechanism of their action has not been fully characterized. Using a novel antibody and C2/C10 double knockout (DKO) cell lines and mouse models, we established steady interactors of C2/C10 in cell culture and in vivo through affinity purification mass spectrometry. We confirmed several previously published interactors and established that OXPHOS subunits are major interactors. By using KO cell lines of individual interactors, we found that the number of C2/C10 interactors was dramatically increased in cell lines with disrupted mitochondrial cristae, including TAZ, SLP2, and MIC60 KO lines. We knocked out C2/C10 from these lines to produce triple knockout (TKO) lines and found that the protein abundance of the increased interactors is downregulated in TKO lines. These TKO cells exhibit severe growth defects in galactose medium, as they can only rely on OXPHOS to produce ATP. In addition, we identified that FIS1 and DRP1 are crucial for DKO cell survival by using a genome-wide lethality screen. It suggests that the disruption of FIS1-DRP1-mediated mitochondrial fission machinery impacts DKO cell survival. Therefore, we hypothesize that C2/C10 may have chaperone-like functions by stabilizing their interactors to maintain mitochondrial function. This function of C2/C10 may be conditionally essential in the setting of cristae disruption or failure of mitochondrial quality control fission.	TH Huang, N Randolph, XP Huang, B Wu, DP Narendra	2023	NEURO
2023-152	Vijay	A	Ramchandani	NIAAA	Clinical Research	Health coping behaviors and alcohol and mental health outcomes during the COVID-19 pandemic	This study aimed to evaluate endorsement of health (coping) behaviors during the COVID-19 pandemic by participants with and without alcohol use disorder (AUD), and the impact of these health behaviors on perceived stress, mental health outcomes, loneliness, and drinking motives and behaviors. Participants (n=448, 52% female, 44% non-White) completed a longitudinal survey that included a scale assessing a range of positive and negative coping behaviors. A latent class analysis (LCA) identified two classes characterized by: high (Class I, 82%) and low (Class II, 17.9%) probability of positive coping behaviors. We examined associations between latent classes of coping behaviors with perceived stress (PSS), anxiety (GAD-7), depression (PHQ-9), loneliness (UCLA), drinking-to-cope (DMQ-Coping) and drinking behavior (total AUDIT), and demographic variables. There were significant differences between AUD and non-AUD groups across coping behavior classes, in PSS, GAD-7, PHQ-9, DMQ-Coping, UCLA and Total AUDIT scores, after covarying for age, gender, race and income level. Class 2 participants with AUD had significantly higher scores for PSS, GAD-7, PHQ-9, Coping DMQ and Total AUDIT scores than participants in Class 1 with AUD. For GAD-7, PHQ-9 and DMQ Coping measures, a high probability of endorsing positive coping behaviors (Class 1) dampened the effect of AUD status on these outcomes. Individuals with a low probability of positive coping behaviors demonstrated significantly greater perceived stress, anxiety and depressive scores, drinking-to-cope motives, and drinking behavior. Endorsement of positive coping behaviors may be especially important for individuals with AUD. Future health interventions should target populations with poor coping behaviors.	EM McCabe, JW Luk, BL Stangl, ML Schwandt, R Momenan, D Goldman, N Diazgranados, VA Ramchandani	2023	CLINICAL
2023-153	Yangyang		Deng	NIMHD	Epidemiology	Identify correlates of the physically active day using machine learning methods on neighborhood environments: ACT24 Data	Background: Previous studies of physical activity (PA) have focused on estimating average levels of PA for people. An alternative perspective is to examine correlates of active days, but little is known about specific factors contributing to an active day and how neighborhoods play a key role. This perspective could inform the development of effective population-level interventions to increase PA. Methods: A total of 2,625 participants (mean age [SD] = 45.2 [15.38]) from the AmeriSpeak panel, aged 20-75, completed up to two activity recalls over 24 hours using the Activities Completed over Time in 24 Hours (ACT24) instrument in 2019. A physically active day was categorized as "sufficient" (≥ 1.6 physical activity levels [PAL]) or "insufficient" (<1.6 PAL). A set of 25 variables were analyzed, including demographics (e.g., age, gender, and occupation), health-related factors (BMI), and neighborhood characteristics (segregation and walkability indices, and county-level census variables). Supervised machine learning (ML) algorithms, including random tree-based models, were used to identify the key correlates of a physically active day. Results: We have identified the top 10 predictors that significantly contribute to a physically active day at individual and neighborhood levels. These predictors were ranked in the following order: population density, age, walkability, education, income, region, race/ethnicity, county-level poverty, marital status, and BMI. Conclusion: Tree-based ML algorithms suggest that both individual and area-level characteristics are associated with active days. Furthermore, some of the identified correlates of active days include modifiable features of the environment and could inform community-level interventions for at-risk areas.	Y Deng, M Moniruzzaman, B Rogers, K Jones, D Berrigan, C Matthews, K Tamura	2023	EPIG
2023-154	Armond	J	Isaak	NCI	Cancer Biology	Investigation of molecular alterations associated with double resistance to BRAF and MEK inhibition in melanoma	A primary cause of melanoma in patients is a mutation of the BRAF protein in the MAPK signaling pathway. Inhibition of mutant BRAF by BRAF inhibitors (BRAFi) in patients with advanced melanoma yields a remarkable initial clinical response. Limited duration response and disease recurrence due to acquired drug resistance continue to be urgent clinical issues. Preclinical studies have suggested concurrent inhibition of BRAF and MEK using inhibitors (BRAFi and MEKi) to block hyperactivated MAPK signaling. However, most patients treated with this combination therapy still relapse due to acquired resistance. Extending our studies to examine the mechanism of both BRAFi and MEKi resistance (double resistance, DR) in mutant BRAF melanomas, we have developed models from four human melanoma cell lines to explore the hypothesis that molecular alterations are related to double resistance to BRAFi and MEKi in melanoma. We have found that BRAFi-MEKi double-resistant models exhibit distinct differences in morphology and growth kinetics. Specifically, BRAFi-MEKi double-resistant human melanomas express a higher level of FGFb and PAI-1 expression. We confirmed that overexpression of FGFb and PAI-1 in parental cells could increase the ability to resist BRAF and MEK inhibition. Additionally, we discovered that decreased expression of FGFb and PAI-1, via knock-down or inhibition in double resistant cells, can restore cell sensitivity to treatments of BRAFi and MEKi. Our findings uncover the mechanism of how melanoma cells escape BRAFi and MEKi attacks and offer a rational strategy to guide clinical treatment.	AJ Isaak, GR Clements, L Huang, Y Qin, Q Zho, G Merlino, Y Yu	2023	CANCER
2023-156	Tiffany	P	Nguyen	NIDCR	Molecular Biology and Biochemistry	Critical Role of Fibrinolysis in Hematopoietic Recovery After Myelosuppression	Bone marrow responds to myelosuppression by expanding the hematopoietic stem cell population. Fibrinolysis is the breakdown of fibrin. Plasmin, a fibrinolytic protease, has been shown to be required for hematopoietic recovery. Fibrin deficiency alleviates many pathologies seen in plasmin-deficient (Plg-/-) mice such as impaired wound healing and periodontitis. 5-Fluorouracil (5-FU), a highly used chemotherapy drug, induces bone marrow injury, and elevated fibrin deposition in bone marrow has been observed within three days after treatment. Our study aims to evaluate the importance of fibrinolysis in hematopoietic recovery by investigating whether fibrin mediates myelosuppression. Using an in vivo model, we determined mouse survival and fibrin deposition after 5-FU treatment to see if hematopoietic recovery is critical for survival. An siRNA targeting fibrinogen (siFibrin) or a scrambled control (siLuciferase) was used to determine whether 5-FU toxicity in Plg-/- mice is fibrin-dependent. We found that plasmin is required for hematopoietic recovery in a 5-FU-induced myelosuppression model, and that reduced fibrin deposition improved survival. Our work suggests that the pharmacological depletion of fibrin via siFibrin partially rescues myelosuppressed Plg-/- mice and improves sustained hematopoietic recovery. Collectively, these data suggest that pharmacological reduction of fibrin may reduce toxicity of myelosuppressive chemotherapy drugs.	TP Nguyen, YG Jiang, LJ Juang, CJ Kastrup, LM Silva, TH Bugge	2023	MOLBIO
2023-157	Kobe	C	Robichaux	CC	Virology	Illuminating the relationship between Hepatitis C Virus and B cell disorders: Detection of viral genome in peripheral B cells using RNAscope	Approximately 58 million people are currently infected with Hepatitis C Virus (HCV). HCV is an enveloped, positive-strand RNA virus that primarily infects hepatocytes but has been reported to infect lymphocytes. Epidemiological studies have shown that chronic HCV infection is associated with increased risk of developing lymphoproliferative disorders, including B cell non-Hodgkin's lymphoma. The mechanism underlying this association is unclear. It may consist of direct oncogenic effects or an indirect mechanism. Direct effects refer to potential HCV infection of B cells, while indirect mechanism includes viral interaction with cell surface receptors via chronic antigen stimulation and/or CD81 engagement. The detection of HCV replication in B cells would support the hypothesis of direct virus-mediated lymphomagenesis, where the virus could trigger oncogenic events via intracellular viral proteins. This study aims to further elucidate these mechanisms by visualizing HCV positive and negative strand RNA in B cells using RNAscope fluorescent in situ hybridization. B cells were isolated from whole blood of HCV-infected patients and healthy donors and probed for CD19 mRNA and HCV positive-strand RNA. CD19 serves as a B cell marker and HCV positive-strand RNA indicates the presence of the virus. Preliminary data show successful visualization of CD19 mRNA and HCV positive-strand RNA. Optimization of the negative-strand HCV RNA probe is ongoing. Visualization of this RNA would indicate viral proliferation within B cells. Results from this study will confirm the existence of extrahepatic reservoirs for HCV and provide more direct evidence of viral protein expression in HCV associated lymphoma.	KC Robichaux, AN Henning, V de Giorgi	2023	VIROL
2023-158	William	J	Becker	NCI	Cancer Biology	Triple synergy between cancer vaccine and checkpoint inhibitors in a pre-clinical tumor model	Despite advances in checkpoint inhibitor (CPI) therapy for cancer, many cancers remain resistant. Tumors deemed 'cold' based on insufficient T cell infiltration into tumors show reduced potential for CPI therapy. Cancer vaccines may overcome this resistance by inducing the needed T cell immune response against the tumor to synergize with CPIs when the absence or low levels of anti-tumor T cells contributes to the primary resistance to CPIs. Here we used a mouse tumor model, TC1, expressing HPV16 E6 and E7 oncogenes, and administered a vaccine consisting of the E7 peptide combined with alpha-galactosylceramide (a potent NKT cell agonist) and GM-CSF as adjuvants. We show the synergy between the tumor-antigen specific vaccine and the combination of two CPIs, anti-TIGIT and anti-PD-L1. The synergistic effect of the triple combination provides more protection against tumor growth than either treatment alone or any pairwise combination and significantly improves survival in a CD8+ T cell-dependent manner. Depletion of CD4 T cells surprisingly improved the vaccine response, and depleting FoxP3+ Tregs via diphtheria toxin in FoxP3-GFPDTR mice revealed Tregs to be the causative agent inhibiting the response. The triple combination induces E7-specific T cells infiltrating the tumors by tetramer staining in young and aged mice, and aged mice show protection albeit less than their younger counterparts. These data show proof-of-concept for a novel combination of a vaccine designed to elicit de novo anti-tumor T cell responses that can be amplified by synergistic CPIs and Treg depletion that lead to greater survival.	WJ Becker, PB Olkhanud, HM Maeng, JA Berzofsky	2023	CANCER
2023-160	Caroline	N	Pruitt	NCI	ACI/IRS	Sociodemographic inequities in carcinogenic industrial air pollution exposures among women in a U.S. Cohort	Introduction: In the United States (U.S.) industrial pollution disproportionately burdens under-resourced communities, but little is known about the amount of exposure to carcinogenic air pollutants. We assessed exposures to carcinogenic industrial emissions by population characteristics in a large cohort. Methods: We used a U.S. Environmental Protection Agency nationwide database of regulated chemical emissions from industrial facilities to estimate historical exposures (1987-1995) to 21 known and 30 probable carcinogens for female participants in the NIH-AARP Diet and Health Study (n=177,806). We estimated emissions from facilities within 2km of the enrollment residence and compared exposure prevalence by race/ethnicity, educational attainment, and a census tract-level neighborhood deprivation index. We used ordinal logistic regression models to estimate odds ratios (ORs) and 95% confidence intervals (CIs) comparing the highest category of emissions (highest tertile (T3) or >90th percentile) to the referent group (zero emissions) for all sociodemographic characteristics. Results: The majority identified as non-Hispanic White, followed by non-Hispanic Black, Hispanic/Latina and Asian. Black women were nearly twice as likely as White women to live within 2km of an exposure source. In adjusted models, compared to White women, Asian (OR=1.4, CI 1.2-1.5), Black (OR=1.4, CI 1.3-1.5), and Hispanic/Latina (OR=1.5, CI 1.4-1.6) women had 1.4-1.6 times greater exposure burden to any known or probable carcinogen. Low educational attainment and high neighborhood deprivation were associated with up to 2-fold higher odds of being heavily exposed. Conclusions: We demonstrated notable disparities in environmental exposure to airborne carcinogens by race/ethnicity and individual and neighborhood-level measures of education and deprivation.	JM Madrigal, CN Pruitt, JA Fisher, BI Graubard, MH Ward, RR Jones	2023	ACI/IRS

2023-161	Zhixiong		Wang	NIBIB	Chemical Biology	Super-resolution imaging of cGAMP-loaded mitochondria-targeting H-aggregation poly-photosensitizer vesicles for cancer photodynamic-immunotherapy	The activation of Stimulator of Interferon Genes (STING) through STING agonists has gained recognition as a robust and highly promising strategy in immunotherapy, with remaining challenges in the immunosuppressive tumor microenvironment and the safety concerns associated with the systemic administration of STING agonists. We have developed a poly-photosensitizer vesicle for encapsulated hydrophilic cGAMP to combine photodynamic therapy and STING activation to improve immunotherapeutic efficacy. The poly-photosensitizer vesicle employs three times higher singlet oxygen and superoxide yields than the small molecule photosensitizer under physiological conditions, owing to H-aggregation improves the energy matching between excited singlet and triplet states to promote the intersystem crossing (ISC) rate. We visualize the entire process of nanovesicles targeting mitochondria using super-resolution microscopy in vitro. Upon 671 nm laser irradiation in vivo, our collaborators have observed that hybrid type I and type II photodynamic therapy effectively kills primitive tumor cells and promote immunogenic cell death. Meanwhile, the cGAMP release activates cGAS-STING and downstream proinflammatory pathways that efficiently prime antigen-specific T cells. This innate and adaptive immunity combination inhibited tumor growth in localized and metastatic murine cancer models. We are developing organ-on-chip models and super-resolution imaging methodologies to bridge these in vitro and in vivo results. Our findings demonstrate that targeted mitochondrial photodynamic therapy and local activation of STING results in systemic antitumor immunity and improve the therapeutic efficacy of checkpoint blockade.	Z Wang, J Chen, D Kiesewetter, RD Leapman, A Jin	2023	CHEMBIO
2023-162	Winston		Hibler	NCI	Cancer Biology	Characterization of anti-AXL CAR-NK cell therapy in the treatment of metastatic melanoma	AXL is a receptor tyrosine kinase (RTK) that is commonly expressed in metastatic melanoma and several other forms of cancer. Activation of AXL signaling is linked to tumor cell growth, invasion, metastatic transformation, drug resistance, and immune response regulation. However, treatment of metastatic melanoma continues to present clinical challenges due to its capacity to rapidly develop drug resistance, which manifests under the influence of AXL signaling. As such, AXL may be a viable antigen target for immunotherapies. Despite their successes in hematological malignancies, chimeric antigen receptor (CAR)-T cell therapies remain limited by their susceptibility to causing off-target toxicity. In contrast, natural killer (NK) cells are not associated with such risks, which makes them clinically appealing as an alternative to T cells. However, studies on the application of CAR-NK cells to treat solid tumors remain acutely scarce. To explore the clinical viability of CAR-NK cells for the treatment of metastatic melanoma, AXL-specific CAR-NK cells were generated by transfecting NK cells obtained from NK cell lines. Preliminary data from a cytotoxicity assay indicated that the cytotoxicity of CAR-NK92-MI cells against AXL-positive melanoma cell lines was significantly stronger (up to a 10-fold difference) than the corresponding parental cells. Further in vitro characterization of this CAR-NK cell line and other CAR-NK cell lines, as well as in vivo evaluation of their efficacy in a mouse xenograft model of melanoma metastasis, will be conducted in future experiments.	WH Hibler, YL Yu, G Merlino	2023	CANCER
2023-163	Matthew	J	Payea	NIA	Cell Biology	Senescent Cells Are Resistant to Activation of the Integrated Stress Response Pathway	Cellular senescence occurs in response to sub-lethal genomic damage and is a central mechanism of aging. Senescence can be induced in any cell type and senescent cells accumulate during aging where they contribute to aging-related disease through a persistent inflammatory program called the Senescence Associated Secretory Phenotype (SASP). The SASP is activated through continuous DNA damage signaling that promotes expression of secretory proteins, thus placing senescent cells in a state of constant unresolved stress. To examine the role of stress in senescence, we conducted a proteomic screen of senescent, quiescent, and cycling cells. We found senescence-specific increases in numerous ER stress response proteins and further investigation showed increased phosphorylation of the translation initiation factor eIF2α, which is a marker of integrated stress response (ISR) activation. However, senescent cells did not express the ISR transcription factor ATF4, even after overexpression of an in vitro transcribed ATF4 mRNA. Ribosome-sequencing analysis revealed that senescent cells failed to bypass the inhibitory upstream ORFs of ATF4 that is normally mediated by eIF2α-P, suggesting that elevated eIF2α-P levels were insufficient to activate the ISR in senescence. In fact, senescent cells showed extreme resistance to expression of ATF4 in response to exogenous oxidative, proteotoxic, and starvation stressors indicating that the ISR response is highly inhibited during senescence. We further found that senescent cells survived even lethal amounts of stress compared to cycling cells and entered a hypersecretory state that lasts long after the stressor was removed.	MJ Payea, S Dar, C Belair, JM Martindale, RB Munk, M Maragkakis	2023	CELLBIO
2023-164	Ballachandra	N	Devaiah	NCI	Molecular Biology and Biochemistry	JNK phosphorylation of BRD4 triggers its transition from a chromatin modifier into a transcriptional activator	BRD4 is a key regulatory factor controlling multiple cancers and cellular stress responses. It regulates chromatin remodeling and transcription through its histone acetyltransferase (HAT) and kinase activities respectively. BRD4 is primarily a chromatin bound protein but is released from the chromatin to recruit and regulate crucial elements of the transcriptional machinery during periods of activated transcription such as immune and inflammatory responses or cancer progression. The mechanism responsible for switching BRD4 from a chromatin to transcriptional regulator is currently unknown. Here, we report that the JNK kinase directly interacts with BRD4 and phosphorylates it specifically at Ser1117, Thr1186 and Thr1212, triggering BRD4 release from chromatin genome wide. Activation of JNK kinase by a broad range of stimuli causes the release of BRD4 from chromatin. JNK phosphorylated BRD4 is dephosphorylated by the PP4 phosphatase in the nucleoplasm, allowing its interaction with RNA Pol II at transcriptionally active sites. JNK phosphorylation of BRD4 blocks its chromatin regulatory HAT function and activates its transcription-enhancing kinase function. Accordingly, JNK activation leads to significantly elevated transcription of BRD4 regulated immune and inflammatory response genes in a manner dependent on the presence of the three JNK phospho-sites on BRD4. JNK phosphorylation of BRD4 is involved in biological processes such as T-cell activation and is required for epithelial to mesenchymal transition (EMT) during cancer progression. These finding thus characterize a hitherto unknown mechanism that allows BRD4 to transition from a chromatin to transcriptional regulator during immune/inflammatory response and EMT.	BN Devaiah, AK Singh, J Mu, Q Chen, D Meerzaman, DS Singer	2023	MOLBIO
2023-165	Abhinav		Saurabh	NHLBI	Health Disparities	Physical activity is associated with monocytes and monocyte subsets in low-resourced neighborhoods: data from the Step It Up physical activity intervention	Background: People living in lower-resourced neighborhoods have higher CVD risk in part due to limited physical activity (PA) access. Monocyte subsets with their platelet aggregates (PlAgg) are key in CVD. We investigated associations between PA and monocyte subsets with PlAgg in African American (AA) women with CVD risk living in resource-limited Washington, DC areas. Methods: Step It Up is a technology-enabled, community-engaged PA intervention. Participants were enrolled in this study and their baseline PA was measured as daily step counts using a FitBit Charge 2. Flow cytometry was used to measure monocyte subsets and PlAgg in fasting blood samples. Multivariable linear regression determined relationships between PA and monocytes adjusting for BMI and ASCVD 10-year risk score. We examined neighborhood deprivation index (NDI), a Census-tract based measure of neighborhood socioeconomic deprivation, as a moderator of associations between PA and monocytes. Results: The study cohort was a sample of AA women with overweight/obesity enrolled in Step It Up (N=106, age=57±12 y, BMI=34.8±6.3kg/m2). We observed that higher baseline PA associated with monocyte subsets, but not overall monocyte presence. Furthermore, higher baseline PA negatively associated with PlAgg on all monocytes. PA and monocyte subsets were most associated among those residing in higher deprivation neighborhoods. Conclusion: Baseline PA was associated with monocyte subsets and lower monocyte-PlAgg formation among AA women living in lower-resourced conditions. Future work should examine the relationship between PA changes and changes in monocyte subsets in community engaged PA interventions like Step It Up, particularly among those residing in limited resource communities.	A Saurabh, H A Tarfa, Y Baumer, A Dave, M A Pita, M A Citron, L R Ortiz-Whittingham, S Reynolds, K A Potharaju, A S Baez, K Thompson, F O Baah, J F Troendle, C Ayers, S J Neally, V M Mitchell, A Wells, M Marah, B S Collins, T M Powell-Wiley	2023	HEALTH
2023-166	Christian	O	Mbulu	CC	Health Disparities	Focusing on whole person health in treatment seeking individuals with alcohol use disorder: A case for universal dental screening, care, and education	Background: Poor oral health in individuals with alcohol use disorder (AUD) can be linked to physiologic changes and health behavior practices including effects of alcohol on local soft and hard dental tissues; the compounding biological effect of alcohol on the human body; and the potential daily neglect in optimal oral care practices within this population. Aim: Determine the behaviors and oral health outcomes of treatment seeking individuals with AUD. Methods: A retrospective review was conducted on 323 of 423 patients admitted for treatment from January 2017 to December 2021. AUD-associated metrics and oral health measures including Becks Oral Assessment Scale (BOAS), oral pain, periodontal disease classification (PD), alveolar bone loss (ABL), oral health and smoking behaviors were collected. Associations were assessed by Pearson correlations, Chi-square test, t-test, and ANOVA. Results: Of the 323 referred for dental consults, 142 individuals (mean age 45.5; male (66.2%); White (52.1%)) were included in the final analyses. Race (p=.045), education (p=.037), age (p<.001), heavy drinking years (p<.001) and pack-years of smoking (p=012) were associated with PD. Oral pain was associated with overall maximum withdrawal score(p<.001) and brushing frequency (p=.045). Heavy drinking years (p=.008) and brushing frequency were associated with BOAS. Age (p=.036) and alcohol type (p=.007) were associated with ABL. Conclusion: Individuals with AUD, High withdrawal severity, heavy drinking years, and high smoking pack years are at increased risk for severe PD. These results demonstrate a need for universal dental screening and interventional dental care in this underserved population. Key words: oral health, periodontal disease.	CO Mbulu, J Diss, L Yang, K Maki, C Crayton, J Barb, M Schwandt, K Herman, S Sharon, N Diazgranados, V Ramchandani, G Wallen	2023	HEALTH
2023-167	Renee		Groechel	NINDS	Epidemiology	Social engagement, amyloid burden, and dementia: the Atherosclerosis Risk in Communities (ARIC) - PET study	Background: Although amyloid deposition in the brain is often associated with subsequent dementia risk, not everyone with brain amyloid will develop dementia. This discrepancy illustrates the potential importance that vascular and lifestyle risk factors may have in modifying this association. Compared to participants with low mid-life social engagement, we hypothesized that participants with high mid-life social engagement will show a weaker association between amyloid burden and incident dementia. Method: Participants in the Atherosclerosis Risk in Communities (ARIC) Study were assessed for social support and social isolation (visit 2; 1990-1992). Through these measures, a composite measure, "social engagement" was generated. Brain amyloid was evaluated with florbetapir PET (visit 5; 2012-2014). Incident dementia cases were identified following visit 5 through December 31, 2019 using ongoing surveillance. Relative contributions of mid-life social engagement and elevated brain amyloid to incident dementia, independently and with multiplicative interaction terms, were evaluated with Cox regression models. Models were adjusted for demographics, APOE𝜀4, and vascular risk factors. Result: Among 310 participants, 48 developed dementia (median follow-up: 4.7 years). Greater mid-life social engagement was independently associated with lower dementia risk. Elevated late life brain amyloid was associated with greater dementia risk. Conclusion: We found no evidence that mid-life social engagement reduces the risk of dementia in participants with elevated brain amyloid burden in late life. Future longitudinal studies evaluating the potential influence of social factors measured throughout the life course are needed to inform our understanding as to what factors may preserve cognition in the presence of brain pathology.	RC Greochel, AC Liu, C Liu, DS Knopman, S Koton, AM Kucharska-Newton, PL Lutsey, TH Mosley Jr, P Palta, AR Sharrett, KA Walker, DF Wong, RF Gottesman	2023	EPIG
2023-168	Fnu		Urvashi	NIAMS	Health Disparities	Functional NOTCH4 variants increase susceptibility for systemic sclerosis in African American patients	Using GRASP cohort, we examined the hypothesis that common noncoding variants are identifying gene regions that are enriched for rare, functional variants that can increase disease burden in African Americans (AAs) with scleroderma (SSc). Exome sequencing and gene-based testing was performed in 969 SSc and 771 controls of African ancestry for 32 genes reported with SSc in GWAS catalog. In both discovery and replication series only functional variants in NOTCH4 remained statistically significant. Majority of NOTCH4 variants were African ancestry-predominant or novel. On analyzing SSc-subsets, diffuse cutaneous SSc, anti-fibrillarin antibody, and severe Raynauds' remained significant. We theorized that the NOTCH4 variants transcriptionally regulate NOTCH4 signaling pathway either by increasing NOTCH4 or downstream signaling molecules- HEY2 and HES1. eQTL analysis using GTEx data showed that NOTCH4 promoter (c.-117G>A) variant increased NOTCH4 transcripts and missense (p.Gly942Arg) variant increased HEY2 in LCLs. RT-PCR and ELISA revealed higher NOTCH4 in LCLs with c.-117A allele. Stimulation of NOTCH4 in LCLs carrying missense variant showed higher HEY2 and HES1 expression than wild type LCLs. SSc patients carrying c.-117A allele had higher NOTCH4 and the missense variant was associated with increased downstream NOTCH4 signaling in skin than WT alleles. Single cell analysis identified NOTCH4 principally being expressed in endothelial cells (ECs). SSc ECs with c.-117A allele had increased NOTCH4, downstream signaling, and decreased tube formation. Inhibiting the NOTCH4 pathway using a NOTCH4-specific blocking antibody, rescued normal tube formation. To summarize, NOTCH4 variants in AA SSc patients increase NOTCH4 expression and signaling that can cause impaired angiogenesis.	U Kaundal, M Sahu, T Talley, K Gudapati, E Stenson, K Thakur, J Wang, D Randazzo, S Dell'Orso, E Tsou, GRASP Collaborators P, Gourh	2023	HEALTH
2023-169	Natalia	J	Martinez	NCATS	Chemical Biology	Identification of broad-spectrum inhibitors against Bunyaviral endonucleases	Bunyavirales is an order of segmented (-) strand RNA viruses. Several families in the Bunyavirales order, such as Phenuiviridae, Arenaviridae, Nairoviridae, and Hantaviridae, cause viral hemorrhagic fevers or pulmonary disorders for which no effective therapy exists. These emerging viruses are considered Category A priority pathogens by the National Institutes of Health due to their potential threat to global health. Bunyavirales share common mechanisms that can be potentially targeted for the development of broad-spectrum antivirals. Like all segmented (-) strand RNA viruses, Bunyavirales rely on their own transcriptional machinery which contains an endonuclease domain that cleaves the 5'RNA cap of host cell mRNAs, a process called "cap-snatching", to prime viral transcription. The endonuclease domain of Bunyavirals is therefore a promising antiviral target. To identify small molecules with potential broad spectrum anti-bunyaviral activity, we developed fluorescence-based enzymatic assays for 4 recombinant endonucleases from Rift Valley Fever, La Cross, Punta Toro, and Hantaan viruses. The assays were miniaturized to 1536-well format to support the quantitative-high throughput screening (qHTS) of a total of ~12K compounds from NCATS-sourced libraries. Hits identified from the screen, were subsequently tested for their ability to engage their intended target in high-throughput enzyme complementation assays. High-throughput viral infection assays were also utilized to further characterize inhibitor activity.	YM Ahn, S Costmire, S Ogden, D Esposito, S Messing, K Shamim, X Hu, L Ye, EM Lee, NJ Martinez	2023	CHEMBIO

2023-170	Martin		Carrasco	NCATS	Neuroscience	Developing a neural spheroid model of amyotrophic lateral sclerosis for high-throughput drug screening	Our group previously established a method for generating functional brain region-specific neural spheroids compatible with high-throughput screening (HTS). This platform can be manipulated to mimic different brain regions and model different diseased states, thereby serving as a robust tool for drug discovery. Building off this work, our goal herein is to develop a HTS-compatible neural spheroid model of amyotrophic lateral sclerosis (ALS) using iPSC-derived motor neurons and astrocytes to mimic the motor cortex of the brain. ALS is a fatal neurodegenerative disease with no cure and whose underlying mechanism is not fully understood. However, mutations in the transactivation response DNA-binding protein 43kDa (TDP-43) have been linked to ALS pathology. Therefore, we include genetically engineered motor neurons with TDP-43 mutations to model this diseased state. Using intracellular calcium activity as a functional readout, our first objective is to establish a baseline phenotype for wild type (WT) "healthy" motor neuron spheroids and validate using control compounds with known effects on different neuronal subtypes.	M Carrasco, J Zhang, S Kundu, E Lee, M Ferrer	2023	NEURO
2023-171	Santhi		Devasundaram	NCI	Immunology	Early biomarkers for an effective antibody responses after SARS-CoV-2 BNT162b2 mRNA vaccination in humans	Background Early innate responses to vaccination are important for shaping both humoral and cellular protective immunity. Dissecting biomarkers induced by BNT162b2 mRNA (Pfizer/BioNtech) vaccine (NCT04743388) may lead to optimization of mRNA and other vaccine strategies. Methods Plasma was analyzed after the 1st, 2nd and 3rd vaccination (NCT04743388). Cytokine/chemokine changes were measured using V-PLEX Human Biomarker Assay (Meso Scale Diagnostics) and ELISA (CXCL13, Invitrogen) at the day of vaccination and 24hrs later. Anti-spike binding and neutralizing Ab were measured over time using in-house ELISA and a pseudotyped virus assay. Results Vaccination induced robust anti-Spike Ab with a significant enhancement upon the 3rd vaccination. We identified a transient systemic signature including increases in IL-15, IFN-gamma, and IP-10/CXCL10 after the 1st vaccination, enriched by TNF-alpha and IL-6 after the 2nd and 3rd vaccination. Changes in biomarker levels and their inter-relationship revealed two major clusters: including (i) IL-15, IFN-gamma, CXCL10/IP-10 and (ii) myeloid cell-associated cytokines CCL2/MCP-1, CCL3/MIP-1a, CCL4/MIP-1b, CXCL8/IL-8. Additionally, CXCL13 induction upon the 3rd vaccination indicated a stronger effect on lymph node activation only upon repeated vaccination. Changes in IFN-gamma and IP-10/CXCL10 correlated with the anti-Spike humoral responses and were predictive of successful antibody development. In contrast, most hematological patients showed diminished IL-15 signature and antibody responses. Patients who failed to develop antibodies, also lacked the IL-15 signature and had an innate systemic response dominated by IL-8 and MIP-1a.	S Devasundaram, M Rosati, C Bergamaschi, J Bear, R Burns, P Homan, MA Dimopoulos, E Terpos, GN Pavlakis, BK Felber	2023	IMMUNO
2023-172	Xinh-Xinh	M	Nguyen	NCATS	Molecular Biology and Biochemistry	3D Biofabricated Immunocompetent Skin Tissue Model of Atopic Dermatitis for Testing the Efficacy of Immunomodulatory Mesenchymal Stromal Cell Therapies	Atopic dermatitis (AD) is a complex inflammatory skin disease that involves multiple cell types and immune system imbalance. During disease progression, T-helper type 2 (Th2) cells migrate to the skin and secrete pro-inflammatory cytokines such as IL-4 and IL-13, which induce AD pathology in the skin. We have established a robust protocol to fabricate normal full thickness skin (FTS) and vascularized (VFTS) and AD-like FTS and VFTS tissues by treatment with IL-4. The IL-4 induced AD skin models recapitulate the hallmarks of AD including spongiosis-like intercellular spaces, epithelial hyperplasia, and the loss of barrier function, further highlighting the rescue of AD-like phenotypes by Tofacitinib, a potent inhibitor of the JAK-STAT pathways. Furthermore, in place of adding IL-4, we have increased the physiological complexity of the previous model by incorporating Th2 cells to induce the AD-phenotype. Our data show that Th2-incorporated skin tissues exhibit AD-like phenotypes including the loss of barrier function, suggesting the barrier function of the skin is impaired, and undifferentiated epidermal keratinocytes by histology. We also utilize our immunocompetent AD model test whether cell-based immunological therapies, such as mesenchymal stromal cells (MSC), can be used to monitor the suppressive T-cells response in the model, and additional MSC treatment helps to restore the vasculature formation in the AD model. Taken together, our 3D fabricated tissue models have potential to improve understanding of immune cell interactions and mechanisms during the initiation and progression of AD, while also providing testing platforms for different therapeutic approaches, including small molecules and biologics.	X-X Nguyen, H Zarkoob, MJ Song, K Sung, M Ferrer	2023	MOLBIO
2023-173	Jeremy	W	Luk	NIAAA	Social and Behavioral Sciences	History of suicidality and pandemic outcomes: Longitudinal associations with anxiety symptoms, depressive symptoms, and problematic drinking	Objective: The COVID-19 pandemic has led to increased anxiety, depression, and alcohol-related mortality. Individuals with a history of suicidality may be especially vulnerable to the adverse impact of COVID-related stressors. This study investigated the longitudinal effects of suicidality history and interactions with COVID-related stressors on anxiety symptoms, depressive symptoms, and problematic drinking. Methods: Longitudinal data from 518 participants were drawn from the NIAAA Natural History Protocol and the NIAAA COVID-19 Pandemic Impact on Alcohol Study. History of suicidality was assessed using the clinician administered Columbia Suicide Severity Rating Scale. Multiple regression analyses tested the interaction between suicidality history and COVID-related stressors on clinical outcomes. Results: Compared with individuals without any history of suicidality (79.7%), individuals with a history of suicide ideation only (14.7%) and suicide attempt (5.6%) had higher anxiety symptoms, depressive symptoms, and problematic drinking during the pandemic. COVID-related stressors were positively associated with clinical outcomes. Moderation analyses indicated that the associations between COVID-related stressors and mental health symptoms were stronger among individuals with suicide attempt history than individuals without suicidality history. Problematic drinking was elevated during the later phases of the pandemic. Conclusions: History of suicide ideation and/or attempt longitudinally predicted higher pandemic mental health symptoms and problematic drinking increased during the later phases of the pandemic. Individuals with a history of suicide attempt may more easily develop mental health symptoms in the face of COVID-related stressors. Suicide risk assessment and surveillance of problematic drinking trends may inform targeted prevention and intervention amidst a global public health crisis.	JW Luk, MF Thompson, LA Novak, BL Stangl, ML Schwandt, D Goldman, VA Ramchandani, N Diazgranados	2023	SOCIAL
2023-174	Liu		Liu	NIDDK	Molecular Biology and Biochemistry	Regulation of α-cell function by Gs and Gq signaling	Glucagon, an important islet hormone released from pancreatic α-cells, regulates systemic glucose homeostasis. Dysregulated glucagon secretion is a key feature of type 1 and 2 diabetes. However, the signaling pathways underlying the regulation of glucagon secretion remain incompletely understood. cAMP and Ca2+, the major intracellular second messengers downstream of Gs and Gq signaling, respectively, have been implicated in the regulation of glucagon secretion from of α-cells. In this study, we explored the relative physiological relevance of these signaling pathways by gene targeting technology in mice. Specifically, we selectively deleted the α subunit of Gs or Gq in α-cells of adult mice (α-GsKO and α-Gq/11KO mice, respectively). Ablation of Gs or Gq signaling in α-cells caused reduced circulating glucagon, most likely due to decreased proglucagon gene expression and islet glucagon content. Disruption of α-cell Gs or Gq signaling also led to impaired glucagon secretion in response to hypoglycemic or glucopenic conditions, supporting the involvement of α-cell Gs- and Gq-coupled receptors in this effect. Perifusion studies showed that treatment of α-GsKO islets with ligands activating Gq-coupled receptors resulted in reduced glucagon secretion. Vice versa, α-Gq/11KO islets released reduced amounts of glucagon in response to ligands able to stimulate Gs-coupled receptors. Overall, these findings suggest that both α-cell Gs and Gq signaling are critical for glucagon secretion under various experimental conditions. Our data suggest that Gq activation engages pathways that require Gs signaling to effectively stimulate glucagon secretion and vice versa.	L Liu, K El, L Barella, Y Cui, M Chen, LS Weinstein, JE Campbell, J Wess	2023	MOLBIO
2023-175	Boah		Kim	CC	Biomedical Engineering and Biophysics	Multi-modal image registration using neural optimal transport: an application to abdominal multi-parametric MR registration	Medical image registration is one of the essential processes in analyzing multiple images and diagnosing diseases. Although classical image registration methods that solve optimization problems for a moving image to be deformed into a fixed image have shown high-quality performance, they have limitations in taking a long time to be processed and extensive computational costs. To accelerate registration while maintaining performance, recently, deep learning approaches have been developed, which train neural networks by minimizing the energy function from the classical algorithms. Since these learning-based methods can learn image registration in an unsupervised manner, they have been applied to various medical image registration tasks such as atlas-based registration and multi-phase image registration. However, multi-modal image registration is still challenging in that the network needs to consider different data distributions from multiple modality images. To address this problem, we propose a domain-transported image registration method, called OTMorph. By employing a recent approach of neural optimal transport for image-to-image translation, we design a novel framework composed of a transport module and a registration module: the former transports data distribution from the moving source domain to the fixed target domain, and the latter provides deformation by taking the transported data. Through end-to-end learning, our proposed method can effectively learn deformable registration for the images in different distributions. Experimental results on abdominal multi-parametric MR image registration show that our method is superior to deform multi-modal images compared to the existing learning-based methods. We expect that our method can be useful for various image modalities.	B Kim, T Mathai, R M Summers	2023	BIOENG
2023-176	Wengang		Zhang	NCI	Computational Biology	Elucidating the conformational landscape of CDKs: implications for cell cycle regulation	Cyclin-dependent kinases (CDKs) play a pivotal role in cell cycle regulation, and their dysregulation is implicated in cancer. We aim to decode the differential activation dynamics and function of cyclin-D/CDK4 and cyclin-E/CDK2 complexes in the G1 phase and G1/S phase transition of the cell cycle, respectively. Through molecular dynamics simulations and protein-protein docking, we analyze the conformational dynamics of these complexes, with a focus on their differential activation kinetics - cyclin-E/CDK2's rapid activation versus cyclin-D/CDK4's slower activation. Moreover, we examine how different conformational ensembles of active CDK complexes relate to their catalytic efficiencies, aiming to uncover key structural characteristics that govern the slow cyclin-D/CDK4 and rapid cyclin-E/CDK2 catalytic activities. Additionally, the study explores the diversity of CDK-cyclin interacting pairs, evaluating whether other CDKs have multiple cyclin partners as observed in CDK2, and the implications of these interactions on cell cycle progression. By integrating computational approaches with available experimental data, this project aims to elucidate the activation mechanisms of CDK complexes, offering insights for drug design and understanding CDK-dysregulated cancers.	W Zhang, Y Liu, M Bergman, H Jang, R Nussinov	2023	COMPBIO
2023-177	Biswajit		Kundu	NIAAA	Chemical Biology	Rational Design, Synthesis, And Biological Validation of Therapeutically Effective Novel Sulfonamide Urea Derivatives as Soluble Epoxide Hydrolase Inhibitors	The enzyme soluble epoxide hydrolase (sEH) plays a pivotal role in the metabolism process of bioactive lipid signaling molecules. The substrate-specific hydrolase activity of sEH transforms epoxyeicosatrienoic acids (EETs) to the corresponding dihydroxyeicosatrienoic acids (DHETs) purported to have inflammatory effects. It has been demonstrated that sEH inhibition leads to elevated levels of EETs, subsequently manifesting anti-inflammatory, analgesic, antihypertensive, cardio-protective, and organ-protective effects. Pharmacological inhibition of sEH in animal models exhibited beneficial effects on the treatment of hypertension, inflammation, and related syndromes. Although existing sEH inhibitors are potent and specific, low solubility and relatively fast metabolism decrease their therapeutic efficiency, stating the requirement for novel sEH inhibitors. Our research features rational design and synthesis of a series of novel compounds having potent soluble epoxide hydrolase inhibitory activity with enhanced solubility. A set of inhibitors have been found to exhibit better druggable properties and nanomolar potency in recombinant assays. We experimentally found these compounds synergistically inhibit sEH & iNOS (inducible Nitric Oxide Synthase), accounting for higher therapeutic efficacy. The potent compounds were evaluated in a panel of in vitro ADME assays and in vivo pharmacokinetic studies. The gene expression data from lipopolysaccharide (LPS)-induced acute lung injury (ALI) studies in mice demonstrated that the lead compound is more efficacious compared to a known sEH inhibitor AUDA to attenuate the inflammation caused by LPS in mice.Multi-target approach for improving the efficacy of sEH inhibitors either as a pro-drug, metabolite or whole drug will be presented.	B Kundu, A Basu, C Wood, KA Kim, L Pommerolle, ER Gibbs, M Behee, R Cinar, MR Iyer	2023	CHEMBIO
2023-178	Jared	A	Shadish	NHLBI	Biomedical Engineering and Biophysics	Photocleavable TDP-43 to Control Subcellular Localization	TAR DNA-binding protein 43 (TDP-43) cytosolic aggregates have been implicated in a host of neurodegenerative diseases such as amyotrophic lateral sclerosis and frontotemporal lobar dementia. Under healthy conditions, TDP-43 is an ubiquitously expressed RNA-binding protein which is primarily located in the nucleus. The mechanism of TDP-43 pathology, going from a functional nuclear protein to an aggregated cytoplasmic inclusion, remains poorly understood. Understanding this process is critical to developing effective therapeutics. In this work, the subcellular distribution equilibrium of TDP-43 is controlled in a spatiotemporal manner through the genetic incorporation of a photocleavable protein, PhoCl. Upon illumination with cellular compatible violet light (λ = 400 nm), the PhoCl protein undergoes a structural rearrangement to generate disease-related N-terminally truncated TDP-43 variants. The position of the truncation is based on the placement of PhoCl in the TDP-43 sequence. Photocleavable TDP-43 constructs were transfected and expressed in HEK293-T cells. Light exposure generates truncations lacking an N-terminal nuclear localization sequence, shifting TDP-43 equilibrium towards the cytosol. Cells are tracked via timelapse confocal fluorescence microscopy, and the cellular distribution of TDP-43 is quantified by cellular fractionation and western blot. Spatial control over the in cellulo generation of truncations facilitates the probing of biological mechanisms of TDP-43 translocation that are not possible by traditional methods.	JA Shadish, JC Lee	2023	BIOENG
2023-179	Daniel	Q	SanGiovanni	NHLBI	Biomedical Engineering and Biophysics	Amyloid formation of alternatively spliced variants of α-synuclein	Intracellular accumulation of α-synuclein (α-syn) amyloid fibrils is the pathological hallmark of synucleinopathies including Parkinson's disease, Lewy body dementia, and multiple system atrophy. The gene that encodes for α-syn (SNCA) engages in alternative splicing, generating at least three other isoforms (SNCA126, SNCA112, and SNCA98). For nearly 30 years, the vast amount of research dedicated to α-syn has overlooked the potential involvement of these alternatively spliced variants. Of note, these alternatively spliced isoforms have been shown to be upregulated in synucleinopathies; however, neither their aggregation behaviors nor their effects on the full length α-syn have been studied. To address this deficiency, we have carried out an in vitro investigation to examine their detailed aggregation behaviors as a function of protein concentration and solution pH and compared them to the full-length protein (SNCA140). Specifically, we are testing the hypothesis of whether specific isoforms can form different fibril polymorphs and facilitate fibril formation of SNCA140 by performing cross-seeding experiments. Aggregation kinetics were assessed by standard thioflavin-T assays, and fibril morphology and β-sheet formation are characterized by transmission electron microscopy and circular dichroism spectroscopy, respectively. It is anticipated that our results would offer new insights on the potential role of these variants in disease.	DQ SanGiovanni, RP McGlinchey, JC Lee	2023	BIOENG

2023-180	Bethany	L	Stangl	NIAAA	Clinical Research	The relationship between COVID-19-related stigma and alcohol use, mental health, fear of COVID-19 and fatigue at 2-year follow-up	Purpose: The negative effect of stigma on mental health has been well documented. However, the stigma associated with COVID-19 has been understudied. We adapted a stigma questionnaire to examine the effect of COVID-19 related stigma on alcohol use, mental health, fear of COVID-19 and fatigue at 2-year follow-up in individuals across a wide range of alcohol use patterns. Methods/Data: Participants (N=250, M=125) previously enrolled in the NIAAA Natural History Protocol were recruited for a 2-year follow-up longitudinal survey study. Alcohol use and consequences were measured using the Alcohol Use Disorder Identification Test (AUDIT). Twelve stigma questions were adapted from a scale of 17 items measuring HIV/AIDS related stigma (Visser et al., 2008). Mental health measures of anxiety and depression included the Generalized Anxiety Disorder (GAD) questionnaire and the Patient Health Questionnaire (PHQ-9), respectively. Fear of COVID was measured using the Fear of COVID-19 Scale (FCV-19S). Fatigue was measured using the Fatigue Assessment Scale (FAS) with three measures of fatigue: physical fatigue, mental fatigue, and pandemic fatigue. Results: The Stigma scale had strong internal consistency (Cronbach's α = 0.80). Correlational analyses revealed that greater COVID-19 related stigma was associated with greater anxiety and depression symptoms, less alcohol use, greater fear of COVID-19, and greater physical and mental fatigue (all p's<0.05). Conclusions: These findings highlight the need to address COVID-19 related stigma and its association with poorer mental health. Future directions include examining the role of race, discrimination, and impact from the COVID-19 pandemic on stigma to better understand sources of vulnerability.	BL Stangl, JW Luk, RV Shah, CL Vaughan, AJ Waters, ML Schwandt, D Goldman, N Diazgranandos, VA Ramchandani	2023	CLINICAL
2023-181	Trevor	A	Christensen	NCI	Cancer Biology	Functional Characterization of Pancreatic Cancer GWAS Signal at PDX1 Promoter	PanScan (Pancreatic Cancer Cohort Consortium), a genome-wide association study (GWAS) to identify common genetic variants associated with increased risk of pancreatic cancer, has been conducted over the past several years to improve detection and treatment of pancreatic cancer. A prominent signal at 13q12.2 was observed, which epigenomic fine mapping and experimental validation revealed to most likely be a functional SNP ~200bp upstream of PDX1. Using a doxycycline-inducible overexpression system, we found that increased PDX1 expression likely inhibits cell proliferation through upregulating apoptosis. We ran a gene set enrichment analysis of time-course RNA-seq data comparing cells with PDX1 overexpression to uninduced cells and found changes in several pathways linked to immune system activity, inflammation, diabetes, and other cancer-related or harmful outcomes. Finally, we used CRISPR to edit pancreatic cancer cells that were wild-type heterozygous (G/A) for the SNP of interest into multiple clones of both homozygous types (G/G and A/A), finding decreased PDX1 expression as well as other changes associated with increased copies of the risk SNP (A).	TA Christensen, JW Hoskins, DR Eiser, E Char, M Mobaraki, I Collins, LT Amundadottir	2023	CANCER
2023-182	Yunliang		Zhang	NIAID	Virology	Vaccinia virus encodes a novel O-GlcNAc protein required for virion assembly	There have been relatively few examples of viral O-GlcNAc proteins relative to the large numbers discovered in animals and plants. Here, we describe the presence of a novel O-GlcNAc protein in vaccinia virus (VACV) infectious particles. VACV, the prototypic member of the Poxviridae family, comprised the live-virus vaccine that eradicated smallpox and harbors a linear, double-stranded DNA genome encoding approximately 200 proteins. Early studies from our laboratory demonstrated the presence of a 40-kDa protein that contains N-acetylglucosamine in purified virions. The small size of the pronase-digestion product and the absence of other sugars suggested one or few glucosamines. In the present study, extracts of purified virions were enzymatically labeled utilizing the mutant β-1,4-galactosyltransferase (Gal-T1 (Y289L)) to specifically transfer azido-modified galactose (GalNAz) from UDP-GalNAz to O-GlcNAc residues. Following copper catalyzed azide-alkyne cycloaddition, the candidate GlcNAc proteins were detected by SDS-polyacrylamide gel electrophoresis and identified by mass spectrometry. Then using strain-promoted cycloaddition chemistry to attach a polyethylene glycol mass tag of 10 kDa on to the GlcNAc protein, a significant shift in the electrophoretic mobility of the VACV A4 protein was documented by Western blotting. The presence of O-GlcNAc and one major modification site in A4 was confirmed by mass spectrometry and specific antibody. Expression of A4 is essential for virus replication and is required for morphogenesis of mature virions. Further studies to determine the serine/threonine residues modified and to determine the role of GlcNAc in the function of A4 are in progress.	Y Zhang, B Moss	2023	VIROL
2023-185	Rodica		Stan	NCATS	Clinical Research	Regulatory Pathway for Gene Therapy for Rare Diseases: An Illustrative Example from the PaVe-GT Platform Program	The Platform Vector Gene Therapy (PaVe-GT) program is an initiative started by a multi-disciplinary group of collaborators to develop adeno-associated virus (AAV) gene therapies for four rare diseases. With approximately 10,000 rare diseases that affect 25 to 30 million people in the US and less than 10% of these diseases having an approved treatment, there is much work to be done. Addressing the need for therapies for rare diseases under a unified platform may serve as a paradigm for reducing process redundancies and increasing efficiencies in the preclinical, regulatory, and clinical activities to broadly enable the development of gene therapies for rare diseases. Here, we showcase the regulatory strategy for the PaVe-GT program's first indication. AAV9-hPCCA gene therapy is being developed to treat propionic acidemia resulting from a deficiency of propionyl-CoA carboxylase, alpha subunit (PCCA). The product's regulatory pathway has thus far progressed successfully through an INTERACT meeting with the FDA and is in pre-IND planning phase. This gene therapy project has also received two valuable designations from the FDA: Orphan Drug and Rare Pediatric Disease, which provide sponsors with financial incentives for research and development of drugs for rare diseases. Lessons learned from our regulatory activities will be presented. In conclusion, the knowledge achieved by advancing PaVe-GT program's first product will be applied to the other three indications under development, to reduce process redundancies and increase efficiencies. PaVe-GT represents a strategy for accelerating therapeutic development for rare diseases that can be disseminated to other AAV gene therapy efforts.	R Stan, RM Lomash, RJ Chandler, OA Shchelochkov, CP Venditti, CG Bönnemann, PJ Brooks, EA Ottinger	2023	CLINICAL
2023-186	Darryl		Owusu-Ansah	CC	Immunology	Assessing the Impact of Cell Isolation Methods on Gene Expression in CD19+ B cells Using Next Generation Sequencing	The targeted isolation of B-cell cell populations is crucial for researchers investigating lymphoproliferative disorders, particularly when investigating non-Hodgkin's lymphoma. Over the years, cell isolation methods have evolved significantly; however, the potential influence of these methods on downstream gene expression in target cell populations remains a subject of interest. It is widely believed that techniques such as positive magnetic activated cell sorting (MACS) and fluorescence-activated cell sorting (FACS) may affect the expression of genes due to the direct interaction of associated antibodies with surface markers. We currently know through literature review that cofactors like pressure, nozzle size, instrument type, have little effect on gene expression profile. We also know that temperature can play a significant role on downstream expression. However, to the best of our knowledge, no specific studies have examined these effects within CD19+ B cell populations. In this study, we plan to isolate B cells from n=4 healthy donors using three distinct methods: positive MACS, negative MACS, and FACS. We will then perform Next Generation Sequencing (NGS) analysis in order to identify differentially expressed genes among the three different isolation methods. In this study we will be comparing the performance of three isolation methods and their effect on gene expression in CD19+ B cells, trying to establish if different cell isolation methods would potentially impact the disease-related signature when analyzing patient samples.	D Owusu-Ansah, A Henning, V DeGiorgi	2023	IMMUNO
2023-187	Catherine	M	Farrell	NLM	Research Support Services	NCBI RefSeq Functional Elements, a growing resource for human and mouse genomic functional discovery beyond genes	To facilitate genomic functional discovery, NCBI provides RefSeq Functional Elements (RefSeqFEs; www.ncbi.nlm.nih.gov/refseq/functionalelements/) for diverse and functionally important non-genic elements in human and mouse, including gene regulatory regions and other regions that have been experimentally validated in the literature. The dataset includes richly annotated sequence records, descriptive records in the Gene database, genomic feature annotation, and interactions between regulatory regions, target genes and each other. We have tremendously scaled up content following our initial publication describing the resource (PMID:34876495). The dataset currently has over 150K features for human and 6K features for mouse (July 2023), with significant at scale growth expected over the coming year. Recent improvements include the addition of thousands of new records, extractable cell type activity data for annotated features, additional fields for data mining in download files, and new CRISPRi-validated target gene linkages. We increased accessibility by providing annotation on the T2T-CHM13v2.0 genome assembly, with periodic updates of GRCh38, GRCm39 and T2T-CHM13v2.0 annotations and the RefSeqFE track hub. Moreover, we improved clinically relevant content by adding features for functionally validated regulatory variants, and we curated regulatory elements for genes associated with coronavirus biology and marked up biological regions that overlap known COVID-19-associated variants. Our freely available resource enables discovery of non-coding function beyond genes, and directly links it to the experimental literature. Further details on RefSeqFE data access, improvements and uses will be presented. We welcome feedback from the NIH research community, with an aim to optimize RefSeqFEs as a reference resource for experimentally validated non-genic regions.	CM Farrell, OD Ermolaeva, CL Wallin, TD Murphy	2023	RSCHSUPP
2023-188	Li		Yin	NIAID	Virology	Pregnant Women with HIV (PWH) induce Pro-Inflammatory Bioprofiles in Their HIV Exposed Uninfected (HEU) Infants That Persisted For At Least Six Months of Age.	Introduction. HEU infants have a higher risk for adverse metabolic, infectious, and neurodevelopmental outcomes. How HEU immunity is influenced by maternal HIV immune status is understudied, and thus a focus of this study. Methods. Blood samples obtained from 46 PWH and their HEU newborns pairs were compared to a reference group of 18 pregnant women without HIV (PWOH) and their HIV-unexposed uninfected (HUU) neonates. HEU infants were evaluated at birth and 6 months along with a longitudinal cohort of 32 HUU infants. Twenty-one biomarkers associated with B-cell development, macrophage or lymphocyte activation, and inflammation were measured by Mesoscale. The Mann-Whiney and Kruskal-Wallis tests compared two and multiple groups respectively. Spearman's test evaluated mother/baby biomarker correlations. Results. Compared to PWOH, biomarkers related to B-cell development (sCD40L, IL-21), immune activation (sCD163, sCD27, IL-22), and inflammation (CXCL9, CXCL10, CCL5, TNF-α, IL-1β) elevated significantly in PWH. In contrast, APRIL, a biomarker of B-cell development, was lower in PWH. HEU neonates showed significantly higher biomarker concentrations of B-cell development (APRIL, BAFF, sCD40L, IL-21), macrophage activation (sCD14), lymphocyte activation (sCD27, IFN-γ, IL-22), inflammatory (CXCL9, CCL4, CCL5, CXCL8, TNF-α, IL-1β, IL-6), and anti-inflammatory (IL-10, IL-1RA) compared to HUU newborns, which persisted through 6 months of life. Among PWOH and PWH mother/neonate pairs there was a positive correlation in BAFF, IL-21, sCD14, IL-17A, and CXCL9. PWH/HEU newborns dyads displayed additional positive correlations in APRIL, sCD163, IFN-γ, CXCL10, CCL4, CCL5, TNF-α, IL-1β, IL-6, and IL-1RA. Conclusions. HEU infants have impaired early immune priming influenced by maternal immune perturbations.	L Yin, BF Fischer, GM Venturi, U Nepal, S Choudhary, J Shen, K Chang, ID Raplee, SA Borkar, JJ Kim-Chang, K D Paris, JW Sleasman, MM Goodenow	2023	VIROL
2023-189	Joseph	J	Shearer	NHLBI	Epidemiology	Frailty and Metabolic Vulnerability in Heart Failure: A Community Cohort study	BACKGROUND: Frailty is common in heart failure (HF) and associated with mortality but not routinely captured clinically. Frailty is linked with inflammation and malnutrition, which can be assessed by a novel plasma multimarker score: the Metabolic Vulnerability Index (MVX). We sought to evaluate the associations between frailty and MVX, and their prognostic impact. METHODS: In a HF community cohort (2003-2012), we measured frailty as a proportion of deficits present out of 32 physical limitations and comorbidities, MVX by nuclear magnetic resonance spectroscopy and collected extensive longitudinal clinical data. Patients were categorized by frailty score (≤0.15; >0.15 and ≤0.27; >0.27) and MVX score (≤50; >50 and ≤60; >60 and ≤70; >70). Cox models estimated associations of frailty and MVX with mortality, adjusted for Meta-Analysis Global Group in Chronic HF (MAGGIC) score and NT-proBNP. Uno's C-statistic measured incremental value of MVX beyond frailty and clinical factors. Weibull's accelerated failure time regression assessed whether MVX mediated the association between frailty and mortality. RESULTS: We studied 985 patients (median age 77, 48% women). Frailty and MVX were weakly correlated (Spearman ρ=0.21). The highest frailty group experienced an increased rate of death, independent of MVX, MAGGIC score and NT-proBNP (HR=3.3, 95% CI: 2.6, 4.2). Frailty improved Uno's c-statistic beyond MAGGIC score and NT-proBNP (0.71 to 0.73). MVX mediated <10% of the association between frailty and mortality. CONCLUSIONS: In this HF cohort, frailty and MVX are weakly correlated. Both independently contribute stratifying the risk of death suggesting they capture distinct domains of vulnerability in HF.	*S Kumar, *KM Conners, JJ Shearer, J Joo, S Turecamo, M Sampson, A Wolska, AT Remaley, MA Connelly, JD Otvos, NB Larson, SJ Bielinski, VL Roger	2023	EPIG
2023-190	Andrea		Krenek	NIDDK	Clinical Research	Recipe for heart health: a randomized crossover trial of extra virgin olive oil within a whole-food plant-based vegan diet on cardiometabolic risk factors	Background: High quality plant-based diets (PBD) are recommended for decreasing atherosclerotic cardiovascular disease (ASCVD) risk. Optimal quantity of dietary fat, particularly extra virgin olive oil (EVOO), within a PBD diet is unclear. Objective: To compare effects of high (4 tablespoon/day) vs low (<1 teaspoon/day) EVOO consumption within a whole-food PBD (WFPBD) on low density lipoprotein (LDL-C) and cardiometabolic markers. Methods: In a randomized, crossover trial, adults with >5% ASCVD risk followed a high to low (H2L) or low to high (L2H) EVOO WFPBD for 4 weeks each, separated by a 1-week washout. Linear mixed models assessed changes between phases. Results: In 40 participants (75% female, age 64+9 years), fat intake comprised 48% and 32% of energy in the high and low EVOO phases, respectively. Both diets comparably reduced LDL-C, total cholesterol, apolipoprotein B, HDL-C, glucose, and hs-CRP (all P<0.05), with diet-sequence interactions for LDL-C (P=0.003). Differences in LDL-C between diets were detected by diet order (H2L: Δ-12.7 mg/dl, P=0.04 vs L2H: Δ+15.8 mg/dl, P=0.02). Similarly, L2H order led to increased glucose, total cholesterol, and HDL-C (all P<0.05). Over period one, greater LDL-C reductions occurred after low-EVOO (-25.5+5.1 mg/dl) vs high-EVOO (-16.7+4.2 mg/dl), P=0.162, diminished over period two (-4.0+4.3 vs -9.7+5.1 mg/dl, P=0.382). Conclusions: Both patterns, containing >30% energy from dietary fat, improved cardiometabolic risk compared to baseline. More robust LDL-C decreases potentially indicates low-EVOO may be more optimal for lowering CVD risk than high-EVOO within a WFPBD. Addition of EVOO after following a low-EVOO pattern may impede further LDL reductions.	AM Krenek, A Mathews, J Guo, ST Chung, AB Courville, M Aggarwal	2023	CLINICAL

2023-191	Kartick		Patra	NIDDK	Cell Biology	Hyperglycemia inhibits ascorbic acid (VitC) mass efflux by Glucose 6 phosphate (G6P) mediated and m-TOR independent translation of a repressor protein	Compared to healthy people, people with diabetes have lower VitC concentrations. VitC is normally reabsorbed by kidney tubules. People with diabetes abnormally lose VitC in urine, independent of glycosuria. We hypothesized that hyperglycemia disrupts VitC efflux from polarized cells that mediate VitC absorption and release in intestine, liver, and kidney. We chose human hepatocytes because if our hypothesis is correct, clinical testing can follow: hepatic VitC sequestration with hyperglycemia may lower plasma VitC concentrations. Cultured hepatocytes were incubated with VitC to achieve physiologic internal VitC concentrations. D-Glucose (2-25 mM) progressively inhibited VitC efflux from hepatocytes as measured by extracellular mass of VitC released. Glucose did not effect VitC uptake into hepatocytes, nor SVCT1 (VitC transporter)-mediated VitC uptake in Xenopus oocytes microinjected with SVCT1 cRNA. In hepatocytes, D-glucose inhibited VitC efflux, but L-glucose and 3-o-methyl D-glucose did not, indicating inhibition required glucose uptake and metabolism. Inhibiting G6P metabolic progression to glycolysis, glycogenesis, and the pentose shunt potentiated glucose inhibition of efflux, indicating glucose-mediated VitC efflux occurred via G6P. As predicted, G6P was increased by inhibiting glycolysis. Chemical or genetically-transient inhibition of protein synthesis abolished inhibitory effects of glucose on VitC efflux, but rapamycin (mTOR inhibitor) had no effect. Together, these data indicate that with hyperglycemia, VitC efflux from polarized epithelial cells was inhibited via G6P-mediated m-TOR independent translation of an as yet unidentified repressor protein. We predict that hyperglycemia in diabetes will cause hepatic sequestration and decreasing plasma VitC concentrations during hyperglycemia. To test this possibility, clinical experiments are underway.	K Patra, H Tu, M Levine*	2023	CELLBIO
2023-192	Hieu	T	Van	NIDDK	Chromosome Biology	Dynamic relationship of MLL4 and BAF in enhancer activation	Enhancers are cis-regulatory elements that, through working with promoters, control cell type-specific gene expression during differentiation and development. Enhancers are highly regulated by epigenetic factors. We previously reported the inter-dependent roles of the chromatin remodeling complex BRG1/BRM-associated factor (BAF) and histone H3K4 mono-methyltransferase MLL4 (KMT2D) in enhancer activation by the adipogenic transcription factor (TF) C/EBPbb in preadipocytes. However, the molecular mechanisms by which MLL4 and BAF regulate enhancer activation are not fully understood. Using MyoD-driven myogenesis in preadipocytes, we investigate the dynamic recruitment and actions of MLL4 and BAF at the early steps of enhancer activation upon differentiation induction. To validate our observations, we also utilize the Auxin Inducible Degron (AID) rapid protein degradation system to acutely deplete MLL4 or the inhibition of BRG1, the enzymatic subunit of BAF complex, and assess the effects on enhancers. This project aims to construct a mechanistic model of lineage-determining TF-mediated enhancer activation.	HT Van, JE Lee, YK Park, K Ge	2023	CHROM
2023-193	Aruba		Chowdhury	NIDDK	Clinical Research	Small and remnant lipoproteins are associated with insulin resistance and subclinical inflammation in Youth-onset Type 2 Diabetes	Youth-onset type 2 diabetes (YT2D) is characterized by severe insulin resistance, elevated triglyceride concentrations, and low HDL-cholesterol (-C). The contribution of triglyceride-rich remnant lipoproteins (TRLp) and remnant-C to overall atherogenic risk in YT2D is unknown, especially in the absence of clinically relevant elevations in LDL-C. We hypothesized that YT2D would have higher remnant TRLp, remnant-C, and greater subclinical inflammation and insulin resistance compared to healthy peers with obesity. We measured fasting lipoprotein particle size and number, GlycA, and lipoprotein insulin resistance index (LPIR) in 61 YT2D (age 17.2 ±2.9 y, mean±SD, BMI 39.1 ±8.4 kg/m2) and 25 healthy peers (age 17.9 ± 5.1 y, BMI 35.8 ±5.7 kg/m2). YT2D had higher HemoglobinA1c (7.6 ± 2.0 vs 5.8 ± 0.8%), GlycA (427 [388, 474] vs 376 [332, 406] nmol/L, median[25th,75th]), LPIR (53.7 ± 23.6 vs 29.6 ± 16.5). YT2D had higher remnant TRLp and remnant-C and a more proatherogenic lipid and lipoprotein profile: LDL-C: 89 ± 23 vs 74 ± 20 mg/dL; total LDLp: 1392 ±368 vs 1075 ±289 nmol/L; small LDLp: 890 ±450 vs 519 ±232 nmol/L, all P<0.01. LPIR was associated with remnant-C (r=0.6, P<0.001) but not with LDL-C (r=0.1, P=0.6). GlycA was associated with remnant-C, remnant TRLp, and small LDLp (all r≥0.3, P<0.01). The proatherogenic profile in YT2D is characterized by higher small LDLp, remnant TRLp, and remnant-C and is related to insulin resistance and subclinical inflammation compared to healthy peers with obesity. Future research should determine whether reducing pro-atherogenic lipoproteins and inflammation will reduce ASCVD risk.	A Chowdhury, F Davis, A Krenek, S Dixon, L Mabundo, S Chung	2023	CLINICAL
2023-194	Elizabeth	E	Sharp	NCI	ACI/IRS	Evaluation of exposure to carcinogenic industrial land pollution among sociodemographic groups across the United States	Introduction: Most evaluations of industrial pollution focus on air emissions. Little is known about who is exposed to carcinogenic waste stored in landfills. We evaluated patterns of population exposure to carcinogenic industrial emissions to land areas in census tracts across the United States (US). Methods: We used data from the US Environmental Protection Agency's Toxics Release Inventory and the 2010 Census. We identified non-air emissions (e.g., landfills and surface impoundments) of 21 known carcinogens as classified by the International Agency for Research on Cancer. Population characteristics included race and ethnicity (e.g., Hispanic, non-Hispanic White, African American) and socioeconomic indicators (e.g., neighborhood deprivation and family poverty). We used multinomial, population density-adjusted logistic regression models to estimate odds ratios (ORs) and 95% confidence intervals (CIs) comparing the highest category of emissions quintiles: Q5) to the referent group of zero emissions (non-exposed). Results: In 2018, 273 million pounds of carcinogens (e.g., asbestos, arsenic, nickel, polychlorinated biphenyls) were stored in landfills and surface impoundments in 1,807 tracts (estimated population: 7.6 million people). The proportion of African American and Hispanic population in the tract was associated with higher odds of having the highest land emissions (Q5), whereas the pattern was inverse for White (and Asian populations. Tracts with the highest quintile of carcinogenic land emissions had lower median	EE Sharp, JM Madrigal, MH Ward, JA Fisher, A Flory, RR Jones, BI Graubard	2023	ACI/IRS
2023-195	Peng		Gao	NCATS	Computational Biology	Deep learning- and biochemical activity-based screening strategy for rapid discovery of COVID19 drug candidates: inhibition for both SARS-CoV-2 cell-entry and 3CL protease replication	To enhance COVID19 treatment development and gain experience for similar pandemic response, a systematic yet comprehensive elucidation of biological mechanism involving the inhibition of severe acute respiratory syndrome coronavirus 2 (SARS-CoV-2) is highly needed. To propose an efficient yet reliable drug discovery strategy to overcome this terrible disease, both cell-entry and intra-cell inhibitions should be considered. The role played by the cell surface biopolymer, heparan sulfate (HS), is crucial for viral entry bio-process. Inside the host cell, the compounds with high-performance inhibition to viral replication should be preferred. Thus, the ideal candidate compound should be competitive in both aspects, instead of being one-sidedly emphasized. In this study, we proposed a combinational drug discovery strategy for anti-SARS-CoV-2 inhibitors screening. The virtual screening part was based on a double-layer deep learning algorithm that consists of both molecular graph processing and descriptors correction. The experimental validations of the screened compounds were crossly conducted upon 3-chymotrypsin-like (3CL) based, pseudotyped particle (PP), S{\alpha}S-Synuclein fibrils uptake and cell-based live SARS-CoV-2 (CPE) assays. Based on this strategy, we successfully identified the lead compounds that display high inhibitions for both viral entry and intra-cell replication; and their efficacy was also verified by PRNT and iPSC-derived 3D lung model. To further elucidate the reaction pathways of these inhibitors, quantum mechanics (QM) calculations were conducted for microscopic binding observations under biological environment. This novel strategy is instructive for future biological investigations; and the proposed virtual screening workflow is also a robust complementary for qualitative high-throughput screening (qHTS) based drug discovery.	P Gao, I Pavlinov, M Xu, X Huang, Q Zhang, M Shen, CZ Chen, W Zheng	2023	COMPBIO
2023-196	Emma		Price	NIAID	Genetics and Genomics	Transcriptional regulation and beyond: uncovering CTCFL functions in spermatogenesis using a novel humanized mouse model.	During the process of spermatogenesis, significant epigenetic reprogramming occurs in the genome. CTCFL, a DNA-binding protein is expressed early in spermatogenesis and is widely recognized as a transcriptional regulator. Recent studies have suggested that CTCFL may have additional functions in organizing chromatin and controlling transposable elements, both of which are crucial for maintaining genome integrity. Our objective is to investigate the potential involvement of CTCFL in these processes. However, two major challenges have hindered progress in this area. Firstly, obtaining human germ cells that express CTCFL involves invasive procedures. Secondly, antibodies that target mouse CTCFL result in non-specific binding profiles in ChIP-seq analysis. Consequently, it is difficult to acquire human germ cells and mouse germ cells are unsuitable for analysis. To overcome these limitations, we have developed a novel humanized mouse model that expresses human CTCFL in mouse germ cells. This model enables us to utilize antibodies that have been verified for their specificity in targeting human CTCFL. By performing ChIP-seq analysis, we have discovered thousands of previously unidentified binding sites of CTCFL in germ cells. This breakthrough has set the foundation for our ongoing multi-omics approach, incorporating single-cell RNA-seq, ATAC-seq, and other NGS techniques to assess the epigenetic landscape in humanized germ cells and perform a comprehensive analysis of CTCFL functions during spermatogenesis.	E Price, EM Pugacheva, YJ Ji, D Loukinov, V Lobanenkov	2023	GEN
2023-197	Noriko		Seishima	NCI	Immunology	Peptide-pulsed MHC class II mutant dendritic cell vaccine has superior efficacy in a murine tumor model.	Autologous dendritic cell (DC) vaccines with tumor antigens have been used clinically with limited therapeutic effects. Semi-allogeneic DC-based immunotherapy is still controversial, but it can be an alternative source and more attractive than autologous DC vaccines because the "off-the-shelf" DCs can be used for multiple patients without lengthy individual manufacturing time and may provide additional "allogeneic help". This study aims to compare efficacy of syngeneic DC vaccines and semi-allogeneic DC vaccines and determine whether a therapeutic semi-allogeneic DC vaccine is more efficacious in tumor suppression. Female C57BL/6 mice were inoculated subcutaneously with human papillomavirus E6 and E7-expressing TC-1 cells. Syngeneic bone marrow dendritic cells (BMDCs) were generated from C57BL/6 and semi-allogeneic BMDCs were generated from two mouse strains, B6.C-H2-Kbm1/ByJ and B6(C)-H2-Ab1bm12/KhEgJ which had limited point mutations in the MHC class I H2-Kb allele or H2-IAb MHC class II allele, respectively. Each BMDC was pulsed with H-2Db-restricted E743-77 peptide and matured before injection. The mice received 4-5 intradermal injections of syngeneic or one of the semi-allogeneic E7-pulsed BMDC vaccines starting 8-9 days after the TC-1 implantation. Compared with saline control, the MHC class I mutant BMDC vaccine had efficacy similar to the syngeneic BMDC vaccine in suppressing TC-1 tumor growth. However, the MHC class II mutant BMDC vaccine had efficacy significantly superior to that of the other BMDC vaccines. Thus, MHC class II semi-allogeneic BMDCs may be more effective than syngeneic DC-based cancer vaccines, presumably because the class II alloantigens induce additional T cell help for anti-tumor immunity.	N Seishima, PB Olkhanud, W Becker, H Maeng, M Lopez-Lago, C Wiseman, WV Williams, JA Berzofsky	2023	IMMUNO
2023-198	Christian	I	Lantz	NINDS	Neuroscience	Elucidating CHCHD10 mutant phenotypes in inducible cell models and designing effective therapeutic strategies	Mutations in the mitochondrial protein CHCHD10 cause autosomal dominant neuromuscular disorders including frontotemporal dementia (FTD)/ALS, mitochondrial myopathy, lower motor neuronopathy (SMAJ, spinal muscular atrophy Jokela type), and a familial form of ALS. These mutations have a strict genotype-phenotype relationship, with the p.G58R mutation causing a pure myopathy and the p.G66V mutation causing a pure lower motor neuronopathy. The molecular basis for this genotype-phenotype relationship is not well understood, and the current model of pathogenicity is toxic gain-of-function, as CHCHD10 knock-in mice but not CHCHD10 KO mice recapitulate the myopathy phenotype seen in patients with the p.G58R or p.S59L variants, as demonstrated by our lab and others. To better understand the genotype-phenotype relationship among CHCHD10 mutations, we are using a robust DOX-inducible system of differentiation of human wild type iPS (induced pluripotent stem) cells into motor neurons and myocytes. After inducing mitochondrial stress, we measured the transcriptional signature of these cells. Using CRISPR Cas9, we've generated an allelic series of iPS cells with the homozygous pathogenic CHCHD10 mutations p.R15L, p.S59L, p.G58R, and p.G66V, as well as CHCHD10 knock-out (KO), that we will differentiate into motor neurons and myocytes to compare transcriptional signatures between mutant lines. Finally, by designing non-allele-specific antisense oligonucleotides (ASOs) targeting CHCHD10 mRNA, we are developing an effective therapy that can target diseased tissues like skeletal muscle and motor neurons. We have screened and identified several ASO candidates that are effective in knocking down CHCHD10.	CI Lantz, JC Mercado, C Grunseich, J Thayer, A Garcia-Guerra, ME Ward, C Rinaldi, DP Narendra	2023	NEURO
2023-199	Charnae'		Henry-Smith	NIA	ACI/IRS	Impact of atherosclerosis-induced cellular senescence on vascular cognitive impairment and dementia (VCID)	Vascular Cognitive Impairment Disease (VCID) is an increasingly prevalent form of dementia that is second only to Alzheimer's disease in incidence. Many risk factors for VCID include cardiovascular diseases (CVD) such as atherosclerosis and hypertension, suggesting a strong link between VCID and CVD. Given the presence of vascular smooth muscle cells, endothelial cells, and immune cells displaying senescent-like phenotypes, i.e., increased activity of SA-β-Gal (senescence-associated β-galactosidase), in atherosclerotic lesions, it has been reported that atherosclerosis can cause cellular senescence within the aorta. Because atherosclerosis is a disease of the largest artery and can impact all organs and tissues, we hypothesize that atherosclerosis can promote senescence in other organs, such as the brain, either by plaque formation in remote locations or by triggering the senescence associated secretory phenotype (SASP). To test our hypothesis, we performed a series of functional and behavior tests on control, atherosclerotic mice fed a high-fat diet (HFD), and atherosclerotic mice treated with a senolytic drug, ABT-737. The preliminary results suggest male HFD mice had reduced homecage locomotor activity during their dark (wake) phase, showed increased anxiety-like behavior in both the open field test and elevated plus maze, and displayed impairment in long-term spatial memory and that this effect was potentially rescued by ABT-737. Pulse wave velocity data revealed increased arterial stiffening in HFD mice compared to control mice and that treatment with ABT-737 rescued this phenotype. Together, these data suggest that atherosclerotic male mice exhibit cognitive decline that may be rescued by senolytic drug, ABT-737.	C Henry-Smith, A Carr, Q Claybourne, R McDevitt, C Rocha Dos Santos, O Fedorova, D Tsitsipatis, J Martindale, R Munk, M Gorospe, AB Herman	2023	ACI/IRS
2023-200	Yili		Zhao	NCCIH	Neuroscience	Domain-general and domain-specific activations of expectancy-based pain modulation as compared to aversive and pleasant tastes	Pain perception's specificity is disputed. Despite previous research identifying pain-specific neural patterns such as the neurologic pain signature (NPS) and the stimulus intensity independent pain signature (SIIPS), these activations often overlap with other salience experiences and a general negative affect pattern. The orbitofrontal cortex (OFC) and the anterior insula have been implicated in value-based learning and expectation across domains including pain. However, the expectation effect and underlying neural mechanisms across pain and both aversive and pleasant sensations lack direct investigation. In this study, we compared pain perception with both unpleasant and pleasant tastes (i.e., heat, salt, and sugar) in sixty participants during fMRI scanning. During conditioning, visual cues were paired with high-intensity (high cue) or low-intensity (low cue) stimulation. Each cue was then equally likely to be followed by its conditioned intensity or a medium intensity stimulus. Intensity and valence were rated after each stimulus. Participants reported higher intensity for medium stimuli preceded by high cues versus low cues. Cue-relevant anticipatory activation in OFC was observed across all groups. While the anterior insula mediated cue effects on intensity ratings for medium trials across all domains, distinct domain-specific effects were uncovered when examining the OFC's moderating role. Notably, the NPS and SIIPS demonstrated greater differentiation in the heat group compared to taste groups, while the affect pattern did not differ between the heat and salt groups. Our findings suggest that predictive cues engage both domain-general and domain-specific mechanisms in pain compared to taste perceptions.	Y Zhao, IS Lee, Q Yu, M Rose-McCandlish, D Mischkowski, J Avery, JE Ingeholm, LY Atlas	2023	NEURO

2023-201	Jennifer		Bowling	CC	Microbiology and Infectious Diseases	Candida parapsilosis sensu stricto: prevalence and antifungal susceptibility profile in patients with underlying immunodeficiencies	Candida parapsilosis sensu stricto (C. parapsilosis SS) is a leading cause of invasive candidiasis in southern Europe, Latin America and Asia. Although it is generally considered susceptible to triazoles, clonal expansion of fluconazole-resistance has been reported in health care settings in some countries. In this study, we aimed to determine the prevalence and associated mutations of fluconazole-resistance phenotypes of C. parapsilosis SS isolated from patients with underlying immunodeficiencies at NIH Clinical Center. A total of 43 C. parapsilosis SS isolates were tested. Species level identification was confirmed by Matrix-assisted laser desorption/ionization time-of-flight mass spectrometry (MALDI-TOF) and PCR-sequencing of the internal transcribed spacer and D1/D2 region of ribosomal DNA gene. Antifungal susceptibility testing was performed using broth microdilution. The results were analyzed using current Clinical and Laboratory Standards Institute (CLSI) M60-Ed2-2020 breakpoints. Overall, C. parapsilosis SS was the primary contributor of yeast related blood stream infections, accounting for 24% of infections. All of the isolates tested were 100% susceptible to anidulafungin, caspofungin and amphotericin B. The susceptibility rate of micafungin was 93.3% and 97.6% of the isolates were found to be susceptible to voriconazole. Of all isolates tested, one was susceptible-dose dependent (MIC 4 µg/ml) and one was resistant (MIC ≥ 8 µg/ml) to fluconazole. Both isolates were sourced from blood. In conclusion, prevalence of C. parapsilosis SS among clinical yeast isolates was significantly high in our Center. Further studies are warranted to explore the molecular mechanism of fluconazole resistance and its association to prior azole use in these isolates.	JD Bowling, CI Aneke, SE Shahegh, J Youn, JM Cuellar-Rodriguez, A Seyedmousavi	2023	MICROBIO
2023-202	Dale	O	Kiesewetter	NIBIB	Research Support Services	Radiolabeling of peptides, nanobodies, and aptamers for positron emission tomography (PET)	Our NIBIB core facility has a mission to provide state of the art positron emission tomography imaging in small animals. Our equipment includes a Mediso nanoScan PET/CT instrument to provide high quality, quantitative images of radioisotope distribution in mice or rats. In addition, we have a radiochemistry facility to synthesize Ga-68 and F-18 labeled radiotracers. We now have available fluorine-18 labeled prosthetic groups that can be attached to peptides, nanobodies, and aptamers. Using copper-mediated radiofluorination of aryl boronates, we have prepared N-hydroxysuccinimidyl [18F]fluorobenzoate for attachment to lysine residues; 1-(3-(4-(4-[18F]fluorobenzyl)piperazin-1-yl)-3-oxopropyl)-1H-pyrrole-2,5-dione (a maleimide) for attachment to free cysteine thiol residues; and 2-azido-1(4-(4-[18F]fluorobenzylpiperazin-1-yl)ethan-1-one for attachment to alkyne residues using copper catalyzed "click" chemistry. The preparation methods for the various compounds utilize the same automated radiosynthesis system with only slight variations in purification conditions. These compounds can be conjugated to appropriate biomolecules and the resulting product used for PET/CT imaging.	DO Kiesewetter, L Lang, Y Ma	2023	RSCHSUPP
2023-203	Katherine	A	Maki	CC	ACI/IRS	Unraveling Gut-Brain Communication Mechanisms using Clinical Phenotype, Microbiome, and Structural MRI Features in Patients with Alcohol Use Disorder	Background: Alcohol misuse is a public health concern and alcohol use disorder (AUD) contributes to chronic health conditions. Studies suggest the gut microbiome plays a role in AUD and its associated symptoms through gut-brain communication. The objective of this study was to 1) evaluate associations between morphometry of stress-associated areas of the brain and the microbiome and 2) characterize longitudinal relationships between AUD-associated symptoms and the gut microbiome. Methods: Subjects undergoing inpatient treatment for AUD were studied (n=20, 35% female). Stool specimens and symptoms of anxiety, depression, withdrawal, sleep disturbance and alcohol cravings were collected weekly while inpatient (4 weeks). Structural MRIs (n=16) were obtained at week 2 and morphometry was quantified in brain regions of interest (ROIs) involved in the hypothalamic-pituitary-adrenal axis. Shotgun metagenomics sequencing was performed and the neuroactive potential of predicted metagenomes was tested using gut-brain modules. Results: Anterior cingulate cortex (ACC) thickness was negatively associated and amygdala volume was positively associated with microbiome alpha diversity (Shannon Index). Several Blautia taxa were associated with amygdala and ACC ROIs, along with AUD-associated symptom severity scores. Longitudinal responses of clinically significant microbiome features will also be presented. Conclusions: In this cohort of subjects, ACC and amygdala morphometry were associated with microbiome features suggesting gut-brain communication with these brain regions in patients with AUD. Ongoing work will quantify longitudinal responses of bacteria and gut-brain modules associated with symptom severity scores in hopes of providing preliminary data to design future studies aimed at improving mental health symptoms in patients with AUD.	KA Maki, JJ Barb, LY Hsu, L Yang, VA Ramchandani, ML Schwandt, N Diazgranados, R Momenan, GR Wallen	2023	ACI/IRS
2023-204	Josette		Wlaschin	NICHD	Neuroscience	Investigating alterations preceding neurodegeneration in TDP-43 deficient motor neurons	Amyotrophic lateral sclerosis (ALS) is a progressive and fatal neurodegenerative disease that affects thousands of patients and their families. 97% of ALS patients display a common pathology where the essential nucleic acid binding protein, TDP-43, is mislocalized outside of neuronal nuclei. Due to its role in RNA splicing, mislocalization of TDP43 results in the aberrant splicing of numerous transcripts, including the inclusion of normally repressed cryptic exons. To understand the early changes associated with nuclear loss of TDP-43, we examined the functional and transcriptomic alterations in a mouse model where TDP-43 is conditionally deleted from motor neurons. These animals develop progressive motor symptoms due to motor neuron loss over the course of 2-3 months of age. However, the exact mechanisms by which loss of TDP-43 results in motor neuron death are not well understood. By compound muscle action potential recordings from the tibialis anterior muscle, we detect a significant reduction in motor neuron function preceding motor neuron loss and muscle denervation. We hypothesize changes in motor neuron gene expression may account for this functional deficit. We performed single nucleus RNA sequencing of lumbar motor neurons to examine changes in gene expression as well as RNA sequencing of the lumbar spinal cord to assess potential mis-splicing of transcripts in this model. We will assess expression of genes involved in establishing motor neuron identity/function, stress response genes, and misregulated pathways to better understand pathological progression associated with loss of TDP-43. Ultimately these findings could provide potential therapeutic approaches for ALS patients.	JJ Wlaschin, P Lee, S Seddighi, M Alkaslasi, H Sliberberg, CE Le Pichon	2023	NEURO
2023-206	Sasha		Coates-Park	NCI	Cancer Biology	Regulation of TIMPs through MMP-dependent cleavage	Tissue Inhibitors of Matrix Metalloproteinases (TIMPs) are a broadly expressed family of matrisome proteins which are the primary regulators of metalloproteinase (MP) proteolytic activity. In addition to their canonically described functions, TIMPs display a broad range of MP-independent functional roles associated with proliferation, apoptosis, migration, and differentiation. MPs are endopeptidases that play an essential role in maintaining the extracellular matrix through proteolytic turnover; a balancing act maintained (in part) by the local MMP:TIMP ratio. Disturbances in the balance between MPs and TIMPs are associated with various disease states, including cancer, heart disease, arthritis, and cognitive dysfunctions. We describe a novel mode of MP-dependent regulation of TIMP function. We show that a molar excess of active matrix metalloproteinase 9 (aMMP9) can cleave TIMP proteins within their C-terminal domains, altering both the MP-dependent and -independent functions of TIMPs. MMP9 abundance and activity is often elevated during the pathogenesis of various diseases, and persistent MMP9 activity is frequently associated with worse prognoses. MMP9 is predominantly produced by stromal cell types such as fibroblasts and myeloid cells. Importantly, myeloid cell types often display low levels of TIMP production and thus may represent a functionally compelling source of TIMP-free MMP9. By stimulating myeloid cells into MMP9 secreting and activating subtypes, we interrogate the conditions that may enable TIMP cleavage in vivo. Investigation of the circumstances which modulate the balance between MPs and TIMPs may reveal new therapeutic opportunities in a range of disease models.	SI Coates-Park, S Gurung, C Lazaroff, JA Rich, W Stetler-Stevenson, D Peeney	2023	CANCER
2023-207	Sandy	T	Reynolds	NHLBI	Health Disparities	The associations between loneliness and circulating lipoproteins as well as diabetes risk in African-American women residing in resource-limited neighborhoods: Data from the Step It Up Physical Activity Intervention	Recent reports suggest that people suffering from loneliness have increased cardiovascular disease (CVD) risk. A potential link between loneliness and CVD is an atherogenic shift in the lipoprotein profile. In this study, we investigated associations between loneliness and lipoproteins in African American (AA) women residing in resource-limited Washington, DC neighborhoods. Participants were enrolled in Step It Up, a technology-based, community-engaged PA intervention. Fasting blood samples were drawn at baseline to measure lipoproteins using NMR technology. The Lipoprotein Insulin Resistance Index (LP-IR), a diabetes risk marker, was calculated. Loneliness was measured using the UCLA Loneliness scale. Associations between loneliness, lipoprotein particles and LP-IR were analyzed using multivariable regression adjusted for BMI, ASCVD 10-year risk score, and lipid-lowering therapy. AA women with CVD risk (N=106, Age 55.9±13, BMI 36.3±6.7) were enrolled into Step It Up. Higher loneliness at baseline was associated with higher Apo-B (beta=0.26,p=0.02), LDL concentration (beta=0.23,p=0.02), and LDL particle number (beta=0.25,p=0.01), but not with LDL particle size. Higher loneliness associated with triglyceride-rich lipoprotein (TRL) size (beta=0.23,p=0.02). This relationship appeared to be due to large and very large TRL particles (p<0.05). No significant associations were found with HDL-related measures. Lastly, loneliness significantly associated with LP-IR, a diabetes risk marker (beta=0.22,p=0.03). Thus, our data show that higher loneliness in AA women from under-resourced neighborhoods is associated with increased hyperlipidemia and diabetes risk. Our findings highlight a potential mechanism by which loneliness may accelerate CVD risk and support the urgent need for multilevel interventions to reduce loneliness and CVD risk in at-risk populations.	S.T Reynolds, Y Baumer, A Dave, M.A Cintron, H.A Tarfa, M.A Pita, L.R Ortiz-Whittingham, L.A Potharaju, A.S Baez, K Thompson, F.O Baah, J.F Troendle, C Ayers, V.M Mitchell, M Marah, B.S Collins, A Saurabh, M Sampson, A.T Remaley, T.M Powell-Wiley	2023	HEALTH
2023-208	Caleb	B	Darden	NIAAA	ACI/IRS	Effects of chemogenetic modulation of MSglu on NAc DA responses during strategy switching	Maladaptation in reward-seeking is an important aspect in the development and maintenance of substance use disorders (SUDs) and understanding brain mechanisms involved in reward-seeking is a crucial first step towards developing therapeutics for SUD. Emerging evidence suggest a brain region called the medial septum (MS) is involved in reward-seeking behaviors. The MS has been found to generate reward signals when electrically stimulated, and it was recently shown that mice lever-press to earn optogenetic stimulation of specifically MS glutamate neurons (MSGLUn). Excitation of MSGLUn can influence canonical reward circuitry leading to dopamine (DA) release in the nucleus accumbens (NAcDA), a primary component of reward-seeking. Our lab found chemogenetic modulation of MSGLUn had little effect on reward-seeking behavior, but these modulations evoked changes in reward seeking strategy. Here we sought to elucidate the regulatory role of MSGLUn on NAcDA that mediate strategy switching. We found that chemogenetic excitation of MSGLUn during strategy switching correlated with increased NAcDA in response to unexpected rewards compared to NAcDA responses expressed in inactivation and control groups. Once cues were learned, chemogenetic excitation of MSGLUn showed higher NAcDA in response to the learned signal than controls, suggesting MSGLUn is involved in NAcDA release during strategy switching tasks. In future studies, we aim to continue using fiber photometry to better understand interactions between MSGLUn and NAcDA amid reward-seeking and strategy switching. Findings may enhance our understanding of how this circuitry may contribute to substance use disorders and guide the development of new therapeutic techniques.	CB Darden, S Ramos-Maciel, N Westcott, AJ Kesner	2023	ACI/IRS
2023-209	Elisa	H	Son	CC	Social and Behavioral Sciences	Digital health engagement behaviors (DHEB) of family caregivers in the United States: A latent class analysis	Digital health technologies can be helpful for family caregivers who need information and resources without time and space restrictions. However, digital health engagement behaviors and associated characteristics of family caregivers remain less explored. The study aimed to identify subgroups of family caregivers in the United States who share similar patterns of digital health engagement behaviors (DHEB), and to investigate factors associated with the subgroup classification. A secondary cross-sectional analysis was performed using the Health Information National Trends Survey 5 Cycle 3 and Cycle 4 datasets. Latent class analysis with sampling weights was used to identify subgroups of 885 family caregivers based on 10 types of DHEB. Two classes were derived: High DHEB (Class 1, 54%), and Low DHEB (Class 2, 46%). Caregivers who owned both a tablet and a smartphone (OR 2.56, CI 1.49 - 4.41) and had a college degree or higher (OR 2.74, CI 1.66 - 4.53) were more likely to be in the High DHEB group. Caregivers with High DHEB were more likely to report better general health status than caregivers with Low DHEB (OR 2.46, CI 1.23 - 4.93). DHEB of family caregivers appeared in distinct patterns based on their level of engagement. Our findings suggest the importance of establishing personalized strategies to encourage DHEB of family caregivers who may benefit most from increasing their use of digital health technologies. Health policymakers might elevate the discussion of digital health engagement to the policy level and use such information to facilitate the best support for caregiver populations.	EH Son, GR Wallen, L Yang, RT Tuason, C Gerrard, LI Lee	2023	SOCIAL
2023-210	Shubhra	J	Saha	NIDDK	Chemical Biology	Binding of nanobody to peptide epitopes facilitate in situ synthesis of GPCR specific agonist	Bioactive compounds possess unfavorable properties for drug development due to on-target, off-tissue mediated side effects. One alternative is to use fragments that can react to form a bioactive product upon exposure to a certain stimulus or chemical. We sought to apply this approach for activation of the parathyroid hormone receptor-1 (PTHR1), which regulates skeletal development, and mineral ion homeostasis. Two fragments (PTH1-11 and PTH12-34) together comprise the prototypical peptide agonist of PTHR1 (PTH1 34). Here we describe methodology for the in-situ synthesis of conjugates that resemble PTH1 34 through peptide template-induced dimerization and click (azide-alkyne) reactions between the fragment peptides PTH1-11 and PTH12-34. Templated dimerization was achieved in presence of a heterodimeric peptide (HDP), fusing PTH fragments containing click chemistry handles to one of two Nbs that bind to short peptide epitopes. HDP was used to bring fusions comprised of Nbs and PTH fragments with complementary click handles, into proximity. Gel electrophoresis analysis of the kinetics of the reaction between azide- and alkyne-functionalized Nbs showed that HDP accelerated product formation. We also used a fluorescence resonance energy transfer assay and fluorophore-labeled Nbs to corroborate the finding that HDP induces proximity between Nbs. During the cell-based assay, HDP facilitated click chemistry-induced dimerization. Whereas PTH fragment-click handle-Nb conjugates were weakly active alone or when added in tandem, the addition of HDP to the tandem mixture resulted in strong activation of the PTHR1. Altogether, this approach entails a new strategy for in situ synthesis of a bioactive agonist from its inactive fragment peptides.	S J Saha, R W Cheloha	2023	CHEMBIO
2023-211	Sarah	G	Castle	NCATS	Molecular Pharmacology	Preparation of Analogs Containing the Minimalist Diazirine Moiety to Identify the Target for the Activation of the Mitochondrial TRAP1 Protein	Lysosomal and mitochondrial dysfunction has been implicated in the pathogenesis of several neurodegenerative disorders, such as Alzheimer's and Parkinson's. Activation of the mitochondrial chaperone tumor necrosis factor receptor-associated protein 1 (TRAP1) has been shown to correct lysosomal storage phenotype in patient cells from lysosomal storage disorders such as Niemann-Pick C1 (NPC1). Small molecules to activate TRAP1 have been shown to restore lysosomal and mitochondrial health. Using high-throughput screening, we identified and optimized hit compounds into lead compounds NCGC00351685 and NCGC00348187. Further studies need to be done to determine the target binding of small molecule agonists to TRAP1. We chose minimalist acetylene-containing diazirine derivatives to help us determine the binding site of these TRAP1 agonists to TRAP1.	SG Castle, RR Calvo, Y Ioannou, J Marugan, S Patnaik	2023	PHARMA

2023-212	Caitlin	N	Strain	NCI	Cancer Biology	Enzymatic Glycosylation of MUC4 Tandem Repeat Sequences	Mucin-type glycosylation, otherwise known as O-GalNAc glycosylation, is the most common form of O-linked glycosylation in mammalian cells. Mucins are a family of ~20 secreted and/or membrane bound high molecular weight proteins and contain long stretches of tandem repeat (TR) peptide sequences with N-acetylgalactosamine (GalNAc)-initiated oligosaccharide chains linked to the hydroxyl group of the TR's serines or threonines. These glycoproteins are essential for processes including cell-cell communication, cellular protection, and signal transduction. In disease states, they are known to resist apoptosis, initiate immunogenic responses, and enhance metastasis, resulting in their over expression in several cancers. Mucin 4 (MUC4) is specifically known for its over expression in pancreatic ductal adenocarcinoma (PDAC), and lack of expression in healthy pancreas tissue, making it a biomarker for the disease. While the mechanism for glycosylation is well understood- involving the interaction of the mucin with uridinediphospho-GalNAc (UDP-GalNAc) and one of the 20 polypeptide N-acetylgalacosaminyltransferase isoenzymes (GALNTs) within the Golgi body- specific glycosylation selectivity towards TR serines and threonines is not as well-known and needs further exploration. We set out to examine the substrate specificity of various TR sequences from MUC4 by replicating mucin-type glycosylation in vitro, with the goals of identifying primary sites of glycosylation on TR sequences and determining patterns of glycosylation across the isoenzymes. Understanding glycosylation specificity and selectivity will expand our knowledge of cancer generation and aid future development of cancer therapeutics.	CN Strain, AN Murphy, J Barchi Jr.	2023	CANCER
2023-213	Allison		Niemiec	CC	Clinical Research	Muscle weakness detected by Maximal Voluntary Isometric Contractions may go undetected by Manual Muscle Testing in men with Spinal Bulbar Muscular Atrophy	Manual Muscle Testing (MMT) is the most common clinical strength assessment. Drawbacks of MMT include poor sensitivity for strong muscles, subjective grading, and examiner stature influence. Alternatively, Maximal Voluntary Isometric Contraction (MVIC) provides precise measurement for all strength levels, but is costly and time-consuming. MMT and MVIC have not been compared in Spinal and Bulbar Muscular Atrophy (SBMA), a progressive neuromuscular disease characterized by muscle weakness. This study compared MMT and MVIC testing in 44 adult men (53y ± 10y) with SBMA. Eight bilateral muscles were tested: elbow flexors, elbow extensors, shoulder abductors, knee extensors, hip abductors, hip extensors, hip flexors, and ankle dorsiflexors. MMT was scored on a 10-point scale. MVIC was converted into percent of predicted strength using normative equations. Correlations were run between strength tests and quality of life/functional measures: Short Form 36 Questionnaire, Activities of Daily Living, Two Minute Walk Test, and Adult Myopathy Assessment Tool. All muscles combined, MVIC revealed more weakness than MMT (MVIC mean 50.6% of predicted, MMT mean 8.9/10). Notably, for knee extensors, hip abductors, and ankle dorsiflexors, ≥ 75% of patients scored 10/10 on MMT, but had an average of only 35-55% of predicted strength. MMT did not correlate with MVIC. Correlations between strength and quality of life/functional measures were stronger for MVIC than MMT. In this population, MMT did not detect significant muscle weakness, therefore clinicians should not interpret an MMT score of 10 as "healthy". MVIC more accurately identified weakness and correlated with function, allowing for earlier intervention strategies.	AC Niemiec, GO Joe, AD Kokkinis, KH Fischbeck, C Grunseich, JA Shrader	2023	CLINICAL
2023-214	Qian		Yao	NCI	Chromosome Biology	Genome-wide profiling of DNA supercoiling domains in human cells	DNA supercoiling is an important feature of the double helix and is critical for regulating chromatin environment and gene expression. However, the understanding of DNA supercoiling in living cells is limited, largely due to a lack of technologies. Here, we developed an azide-psoralen based quantitively detection DNA supercoiling method, termed ATMP-seq, which profiled the human genome is organized into supercoiling domains (SDs). We further revealed such SDs were shaped by balancing transcription-generated supercoiling propagation along chromatin and relaxation by actively regulated topoisomerase. Relaxation of SDs by topoisomerase is actively regulated via 3D chromatin organization. We also found accumulation of negative supercoiling around the boundaries of topologically associating domains. Finally, we demonstrated the dynamics of SDs and supercoiling in human cells, that contribute to the chromatin environment affecting DNA-related processes.	Q Yao, L Zhu, Z Shi, S Banerjee, C Chen	2023	CHROM
2023-215	Samiksha	A	Borkar	NIAID	Virology	Unique Gene Expression Profile in Youth with Human Immunodeficiency Virus (HIV) Suppression on ART: Implications for Novel Diagnostic or Therapeutic Targets	Background. Antiretroviral therapy (ART) suppresses HIV replication, but viral infection persists. We analyzed gene expression in youth with HIV (YWH) on ART with or without sustained viral suppression and youth without HIV (YWOH) to reveal molecular bioprofiles associated with control or persistence of viral replication. Methods. Peripheral blood cell mRNA was profiled using Affymetrix HG-U133 Plus 2.0 Arrays for 52 participants (27 YWH and 25 YWOH) balanced for age, gender, and race. Among 27 YWH (18-23 years), 19 achieved sustained viral suppression (VS) (< 50 RNA copies/ml plasma), while 8 had detectable viral replication (VNS). Differentially expressed genes (DEGs) were identified using samr package (FC ≥ 1.3 and FDR ≤ 0.05). Pathway analyses were based on the Gene Ontology database, while Protein-Protein Interaction networks were inferred from the STRING database. Results. Compared to YWOH, VNS YWH showed 1003 DEGs with 47 perturbed pathways related to interferon signaling and defense against viruses, while VS YWH had 14 perturbed pathways with 367 DEGs, including platelet activation and regulation of serine/threonine protein kinase. Unique hub genes regulating chronic inflammation (HSP90AB1, RhoA, PDGFA, and STK4) were observed in youth with VS compared to YWOH. Direct comparison between VS or VNS YWH identified 131 DEGs involved in DNA repair, RNA processing, and negative regulation of RNA polymerase II transcription pathways, while YY1, Dicer1, and XRCC2 were hub genes associated with viral suppression in youth. Conclusions. Youth on ART with viral suppression display distinct molecular profiles that could guide personalized treatment and diagnostics for HIV resurgence.	SA Borkar, L Yin, KF Chang, J Shen, BM Fischer, GM Venturi, JJ Kim-Chang, U Nepal, ID Raplee, KD Paris, JW Sleasman, MM Goodenow	2023	VIROL
2023-216	Dara	N	Love	NCATS	Molecular Pharmacology	Discovery and optimization of a LATS1/2 kinase inhibitor for applications in wound healing and regenerative medicine	The evolutionarily conserved Hippo pathway plays a key role in organ size regulation and homeostasis by acting as a "brake" on the activity of transcriptional coactivators YAP and TAZ. Central to the activity of this pathway is a kinase cascade involving LATS1/2, which inactivates the YAP/TAZ complex through serine phosphorylation and maintains its subcellular localization in the cytoplasm. In healthy cells, inhibition of LATS1/2 allows the YAP/TAZ complex to remain active and translocate to the nucleus, resulting in cell proliferation via mitosis. Recent studies indicate that LATS1/2 inhibition may have highly beneficial effects in the fields of regenerative medicine and wound healing, but the small number of potent, selective pharmacological options for LATS1/2 inhibition limits exploration of this hypothesis. In order to examine this potential, we endeavored to develop a selective kinase inhibitor for LATS1/2 suitable for use in animal models. A kinome-wide screen of existing commercial kinase inhibitors led us to our initial hit compound; further optimization of the hit simultaneously enhanced its activity against LATS1/2 and reduced activity against its original kinase target. Further optimization of its ADME properties resulted in our lead compound, which demonstrates excellent inhibition of LATS1/2 in murine models and may prove suitable for testing our regenerative medicine hypothesis.	DN Love, PJ Morris, DY Duveau, GR Bantukallu, M Ceribelli, L Evsen, SB Hoyt, FA Tosto, CJ Thomas	2023	PHARMA
2023-217	Jihye	L	Golino	NCI	Cancer Biology	The anti-tumoral effect of verteporfin via modulation of immune response and cancer stemness in a murine cholangiocarcinoma model	Cholangiocarcinoma (CCA) is a heterogenous malignancy derived from the epithelium in the biliary tree system with poor prognosis. Yes-associated protein (YAP) pathway was reported to affect various aspects of tumorigenesis and higher expression of YAP is negatively associated with the survival rate in CCA patients. Moreover, overexpression of YAP along with AKT in mice triggers CCA formation, suggesting YAP pathway is a potential target to control CCA. Verteporfin was reported as inhibitory effect of overgrowth of the liver induced by overexpression of YAP with cancer stemness markers. Thus, we investigated the antitumoral effect of verteporfin, a YAP inhibitor, in the YAP/AKT hydrodynamic tail vein injected murine model. The results demonstrated reduced liver weight and tumor formation in the verteporfin treated group compared to the vehicle treated group. Immune cell profiling using flow cytometry indicated verteporfin induced higher ratio of tumor-associated macrophage (TAM) M1/M2, indicating verteporfin treatment induced M2 to M1 phenotype transition. The percentage of activated CD8 T cell population was also induced by the verteporfin treatment, suggesting T cell activation might be the mechanism of verteporfin suppresses tumor progression. PD-1+CD39+CD8+ T cells were significantly reduced in the verteporfin treated group, indicating verteporfin may inhibit complete/terminal exhaustion of CD8 T cells. Single cell RNA sequence analysis showed that TAM M1 populations increased following verteporfin treatment. The verteporfin treated group decreased proportions of stemness-related expressing cells among malignant cell populations. In summary, verteporfin reduces tumorigenesis in CCA by modulation of immune cells, including anti-tumoral TAM M1, T cell activation and stemness.	JL Golino, X Wang, J Bian, B Ruf, M Kelly, BO Karim, MC Cam, C Xie	2023	CANCER
2023-218	Ivan		Pavlinov	NCATS	Microbiology and Infectious Diseases	Modeling neuroinvasion of SARS-CoV-2 variants in human iPSC-derived brain organoids	While SARS-CoV-2 is predominantly recognized as a respiratory virus, its infection has been linked with neurological manifestations. It remains uncertain whether these symptoms result from the direct viral invasion of the Central Nervous System (CNS) or are secondary to other mechanisms like inflammation or hypoxia. Post-mortem examinations of COVID-19 patients have revealed the presence of viral RNA and protein in brain tissues. Furthermore, there are reports suggesting that the original strain of SARS-CoV-2 can infect and replicate within iPSC-derived neurons, glial cells, and brain organoids. Nevertheless, the capacity of SARS-CoV-2 variants to infect or replicate within the CNS remains largely unexplored. In this study, we leveraged iPSC-derived cortical organoids to investigate the differential neurotropism of the WA1, Alpha, Beta, Gamma, Delta, and Omicron BA.5 variants of SARS-CoV-2. Our preliminary findings reveal that some variants exhibit a heightened infection rate that can't be solely attributed to the differential affinity of each variant's Spike protein for the ACE2 receptor. Moreover, we employed a multi-omic approach to study whether these variants induce distinct immunological and metabolic responses in the brain organoids. Going forward, we aim to use this data to decipher the potential mechanisms underlying the neurological symptoms observed in clinical settings and to develop targeted therapeutic interventions.	I Pavlinov, Q Zhang, M Kosikova, HN Nguyen, H Xie, W Zheng	2023	MICROBIO
2023-219	Wan-Chun		Su	NICHD	Neuroscience	The Use of Functional Near-Infrared Spectroscopy in Tracking Neurodevelopmental Trajectories in Infants and Children with or without Developmental Disorders: A Systematic Review	Understanding neurodevelopmental trajectories in children is crucial for early identification of disorders, exploring neural mechanisms, and predicting outcomes. Functional Near-Infrared Spectroscopy (fNIRS) is an infant-friendly neuroimaging tool that allows monitoring of cerebral hemodynamic responses. With its advantages, fNIRS holds promise for studying neurodevelopmental trajectories. While many researchers have used fNIRS to investigate neural development in infants and children, there is a lack of synthesized evidence on its application for tracking neurodevelopmental trajectories. In this systematic review, we summarized findings from 84 original fNIRS studies and compared them with studies using other neuroimaging tools like EEG and fMRI. Our results revealed age-related increases in network integration and segregation, interhemispheric connectivity, leftward asymmetry, and differences in phase oscillation during resting-state. Typically developing infants and children showed more localized and differentiated activation when processing sensory information, indicating more mature and specialized sensory networks. Developmental changes were observed in language processing and executive functioning tasks. However, children with developmental disorders displayed distinct trajectories, with autism spectrum disorder showing initial overconnectivity followed by underconnectivity during resting-state, and attention-deficit/hyperactivity disorder exhibiting lower prefrontal cortex activation during executive functioning tasks. This review supports the use of fNIRS in tracking neurodevelopmental trajectories. Further longitudinal studies are needed to validate these trajectories and explore the potential of neurobiomarkers for early identification of developmental disorders and evaluating intervention effects.	WC Su, R Colacot, N Ahmed, T Nguyen, A Gandjbakhche	2023	NEURO
2023-220	Matthew	D	Watson	NHLBI	Biomedical Engineering and Biophysics	Interplay between phase separation and amyloid formation: a Raman microscopy study of the TDP-43 C-terminal domain	The transactive response DNA binding protein of 43 kD (TDP-43) is an important regulator of RNA processing, but cytoplasmic accumulation of TDP-43 is associated with several neurodegenerative diseases including amyotrophic lateral sclerosis (ALS), frontotemporal lobar dementia (FTLD), and Alzheimers disease (AD). TDP-43 has been shown to form liquid protein droplets via liquid-liquid phase separation (LLPS)—which may be involved in biological function—as well as amyloid formation, which is characterized by the self-catalyzed growth of filamentous structures associated with a number of distinct proteins and diseases. Both processes are known to be driven by the C-terminal domain (TDP-43(CTD)), and LLPS has been theorized to be on-pathway to amyloidogenesis, with liquid droplets promoting amyloid nucleation. Further, TDP-43(CTD) droplets have been shown to gelate over time, which we have shown to be associated with an increase in amyloid-like β-sheet content via Raman microscopy. In order to examine the structural differences between droplets and amyloid fibrils, an alkyne (C≡C) containing Raman probe—4-ethynylphenylalanine (Fcc)—was substituted at aromatic sites throughout TDP-43(CTD) via Amber codon suppression. Analysis of the amide I, III and Fcc C≡C stretching bands revealed that although β-sheet structure is enriched in both gelated droplets and amyloid fibrils, there are key local environmental and tertiary contact differences between the two species. These results demonstrate that although TDP-43(CTD) gelation is associated with development of β-sheet structure, these structures are distinct from filamentous amyloids. This suggests that TDP-43(CTD) droplet gelation, rather than being on-pathway to amyloidogenesis, instead represents a trapped, non-productive β-sheet structure.	M D Watson, J C Lee	2023	BIOENG
2023-221	Bishwanath		Chatterjee	NCI	Cancer Biology	Role of Myc Family Proteins in Fusion-Positive Rhabdomyosarcoma	Fusion-positive rhabdomyosarcoma is a pediatric cancer characterized by a PAX3-FOXO1 (P3F) fusion gene and high-level expression of MYCN and/or MYC. To model interaction of P3F with Myc family proteins, we generated human myoblasts with doxycycline-inducible P3F (iP3F) with or without constitutively expressed MYCN. Myoblasts expressing both MYCN and P3F (MYCN-iP3F) form foci in vitro and tumors in vivo, while myoblasts expressing only P3F (iP3F) do not form foci and form tumors more slowly. Protein expression analysis revealed very high MYCN and low MYC levels in parental and tumor-derived (TD) MYCN-iP3F lines, moderate MYC and very low MYCN levels in parental iP3F lines, and high MYC and moderate MYCN levels in TD iP3F lines. Using CRISPR-Cas9 technology to knockdown MYCN or MYC, oncogenic activity in parental and TD MYCN-iP3F lines is primarily dependent on MYCN whereas oncogenicity in TD iP3F lines is primarily dependent upon MYC. To elucidate whether Myc proteins regulate P3F target genes, we measured RNA expression of multiple targets in parental and TD lines. Several targets (such as FGFR4) showed comparable upregulation by P3F in parental and TD lines with or without high MYCN. In contrast, a few targets (such as FGF8) were stimulated by P3F at low levels in parental iP3F lines and at much higher levels in TD iP3F lines and both parental and TD MYCN-iP3F lines. We postulate that the dependence of fusion-positive rhabdomyosarcoma on high-level Myc family expression is at least partly due to the need to stimulate P3F targets in this latter category.	B Chatterjee, S Boudjadi, PR Pandey, H Kim, W Sun, FG Barr	2023	CANCER

2023-222	Ghadi		Salem	NIBIB	Social and Behavioral Sciences	Compact Video System for Automated Mouse Home Cage Activity and Behavior Monitoring	Video monitoring of mice in the home-cage unveils behavior profiles without the restraints associated with specialized test equipment and disruptions caused by human interference. It is also key for behavior that is sensitive to changes in circadian rhythms which require long-term observations in their home environment. We present a system for video monitoring in the home-cage that allows for unrestrained activity and behavior in the mouse over long-time scales. The system is designed for integration with Allentown NexGen ventilated racks but can also be operated out of rack. The system has an easy to duplicate and assemble home-cage design along with a video acquisition solution. The system utilizes a depth video camera, and we demonstrate the robustness of depth video for home-cage mice monitoring. For researchers having no access to Allentown NexGen ventilated racks, we provide designs and assembly instructions for a standalone non-ventilated rack solution that holds three systems for more compact and efficient housing. Algorithms are being developed to automatically quantify activity and behavior for mice.	G Salem, M Garmendia-Cedillos, A Somenhalli, S Qin, L Argueta, N Cubert, J Krynitsky, S Bradley, G Dold, D Kendricks, Y Chudasama, J Cushman, D Coble, J Dennis, T Pohida	2023	SOCIAL
2023-223	Ghadi		Salem	NIBIB	Social and Behavioral Sciences	Video Analysis System for Behavior and Activity Assessment of Fruit Flies in High Throughput Studies	We present a novel monitoring system focused on advancing high-throughput automated activity assessment of Drosophila. The video-based system reports on the activity of each fly within each well of custom designed 24-well plate that conforms to the standard dimensions. The housing plate builds on the previously innovative Whole Animal Feeding Flat (WAFFL) system which was designed to streamline high-throughput feeding and toxicology studies for fruit flies. The custom designed plates, however, have been modified to optimize video quality and to make the plates injection moldable. Additionally the system has built in illumination to allow for full circadian cycle studies. The overall system is compact with a small benchtop footprint that should facilitate scale-up to large studies employing multiple units. Algorithms are being developed to automatically quantify activity and behavior for each individual fly.	G Salem, M Garmendia-Cedillos, A Somenhalli, N Khandekar, L Argueta, N Cubert, I Farooq, M Jaime, T Kaufman, J Holsopple, S Smoot, T Kaufman, J Tennessen, B Oliver, T Pohida	2023	SOCIAL
2023-224	Amitava		Roy	NIAID	Computational Biology	Drugsniffer: An open source workflow for virtually screening billions of molecules for binding affinity to protein targets	The SARS-CoV-2 pandemic has highlighted the importance of efficient and effective therapeutic drug identification. In particular, the pandemic has laid bare the need for ways to explore the full diversity of synthesizable small molecules. While classical high-throughput screening methods may consider up to millions of molecules, virtual screening methods promise to appraise billions of candidate molecules, thus expanding the search space while concurrently reducing costs and speeding discovery. Here, we describe a new screening pipeline called Drugsniffer, which can rapidly explore drug candidates from a library of billions of molecules and is designed to support distributed computation on cluster and cloud resources. As an example of performance, our pipeline required ~40,000 total compute hours to screen for potential drugs targeting three SARS-CoV2 proteins among a library of ~3.7 billion candidate molecules.	V Venkatraman, TH Colligan, GT Lesica, DR Olson, J Gaiser, CJ Copeland, TW Wheeler, A Roy	2023	COMPBIO
2023-225	Gergo		Gulyas	NICHD	Molecular Pharmacology	DISSECTING THE ROLES OF ENDOCYTIC EVENTS IN GPCR DESENSITIZATION AND INTERNALIZATION	G protein coupled receptors (GPCRs) are the target of about 35% of FDA-approved drugs, which underlines their importance in pharmacological interventions. Agonist binding to GPCRs activates heterotrimeric G-proteins and β-arrestins to initiate downstream signaling, followed by receptor desensitization and endocytosis. β-arrestins terminate G-protein signaling and promote GPCR internalization thereby reducing the number of receptors in the plasma membrane (PM). and causing loss of responsiveness to agonists. Based on the current view, GPCRs must reach the endolysosomal system to uncouple from their arrestin partner followed by dephosphorylation to regain their resting state, thus becoming capable to fulfil their function in the recurring signaling cycle. Phosphatidylinositol 4,5-bisphosphate (PIP2) is known to affect several proteins that play key roles in endocytosis, but their role in GPCR desensitization is unknown. We found that knock down (KD) of either EFR3A or PIP5K1A (but not B or C), key players in PIP2 synthesis promoted receptor desensitization without changing the overall PIP2 levels in the PM. We also identified that silencing AP2, but not clathrin heavy chain, dynamin 1 or -2, accelerated AT1R desensitization, while all these manipulations inhibited receptor endocytosis. As expected, β-arrestin2 KD prevented receptor desensitization, but unexpectedly, KD of βarr1 promoted desensitization of AT1Rs. None of the manipulations affected signaling of the truncated desensitization deficient AT1R confirming that these effects were specific for receptor desensitization. These results suggest, that contrary to current believes, re-sensitization of GPCRs can occur without their endocytosis and likely occurs at the PM at specific steps during clathrin-coated pit maturation.	G Gulyas, YJ Kim, T Balla	2023	PHARMA
2023-226	Xiaoyu		Duan	NIDDK	Computational Biology	Inferring physiological values of model parameters with deep learning: a lipolysis example	Inference of nonlinear dynamics and parameters in biological modeling is a challenging task. Approaches relying on hypothetical underlying mechanisms can complicate the inference process because standard parameter optimization methods are difficult to constrain to physiological ranges. Is the model at fault or the parameter optimization? We propose an approach that utilizes neural networks to address parameter inference and physiological modeling simultaneously. In this study, we solve an optimization problem using a lipolysis model to obtain parameter values for a physiological model of the dynamics of glucose, insulin, and free fatty acids. First, we generate sample parameters, integrate the model with the sample parameters, and obtain simulated data. We then train a convolutional neural network to output the model parameters and evaluate its performance in reconstructing simulated or experimental data. Our objective is to use the power of deep learning methods to enhance modeling techniques and improve training processes by incorporating more nonlinear terms of state variables as inputs to the network.	X Duan, V Periwal	2023	COMPBIO
2023-227	Alexandra		Bernardo -Colon	NEI	Molecular Biology and Biochemistry	Ablation of Pigment Epithelium-derived Factor (PEDF) and Pigment Epithelium-derived Factor Receptor (PEDF-R) is Detrimental for Photoreceptors	The SERPINF1 gene encodes the retinoprotective pigment epithelium-derived factor (PEDF). Photoreceptor cells express the PNPLA2 gene for its receptor PEDF-R, which is responsible for PEDF-mediated neurotrophic activities. To determine whether the PEDF/PEDF-R axis plays a regulatory role in photoreceptor structure and function, we characterized photoreceptors deficient in PEDF and PEDF-R. CRISPR Pnpla2 knock-out mouse was crossbred with Serpinf1 null, and three genotypes were generated: wild type, Serpinf1+/-/Pnpla2-/- and Serpinf1-/-/Pnpla2-/-. Gene expression was determined in dissected retinas by RT-PCR. Mice were evaluated for electroretinography (ERG), fundoscopy and autofluorescence angiography. Whole eyes were enucleated and processed for histology, immunofluorescence, TUNEL, confocal microscopy, and transmission electron microscopy. At 3 months of age, Serpinf1+/-/Pnpla2-/- and Serpinf1-/-/Pnpla2-/- mice had decreased and undetectable retinal Serpinf1, respectively, relative to their Serpinf1+/+/Pnpla2+/+ littermate controls and both had undetectable Pnpla2 expression levels. The Serpinf1+/-/Pnpla2-/- mice had higher lipid droplet density in their retinal pigment epithelium and Bruch's membrane and the vasculature was more ectatic relative to controls. The Serpinf1-/-/Pnpla2-/- photoreceptors had morphological abnormalities. The ERG a- and b-waves of Serpinf1+/-/Pnpla2-/- and Serpinf1-/-/Pnpla2-/- mice were attenuated relative to controls. Loss of both PEDF and PEDF-R caused retinas to have thinner outer nuclear layers with TUNNEL positive photoreceptor cells, as well as decreased levels of rhodopsin, opsin, PKCα, and synaptophysin compared to controls. Ablation of both PEDF and PEDF-R in mice causes defects in photoreceptor development resulting in suboptimal photoreceptor performance and increases in lipid accumulation. These data identify the PEDF/PEDF-R axis as a critical component for photoreceptor structure and function.	A Bernardo -Colon, S.E Crawford, S.P Becerra	2023	MOLBIO
2023-228	Sanam		Yaghoubi	NCI	Cancer Biology	Intratumor genetic heterogeneity dictates metastatic subclones in stage II colon cancer	Although standard therapies are highly effective in stage II colon cancers (CC), some patients show disease relapse within the next 5-year period after intended curative surgery. We hypothesize that genomic instability and intratumor heterogeneity fuel the formation of subclonal populations in the primary tumor that might promote metastasis. Our study assesses the presence of intratumor heterogeneity in CC using multiplex interphase FISH and whole-exome sequencing in nine primary stage II colon tumors and their patient-matched liver metastases using multi-region sampling. We observed high similarities regarding copy-number alterations (CNA) and ploidy between primary tumor and metastasis for three of four cases analyzed. Two of these cases showed either triploid or highly aneuploid genomes with different degrees of genomic instability. Both matched lesions for the third case displayed diploid clones, however, the primary tumor revealed two distinct cell populations with either CDX2 diploid or gained. The metastasis seems to originate from the CDX2 diploid clone. Conversely, the fourth case revealed a triploid baseline for the primary tumor while diploid for the metastasis. Although five of the CNA observed in the tumor and metastasis major clone populations were similar, two highly clonal gains observed in the tumor, EGFR and MYC, were not present in the metastasis. In summary, we show that the combined analysis of WES and miFISH can describe the subclonal composition of CNA in primary tumors and their liver metastases. Future perspectives include the assessment of subclonality affecting single-nucleotide variants to complete the genomic landscape of tumor evolution and clonal development.	S Yaghoubi, K Heselmeyer-Haddad, I Archilla, C Parra, D Wangsa, G Castellano, S Lahoz, V Pablo-Fontecha, D Hirsch, W Chen, T Ried, M Cuatrecasas, PS Meltzer, J Camps	2023	CANCER
2023-229	Sangeetha		Hareendran	NICHD	Neuroscience	Dual leucine Zipper kinase regulates onset and maintenance of nerve injury signaling, neuroinflammation and mechanical allodynia in a neuropathic pain model	Peripheral nerve lesions can cause neuropathic pain; however, the key molecule(s) that coordinate pain transmission are still poorly understood. We have shown that dual leucine zipper kinase (DLK) is a critical upstream regulator of transcriptional changes in injured sensory neurons and of a microglial response, leading to pain sensitization. Inhibition of DLK by GNE-3511 effectively prevents pain signaling and hypersensitive response after nerve damage. Here, we asked two questions: (1) is initial suppression of DLK sufficient to block pain response? (2) is delayed inhibitor treatment helpful in controlling neuropathic pain? Using a spared nerve injury (SNI) model, we assessed the induction of injury (ATF3, pc-JUN, CSF1) and microglial activation markers (IBA1) either in the DRG or the spinal cord and performed von Frey behavior assay. First, we utilized an 'on/off' approach, where we administered GNE-3511 for five days post SNI, and then discontinued it until D10. A reverse 'off/ on' scheme was adopted to determine the delayed effect of GNE-3511 treatment. Our data revealed that the DLK pathway can be activated to initiate pain signaling days after the actual neuronal insult, and that continuous DLK inhibition is required to prevent chronic pain. Further we found that DLK inhibition is nevertheless beneficial in treating neuropathic pain days after the injury occurs. In conclusion, we show that DLK is essential not only for the onset of neuropathic pain signaling but also for the disease maintenance. Insights gained from this study are clinically relevant in the development of DLK inhibitors for pain management.	S Hareendran, JJ Wlaschin, H Silberberg, CE Le Pichon	2023	NEURO
2023-230	Kathleen		Gwilliam	NIDCD	Genetics and Genomics	RFX2 Compensates for the Loss of RFX1 and RFX3 in the Vestibular System	The group 1 RFX transcription factors (TFs), RFX1, RFX2, and RFX3, are master regulators of ciliogenesis. Our laboratory showed that conditional deletion of Rfx1 and Rfx3 (Rfx1/3;Gfi1-Cre) from mouse hair cells (HCs) results in profound hearing loss, an abrupt loss of all outer HCs shortly after the onset of hearing, and a late mild vestibular phenotype. However, Rfx1/3;Gfi1-Cre mutant HCs have no kinocilia defects. Due to significant homology in functional domains, similar role in ciliogenesis, and expression in cochlear and vestibular HCs, we hypothesized that RFX2 functions to compensate for the loss of RFX1/3 in inner ear HCs. We investigated the compensatory role of RFX2 for RFX1/3 in kinocilia development and maintenance and function in the vestibular system and explored the signaling cascade downstream of the group 1 RFX TFs in vestibular HCs. A conditional knockout (cKO) mouse of the group 1 RFX TFs (Rfx1/2/3 cKO) underwent vestibular sensory evoked potential (VsEP) testing to measure vestibular function. Rfx1/2/3 cKO mice had significantly elevated VsEP thresholds as early as 1-month-old. Additionally, Rfx1/2/3 cKO kinocilia were shortened in vestibular HCs at postnatal day(P)10 to 6-months-old. Single cell RNA-sequencing of P5 Rfx1/2/3 cKO vestibular HCs identified significantly downregulated genes in Rfx1/2/3 cKO with known ciliogenesis roles. Therefore, RFX2 compensates for RFX1/3 within the vestibular system and the group 1 RFX TFs have an essential role in vestibular function and kinocilia development or maintenance. We reveal part of the group 1 RFX signaling pathway in vestibular HCs, identifying candidate genes for maintaining vestibular function.	K Gwilliam, B Milon, M Eshel, M McMurray, Y Song, I Belyantseva, S Jones, MR Bowl, R Elkon, R Hertzano	2023	GEN
2023-232	Lili		Masoumzadeh	NIDDK	Structural Biology	Slow Proline Isomerization as a Kinetics Barrier for Protein Folding	Slow proline cis-trans isomerization can serve as a rate-limiting step in protein folding by creating energy barriers that must be overcome to achieve the native structure. Several studies have reported that the cis isomer of proline can act as a kinetic trap during protein folding, thereby altering the folding pathway, or preventing folding, while the trans isomer is usually preferred in folded proteins. Therefore, the presence of proline residues within protein domains can significantly impact their function, and ability to fold correctly. In this study, we utilize NMR spectrometer-controlled hardware that performs rapid and repeatable pressure switching within a sample cell from 1bar (folding condition) to 2.5kbar (unfolding condition) to alter the population of cis proline isomers. Hydrostatic pressure can reversibly shift the thermodynamic equilibrium between folded and unfolded states, enabling the experimental control over folding and unfolding under physiologically relevant conditions. Single and double pressure-jump techniques enable us to measure cis-trans isomerization time constants ranging from seconds to many minutes and to record specific rates for each proline. Ubiquitin L50A, used as a model system in this study, contains three proline residues with cis fractions of 9.5%, 6.5% and 3% for P19, P37, and P38, respectively, under unfolding conditions.	L Masoumzadeh, J Yang, A Bax	2023	STRUCTBIO
2023-233	Amit	K	Singh	NCI	Molecular Biology and Biochemistry	Cohesin Regulates Alternative Splicing in Acute Myeloid Leukemia	Cohesin is a ring-shaped complex with multiple functions throughout cell cycle. Cohesin establishes sister-chromatid cohesion, organizes chromatin into functional domains, regulates transcription and DNA repair. The high frequency of cohesin mutations and of changes in alternative splicing in acute myeloid leukemia (AML) led us to ask if cohesin regulates alternative splicing. Targeted depletion of cohesin in HCT-116 cells led to changes in splicing patterns, demonstrating that cohesin regulates alternative splicing. Mechanistically, cohesin colocalizes and directly interacts with core components of splicing machinery including U1-70, and regulatory factor FUS. Acute cohesin depletion did not affect mRNA levels, rate of transcription and splicing factor levels. Furthermore, in two independent datasets, primary AML patient samples with cohesin mutations show aberrant splicing patterns relative to healthy controls. Importantly, cohesin point mutations observed in AML samples display reduced in-vitro interactions with U1-70. Introduction of a point mutation in the SMC1 subunit in mES cells reduces the in-situ proximity of cohesin with U1-70 and alters splicing patterns. This finding demonstrates a direct relationship between cohesin and splicing. BRD4, like cohesin, regulates alternative splicing. Interestingly, cohesin and BRD4 together regulate the splicing of a gene subset that is distinct from those regulated by either protein alone. Consistent with their co-regulation of splicing, cohesin and BRD4 colocalize across the genome, directly interact and exist in a complex in cells. Together these studies establish a novel role of cohesin in regulating alternative splicing alone or in conjunction with BRD4 and have implications in the characterization of human AML cancers.	AK Singh, Q Chen, C Nguyen, D Meerzaman, DS Singer	2023	MOLBIO

2023-234	Shaun	R	Abrams	NIDCR	ACI/IRS	Central role of centrioles: tissue-specific requirements for coordinating facial development	Centrioles make up the core of centrosomes which function as microtubule-organizing centers of the cell. Centrioles perform two distinct cellular functions: (i) they form core components required to build the centrosome and (ii) they form the basal body that templates formation of the cilium, a microtubule-based specialized signaling organelle. CENPJ is a central component of centrioles required for centriole duplication. Mutations in CENPJ cause Seckel syndrome and primary microcephaly, leading to facial defects including hypoplasia of the lower jaw (micrognathia), facial midline abnormalities, premature closure of cranial sutures (craniosynostosis), and tooth abnormalities. Understanding how centriole loss affects facial development is critical for developing novel therapeutic interventions. To investigate the role of centrioles in craniofacial development, we conditionally deleted CenpJ in craniofacial tissues of mouse embryos using the Sox9-cre driver. The resulting mice displayed underdeveloped jaws, midline facial defects, and skull abnormalities similar to Seckel syndrome patients. Defects appeared at embryonic day 10.5 (E10.5), starting with a smaller jaw and widened midface. By E11.5-12.5, midline facial clefting occurred. Increased cell death in the mandibular arch and p53 activation were observed. Remarkably, deleting p53 fully rescued the craniofacial phenotypes in CenpJ-deficient mice, emphasizing p53's role in facial dysmorphology due to centriole loss. This discovery sheds light on the pathways involved in facial development and highlights p53 as a potential target for therapeutic interventions.	SR Abrams, CE Foster, C Xie, JF Reiter, L Kerosuo	2023	ACI/IRS
2023-235	Ryan		McGlinchey	NHLBI	Biomedical Engineering and Biophysics	Effect of N- and C-terminal truncations on α-synuclein amyloid formation and fibril structure	The generation of α-synuclein (α-syn) truncations from incomplete proteolysis plays a significant role in the pathogenesis of Parkinson's disease. Here, we report fibril structures of full-length acetylated (Ac) protein (Ac1–140), two C-terminally truncated α-syn (Ac1–122 and Ac1–103), and an N-terminally truncated α-syn (41–140) solved by cryoelectron microscopy. For the C-terminal truncations, both proteins exhibited faster aggregation kinetics and Ac1–103 fibrils efficiently seeded the full-length protein, highlighting their importance in pathogenesis. The removal of C-terminal residues resulted in increased fibrillar twist, accompanied by modest conformational changes in a more compact amyloid core. For 41–140, a novel amyloid structure with two asymmetric protofilaments was found. While one protomer resembled the previously characterized bent β-arch kernel, comprised of residues E46–K96, the other protomer is folded into an extended β-hairpin conformation with fewer residues (E61–D98) that does not resemble other reported structures. In stark contrast to the C-terminal truncations, fibrillar 41–140 had little effect on full-length α-syn aggregation and fibril propagation. Together, these results offer new insights into α-syn fibril polymorphism and the interplay between full-length and its truncations.	RP McGlinchey, X Ni, J Jiang, JC Lee	2023	BIOENG
2023-236	Nishanth		Anandanadarajah	NIEHS	Computational Biology	Automatic loose lead detection in sleep EEG data	Polysomnography is an overnight sleep study used for diagnosis of sleep disorders. In polysomnography, a patient's brain activity is measured using electroencephalography (EEG) through six leads placed on the scalp: frontal (F3 and F4), central (C3 and C4), and occipital (O1 and O2). Large artifacts caused by loose leads can distort EEG measurements, but manual checking for such artifacts is prohibitively time-consuming. We developed a method to automatically identify large artifacts in an EEG trace. After multitaper spectral analysis extracts power for specific frequency bands, we compute, for every 1s time segment, the correlation of band-specific power levels between all pairs of leads. For each lead, we average the pairs involving that lead (e.g., C3-C4, C3-F3, C3-F4, C3-O1, C3-O2 for C3), creating a time series of segment-specific average correlations for each lead. Next, our algorithm scans each time series separately for "bad" segments using a local moving window. A segment is designated "bad" when its correlation is less than half of median correlation among all segments in the window; otherwise, the segment is designated "good". In a second pass, a segment is declared an outlier and assigned value '1' when its correlation is less than ¼ of the 75th percentile among all "good" segments; otherwise, a segment is assigned value '0'. A continuous period of outliers reveals a loose lead. We scan the temporal sequence of segments by summing outlier values within moving 300s windows and declare a loose lead present within a window when the sum exceeds five.	N Anandanadarajah, D Yeung, Y Li, A Talukder, DM Umbach, Z Fan, L Li	2023	COMPBIO
2023-237	Stephanie		Pitts	NCI	Immunology	Immune correlates with response in patients with metastatic solid tumors treated with a tumor targeting immunocytokine NHS-IL12	Background: NHS-IL12 (now designated PDS0301) is a tumor-targeting immunocytokine targeting DNA/histones in necrotic areas of the tumor microenvironment. NHS-IL12 has shown promising results in preclinical studies as a monotherapy and in combination with other anti-cancer therapies such as the HDAC inhibitor Entinostat. The first-in-human clinical trial (NCT01417546) administered NHS-IL12 subcutaneously every four weeks (Q4W) and was expanded to include cohorts with bi-weekly treatment (Q2W). Here, we present immune correlates in peripheral blood to determine the impact of the dose level and schedule of NHS-IL12 on immune activation and evaluate immune correlates of clinical response. Methods: Serum was evaluated for levels of cytokines/soluble factors by Elisa and Mesoscale assays, and peripheral blood mononuclear cells were assessed for 158 immune cell subsets by multicolor flow cytometry. New assays to detect soluble NK ligands and more extensively characterize the association between NK lysis and phenotype were developed in healthy donor samples. Results: Patients treated in the Q2W cohort with a dose of 16.8 mcg/kg NHS-IL12 (versus those with 12.0 mcg/kg) exhibited greater increases in serum IFNγ, TNFα, and sPD-1, and greater increases in peripheral ki67+ mature NK, CD8+ T, and NKT cells. Greater immune activation was also seen in the Q2W versus Q4W cohort. Lower baseline levels of monocytes and plasmacytoid dendritic cells and greater increases after treatment in NK and CD8+ T cell subsets associated with improved clinical outcome. Conclusions:	SC Pitts, NJ Toney, ME Gatti-Mays, NP Tschernia, J Strauss, JL Gulley, J Schlom, RN Donahue	2023	IMMUNO
2023-238	Michael	H	Ronzetti	NCATS	Chemical Biology	The Real-Time Cellular Thermal Shift Assay to Monitor Target Engagement	Evaluating a small molecule's mechanism of action is crucial for drug discovery and the development of chemical probes. The Cellular Thermal Shift Assay (CETSA) provides a means for conducting direct target engagement studies by measuring protein thermal stability alterations upon ligand binding. However, conventional CETSA methods are low-throughput, requiring considerable optimization and sample allocation. We present a real-time CETSA (RT-CETSA) platform designed to overcome these shortcomings. This platform combines a bioengineered, thermally stable Nanoluciferase variant, known as ThermLuc, with a prototype real-time PCR instrument equipped with a CCD camera for luminescence detection. This configuration enables the generation of a comprehensive protein aggregation profile from a single sample. The novel Nanoluciferase variant, ThermLuc, designed for enhanced thermal stability, resists denaturation even at temperatures above 90 °C, demonstrating its compatibility with monitoring target engagement across a spectrum of targets. The effectiveness of the RT-CETSA was validated using well-studied inhibitors of lactate dehydrogenase alpha. This validation revealed a significant correlation with established enzymatic, biophysical, and cell-based assays. A dedicated data analysis pipeline accompanies RT-CETSA, heightening sensitivity in the detection of on-target binding. This innovative approach broadens the capabilities of CETSA, facilitating real-time, target-agnostic, and high-throughput evaluations of ligand-target interaction, a key component in determining a small molecule's mechanism of action.	MH Ronzetti, TW Sanchez, B Baljinnyam, AE Owens, M Antony, T Voss, E Wallgren, D Talley, K Balakrishnan, SE Leyes Porello, G Rai, JJ Marugan, SG Michael, B Baljinnyam, N Southall, C Klumpp-Thomas, A Simeonov, MJ Henderson	2023	CHEMBIO
2023-240	Ashwaq	K	Aljabri	NCI	Molecular Biology and Biochemistry	The role of SMARCA1 in Rhabdomyosarcoma and Skeletal Muscle Differentiation	Background: Rhabdomyosarcoma (RMS) is the most common soft tissue of pediatric sarcoma, and studies demonstrate that RMS arises from skeletal muscle precursor cells. RMS, genetically and histologically, is divided into two subtypes: PAX-FOXO1 fusion positive (alveolar) RMS, which is driven by chromosomal translocation involving PAX3 or PAX7 genes with FOXO1 and PAX-FOXO1 fusion negative (embryonal) RMS, which is marked by mutations in RAS isoforms and some genes such as TP53, PIK3CA, CTNNB1 and FGFR4. Chromatin was one of the earliest identified targets for cancer therapy. Several chromatin remodeling proteins are associated with cancer progression processes such as proliferation, differentiation, apoptosis, and tumorigenesis. The ISWI family protein, SMARCA1, has been implicated in tumorigenesis for several cancer types. ISWI complexes regulate cell differentiation and proliferation in other cell systems, but their impact in myogenesis is not well understood. In this study, we will characterize the function of SMARCA1 in RMS cells and skeletal muscle. We hypothesize that SMARCA1 acts to modulate chromatin accessibility, and drive RMS tumorigenic growth. Methods: We will use RNA-seq, ATAC-seq, and ChIP-seq to study the impact of SMARCA1 deletion in RMS cells. Furthermore, phenotypic experiments will be performed to determine the influence of SMARCA1 on differentiation. Results: SMARCA1 is expressed highly in RMS tissues but not in muscle tissues. In addition, we show that SMARCA1 interacts with HDAC2 in rhabdomyosarcoma cells. Conclusions: This study will deepen our understanding of how SMARCA1 impacts RMS differentiation and tumor growth and may credential SMARCA1 as a novel therapeutic target in rhabdomyosarcoma.	A.K Aljabri, K.E Hebron, Y Kariga, J.M Caravaca, J Shetty, B Tran, S Stauffer, L Stoak, M Porter, J Davie, M.E Yohe	2023	MOLBIO
2023-241	Andrew		Zhang	NIDCR	Cancer Biology	Visualization of Anthrax Toxin Intoxication in Mice	Morbidity and mortality of B. anthracis is attributed to secretion of anthrax lethal toxin (LT) and anthrax edema toxin (ET). LT and ET consist of a common protein, protective antigen (PA) and, respectively, lethal factor (LF) or edema factor (EF). Intoxication by LT or ET is initiated by binding of PA to widely expressed receptors, followed by cleavage of PA by furin and furin-like proteases. Cleavage of PA allows for cytoplasmic entry of LT and ET to exert their cytotoxicity. We have previously reengineered PA to require single or dual cleavage by the tumor-associated proteases uPA and MMPs for cellular intoxication, thereby achieving high tumor selectivity when combined with LF. The mutant toxins display low systemic toxicity and high antitumor activity towards human and mouse tumors xenografted or syngrafted to mice, as well as towards naturally occurring oral squamous carcinomas and oral melanomas in feline and canine veterinary patients. We recently generated an assay that allows for single-cell resolution imaging of anthrax toxin intoxication of animals. This was achieved by using an LF-Cre fusion protein in combination with a Cre-reporter transgenic (mT/mG) mouse. When PA and LF-Cre are co-administered to mT/mG mice, intoxicated cells display membrane-localized green fluorescence, while non-intoxicated cells display membrane-localized red fluorescence. Cellular intoxication is visualized by confocal microscopy of intact tissues or flow cytometry of single cell suspensions. We use the imaging assay to catalogue on- and off-targets for a variety of engineered toxin variants currently in preclinical development. Data from these studies will be presented.	A Zhang, M Moayeri, SH Leppla, TH Bugge	2023	CANCER
2023-242	Bikash		Santra	CC	Clinical Research	Anatomical location-guided deep learning-based genetic cluster identification of pheochromocytomas and paragangliomas from CT images	Pheochromocytomas and paragangliomas (PPGLs) are respectively intra-adrenal and extra-adrenal neuroendocrine tumors whose pathogenesis and progression are greatly regulated by genetics. Identifying PPGL's genetic clusters (SDHx, VHL/EPAS1, kinase signaling, and sporadic) is essential as PPGL's management varies critically on its genotype. Genetic testing for PPGLs is expensive and time-consuming. Contrast-enhanced CT (CE-CT) scans of PPGL patients are acquired at the beginning of patient management for PPGL staging and determining the next therapeutic steps. Given a CE-CT sub-image of the PPGL, this work demonstrates a two-branch vision transformer (PPGL-Transformer) to identify each tumor's genetic cluster. The standard of reference for each tumor included two items: its genetic cluster from clinical testing, and its anatomical location. One branch of the PPGL-Transformer identifies PPGL's anatomic location while the other one characterizes PPGL's genetic type. A supervised contrastive learning strategy was used to train the PPGL-Transformer by optimizing contrastive and classification losses for PPGLs' genetic group and anatomic location. Our method was evaluated on a dataset comprised of 1010 PPGLs extracted from the CE-CT images of 289 patients. PPGL-Transformer achieved an accuracy of 0.63 ± 0.08 and balanced accuracy (BA) of 0.63 ± 0.06 on five-fold cross-validation and outperformed competing methods by 2-29% on accuracy and 3-18% on BA. The performance for the sporadic cluster was higher on BA (0.68 ± 0.13) while the performance for the SDHx cluster was higher on recall (0.83 ± 0.06). The proposed method may lead to faster and more widely available PPGLs' genetic characterization offering PPGLs' timely personalized management.	B Santra, A Jha, P Mukherjee, M Patel, K Pacak, RM Summers	2023	CLINICAL
2023-243	Dale	E	Lewis	NCI	Molecular Biology and Biochemistry	RNA Polymerase and CI Regulator Interactions in Gene Regulation in Bacteriophage Lambda Re-visited	Background: The bacteriophage lambda paradigm in gene regulation revealed several basic principles of transcription regulation. After infection with E. coli, lambda follows either a lytic growth or a lysogenic growth cycle. The CI represses the lytic promoters (PR and PL) and activates and represses the lysogenic promoter (PRM) at low and high concentrations, respectively. CI regulates PRM by binding to tripartite, OR1, OR2 & OR3 located between PRM and PR. CI binds to OR1 and OR2 represses PR. CI bound to OR2 activates PRM through direct contact between RNAP~PRM and CI ~OR2. CI binding to OR3 represses PRM. Methods: In an in vitro transcription system, we analyzed the RNA polymerase and CI interactions by monitoring PRM levels by using DNA and CI mutants. Results: We obtained unexpected findings. First, DNA mutants resulted in PRM repression. This repression is depending on DNA looping and CI~OR2. CI mutant, E34K, resulted in PRM repression at the same CI concentration for PR repression. Conclusion: Attempted disruption of the activation complex between RNAP at PRM and CI at OR2 by mutating CI or inserting or deleting base pair to change the angular orientation and distance between RNAP and CI unexpectedly led to CI-dependent repression of PRM. From these unexpected results, we propose that under all three conditions, the OR2 bound CI is creating an inhibitory contact with RNA polymerase at PRM preventing the latter to escape the promoter and repressing transcription. Studies are being conducted to test the model.	DEA Lewis, S Adhya	2023	MOLBIO

2023-244	Yi-Han		Lin	NCATS	Chemical Biology	High-throughput MS-based cholesterol quantitation assay for Niemann-Pick Disease type C (NPC)	Quantification of cellular lipids is a key step for the development of therapeutics for lipid storage diseases. For Niemann-Pick Disease Type C (NPC), a genetic disorder characterized by the accumulation of unesterified cholesterol in late endosome/lysosome, filipin staining was used traditionally for cholesterol quantification. However, due to the non-specific binding of filipin to other sterol derivatives and its sensitivity to photobleaching, using filipin staining in high-throughput assay for compound screening is not ideal. We have developed an automated protocol for extracting cellular cholesterol and quantifying it using the high-throughput LC/MS system RapidFire 360. Neuronal stem cells derived from human NPC fibroblasts were optimized to grow in 384-well format, and cholesterol was extracted using methyl-tert-butyl ether (MTBE). 13C-labeled cholesterol was added to MTBE so that signal of native cholesterol could be normalized to it to account for variations introduced during multiple liquid transfer steps. This assay allows lipid extraction and analyses by MS for 384 samples to be completed in 1.5-2 hours. Using this assay, we screened a 248-compound library of investigational agents for NPC in dose-response, benchmarking this efficient, label-free cellular cholesterol quantification assay for high-throughput applications.	Y Lin, ML Gosztyla, Y Fang, E Zhu, AD Garcia, DC Talley, A Kapoor, MJ Henderson, X Hu, W Zheng, CA LeClair, A Simeonov, JJ Marugan, D Tao, B Baljinnyam	2023	CHEMBIO
2023-246	Soongho		Park	NICHD	Cell Biology	Real-time Diagnosis of Cellular Metabolism through Optical Imaging and AI Methods	Detecting changes in cellular metabolism and viability is vital in various fields such as modern biology, drug development, toxicology, and cell biology research. To achieve this, real-time observation of dynamic activity in cells or tissues is essential. Such observations provide valuable insights into the underlying physiological and pathological processes, including intricate signaling pathways and cellular interactions. However, traditional methods like fluorescence imaging or dye analysis have limitations that hinder their effectiveness in observing intracellular activity and viability. In this regard, we propose a label-free, non-invasive, and automated method for evaluating dynamic activity in cells or tissues and assessing cell viability. Our approach utilizes high-speed optical imaging techniques and artificial intelligence (AI) methods, enabling objective assessment. Unlike traditional methods that may yield subjective results based on expert interpretation, our method facilitates the study of complex signaling pathways and cellular interactions in a comprehensive and unbiased manner.	S Park, T Nguyen, J Park, A Gandjbakhche	2023	CELLBIO
2023-247	Pierre	V	Daude	NHLBI	Biomedical Engineering and Biophysics	Automatic SNR-driven quality control of 2D Phase-Contrast MR imaging using closed-loop feedback between image reconstruction and acquisition	Conventional MRI uses predefined parameters with a fixed acquisition time to provide suitable image quality for most patients. Nevertheless, image quality is patient-dependent. Therefore, we propose using a closed-loop feedback framework between data acquisition and the image reconstruction to efficiently achieve consistent diagnostic image quality for quantitative flow measurements with MRI. The workflow is designed as follows: the "FIRE" framework (Siemens Healthcare) handles the communication between the image acquisition software and the Gadgetron reconstruction software, which rapidly generates images. When the target signal-to-noise ratio (SNR) is achieved, a message is sent from Gadgetron to the acquisition software to stop the data acquisition. A volunteer was imaged on a 0.55T Free.Max MRI scanner (Siemens Healthineers, Erlangen, Germany). The flow measurement sequence was run with or without closed-loop feedback (every 20s), with a total duration of 4min30s. A target SNR of 120 in the aorta was selected to demonstrate the stopping criterion. The acquisition stopped when the target SNR was reached after 140s, saving >2 minutes of scan time. The absolute relative difference of quantitative parameters (peak flow and cardiac output) was <5 % between acquisitions with or without feedback. We have demonstrated a proof-of-concept framework for adaptive MRI and applied it to SNR quality control imaging. It can improve MR value by removing inefficiencies in imaging by reducing scan time or avoiding sequence repetition due to poor image quality. This framework will be extended for diverse applications such as real-time image quality assessment and adaptive sampling for efficient dynamic imaging.	PV Daude, R Ramasawmy, A Javed, H Xue, P Kellman, K Chow, AE Campbell-Washburn	2023	BIOENG
2023-248	Shreya		Rajhans	NCI	Cancer Biology	Single-nuclei RNA and ATAC Sequencing Uncovers Subtypes In Pancreatic Neuroendocrine Tumors	Pancreatic neuroendocrine tumors (PNETs) are a rare form of cancer, thought to originate from the endocrine lineage of the pancreas—which generates hormone producing cells. PNETs have limited curative options with rising incidence, and are categorized into grades based on Ki67, a generic replication marker. To improve diagnosis and treatments, it's critical to move beyond current diagnostic approaches that rely on incomplete understanding of PNET markers and subtypes. In this study, we used single-cell multiome assays on cryopreserved primary PNETs of varying grade, stage, and metastasis to characterize their chromatin and transcriptome profiles at single-cell resolution. Additionally, we performed multiome analysis on normal endocrine and exocrine pancreas for comparison between healthy pancreas and PNETs at the single-cell level. Our multimodal analysis revealed extensive inter-tumor heterogeneity with few shared genes across the PNET cohort. In contrast, we found minimal heterogeneity within each tumor, suggesting originating from a single founder cell. Using differential gene expression analysis, we identified distinct cell populations within PNETs, including tumor, endothelial, and immune cells. The tumors had distinct gene profiles: cell markers (PDX1/ARX), cancer metabolism (VHL and HIF1a/HIF2a), and chromatin regulation (DAXX/ATRX). We performed ligand-receptor analysis to find communication networks associated with PNETs, comparing findings to normal pancreas. For a subset of tumors, we identified interactions previously understudied in PNETs. We observed diverse molecular profiles of PNETs with little overlap between patients, explaining the difficulty finding successful treatments for most cases. Our results can help develop personalized medicine by elucidating molecular markers varying between PNETs, by further classification.	S Rajhans, E Mondell, J Madigan, N Truongvo, L Wang, M Kelly, SM Sadowski, HE Arda	2023	CANCER
2023-249	Meagan		Jezek	NCI	Genetics and Genomics	Characterization of cell type-specific enhancers in the human pancreas using a massively parallel reporter assay	Accurate control of cell identity is integral to maintaining healthy, functional systems, and deviations can lead to developmental defects and diseases, including cancer. Therefore, it is crucial to understand the regulatory mechanisms that drive cell type-specific functions. Enhancers are non-coding genetic elements that regulate transcription and are overwhelmingly responsible for cell type-specific gene expression. Additionally, over 80% of disease-associated genetic variants map to enhancer regions, emphasizing the need to understand their function. While nearly one million candidate enhancer regions have been identified, the functional characterization of enhancers has been a daunting challenge, particularly at genome-scale. The pancreas is a vital organ composed of multiple cell types. Our lab has identified candidate enhancer elements unique to the five major human pancreas cell types, and digital footprint analysis of chromatin accessibility data revealed that these regions are likely bound by cell type-specific transcription factors, underscoring the cell specificity. To systematically characterize the drivers of cell identity among the unique cell types, we are using a novel massively parallel reporter assay to quantify enhancer activity. We have prioritized candidate enhancers which contain differentially enriched transcription factor motifs, and those containing motifs of additional highly cell type-specific transcription factors. We have cloned thousands of candidate enhancers into lentiviral reporter libraries and are assessing activity of these elements in primary pancreas cells obtained from healthy donors. These results will yield the first functional enhancer map of human pancreas cells and advance our understanding of how these enhancers orchestrate the remarkable cell type-specific gene expression programs.	MM Jezek, L Wang, S Baek, HE Arda	2023	GEN
2023-250	Georgia	L	Krikorian	NICHD	Developmental Biology	Evaluating the role of novel candidate gene IDH1 in lymphatic development and malformation	The lymphatic system provides essential functions to human health including tissue fluid homeostasis, immune cell transport, and dietary lipid absorption. However, developmental errors, some due to genetic pathogenic variants, lead to lymphatic malformations. Although these may be managed with interventions, understanding the molecular cause of the lymphatic malformation is essential for combinatorial medical therapy that may target the underlying dysregulation of signaling pathways. We identified a recurrent mosaic variant in IDH1 in macrocystic lymphatic malformation tissue that was absent in a saliva sample. IDH1 encodes the enzyme isocitrate dehydrogenase which catalyzes the oxidative dephosphorylation of isocitrate to alpha-ketoglutarate in fatty acid synthesis. Pathogenic variants of IDH1 have been found in a variety of cancers, spindle cell hemangiomas and endochondromas, but have not been previously identified in lymphatic malformations. To test the hypothesis that this pathogenic variant in IDH1 can cause lymphatic malformations, we created transient transgenics using the Tol2 system to simulate the mosaicism seen in the patient. Using the mrc1a promoter, wild-type IDH1 or IDH1 c.295G>A expressed in venous and lymphatic endothelium resulted in lymphovenous cysts and dilated intersegmental vessels by 3 days post-fertilization and pericardial edema by 7 days post-fertilization. Applying deep phenotyping and functional analysis to these mutants will elucidate the role IDH1 and its downstream products in the regulation of gene expression and cell proliferation. Establishing our model for the patient-derived IDH1 pathogenic variants will allow us to better understand the variety of disease mechanisms and evaluate potential new treatments for patients with these rare conditions.	GL Krikorian, SM Paulissen, SE Sheppard	2023	DEVBIO
2023-251	Thien		Nguyen	NICHD	Biomedical Engineering and Biophysics	A point-of-care multimodal biosensor for screening and monitoring patients with respiratory infectious diseases	The worldwide COVID-19 pandemic has challenged the health care community to develop multimodal biosensors to identify patients with critical signs of a respiratory infection. As a result, we have developed and tested an integrated device consisting of a near-infrared spectroscopy (NIRS) sensor, along with an accelerometer and temperature sensor, capable of monitoring skin temperature, tissue oxygenation and significant respiratory and cardiac parameters. Respiratory and cardiac signals collected from the NIRS device was evaluated using physiological data collected from a commercial system during a pilot study in healthy subjects. During experiment, subjects experienced different breathing exercises including breath holding, paced breathing, and hypercapnia. Preliminary data showed a consistent agreement between measurements from our device with signals measured from the commercial system. In addition, tissue oxygenation measured with our device is better than blood oxygenation measured with a pulsed oximeter in detecting breathing pattern change. In future work, we will use our device to collect data from patients with respiratory infectious diseases and apply a deep learning algorithm to classify signals between healthy volunteers and infected patients using our measured parameters.	T Nguyen, S Park, A Gandjbakhche	2023	BIOENG
2023-253	Amir		Seyedmousavi	CC	Microbiology and Infectious Diseases	Efficacy of intravenous posaconazole for the treatment of azole-resistant invasive aspergillosis	Objectives: In the current study we aimed to evaluate the efficacy of the new intravenous formulation of POS in a non-neutropenic murine model of invasive aspergillosis (IA) using POS-susceptible and POS-resistant A. fumigatus isolates. Methods: A total of 240 outbred CD-1® female mice were randomized into groups of 10. The treatment groups consisted of intravenous POS monotherapy at 0.25, 1, 4, 16 and 64 mg/kg/day for seven consequtive days. The control mice received PBS via intravenous injection. The in vivo efficacy of inravenous formulation of POS was assessed against infection with two isolates: a wild type (MIC, 0.031mg/L) and an azole-resistant A. fumigatus (MIC, 0.5 mg/L) harboring TR34/L98H mutation in Cyp-51A gene. Results: The efficacy of posaconazole treatment at the dosing regimens ≤ 4 mg/kg/day depended on the MIC. However, the maximum effect (100% survival at day 14 post infection) was achieved with a POS dose of ≥ 16 mg/kg for both wild-type and mutant isolates, and histopathological slides revealed limited number of inflammatory foci with or without detectable fungal elements in the Kidneys. The Hill-type model with a variable slope fitted the relationship between the dose and 14-day survival well (R2 of 0.99 for wild type, and 0.95 for TR34/L98H isolate). Conclusion: Overall, treatment with intravenous formulation of posaconazole improved the survival of the mice in a dose-dependent manner. A dose-response relationship was observed regardless of the underlying azole-resistance mechanism. These results show intravenous formulation of posaconazole provide higher exposure than the oral suspension for treatment of azole-resistant IA.	A. Seyedmousavi, C.I Aneke, K.J Kwon-Chung, P.E Verweij	2023	MICROBIO
2023-254	Tracy	S	Williams	CC	Clinical Research	Challenges with end-of-life clinical pain trials	Clinical trial participation for refractory cancer pain in end-of-life patients presents numerous barriers that challenge study design and execution. By intent, patient recruitment involves participants that are medically unstable, with a multitude of complex issues, both physical and emotional. Patients with refractory pain often are taking opioid pain medications of various formulations, durations of action, and routes of administration that can complicate recruitment, pain measurement and produce an unacceptable set of side effects. Given this complex background and the high risk of disease-related serious adverse events, targeted development of analgesics in this patient population has been a neglected indication. The objective of this abstract is to examine the multiple considerations that can impede drug testing in this population spanning psychosocial issues to clinical trial design. All studies involving patients at the end of life require a delicate balance of collecting data while minimally impacting their remaining life. In a phase I study, a patient may not receive benefit if treated early in a study (e.g. sub-therapeutic dose or placebo). Patient study visits and frequency as well as types of interventions need to be thoughtful and minimized. These studies are essential for improving the quality of life for this patient population but it is essential that all efforts are made to lessen interference with family interaction and end of life issues.	TS Williams, MJ Iadarola, MR Sapio, AJ Mannes	2023	CLINICAL
2023-255	Darawalee	W	Zong	NCATS	Clinical Research	i3D-RARE: A Precision Medicine Platform of iPSC-derived 3D Cellular Models to Accelerate Therapeutic Development for Rare Diseases	The development of therapies for rare diseases remains a huge challenge, with ~10,000 rare diseases affecting 10% of the US population, and only ~5% having an FDA approved treatment. The lack of disease relevant in vitro and animal models, the small numbers of patients and heterogeneous genetic mutations make it difficult to efficiently find treatments for rare disease patients. Therefore, there is a critical need for personalized and clinically predictive assays for the development of effective therapies for rare diseases. The recent FDA Modernization Act 2.0 allows for alternative to animal testing for purposes of drug and biological products applications for clinical testing. 3D cellular models with patient primary cells and iPSC-derived cells that mimic the physiological complexity of human tissues and organs are being developed as predictive assays for drug discovery and therapeutic development. At NCATS, we are addressing the need for predictive cellular models for rare disease by implementing a collaborative platform (i3D-RARE) of stem cell derived 3D cellular models (e.g., spheroids, organoids, bioprinted tissues, and tissue chips). The i3D-RARE platform has four key strategic goals: (1) production of rare disease patient iPSCs and iPSC-differentiated cells, (2) production of personalized rare disease iPSC-derived 3D organotypic cellular models, (3) operationalization of the use of these 3D organotypic models for therapeutic testing and drug development, and (4) dissemination of acquired knowledge to the public. We believe that i3D-RARE will foster the use of alternative methods to animal testing and accelerate the development of more effective treatments for rare diseases.	DW Zong, RM Lomash, CZ Chen, MJ Song, DD Rudnicki, BJ Traynor, S Michael, CA Tristan, A Simeonov, W Zheng, DA Tagle, M Ferrer, EM Ottinger	2023	CLINICAL

2023-256	Guojia		Xie	NIDDK	Genetics and Genomics	MLL3/MLL4 methyltransferase activities control early embryonic development and ESC differentiation in a lineage-selective manner	Enhancers are cis-regulatory elements controlling cell-type-specific gene expression and are marked by H3K4me1. MLL3 (KMT2C) and MLL4 (KMT2D), the major mammalian H3K4me1 methyltransferases, are critical for enhancer activation and cell-type-specific transcription during development and cell differentiation. However, roles of MLL3/4 enzymatic activities and MLL3/4-mediated enhancer H3K4me1 in these processes remain unclear. Using MLL3/4 enzyme-dead single and double knockin mice generated by CRISPR/Cas9, we report that enzymatic activities of MLL3 and MLL4 are redundant during early embryonic development. Simultaneous elimination of both leads to gastrulation failure and early embryonic lethality around E6.5. Embryonic stem cells (ESCs) lacking MLL3/4 enzymatic activities can differentiate towards the three embryonic germ layers including endoderm, mesoderm and ectoderm. However, they fail to differentiate to extraembryonic endoderm cells due to markedly reduced enhancer binding of GATA6, the lineage-determining transcription factor driving extraembryonic endoderm development. Moreover, loss of MLL3/4 enzymatic activity blocks induction of Elf5 during ESC to trophectoderm transition and thus leads to precocious terminal trophoblast differentiation. Consistent with ESC data, Sox2-Cre-mediated elimination of MLL3/4 enzymatic activities in epiblast, but not in early extraembryonic tissues, leaves gastrulation largely intact. These conditional MLL3/4 enzyme-dead mice survive until mid-gestational stage beyond E10.5. Furthermore, we show that MLL3/4-catalyzed H3K4me1 is largely dispensable for enhancer activation during early EB differentiation and neural differentiation of ESCs. Together, our findings highlight a lineage-selective, but enhancer activation-independent, role of MLL3/4 methyltransferase activities in mammalian embryonic development and ESC differentiation.	G Xie, J Lee, AD Senft, Y Park, Y Jang, S Chakraborty, JJ Thompson, K McKernan, C Liu, TS Macfarlan, PP Rocha, W Peng, K Ge	2023	GEN
2023-257	Songjoon		Baek	NCI	Genetics and Genomics	Identifying Cell-Specific Enhancer Loops and Their Impact on Transcription Activities in Donor Pancreas Tissues: Implications for Gene Regulatory Mechanisms and Therapeutics	This study aims to identify enhancer loops in donor pancreas tissues by performing ATAC-seq and Hi-ChIP on purified major cell types. We transformed these loops into networks, where nodes denote looping regions and edges denote interactions. We further simplified EP networks to a collection of EP trees, each consisting of a root promoter and its associated enhancer nodes. Through annotation of the EP trees with genomic data (accessibility, interaction frequency, transcripts of root promoters), we observed a strong correlation between enhancer accessibility and interaction frequency within EP trees. This relationship provides a comprehensive measure of enhancer activity on the corresponding promoter. Moreover, cell-specific promoters have unique EP trees, indicating that enhancer activities are associated with promoter activities in a cell-type specific manner. To validate this finding, CRISPR-perturbation and RNA-FISH were performed in donor tissues at PCSK1, a beta cell-specific gene. We targeted two enhancers with beta-specific activities based on EP tree analysis, and observed the effect on PCSK1 promoter specifically in beta cells but not in exocrine cells where PCSK1 is inactive. In our initial simulation analysis, we were able to identify redundant loops that are likely artifact of crosslinking. The redundant loops (~2%) were removed to help simplify EP tree structure and reduce ambiguity in assessing enhancers impact on root promoter. Our study will provide guidance for prioritizing critical enhancers to understand gene regulatory mechanisms controlling pancreatic cell identity and function, which could lead to the development of therapeutics for pancreatic diseases.	SJ Baek, L Wang, E Arda	2023	GEN
2023-258	Shareef	F	Syed	NIDCR	Developmental Biology	Elucidating the role of Mab21l2 -expressing cells during synovial joint development using a flox-cre mouse model	Synovial joints are important components of the skeletal system and consist of bone-lining cartilage, synovial membranes and fluids that endow us with our mobility. How these tissues develop during embryogenesis, are maintained during life, and how they degenerate during aging and in disease is a major interest in our group. Previously, we used scRNA-seq to characterize synovial joint formation in the murine knee during fetal development. We identified a gene called Mab21l2 that was expressed in a unique population of neural/neuronal progenitor cells, and in a subset of early joint precursor cells. While little is known about Mab21l2, certain mutations of this gene lead to osteochondral anomalies in humans and mice. We hypothesize that Mab21l2-expressing cells may represent a chondrogenic progenitor cell or a cell type that guides cartilage development in the morphogenetic field. In this study, Tamoxifen-inducible Mab21l2-iCreERT2;R26R-EYFP mice will be used that employs a flox-cre reporter system to trace Mab21l2-expressing cells during synovial joint development. Pregnant mice will be injected with tamoxifen at E11.5 to induce Cre recombinase activity, which results in an eYFP fluorescence signal in Mab21l2-expressing cells and their progeny. Following induction, mice will be collected on embryonic days specific to critical events during joint development (E11.5-E18.5). eYFP expressing cells will be enriched for by using FACS and then analyzed using scRNA-seq for cell cluster annotation. Additionally, the mediolateral knee section will be analyzed using immunohistochemistry methods. We hope that this study will help elucidate the role of Mab21l2-expressing cells during joint development.	SF Syed, PG Robey, K Futrega	2023	DEVBIO
2023-259	Anas	H	Awan	NHGRI	Genetics and Genomics	Phenome-wide association study of Sickle Cell Trait in NIH's All of Us Research Program	The HbS variant is widespread, particularly among individuals of African descent. While most people with Sickle Cell Trait (SCT) carrying one HbS allele remain symptom-free, some rare cases link carrier status to adverse outcomes. All of Us is a diverse biobank with participants' genomic and health data. This study aimed to investigate the association of SCT with clinical outcomes, focusing on vascular occlusive complications. Among 39,020 individuals of African descent with genomic and health records, 3,363 carried one HbS allele, while 73 carried two and were excluded. We ran a PheWAS comparing single HbS allele carriers to non-carriers and found strong associations with anemia during pregnancy, iron deficiency anemias, aseptic necrosis of bone, and pulmonary embolism/infarction. To assess the impact of other hemoglobinopathies, ClinVar variants of the HBB gene were examined, excluding non-HbS variants like beta-thalassemia and HbC. This resulted in 3,162 single HbS carriers and 31,798 non-carriers. A second PheWAS identified the most strongly associated phenotypes in this group as anemia during pregnancy, iron deficiency anemias, gout, and abnormal results of kidney function. The association with aseptic necrosis of bone and the association with pulmonary embolism/infarction decreased. These findings align with previous research, suggesting that the reported associations between SCT and vascular occlusion phenotypes, except for kidney issues, may be influenced by concomitant hemoglobinopathies. The study provides new insights into phenotypic variations among individuals with SCT. Considering the prevalence of HbC and beta-thalassemia alleles, clinicians should investigate other hemoglobinopathies to determine the risks of vascular occlusive complications in SCT.	AH Awan, HC Ramirez, TM Ferrara, A Williams, A Buscetta, RP Naik, P Joseph, JM Keaton, JC Denny, VL Bonham, H Mo	2023	GEN
2023-260	Nafiseh		Ghazanfari	NIMH	Molecular Biology and Biochemistry	The PET radioligand [11C]PS13 shows high specific binding in human brain of cyclooxygenase-1, a biomarker for microglia	Purpose/ Background: Neuroinflammation is associated with various neurodegenerative forms of dementia, including Alzheimer's disease. Such diseases may be associated with neuroinflammation. Cyclooxygenases (COX) produce inflammatory mediators Thus, PET radioligands for COX are potentially useful for the study of neuroinflammation. We recently developed [11C]PS13, a highly selective radioligand for COX-1, a major isoform of COX. Our objective was to accurately estimate the specific binding of [11C]PS13 to COX-1 in healthy human brain using scans performed at baseline and after treatment with ketoprofen. Methods: Eight healthy volunteers underwent two 90-minute [11C]PS13 PET scans (injected activity 743±37 MBq) at baseline and at least two hours after oral administration of ketoprofen (75 mg). During each scan, the radiometabolite-corrected arterial input function was measured. VT values were obtained with both a two-tissue compartmental model (2TCM) and Logan graphical analysis. Results: Brain radioactivity concentration peaked at about 3 minutes after [11C]PS13 injection, with SUV values of 2.9±0.7 at baseline and 3.3±0.8 after ketoprofen treatment. The time-activity curve for parent radiotracer in plasma had a higher peak after ketoprofen treatment (12.5±5.1 SUV) than at baseline (7.5±2.0 SUV). 2TCM analysis fitted the brain time-activity curves well at both baseline and after ketoprofen treatment (SE <5%). VT values were 2.7±0.5 at 1.6±0.5 for baseline and after treatment, respectively. The Lassen plot revealed an occupancy of 80% by ketoprofen and a VND of 1.4. Whole brain BPND was calculated at 1.3. Conclusion: [11C]PS13 binds specifically to COX-1 in the human brain and can be blocked by the selective inhibitor ketoprofen.	N Ghazanfari, M.J Kim, C Knoer, J Hong, F Ahmadi, J.M Montero Santamaria, S Zoghbi, J.S Liow, V.W Pike, R.B Innis, P Paolo Zanotti-Fregonara	2023	MOLBIO
2023-261	Britney		Campbell	NIA	Immunology	Peripherally activated brain CD8+ T cells promote AD in mice with Alzheimer's Disease	Alzheimer's Disease (AD) is neurodegenerative disease linked to accumulation of Aβ plaques, neurofibrillary tangles, and chronic neuroinflammation. Although the role of the adaptive immunity in AD remains poorly understood, recent findings indicate that CD8+ T cells increase in the AD brain. Our aim was to characterize CD8+ T-cells and to investigate if they are required in AD progression. We immunized female 5xFAD mice at pre- (2-3 months) and post-onset of AD (7-8 months) with an Aβ-CoreS RNA vaccine encoding Aiff1-11 on the surface of HBsAg particles. The CD8+ T cells were quantified from the brain of these mice and unvaccinated 5xFAD mice using immunofluorescence (IF) staining (n=4-7). We further characterized the activation state of brain CD8+ T cells from saline perfused 5xFAD mice using flow cytometry (n = 8-11). Similarly, stained humans tissued with AD (79-90 years old) were quantified for CD8+ T-cells. Our results reveal that compared to WT, AD significantly increases brain CD8+ T cells exhibiting cytotoxic but exhausted phenotype. These affects were significantly increased in vaccinated mice, linking the increase of brain CD8+ T cells to the exacerbation of AD. The brain CD8+ T cells positively correlated with cognitive decline and Aβ plaque accumulation with their activation induced in the periphery. To do this, they likely target microglia, as in both mice and humans with AD we detected significantly more brain CD8+ T cells tightly attached to activated microglia than in non-AD groups. Overall, our results indicate that brain CD8+ T cells play pathogenic role in AD.	B Campbell, M Bodogai, X Wang, RA McDevitt, K Konda, H Ishikawa-Ankerhold, A Biragyn	2023	IMMUNO
2023-262	Shweta		Tiwary	NCI	Immunology	Endogenously High Omega-3 levels lead to a less exhausted T cell phenotype in tumor microenvironment	Cancer causes multiple changes in the cellular pool of nutrients and macromolecules, including lipids. Tumors switch to the de novo lipid pathway and preferentially accumulate some lipids while excluding others, such as omega-3 (n-3) fatty acids and bioactive lipids derived from them, from the tumor microenvironment. These lipids, known as specialized pro-resolving lipids (SPM), may affect cancer development. Although their roles in decreased cancer risk and inflammation are well studied, their effects on anti-tumor immunity are still poorly understood. Here, we report the consequences of high n-3 levels on tumor growth and anti-tumor immunity. We have utilized a FAT-1 transgenic mouse model with an endogenously high n-3: n-6 ratio due to a transgenic enzyme making n-3 fatty acids and EO771 mammary tumor model. Our data show a decreased tumor growth rate in FAT-1 mice associated with increased tumor-infiltrating cells (TILs). In preliminary studies, we found that CD8 and CD4 T-cells in TILs isolated from tumors growing in FAT-1 mice display a more active and proliferative phenotype. Also, the T-cells had decreased exhaustion markers such as TIM-3, LAG-3, and TIGIT in the TILs isolated from tumors growing in FAT-1 animals, and there were fewer FOXP-3 positive T-cells. Together our data suggest a less suppressive anti-tumor immune environment in FAT-1 animals. Currently, we are performing mechanistic studies to understand the role of high omega-3 in the expression and function of these exhaustion markers. We are also exploring the therapeutic benefit of CPI and cancer vaccines in combination with high omega-3 fatty acids.	S Tiwary, X Zheng, P Olkhanud, JA Berzofksy	2023	IMMUNO
2023-263	Amlan		Talukder	NIEHS	Neuroscience	Patients with Down syndrome differ from matched controls in their EEG power spectra during sleep	Electroencephalogram (EEG) can capture brain oscillatory activities during sleep as a form of electrophysiological signals. Unique brain wave activities may be present in patients with neurological disorders such as Down Syndrome (DS) when compared to healthy controls. In this study, we analyzed 97 full night in-laboratory polysomnography EEG recordings of DS subjects along with age- and sex-matched controls. We aimed to identify EEG features that are distinctive to patients with DS. From each subject's EEG, we extracted the relative power at six frequency bands (delta, theta, alpha, slow spindle, fast spindle, and beta) for each of the five sleep stages (N3, N2, N1, R, and W) and six channels (frontal F3 and F4, central C3 and C4, and occipital O1 and O2) – 180 features in all. We applied statistical and machine learning methods to the data including paired t-tests and Extreme Gradient Boosting (XGBoost). We showed that EEG features identified by XGBoost can distinguish between DS patients and healthy controls. Our results also revealed that, in N1 sleep, DS patients had significantly lower power in the alpha band (8-10.5 Hz) but higher power in the delta band (0.25-4.5 Hz). We also noticed that, during N1 sleep, the power difference between DS patients and matched controls gradually increased with age in both the alpha and the delta bands. Our findings suggest that unique EEG features can be identified in DS patients and that those features may be used as markers for disease management.	A Talukder, D Yeung, Y Li, N Anandanadarajah, DM Umbach, Z Fan, L Li	2023	NEURO
2023-264	Victoria	I	Dulemba	NCI	Immunology	Significance of tumor reactivity in draining lymph nodes	CD8+ T cell responses play a pivotal role in promoting immune recognition against tumors, and the abundance of T cells existing in a stem-like phenotypic state have been associated with increased response to therapy. In scenarios characterized by persistent exposure to antigens, such as cancer and chronic infections, CD8+ T cells with specificity towards these antigens may undergo exhaustion or dysfunction that can manifest through increased expression of inhibitory receptors. Extensive transcriptomic profiling of Tumor Infiltrating Lymphocytes (TIL) across metastatic tumors has demonstrated that anti-tumor T cells tend to exist in an exhausted or dysfunctional state, allowing for successful TCR prediction based on a common exhaustion gene signature. Recent investigations in murine models have revealed the significance of T cells located in peripheral regions, specifically secondary lymphoid organs such as tumor-draining lymph nodes. However, the anti-tumor properties and phenotypic states of T cells within DLNs remains to be fully understood. Fresh Tumor Digest (FTD), Draining Lymph Node (DLN), and/or PBL sample were obtained from patients undergoing oncologic resections. Single cell transcriptomic analysis was performed for FTD and DLN samples, and TCRs within likely reactive clusters were ordered for functional screening based on neoTCR signature. TCR encoded DNA plasmids were retrovirally transduced into donor PBL using a gp100 cell line, allowing for functional screening of TCRs against neoantigen candidates and patient derived organoid by ELISpot and Flow Cytometry. Reactive TCR clones were then back projected onto single cell transcriptomic data to determine phenotypic states allowing for comparison between sites.	V Dulemba, K Hitscherich, S Sivashish, A Dinerman, F Lowery, P Robbins, J Hernandez, S Krishna	2023	IMMUNO

2023-265	Catherine		Kwiat	NINR	Clinical Research	Relationships of BDNF single nucleotide polymorphisms and perceived stress in cancer survivors	Stress related to cancer and its treatments is commonly experienced by cancer survivors. When cancer-related stress becomes overwhelming, it can negatively affect various bodily processes and quality of life. A single nucleotide polymorphism (SNP) of brain-derived neurotropic factor (BDNF), called rs6265, is known to contribute to the inter-individual perception of psychoneurological (PN) symptoms in cancer survivors. Given the roles of BDNF in neurotransmitter modulation and of rs6265 in PN symptom perception, we hypothesize that rs6265 can also influence inter-individual stress perception in cancer survivors, which can vary between cancer types. The Perceived Stress Scale (PSS) was used to assess stress scores of 413 breast cancer and colorectal cancer survivors. Buccal swabs were used to obtain genotypes for BDNF rs6265 (Val/Val, Val/Met, or Met/Met). PSS scores were compared across genotypes and between cancer types. The study results showed no significant relationship between the presence of the BDNF Val/Met rs6265 polymorphism and perceived stress in cancer survivors. Among Val/Val homozygotes, but not among those with the Met allele, the results revealed higher perceived stress scores among colorectal cancer survivors compared to breast cancer survivors. This suggests that carrying the Met allele may have a mitigating effect on stress perception among colorectal cancer survivors. Risk identification for long term toxicities related to cancer and its treatment is critical to provide precise and optimal supportive care to cancer survivors.	C Kwiat, T Goto, L Saligan	2023	CLINICAL
2023-266	Amy	Q	Wang	NCATS	Molecular Pharmacology	Ultra-Performance Liquid Chromatography-Tandem Mass Spectrometry Method Development and Pharmacokinetics of PTH-IA in Mice	PTH-IA (parathyroid hormone receptor-inverse agonist) is a drug candidate under investigation for the treatment of Jansen's Metaphyseal Chondrodysplasia (JMC) which is a rare disease of abnormalities in bone development and mineral ion homeostasis. The objective of the present study was to develop a rapid, accurate, and selective ultra-performance liquid chromatography-tandem mass spectrometry (UPLC–MS/MS) method to quantify PTH-IA in plasma samples and to assess PTH-IA pharmacokinetic (PK) properties in mice. The developed UPLC-MS/MS method was successfully applied in PK studies of PTH-IA in mice. Following a single SC administration of 1.52 mg/kg to male C57Bl6 mice, the mean maximum plasma concentration (Cmax) was 152 ng/mL at the first sample collection time of 0.083 h. The terminal half-life (t1/2) was 2.3 h. The corresponding AUC0-∞ was 101 ng-h/mL. Following a single IV administration of 1.44 mg/kg, the mean plasma clearance (CLp) was relatively low, in the range of 10 - 15 mL/min/kg. The volume of distribution at steady-state (Vdss) was in the range of 0.21 - 0.45 L/kg. Based on the dose normalized AUC0-∞ values between the SC and the IV studies, the estimated SC bioavailability for PHT-IA was 4 - 6% in mice. An accurate, selective, rapid, and robust UPLC-MS/MS method to quantify PTH-IA in mouse plasma was developed. This method was applied successfully to the mouse PK studies.	AQ Wang, C Ryu, NR Hagen, X Xu	2023	PHARMA
2023-267	Shawn	A	Bryant	NCI	Immunology	Differential efficacy of TLRL adjuvants in COVID-19 protein subunit vaccines	Although COVID-19 may no longer be a Public Health Emergency, its effects are still being felt both here and throughout the world. Universal access to cheap, transportable, and effective vaccines is critical to ensuring public health and safety. Protein subunit vaccines are safer and easier to transport than live virus or mRNA vaccines, but they are less immunogenic. To create an effective protein subunit vaccine, immunostimulatory substances known as adjuvants must be added. Adjuvants both stimulate and shape the immune response, allowing an otherwise weakly immunogenic protein to provide full protective immunity. This research examines the efficacy of toll-like receptor ligands (TLRLs) as adjuvants in an S1 COVID-19 protein subunit vaccine. Vaccines containing these adjuvants have previously been shown to induce a stronger immune response than the protein alone. Healthy mice were given an S1 protein vaccine which contained various combinations of TLRL adjuvants. The immune response was characterized at each dose and at the end of the study to track changes over time. Humoral immunity was characterized by determining the blood concentration of anti-S1 antibodies produced in response to the vaccine, as well as the neutralizing capability if these antibodies. Cellular immunity was characterized using flow cytometry to follow changes in the T cell populations following vaccination. These data highlight the potential of TLRL adjuvant vaccines and demonstrate the need for future investigations into their use for current and emerging viral diseases.	SA Bryant, W Becker, JA Berzofsky, PB Olkhanud	2023	IMMUNO
2023-268	Anusha		Ebrahim	NHGRI	Genetics and Genomics	Introducing "Leptomeningeal Cavernomatosis": A neologism for an unusual case of familial cerebral cavernous malformations	Introduction: Cerebral cavernous malformations (CCM) are structurally abnormal, irregularly clustered, and dilated capillaries found in the brain and spinal cord. While isolated CCMs are common and often discovered incidentally, familial cerebral cavernous malformation (FCCM), an autosomal dominant disease in which innumerable CCMs could form, results in a variety of neurological symptoms. The three genes associated with FCCM are KRIT1, CCM2, and PDCD10, but mutations in KRIT1 are the most frequent cause of FCCM. While many patients might remain asymptomatic, others experience seizures, focal neurological deficits, headaches, vision changes, strokes, and intracerebral hemorrhages. Multiple focal lesions with hemosiderin deposits are prototypical in FCCM. Here we describe a patient with a novel VUS in KRIT1 (c.1942 G>A, p.A648T) identified on clinical WES and WGS, with leptomeningeal cavernomas, diffuse superficial siderosis, and numerous brainstem lacunar strokes including several without hemosiderin deposits. Case Presentation: The proband, a now 29-year-old African American male, presented to the NIH Undiagnosed Diseases Program (UDP) with progressive stepwise cognitive decline, balance issues, dysarthria, and spasticity. His MRI was atypical in that multiple non-hemorrhagic brainstem lacunae coexisted with more typical CCM features. Conclusions: This is the first association of this specific variant of KRIT1 (c.1942 G>A, p.A648T) with FCCM. The presentation of ischemic non-hemorrhagic lacunar strokes restricted to the brainstem as well as a single leptomeningeal cavernoma with subarachnoid hemorrhage would be unusual for FCCM. Other monogenic vasculopathies associated with mutations in NOTCH3, COL4A1, NEU1, HRTA, and GLA were excluded.	A Ebrahim, Z Wolfenson, O Jean-Marie, C Wahl, LG Vezina, WA Gahl, C Toro	2023	GEN
2023-269	MG		Hirsch	NLM	Computational Biology	Identification of genes with adaptive expression results in distinct transcriptional states of tumor subclones	Cancer growth is an evolutionary process involving cells acquiring mutations, epigenetic reprogramming, and differentiation into distinct subclones. It is assumed that this clonal evolution is driven by the selection of cells exhibiting properties related to growth advantage, like immunoevasion and cell growth, which are phenotypic hallmarks of cancer. Studying the evolution of gene expression is critical to understand the driving selective pressures of these phenotypic traits. This is particularly important in the context of drug response, where treatment-induced effects modulate gene expression. To investigate the role of selection on gene expression in subclonal evolution, we model changes in gene expression along trajectories defined by the evolutionary tree as Ornstein-Uhlenbeck processes. Our approach differs from prior approaches, like differential expression analysis, by jointly leveraging the evolutionary history of tumor subclones (inferred from mutation data) and single-cell subclone-specific expression data. Applying our model to sublines derived from a B2905 cell line revealed that sublines with different growth rates and immunotherapy treatment responses have distinct patterns of gene expression adaptation. Specifically, sublines that showed resistance to treatment had genes with adaptive expression related to immunoinvasion, whereas sublines that responded to treatment had genes with adaptive expression related to increased growth rate. Further, we observed that tumors derived from the parental line and then given anti-CTLA-4 treatment were enriched with genes identified to have adaptive expression corresponding with their treatment response. Together, our results suggest that the adaptivity identified is associated not just with individual sublines but also with the broader phenotypic characteristics.	MG Hirsch, S Pal, FR Mehrabadi, S Malikic, E Perez-Guijarro, G Merlino, SC Sahinalp, EK Molloy, CP Day, TM Przytycka	2023	COMPBIO
2023-270	Savanah	L	Shumaker	NCATS	Research Support Services	Development of the NCATS automated sample preparation workflow for NMR-based analysis platforms	Analytical chemistry is crucial for drug discovery, providing vital data like compound identity, purity, structure, target engagement, therapeutic activity, efficacy, and biomarkers. However, current methods are outdated, time-consuming, and detached from research workflows. To overcome these challenges, the Analytical Chemistry Core (ACC) at NCATS is developing automated workflows to enhance speed, efficiency, and reproducibility. The ACC focuses on automating NMR sample preparation, standardizing steps, and utilizing adaptable liquid handling platforms. This enables handling routine 1D and 2D NMR samples and specialized samples for NMR-based fragment screening and quantitative NMR analysis. The sample preparation workflow involves (i) stamping of stock solutions into 96-deep well plates, as well as 96-well LCMS plates for quality control handling a Beckman Coulter Biomek i7, (ii) dilution of the deep-well plates to desired concentration with desired deuterated solvent using a Beckman Coulter Biomek FXP, and (iii) sample transfer from plates to NMR tubes using a Sirius Automation MicroTasker. Customized protocols are being developed for this process to accommodate a variety of NMR analysis requirements. After data acquisition is complete, automated processing and analysis are performed through custom pipelines in Mestrelab Mnova Gears (MGears) software platform. The resulting spectral data is managed within Mnova DB, which can be accessed remotely through a web-based interface. The process thus far marks a significant advancement in our goal of a fully automated NMR platform for the preparation, data acquisition, data processing, and analytical analysis of chemically diverse samples as part of drug discovery and development initiatives.	SL Shumaker, SA Kotler, KA Butler, JC Klein, DR Calabrese, GY Gomba, KM Wilson, CA LeClair	2023	RSCHSUPP
2023-271	Jessalyn	M	Grant-Bier	NIDDK	Molecular Biology and Biochemistry	Proximity dependent biotin-tagging to screen for proteins involved in FMR1 gene silencing in Fragile X syndrome	Repeat Expansion Diseases (REDs) are a group of more than 40 human diseases caused by expansion of a disease-specific short tandem repeat tract within a gene. Fragile X syndrome (FXS), the most common heritable form of intellectual disability, is caused by the expansion of a CGG-repeat tract in the 5' UTR of the FMR1 gene. FMR1 alleles with >200 repeats are hypermethylated and transcriptionally silenced. Repeat-induced gene silencing is also seen in other REDs; however, the underlying mechanism is not completely understood. To identify proteins involved in FXS gene silencing, I am developing an unbiased proximity-labeling screen to identify proteins that associate with FMR1 in stem cells derived from unaffected and affected individuals. I have generated FXS embryonic stem cell lines expressing doxycycline-inducible dCas9-APEX2 and repeat-specific CRISPR guide RNA. I will use Chromatin Immunoprecipitation to confirm targeting of dCas9-APEX2 to the FMR1 locus. Addition of doxycycline, together with biotin-phenol and H2O2, will biotin-tag proteins within a ~20 nm radius of the APEX2 peroxidase. Biotinylated proteins will then be purified by streptavidin pull-down and identified by mass spectrometry. Additional cell lines will be produced to assess the proteomic landscape at FMR1 when the gene is experimentally reactivated and in cells with repeat numbers below the silencing threshold. Comparison of these different proteomes should allow proteins contributing to the initiation and maintenance of silencing to be identified. The results obtained from this study may contribute to the understanding of repeat-induced gene silencing in FXS and other REDs.	J M Grant-Bier, B E Hayward, K Usdin, G A Nardone, K W Cormier, L R Olano, D Kumari	2023	MOLBIO
2023-272	Susanna		Barber	NIAID	Microbiology and Infectious Diseases	Global challenges of antimicrobial resistance	Antimicrobial resistance—the ability of micro-organisms (bacteria, viruses, fungi, parasites) to resist drug therapy—is a complex and serious public health problem. The WHO considers AMR to be one of the top ten threats to global health and one of the biggest public health challenges of our time. The systemic / holistic approach to AMR focuses on five main components: (1) Lack of water, sanitation and hygiene (WASH) infrastructure in the developing world, (2) overuse of antibiotics by the food supply industry; (2) overuse of pesticides in agriculture; (3) overprescribing and inappropriate prescribing of antibiotics by the medical profession; (4) poor hand hygiene in hospitals and healthcare facilities, and (5) low incentives for pharmaceutical companies to invest in development of new antimicrobial drugs. There is also growing evidence that the environment plays a key role in the evolution, transmission and spread of AMR. The triple planetary crisis of climate change, biodiversity loss, pollution and waste is propelling AMR. Solutions must be driven by a multi-systems approach: (1) Accelerate WASH infrastructure programs to ensure that all populations have sustainable access to clean water and sanitation; (2) address climate change and environmental degradation, including ending pollution from agriculture, animal and fish production, pharmaceutical manufacturing, and healthcare facilities; (3) phase out mass housing of animals and birds in close-proximity to decrease the need for antimicrobials; (4) increase antimicrobial stewardship in hospitals and healthcare to lower antimicrobial prescribing; (5) Increase financial incentives for innovative research to produce new antimicrobials and bio-degradable antimicrobials; and (6) increase governance and enforcement to deter overuse of antimicrobials.	S R Barber	2023	MICROBIO
2023-273	Liangchen		Liu	CC	Biomedical Engineering and Biophysics	IMPROVING AUTOMATIC SEGMENTATION OF LYMPHOMA WITH ADDITIONAL MEDICAL KNOWLEDGE PRIORS	Lymphoma is a type of malignant tumor that is often fatal to people of all ages. Positron Emission Tomography (PET) / Computed Tomography (CT) is the primary imaging method to assess lymphoma and monitor treatment response. As PET is sensitive to identify lymphoma regions while CT provides detailed anatomic information, the two imaging modalities can complement each other to enable improved diagnosis. However, automatic lymphoma segmentation is still challenging due to its substantial size and shape variability and limited datasets for training. To that end, we create a new whole-body lymphoma dataset. We design pre- and post- processing mechanisms particularly for lymphoma lesion segmentation according to medical knowledge priors. We designed an automatic lymphoma segmentation model with nnU-net as the backbone. Our pipeline incorporates pre- and post- processing mechanisms to remove regions of normally increased radiotracer uptake, and augment training with non-lymphoma samples. The proposed method was validated on the PET/CT scans of 46 patients. Experiments showed that by incorporating these additional steps, segmentation performance was further improved from 0.263 (LPMM-nsa) and 0.456 Dice (baseline nnU-Net) to 0.477 Dice (full pipeline). The results and analysis demonstrate the efficacy of the proposed method. Furthermore, the use of the AI model reduced the time required for segmentation by 55.7% compared to the reference manual segmentation. The mean Total Metabolic Tumor Volume (TMTV) calculated using the AI-predicted labels was not significantly different from those calculated using the manual labels (P = 0.153). This indicates that AI-based segmentation was comparable to manual segmentation.	L Liu, B Hou, MK Nag, J Liu, N Hasani, TC Shen, Y Zhu, B Sabourry, X Jing, RM Summers	2023	BIOENG
2023-274	Nouhou		Ibrahim	NCATS	Virology	A cell-based luminescence high-throughput screening to identify antivirals for EV-D68	The NIH Antiviral Program for Pandemics (APP) was created in June 2021 as a response to the global pandemic of coronavirus disease 2019 (COVID-19). This program identified 11 viral families for developing safe and effective antivirals based on their pandemic potential. One of these families of interest is the Picornaviridae, a large family of small, positive-sense RNA viruses, that includes the genus Enterovirus. Enterovirus D68 (EV-D68), a non-polio enterovirus, is transmitted through the respiratory tract contrary to the fecal-oral route of poliovirus. It mainly infects children and causes flu-like symptoms and can lead to acute flaccid paralysis. In 2014, there was an EV-D68 outbreak in the USA. To date, no vaccine is available against enterovirus infection. In line with the APP goals, there is an urgency for safe antivirals against EV-D68, and we developed a cell viability-based, 1536-well assay for high throughput screening (HTS) to identify candidate antiviral compounds for enterovirus D68. One of the EVD68-induced cytopathic effects in vitro is extensive cell death, therefore our HTS is based on a luminescence readout to measure intracellular ATP using CellTiter Glo (CTG) as a function of cell viability. Here, the optimized steps of the HTS will be described. To validate our CTG-based EVD-68 assay, the NCATS Anti-infective library was screened. Several previously reported compounds were re-identified as antiviral in this screen. Our HTS is suitable to screen other NCATS libraries and will be used for drug repurposing other chemically diverse libraries and the development of computational modeling to predict anti-EV-D68 compounds.	N. Ibrahim, E. Lee	2023	VIROL

2023-275	Samantha		Cotsmire	NCATS	Virology	Characterization of SARS-CoV-2 infection in primary human lower respiratory tract and small intestinal tissue models	While the global and public health emergencies were declared ended in May 2023, there is still concern surrounding both new acute SARS-CoV-2 infections, variant emergence, and the role of persistent infections and symptoms (e.g. long COVID). Because of the continued spread and subvariant emergence, it is critical that the scientific community quickly assess the public impact and dangers of emerging SARS-CoV-2 variants, including changes in infectivity, disease burden, tissue tropism, drug sensitivity, and immunological escape. To achieve this goal, the Antiviral Program for Pandemics Advanced Models & Cell-Based Discovery Team at NCATS, in collaboration with the 3D Tissue Bioprinting Lab, are using human SARS-CoV-2 infected air liquid interface (ALI) primary human airway and alveolar tissues to monitor various infection parameters. In the work presented here, we have infected these tissues with early and current SARS-CoV-2 variants/subvariants and measured temporal and tissue specific 1) variant infectivity/replication, 2) transcriptomic changes, and 3) secreted cytokine responses, and 4) sensitivity to select approved anti-SARS-CoV-2 small molecules. In addition, we also established a long-term human gut infection model by SARS-CoV-2 and investigated variant-specific infectivity profiles in this model for up to 21 days after infection. During these 21 days, we measured sustained intracellular SARS-CoV-2 RNA levels, as well as investigated infectious virion production, tissue transcriptomic changes, and secreted cytokine responses over time.	S Cotsmire, A Medina Farias, K Derr, P Derr, YC Chen, M Ferrer, E Lee	2023	VIROL
2023-276	Amanda	K	Small	NCI	Social and Behavioral Sciences	Relationships between COVID-19 illness experience and risk perceptions in U.S. adults	Background: More than half of U.S. adults report having experience with a COVID-19 infection, in either themselves or a household member. Yet, little is known about how these experiences might relate to risk perceptions about COVID-19 infection/reinfection. Methods: Survey weighted linear regressions were used to examine relationships of risk perceptions with self-reported COVID-19 experiences (personal infection status, household infection status, symptom length, and severity) using data from an online survey of a nationally representative sample of U.S. adults (n=5494) in November 2020. Participants reported perceived likelihood of getting COVID-19 (absolute risk and compared to an average person), worry about COVID-19, vulnerability to COVID-19, perceived probability of death from COVID-19, and judgments about the usefulness and ambiguity of mitigation efforts and prevention guidance. Covariates included gender, age, race/ethnicity, education, income, and marital status. Results: Associations among risk perceptions and personal or household experiences of COVID-19 were complex and varied by risk perception type. Perceived likelihood of COVID-19 was lower for respondents who reported having had COVID-19 ($p < 0.001$), but higher in people reporting a household member who had had COVID-19 ($p = 0.001$). Symptom severity and length also related to perceptions. Notably, both were positively associated ($p </= 0.008$) with worry about getting COVID-19 and feelings of vulnerability to COVID-19. Conclusions: Different types of risk perceptions are associated with personal and household experience with COVID-19 and with the length and severity of symptoms. Understanding these associations could inform efforts to improve mitigation behaviors for COVID-19 and infectious disease more generally.	AK Small, WM Klein, A Kaufman, R Ferrer, CE Matthew, D Berrigan	2023	SOCIAL
2023-277	Favour	O	Nwagugo	NCI	Cancer Biology	Exploring Immune Infiltration in Triple Negative Breast Cancer: Spatial Analysis of 3D Tumor Microenvironment for Therapeutic Insights	Clinically, most diagnoses of cancer are based upon biopsies sectioned into thin 2D slices and analyzed by pathologists. These slices provide information about pathology and specific biomarkers, but not the spatial organization of the 3D tumor microenvironment. Since tumors are heterogeneous, thin sections may fail to capture important spatial information crucial for selecting therapeutic approaches. In this study, we use the 4T1 mouse model, which mimics human triple negative breast cancer, which is notoriously hard to treat. The tumor microenvironment of this cancer is not fully understood and is often classified as an “immune desert”. Therefore, analyzing the spatial characteristics of the 3D tumor microenvironment is pivotal in assessing metabolism, oxygenation, nutrient status, and immune cell infiltration, all important for predicting patient outcomes. We hypothesize that increasing immune cell entry into “immune deserts” could improve patient outcomes. In the 4T1 mouse model, we studied the effects of different treatments on immune cell infiltration. Tumors from untreated and treated mice were collected, fixed, and sectioned into 200㎛ slices, immuno-stained, cleared and imaged using confocal microscopy. This enabled measurement of distances between the cytotoxic T cells (CD8+ cells) and cancer cells with damaged DNA. The increased number of CD8+ cells in the tumor during treatment suggests enhanced immune cell entry into the tumor, indicating stronger immune response. Future investigations will explore drug therapies impacting the immune response after treatment.	FO Nwagugo, V Magidson, SW Feng, KE Delas Peñas, L Ridnour, D Wink, RJ Kinders, J Rittscher, SJ Lockett, DA Scheiblin	2023	CANCER
2023-278	Kaustubh		Wagh	NCI	Chromosome Biology	Dynamic switching of transcriptional regulators between two distinct low-mobility chromatin states	Transcription factors (TFs) scan the nucleus in search of their consensus binding motifs located within enhancers or promoter-proximal regions. The mechanism by which TFs navigate the complex nuclear environment to assemble the transcriptional machinery at specific genomic loci remains elusive. Technological advances over the past 20 years have enabled us to follow single TF molecules within live cells as they interact with chromatin. Using single-molecule tracking, coupled with machine learning, we developed a framework to study the mobility of chromatin and transcriptional regulators within the nucleus. We show that histone H2B and multiple chromatin-bound transcriptional regulators display two distinct low-mobility states. Ligand activation results in a dramatic increase in the propensity of steroid receptors to bind in the lowest mobility state. Mutational analysis revealed that interactions with chromatin in the lowest mobility state require an intact DNA-binding domain as well as oligomerization domains. Importantly, these states are not spatially separated as previously believed but in fact, individual chromatin-bound TF molecules can switch between two dynamic chromatin polymer states (marked by H2B) on timescales of seconds. Single bound-TF molecules with different mobilities exhibit different dwell time distributions, suggesting that the mobility of TFs is intimately coupled with their binding dynamics. Together, our results identify two unique and distinct low-mobility states that appear to represent common pathways for transcription activation in mammalian cells.	K Wagh, DA Stavreva, RAM Jensen, V Paakinaho, G Fettweis, RL Schiltz, S Mandrup, DM Presman, A Upadhyaya, GL Hager	2023	CHROM
2023-279	Elias		Carvalho Padilha	NCATS	Chemical Biology	Metabolism of DHED In Vitro and In Vivo to Support Drug Optimization	DHED (10β,17β-dihydroxyestra-1,4-dien-3-one) is a prodrug of 17β-estradiol which selectively releases 17β-estradiol within the central nervous system. DHED has been demonstrated to have neuroprotective and antidepressant effects in animal models, without peripheral estrogenic effects. However, when the pharmacokinetics of DHED were examined in mice, a high clearance was observed and the vast majority of the prodrug was metabolized into unknown non-17β-estradiol products. This study aims to investigate the cause of the observed high clearance of DHED in PK studies. Studies using liver microsomal fractions, hepatocytes, and in vivo analysis of PK samples were used to fil the knowledge gaps in the metabolism of DHED. The metabolite profiles of the compound in these different systems were analyzed using LC-UV-HRMS on a Synapt G2 TOF system. We found that although minimal turnover occurred in liver microsomes, clearance was extensive in human and mouse hepatocytes, resulting in a major metabolite in human hepatocytes, the dehydrogenated metabolite M286. The formation of M286 is likely attributed to the olefination of the steroid's B-ring or the oxidation of the 23C-hydroxyl group to a ketone. In mouse PK samples, the metabolite M286 was confirmed as the main metabolite. In conclusion, hepatocytes but not microsomes or cytosols, replicated the DHED rapid in vivo clearance in PK studies and produced the major plasma circulating metabolite. Therefore, to prevent the rapid clearance of DHED in humans, structural modifications should be considered to inhibit the formation of M286 identified in this study.	E Carvalho Padilha, PJ Morris, TD Gould, AQ Wang, I Merchenthaler, P Georgiou, A Postle, X Xu	2023	CHEMBIO
2023-280	Maryam		Hashemian	NHLBI	Epidemiology	Awareness of Heart Failure and Associations with Blood Pressure Management and Self-Efficacy in Women	INTRODUCTION: Heart failure (HF) prevalence is increasing in the U.S and hypertension, which affects ~50% of U.S. adults is the leading cause of HF. Awareness of HF and effective management of hypertension is critical for reducing subsequent HF. OBJECTIVES: Assess HF awareness, its association with adherence to antihypertensive medication, and explore the role of self-efficacy in these relationships. METHODS: Three electronic surveys, distributed to 18,849 women ≥18 years in the U.S. via American Heart Association's Research Goes Red platform, assessed HF awareness, blood pressure management in hypertensive participants, and self-efficacy in diabetic and/or hypertensive participants. HF awareness scores were calculated. RESULTS: 2,320 women took the HF awareness survey, 678 the blood pressure management survey, and 755 the self-efficacy survey. Participants were predominantly Non-Hispanic White (80%), median age 51 (IQR: 39, 62), 39% had hypertension and/or diabetes. Mean HF awareness score was 4.4/5 (SD: 0.8). Respondents with high (vs low) HF awareness were older ($p<0.001$), more likely to be Non-Hispanic White ($p<0.001$), and less likely to smoke ($p<0.001$) or have depression ($p=0.03$). Among hypertensive respondents, 89% reported taking prescribed medication, which was not associated with HF awareness or self-efficacy. Respondents with greater (vs lesser) self-efficacy had higher HF awareness score ($p=0.04$), were older ($p=0.01$) and less likely to report depression ($p=0.01$). CONCLUSION: Overall, awareness of HF and adherence to antihypertensive medication were high in this cohort. Depression and younger age may be important factors affecting HF awareness and confidence in managing chronic diseases.	KM Conners, M Hashemian, C Kinzy, JL Hall, C Herr, R Sharma, N Ibrahim, VL Roger	2023	EPIG
2023-281	Miyeon		Jung	NINDS	Cancer Biology	Primary cilia modulate extracellular vesicle-mediated immunosuppression in human glioblastoma cells	Glioblastoma is the most common malignant primary brain tumor. Median survival is 15 months despite surgery, radiation, and chemotherapy. The disease is universally fatal with 5-years survival only 3-5%. Immunotherapy is promising but glioblastoma-mediated immunosuppression remains a barrier. Extracellular vesicles (EVs) comprise a heterogeneous group of small, membrane-bound particles released from all cell types. Tumor-derived EVs induce immunosuppressive myeloid-derived suppressor cells (MDSCs) which in turn inhibit T-cell proliferation and activation. This appears to be a pan-cancer phenomenon which is also active in glioblastomas. Primary cilia are ubiquitous microtubule-based organelles that project from the mother centriole. They are present on glioblastomas and multiple additional cancer cells. We provide evidence that inhibition of glioblastoma ciliogenesis through genetic depletion of KIF3A, IFT88, or ARL13B–structural ciliary proteins necessary for ciliogenesis–reduces MDSCs induction following exposure of normal human monocytes to glioblastoma-derived EVs. Loss of primary cilia also rescues impairment of T-cell proliferation and activation. Biophysical characterization of EVs derived from glioblastoma cells are unchanged following cilia loss. However, LC-MS proteome analysis confirms profound changes in EV content including upregulation of genes and pathways involved in tumor cell death and downregulation of genes and pathways involved in tumor immune regulation. These data suggest a novel role for primary cilia in modulating glioblastoma-mediated immunosuppression and likely, cancer-mediated immunosuppression more broadly. These findings have potential implication for improving the efficacy of immunotherapy in glioblastoma, a universally fatal disease for which this class of therapy remains ineffective.	M Jung, J Trichka, M Oishi, A Agyeman-Andoh, J Welsh, J George, M Laws, A Roehrkasse, J Jones, S Adoro, IF Parney, DA Brown	2023	CANCER
2023-282	Jailyn	M	Izu	NIMH	Immunology	A TBK1 N455S variant in a woman with refractory psychosis and catatonia	Systemic autoimmunity and severe infections are associated with an increased risk of developing a psychotic spectrum disorder. We present a young woman who, three weeks after a high school wilderness retreat, developed subacute psychosis characterized by behavioral disorganization, memory loss, nonsensical speech, mood lability, ritualistic behaviors, and features of catatonia. Three months later, she was diagnosed with Lyme disease (B. burgdorferi) by immunoblot. She was unable to take oral antibiotics due to paranoia and behavioral disorganization. Two months later, a lumbar puncture revealed neuroinflammation indicated by a mild pleocytosis, 16 oligoclonal bands, and an elevated IgG index. Her cerebrospinal fluid (CSF) was negative for infectious encephalitis and paraneoplastic and anti-neural autoantibodies. Blood labs revealed thyroglobulin autoantibodies and subclinical hyperthyroidism. She returned to baseline after intravenous immunoglobulin but relapsed nine months later. She was referred to NIMH where whole genome sequencing identified a heterozygous variant in TANK-binding kinase 1, TBK1 N455S. TBK1 mediates type I interferon production in response to microbial double-stranded RNA and DNA, including B. burgdorferi, and is implicated in autoimmunity. Heterozygous TBK1 variants predispose to herpes simplex encephalitis, frontotemporal dementia, and amyotrophic lateral sclerosis via impairment of kinase activity, homodimerization, protein-protein interactions, TBK1 stability, or autophagy—however TBK1 N455S has not been characterized. Western blotting revealed unaffected TBK1 N455S autophosphorylation but modestly lower expression than wild type TBK1. Additionally, rodent brain tissue staining with her CSF revealed an unclassified anti-glial autoantibody. Studies to assess additional functional consequences of TBK1 N455S and to identify the glial antigen are ongoing.	JI Izu, TT Ngo, SJ Pleasure, MR Wilson, A Nath, CM Bartley, GC Mooneyham	2023	IMMUNO
2023-283	Le		Hoang	NCI	Cell Biology	Effects of Concentration, Timing, and Pattern of Hormone Stimulation on Gene Regulation in vivo Mediated by Estrogen Receptors	Previous studies have established a strong relationship between circadian rhythms and endocrine homeostasis. However, the secretion of many hormones follows both circadian and ultradian patterns. Utilizing the glucocorticoid receptor (GR) as a model system, the impacts of the stimulation patterns of hormones on GR dynamics and downstream gene regulation have been thoroughly examined (Flynn et al. (2018), Stavreva et al. (2019), Stafford et al. (2020)). Building upon the existing knowledge of GR, we employ techniques, including genomics, single molecule tracking (SMT), and high throughput microscopy, to investigate the effects of ultradian and constant hormone stimulation on the mobility of the estrogen receptor (ER) and regulation of ER target genes. We have successfully tagged endogenous ER in MCF7 cells, allowing us to study the spatiotemporal dynamics of ER under estrogen (E2) treatment. Furthermore, we visualized RNA synthesis at both the single-cell and single-promoter levels by using a previously established cell line with 24xMS2 repeats integrated into the 3' UTR of the ER-responsive TFF1gene. Our data revealed that in contrast to GR, E2 hormone fluctuations have much weaker impacts on ER dynamics and no effect on ER-mediated gene responses. This is likely due to the strong ER affinity to E2 and the preservation of the ER-E2 complex even after the depletion of E2 from the growth media. Understanding ER dynamics and its role in gene regulation has the potential to aid in the development of advanced treatment strategies targeting cancers that arise from the dysregulation of ER.	D Stavreva, K Wagh, L Hoang, G Hager, A Upadhyaya, R Chari, L Schiltz	2023	CELLBIO

2023-284	Sofia	A	Nakuchima	NIBIB	Structural Biology	Improved characterization of the Plasmodium falciparum circumsporozoite protein	Malaria is a life-threatening disease that affects a quarter of a billion people each year through the bite of female Anopheles mosquitoes. Currently there are two approved anti-infection vaccines, both contain essentially the carboxyl-terminal half of the Plasmodium falciparum circumsporozoite protein (CSP). In addition, a human monoclonal antibody (mAb) that binds an epitope in the amino-terminal region, not currently in either vaccine, has been shown to passively protect in human clinical trials. Given the partial efficacy of the anti-infection vaccines, we are further investigating the biology, subcellular localization, and structure of the CSP. We previously observed that native CSP, a disordered protein, may undergo structural changes on the surface of infectious sporozoites. Furthermore, efforts to crystallize a near full-length recombinant PfCSP protein, identified as PfCSPM3, using different enriched fractions yielded crystals that unfortunately did not diffract. To pursue a different approach, we have developed a recombinant CSP specific murine mAb with a human Rhinovirus 3C proteolytic site for planned electron microscopy studies. We will initially study PfCSPM3 and subsequently, if possible, native CSP from enriched preparations of whole or fractionated sporozoites. The results from these ongoing efforts will be presented. An improved understanding of native CSP may further support the evaluation of a full-length recombinant CSP malaria vaccine.	A Gittis, RD Leapman, PE Duffy, A Jin, DL Narum	2023	STRUCTBIO
2023-285	Harrison	E	Gichini	NIAID	Clinical Research	Installation and evaluation of the laboratory-grade water filtration system at the Liberia Institute for Biomedical Research Laboratory and its utility in performing FANG ELISA for Ebola virus antibody detection	Partnership for Research on Vaccines and Infectious Diseases in Liberia (PREVAIL) conducts collaborative biomedical and public-health research to advance science, strengthen health policy and practice, and improve the health of Liberians and people worldwide. Performance of clinical research assays to support PREVAIL requires ultra-pure laboratory-grade water, the shipping of which from the United States to Liberia has been affected by supply-chain challenges and has cost up to $115,000 per year. Towards building a sustainable and cost-effective approach, a nonconventional and low-cost water-filtration system was installed at the Liberia Institute for Biomedical Research (LIBR) laboratory to generate laboratory-grade water. Two polymer double-walled 3,000-gallon tanks were installed in a concrete shelter to store water that was purchased from a drinking water company in a nearby town and brought in by water trucks. Electric pressure-boosting water pumps sent water from the tanks to the filtration system, which was fitted with ultraviolet lamps for irradiation treatment. The filtered and irradiated water was distributed to the LIBR laboratory. Within the laboratory, the water was further treated by a Milli-Q purification system. Preliminary results from Filovirus Animal Non-Clinical Group (FANG) Ebola virus immunoassay experiments using each water source yielded comparable results. This work demonstrates that laboratory-grade water can be generated locally in a low-resource setting by installing appropriately designed water-filtration systems, thereby providing a cost-effective and sustainable alternative to shipping water from outside of the country.	HE Gichini, TA Hoeltermann, M Joe, E Towalid, M Chea, Y Quiawiah, M Kopah, L Marron, M Gboue, B Dighero-Kemp, J Kuhn, P Chandrasekaran, IB Maljkovic	2023	CLINICAL
2023-286	Paniz		Rezvan Sangsari	NIBIB	Biomedical Engineering and Biophysics	Microfabrication for Biomedical Research	The use of microfabricated and microfluidic structures in biomedical research continues to expand, but many research applications for these devices require customization, and new applications typically require several design iterations for troubleshooting and optimization. These devices, with length scales ranging from a few microns to a few millimeters, can be particularly useful for controlling cellular environments, either for improved culture models, mechanistic studies, or downstream analysis. We describe our collaborative process in designing, making, and using these structures with an example project, and then discuss in detail a few other examples, including the development of a high-density axonal isolation culture chamber currently in use by several IRP groups, and microfluidic encapsulation protocols to enable the selective analysis of rare cells using downstream sorting. We will also discuss recent efforts to develop vascular models aimed at understanding the interplay of shear forces and vessel geometry on endothelial cells.	P Rezvan Sangsari, NY Morgan	2023	BIOENG
2023-287	Jasmine		Meltzer	NIAMS	ACI/IRS	The Paranuclear Dot Inhibits Apoptosis in Merkel Cell Carcinoma	Merkel cell carcinoma (MCC) is a rare and aggressive neuroendocrine skin cancer that is caused by either integration of the Merkel cell polyomavirus or UV damage. Due to its rarity, MCC is under-researched and poorly understood. Staining for Cytokeratin 20 and other intermediate filaments in a paranuclear dot pattern is a diagnostic marker for MCC, however the functional significance of these protein aggregates is unknown. We sought to investigate the structure and function of the paranuclear dot in MCC. Using pan-cytokeratin immunostaining, we found that 94% of MCC tumors contained cells with paranuclear dots. There were more dot-positive cells in virus-positive MCC than in virus-negative MCC. Electron microscopy and immunofluorescent staining showed that the paranuclear dot forms around the centrosome of interphase cells. However, the dot disaggregated during mitosis, suggesting a dynamic structure that reforms with each cell division. Interestingly, dot cytokeratins colocalized with FADD, the cytoplasmic mediator of death receptor signaling. Dot-positive MCC cells were resistant to apoptotic induction by FasL and TNF-β, suggesting that FADD is sequestered in the dot. Overexpression of FADD in dot-positive cells resulted in diffuse cytoplasmic localization of FADD and apoptotic cell death. Microtubule modulating drugs disrupted the dot and sensitized cells to TNF-β induced extrinsic apoptosis. Taken together, the paranuclear dot is an aggregate of intermediate filaments that is maintained by microtubules and functionally sequesters FADD to block death receptor-mediated apoptosis. Therefore, anti-cancer drugs that target microtubules may also enhance anti-tumor immune responses in MCC.	JC Meltzer, DJ Reed, J Jarvis, L Collado, T Kellenberger, K Nagashima, F Soheilian, S Vilasi, PW Harms, I Brownell, NT Hill	2023	ACI/IRS
2023-288	Blake		Wilson	NIDDK	Structural Biology	Experimental evidence from time-resolved solid-state NMR for millisecond structural annealing of the ultra-fast folding villin headpiece subdomain HP35 triggered by rapid negative temperature jumps	Protein folding is a complicated structural conversion process which lies at the heart of many biophysical and biological systems of interest. Time-resolved solid-state nuclear magnetic resonance (ssNMR) probes structural conversion processes by first triggering, then taking "snapshots" of structural changes by rapidly freezing after a variable evolution delay. Here we use sub-millisecond negative temperature jumps to trigger folding of the 35-residue villin headpiece subdomain (HP35), an ultra-fast folding protein studied extensively and widely used as a folding benchmark. A specially constructed temperature-jump apparatus utilizing copper capillary tubes anchored to temperature-controlled copper plates first heats HP35 solutions 95 °C, causing unfolding, then rapidly cools solutions to 30 °C in 0.6 ms to trigger folding. After a variable evolution time at 30 °C, HP35 is frozen in ~0.1 ms in a -145 °C isopentane bath. Frozen ensembles are studied using low-temperature ssNMR enhanced with dynamic nuclear polarization (DNP). 1D and 2D ssNMR spectra acquired as a function of the variable evolution time show signals consistent with native secondary structure forming on the sub-millisecond timescale, as expected from previous studies, but crucially provide evidence that full structural order, including the alignment of native sidechain configurations, forms much slower through a millisecond structural annealing process. Time-resolved ssNMR triggered by rapid temperature jumps offers direct access to short-lived structures and complexes and is applicable to diverse biomolecular and biophysical systems, and provides quantitative, atomistic information necessary to characterize this previously unobserved annealing process.	CB Wilson, WM Yau, R Tycko	2023	STRUCTBIO
2023-289	Jongeun		Rhee	NCI	Epidemiology	Serum concentrations of per- and polyfluoroalkyl substances and risk of renal cell carcinoma in the Multiethnic Cohort Study	Per- and polyfluoroalkyl substances (PFAS) are environmentally persistent organic pollutants detectable in the serum of most U.S. adults. We previously reported that serum concentrations of perfluorooctanoate (PFOA), one of the most studied PFAS, were positively associated with risk of renal cell carcinoma (RCC) within the Prostate, Lung, Colorectal and Ovarian (PLCO) Cancer Screening Trial, comprising predominantly White individuals. To extend our investigations to a larger and more racially and ethnically diverse population, we conducted a nested case-control study of pre-diagnostic serum concentrations of nine PFAS and RCC (428 cases, 428 individually matched controls) within the Multiethnic Cohort Study. We estimated odds ratios (ORs) and 95% confidence intervals (CIs) for risk of RCC related to each PFAS using multivariable conditional logistic regression. PFOA was not associated with RCC risk overall [doubling in serum concentration, ORcontinuous=0.89 (95%CI=0.67,1.18)]. However, we observed a suggestive positive association among White participants [2.12 (0.87,5.18)]. Furthermore, higher perfluorononanoate (PFNA) concentration was associated with increased risk of RCC overall [fourth vs. first quartile, OR=1.84 (0.97,3.50), Ptrend=0.04; ORcontinuous=1.29 (0.97,1.71)], with the strongest association observed among African American participants [ORcontinuous=3.69 (1.33,10.25)], followed by Native Hawaiian [2.24 (0.70,7.19)] and White [1.98 (0.92,4.25)] participants. While PFOA was not associated with RCC risk overall, the positive association observed among White participants is consistent with previous PLCO findings. Our study provided new evidence of a positive association between PFNA and RCC risk that was strongest in African American participants. Additional investigations of PFAS exposures and RCC in large racially and ethnically diverse populations are needed.	J Rhee, VC Chang, I Cheng, AM Calafat, JC Botelho, JJ Shearer, JN Sampson, VW Sfetiawan, LR Wilkens, DT Silverman, MP Purdue, JN Hofmann	2023	EPIG
2023-290	Benjamin		Chimukangara	CC	RNA Biology	Characterization of gene expression by single-cell transcriptomics during Pneumocystis infection in immunocompetent mice	Pneumocystis is an opportunistic fungal pathogen that causes asymptomatic infection in immunocompetent hosts but life-threatening pneumonia (PCP) in immunosuppressed hosts. Understanding immune mechanisms by which Pneumocystis is cleared will give valuable insights into strategies for reducing risk of PCP. We used a co-housing exposure model of mouse Pneumocystis infection to determine gene expression levels of host cells from the lungs of immunocompetent (C57BL/6) mice. We applied single-cell RNA sequencing combined with flow cytometry, qPCR, ELISA, and pathway analyses, to better characterize host immune responses during infection. We observed a peak in Pneumocystis organism load at day 35 post-infection. All infected mice cleared Pneumocystis and developed anti-Pneumocystis antibodies. CD4+ T cells increased at days 35 and 42 post-infection, primarily involving Th1-effector cells during clearance. An IFN-γ centered cytokine signaling pathway was identified at peak of infection. The top differentially expressed genes in infected mice included pro-inflammatory cytokines IL-21 and CXCL9, co-stimulatory molecule Ox-40 (CD134), and regulatory genes CTLA4, LY6A, and IRF4. These data support a CD4 Th1 cell-driven response in immunocompetent hosts and suggest that a regulated IFN-γ-rich milieu is necessary to enhance phagocytosis of Pneumocystis organisms by macrophages, leading to efficient clearance of Pneumocystis without the development of severe symptoms. More research on the roles of B cells, epithelial cells, and endothelial cells will help to further elucidate the diverse host-pathogen interactions required to prevent PCP in immunosuppressed hosts.	B Chimukangara, S Curran, L Bishop, X Li, W Chang, O Cisse, L Ma, J Kovacs	2023	RNA
2023-291	Shantelle	A	Graff	NINDS	Clinical Research	Comparison of Manual and Automated Methods for Measuring Syrinx Volume	Neurosurgeons assess syrinx reduction after surgery using MRI. Manual syrinx volume measurement is laborious. Semiautomated syrinx volume measurement is faster and may be accurate enough to detect surgically-related syrinx volume reductions reliably. We analyzed pre- and post-operative SPGR axial MRI scans from syringomyelia patients using the manual Cavalieri method (CAV) (n=15) and two semiautomated methods: Spinal Cord Analysis Tool, SCAT (n=15) and 3DQI (n=8). Pre- and post-operative spinal cord and syrinx volumes were compared using the paired t-test. Syrinx volumes (mm3) were significantly larger before (pre) than after surgery (post) across all methods. CAV syrinx volume was: pre, 4515 mm3 ± 3720, post, 1109 mm3 ± 1469 (p=0.0004). SCAT syrinx volume was, pre, 4584 mm3 ± 3826, post, 1064 mm3 ± 1465 (p=0.0014), and 3DQI was, pre, 3540 mm3 ± 2666, post, 751 mm3 ± 810 (p=0.008). CAV detected fluid in irregular, discontinuous, and narrow syringes. Spinal cord volumes were CAV, pre, 13342 mm3 ± 6198, post 8721 mm3 ± 3389 (p=0.0002). SCAT, pre, 11290 mm3 ± 5727, post, 7530 mm3 ± 3210 (p=0.0009), and 3DQI, pre, 11888 mm3 ± 6108, post, 7873 mm3 ± 3785 (p=0.031). Mean spinal cord volumes measured before operation (pre) differed significantly: CAV and SCAT (p=0.003), paired t-test); CAV and 3DQI (p=0.01). Likewise, mean spinal cord volumes after operation (post) also differed significantly (CAV vs. SCAT, p=6.5E-05; CAV vs. 3DQI, p=0.01). The semiautomated methods, SCAT and 3DQI, provided acceptably-precise syrinx volume measurements in less time than the manual method.	EA Kohut, SA Graff, SH Wakelin, M Arhin, G Bhagavatheeshwaran, JD Heiss	2023	CLINICAL
2023-292	Sitanshu	S	Singh	NCI	Immunology	Cyclization and fatty acid derivatization of CD206 activating peptide RP-182 improves anti-tumor function via effective targeting of CD206high M2-like macrophages	Many immunologically cold, solid organ cancers attract and reeducate innate immune cells to promote tumor growth and cancer progression. Tumor-associated macrophages (TAMs) have been increasingly recognized as a de novo target in the field of cancer immunotherapy. Our group has previously shown that targeting the mannose receptor CD206 expressed on tumor-promoting TAMs with the synthetic peptide RP-182 reinvigorates innate and adaptive immune responses for effective tumor control and improved outcome in human and murine preclinical models of cancer. However, due to the linear, unprotected nature of RP-182, it is notoriously prone to enzymatic degradation, and thus not a clinical drug candidate. Here, we designed and synthesized a series of RP-182 derivatives to improve its stability and possibly enhance biological activity. Out of 20 peptide derivatives, three peptides, NCGC00857950, a cyclic analog, NCGC00857001, connecting a lysine-coupled palmitic acid tail, and NCGC00591015 carrying a 10-carbon acyl group, were found to be 5- to 10-fold more potent in cell-based assays than parent peptide RP-182. Liver microsomal study and MetID studies confirmed improved stability, reduced metabolism, and improved pharmacokinetics profiles compared to the parent RP-182. These analogs were further investigated for the induction of apoptosis in CD206high TAMs, TAM reprogramming, reprogramming of the TME, and tumor control. We found that these analogs effectively shifted M2-like TAMs towards a pro-inflammatory phenotype, increased innate and adaptive anti-tumor immunity, and mediated anti-tumor activity in the preclinical model. In particular, the most active, NCGC00857001 appears to be a promising candidate for further preclinical development and clinical translation.	SS SINGH, R CALVO, A KUMARI, D TAO, RV SABLE, E KHLUDENEV, M HENDERSON, J MARUGAN, U RUDLOFF	2023	IMMUNO
2023-293	Mary		Czech	NIAID	Microbiology and Infectious Diseases	Clinical significance and antifungal susceptibility profile of 103 clinical Scedosporium species complex and Lomentospora prolificans isolated from NIH hospitalized patients	Scedosporium species and Lomentospora have been increasingly recognized as emerging opportunists affecting immunocompromised patients. Reduced susceptibility to systemic antifungals is common, and optimal treatments are incompletely described. 103 clinical isolates from NIH were investigated. The identity of each isolate was confirmed at the species level via PCR-sequencing of internal transcribed spacer (ITS) of the ribosomal DNA (rDNA) region and the calmodulin gene. Antifungal susceptibility testing was conducted in accordance with the CLSI M38-A3 guidelines. Patient data were collected retrospectively. The most frequent species were Scedosporium apiospermum, Scedosporium boydii, and Lomentospora prolificans. The novel antifungal olorofim showed the lowest MICs against all Scedosporium and L. prolificans, followed by micafungin. Among triazoles, voriconazole (VRC) showed lower MIC values against clinical members of Scedosporium. Amphotericin and posaconazole (POS) demonstrated species-specific and inter-species variable activity. Itraconazole, isavuconazole, and terbinafine had high MICs against Scedosporium and L. prolificans. Clinical data were available for 90 isolates. 9 patients (28 isolates) had disease or infection. All but one case occurred in immunocompromised hosts, and all patients were treated with a regimen that included VRC or POS. Five patients died. 24 patients (62 isolates) had colonization, of which 58 isolates reflected respiratory colonization in patients with bronchiectasis. Our data support that species-specific and inter-species differences exist in the distribution of antifungal susceptibility patterns among Scedosporium and L. prolificans. Olorofim may be a promising therapy for Scedosporium and L. prolificans. Host status, in conjunction with effective antifungal therapy, is an important determinant in treatment outcomes.	MM Czech, F Stock, CI Aneke, M Lionakis, J Cuellar-Rodriguez, A Seyedmousavi	2023	MICROBIO

2023-294	Faith	S	Davis	NIDDK	Clinical Research	Increased predicted risk for fatal/non-fatal cardiac events in youth-onset type 2 diabetes	Youth-onset type 2 diabetes (YT2D) is associated with traditional markers of cardiovascular disease (CVD), but the relative risk for fatal/non-fatal cardiac events in YT2D compared to their peers is unknown. Our objectives were to quantify CVD risk in youth and young adults (YYA) to inform primary prevention efforts in YT2D. Risk for fatal/non-fatal cardiac events were calculated in a pooled cohort analysis of 146 YYA, including 112 YYA<20y (15.8 (15.4-16.3y), mean (95% CI)) and 34 25y≥YYA≥20y (22.2 (21.6-22.8y)). The i3C 35-year combined risk z-score was used for YYA<20y. The ASCVD Lifetime and Framingham Lipid and BMI 30-year risk scores were used for YYA≥20 years. High sensitivity C-reactive protein (hsCRP) was measured as a CVD risk biomarker. ANOVA models with Bonferroni corrections were used to compare groups. YT2D had higher HbA1c and BMI, with no differences by age category. All YYA with YT2D had 3-fold higher hsCRP, and higher i3C z-score (YT2D: 0.52 (0.38-0.66); OW/OB: 0.20 (0.0-0.41); Lean: -0.53 (-0.78--0.27), P<0.01), ASCVD Lifetime risk score (YT2D: 50 (44-57%); OW/OB: 28 (12-37%); Lean: 26 (10-40%), P<0.01), Framingham BMI risk score (YT2D: 15 (11-19%); OW/OB: 5 (4-6%); Lean: 4 (2-5%), P<0.01), Framingham lipid risk score (YT2D: 10 (7-13%); OW/OB: 4 (3-6%); Lean: 4 (2-5%), P<0.01) compared to OW/OB and Lean. Youth/young adults with YT2D are predicted to have at least twice the lifetime or 30-year risk for fatal/non-fatal cardiac events compared to age-matched peers with OW/OB or normal weight. Future studies are needed to verify predicted risk, especially in the YYA population.	FS Davis, SA Dixon, A Chowdhury, AM Krenek, NL Sala, L Mabundo, ST Chung	2023	CLINICAL
2023-295	Belmaliz		Cardona	NIDCR	Immunology	Oral mucosa dissociation protocols for targeting fibroblasts	Periodontitis is one of the most common diseases associated with the oral cavity resulting in mucosal inflammation and bone loss. It has been shown that immune cells such as neutrophils play pathogenic roles in periodontitis, however, we do not know the role of non-immune cells. Our lab recently published scRNAseq data in humans showing that stromal cells may recruit neutrophils to the oral mucosa leading to inflammation. Oral fibroblasts play an important role in wound healing and tissue repair in the gingival connective tissue. During further studies of oral fibroblasts in mice, we discovered that the enzyme selection for tissue dissociation influences the amount of fibroblasts recovered. In this current study, we compared three different tissue dissociation methods: collagenase Ⅳ, collagenase Ⅱ and enzymes in Miltenyi Whole skin dissociation kit in the process of oral mucosal tissue dissociation to obtain fibroblasts as single cells. We evaluated fibroblasts using flow cytometry by cell surface markers. There were significant differences in the viabilities and fibroblasts proportions between the methods. We conclude using collagenase Ⅱ is the best dissociation method to obtain high viability and amount of fibroblasts from oral mucosa.	B Cardona, R Akhi, N Moutsopoulos, T Ikeuchi	2023	IMMUNO
2023-296	Philip	P	Adams	NICHD	ACI/IRS	Transcriptome mapping: discovering regulation in the Lyme pathogen	All steps in gene expression – transcription, RNA processing, translation, and protein turnover – determine the ability of a cell to survive. Thus, they are highly regulated in all domains of life. While these regulatory mechanisms have been studied extensively in multiple model systems, such as Escherichia coli and Bacillus subtilis, much less is known about these processes in other important organisms, such as bacterial pathogens. For example, the fundamental aspects of gene expression have not been studied extensively in the spirochete Borrelia (Borreliella) burgdorferi, the etiological agent of Lyme disease – the foremost vector-borne illness in the United States. The bacterium exists in a complex enzootic cycle that requires acquisition and transmission of B. burgdorferi between Ixodes scapularis ticks and small vertebrates. The Adams lab studies the basic biology and molecular mechanisms of B. burgdorferi infectivity, to ultimately better diagnose and treat Lyme disease.	M Zamba-Campero, D Tetreault, E Petroni, D Soliman, J Silberman, R Fishman, P Adams	2023	ACI/IRS
2023-297	Pranav		Narnur	NIMH	Neuroscience	Inference of neural cell-cell communication networks using single-cell RNA sequencing data	Background: Cell-cell communication (CCC) coordinates brain activity through interactions between ligands and receptors. A recently developed method named CellChat used both single-cell RNA-sequencing (scRNA-seq) and a curated database of ligand-receptor pairs to infer CCC networks. However, applying this method to infer nervous system signaling is currently limited due to a lack of neural pathways in the CellChat database. Methods: We curated a database of 207 neural ligand-receptor pairs, along with their cofactors and co-receptors, for both humans and mice using KEGG, Ingenuity pathway analysis, and literature review. We tested our database by applying CellChat on scRNA-seq data of adult mouse neocortex (ALM and VISp) obtained by the Allen Brain Institute to infer cell-type specific communication networks. We compared our predicted networks to known molecular interactions between cell types. Results: CellChat predicted the following interactions in both the ALM and VISp: 1) neuregulin-ERBB signaling from Cajal-Retzius cells onto Pvalb+ chandelier and basket cells; 2) cholecystokinin signaling from Sncg+ interneurons onto layer 6b glutamatergic neurons; and 3) oxytocin signaling from L2/3 intratelencephalic neurons onto Sst+ interneurons. Previous studies support the predicted cholecystokinin network, but not the dominant sender statuses of Cajal-Retzius cells within neuregulin signaling or that of L2/3 neurons within oxytocin signaling. Conclusion: Our curated database extends RNA-based inference of cell-cell communication to predicting neural signaling across cell classes and can identify known cell-cell interactions in the mouse brain. We plan to extend these studies to examine whether these same cell-cell communication patterns are conserved in humans.	P Narnur, D Kim, A Schulmann, PK Auluck, S Marenco	2023	NEURO
2023-298	Kenneth		Canubas	NCI	Clinical Research	Tumor immune microenvironment (TIME) characterization of prostate cancer bone metastasis may guide future immunotherapies	Background: Prostate cancer (PCa) is the most common malignancy among men in the US.1 PCa is considered a cold tumor because immune cells (IC) are suppressed. PCa can spread to bone (bone metastasis, or "mets"). To design immunotherapies that target PCa bone mets, it is important to characterize their TIME. Methods: We procured bone mets tissue samples (n=13) from 9 patients with castration-resistant PCa. EDTA was used to optimally preserve bone tissue. Adjacent FFPE bone mets were stained using 3 validated multiplex immunofluorescence panels and opal technology. We identified the lymphocytes (CD4+ and CD8+ T cells), tumor-associated macrophages (M1 and M2), and myeloid-derived suppressor cells (M-MDSCs and PMN-MDSCs) infiltrating the bone mets. Densities of these cells were calculated per mm2 of the analytes. Results: In all PCa bone mets samples, suppression of ICs was apparent. On average, M2 macrophages, important pro-metastatic cells, were almost 4-fold and 52-fold greater than CD8+ and CD4+ T cells, respectively. M2:M1 macrophage ratio was 1.44. PMN-MDSC and M-MDSC were 38 and 9, respectively. HLA-DR– expression was 27-fold greater than HLA-DR+. HLA class I will be examined in future endeavors. Conclusion: Our data agree with previous studies about the immune-excluded TIME of PCa. HLA-DR–, MDSCs, and M2 macrophage predominance over T lymphocytes promotes IC suppression. Thus, there is agreement that targeting M2 macrophages and promoting M2 to M1 polarization may control PCa bone mets. 1. Siegel, R., Miller, K., Wagle, N., Jemal, A. Cancer statistics, 2023. CA: A Cancer Journal for Clinicians. 2023; 73: 17–48.	K Canubas, M Xu, WK Kelly, J Marte, HA Sater, JL Gulley, W Lassoued	2023	CLINICAL
2023-299	Yunna		Kwan	NIMH	Epidemiology	The structure of mania symptoms in a community-based samples of adults and adolescents: Associations with clinical severity, suicide attempts, comorbid disorders, and service use	There is now compelling evidence that bipolar disorder can begin in childhood and adolescence, particularly among offspring of parents with bipolar disorder. Therefore, prevention of the consequences of bipolar disorder including the development of substance use disorders, physical morbidity and suicide attempts is paramount. However, many youths with emerging symptoms of mania and depression are not detected because they fail to manifest the full clinical syndrome. Here we examine the symptom structure of mania and depression in adults and youth and their developmental specific correlates in from two large scale U.S. nationally representative sample of adults and youth over age 12. Latent class analysis of mania symptoms yielded four classes that represented the full clinical syndrome in both adults and youth, as well as two subthreshold classes characterized by the salience of attention/ distractibility on the one hand, and behavioral symptoms with motor activity and energy changes on the other. There was remarkable similarity of profiles in youth and adults, with changes in motor activity as the most common manifestation of mania across the lifespan. Youth were much less likely to exhibit consequences of the conditions and sleep disturbances than adults. The underlying classes were better characterized by the nature of the rather than the number of the mania symptoms. These findings have important implications for identifying early manifestations of bipolar disorder in adolescents and young adults that could reduce the risk of serious lifetime consequences of this condition.	Y Kwan, L Cui, K R Merikangas	2023	EPIG
2023-300	Kimia	N	Shamsian	NCATS	RNA Biology	A genome-wide siRNA screen for regulators of EWSR1 in Ewing Sarcoma	Chromosomal translocations in the EWSR1 locus and a second breakpoint, are known as the initiating mutation and catalyst for several cancer types. Ewing Sarcoma (EWS), a soft tissue and bone cancer, is a cancer that is associated with rearrangements between the EWSR1 gene and a gene from the ETS DNA binding proteins. Treatments for EWS include harmful and general methods like surgery, radiation, and chemotherapy and, unfortunately, investigations into more targeted treatments have not proven fruitful. Therefore, to target the EWSR1-fusion-driven cancers more efficiently, we conducted RNAi screens aimed at identifying regulators of the EWSR1 gene, with future aims to conduct a similar screen for the EWSR1-fusion oncoprotein. To accomplish this, our team utilized CRISPR-Cas9 gene editing to create a TC32 cell line containing the EWSR1 gene tagged with a HiBiT luminescence reporter. With the cell line, we validated our negative, positive, and biological siRNA controls, and then optimized three assay parameters: the TC32 cell number, lipid transfection reagent concentration, and incubation time point. Then, we conducted the genome-wide RNAi screen in a 384-well arrayed format. From our analysis of the luminescence readings, we found genes that when silenced could effectively downregulate or upregulate EWSR1 expression. Our results suggest that these gene hits could be utilized as effective regulators of EWSR1 and therapeutic targets of EWSR1-driven cancers.	KN Shamsian, S Lin, SS Rajan, NJ Caplen, KC Cheng	2023	RNA
2023-301	Igor		Shats	NIEHS	Virology	Development of a novel anti-coronaviral lead compound UNC7844	Although several drugs and vaccines targeting viral proteins have been deployed against SARS-CoV-2 continued emergence of new variants will likely lead to rapid development of resistance to these therapeutics. An alternative approach is to target host mechanisms essential for the viral life cycle. Here we describe the development of a new anti-viral lead compound, UNC7844, which targets multiple host pathways. UNC7844 inhibits replication of several coronavirus types by more than four orders of magnitude in different cell lines in a low micromolar range. This compound also significantly inhibits liver infection in mice infected with MHV accompanied by reduced expression of inflammatory and fibrosis genes. Preliminary data points to potential in-vivo activity against SARS-CoV-2 in ACE2-expressing mice. Kinetics analysis and time of addition assays revealed that UNC7844 inhibits early phases of viral life cycle between viral entry and replication. UNC7844 inhibits several kinases in the inositol (pyro)phosphate pathway, including IP6K and IPMK, in a low nanomolar range. Overexpression of IPMK in IPMK KO cells elevated viral RNA levels of 229E coronavirus demonstrating a positive role of this kinase in viral replication. Specific IPMK and IP6K inhibitors brought the levels of MHV RNA in IPMK-overexpressing cells to those found in IPMK KO cells. However, UNC7844 exhibits superior inhibition of viral replication, suggesting its mechanisms of antiviral action include additional targets. In summary, our work identifies a novel role of inositol phosphate kinases in coronavirus replication and discloses a new lead compound for targeting host processes involved in viral replication.	I Shats, H Wang, Y Zhou, C Gu, R Blind, X Wang, X Li	2023	VIROL
2023-302	Lindsay	S	Farr	NCI	Virology	Neutral Sphingomyelinase 2 Required for HIV-1 Maturation: Selecting for Resistance	HIV-1 assembly occurs at specific membrane microdomains of the plasma membrane (PM) called lipid rafts, regions typically high in cholesterol, sphingomyelin, and ceramide. Sphingomyelinases (SMases) are key enzymes that produce ceramide through the hydrolysis of sphingomyelin. Neutral sphingomyelinase 2 (nSMase2) is the primary sphingomyelinase in mammalian cells that generates ceramide at the PM. In our recent study, we have shown that inhibition of nSMase2 via either a highly potent and selective inhibitor, phenyl(R)-(1-(3-(3,4-dimethoxyphenyl)-2,6-dimethylimidazo[1,2-b] pyridazin-8-yl)pyrrolidin-3-yl)carbamate (PDDC), or siRNA knockdown disrupts HIV-1 Gag and GagPol polyprotein processing, thereby inhibiting maturation and infectivity of viral particles (Waheed et al., PNAS 2023). However, the precise mechanism by which nSMase2 inhibition affects viral protein processing and maturation remains unknown. To elucidate the mechanism of action of PDDC we passaged HIV-1 in immortalized T cell lines under suboptimal concentrations of PDDC. We were able to select for and identify mutations in the HIV-1 structural proteins and enzymes that confer partial resistance to the nSMase2 inhibitor. This PDDC resistance was confirmed in single-cycle HIV-1 infectivity and viral replication assays. By elucidating the mechanism of viral escape, we will shed light on the role of nSMase2 in HIV-1 maturation.	LS Farr, AA Waheed, EL Agostino, L Naing, B Slusher, N Haughey, EO Freed	2023	VIROL
2023-303	Pinaki		Bhattacharjee	NIAAA	Molecular Pharmacology	Design and synthesis of peripherally selective dual CB1R antagonist/iNOS inhibitors for Metabolic disorders	There is a pressing need for innovative therapeutic approaches to the growing global epidemic of obesity. As part of the endocannabinoid system, cannabinoid receptors are involved in a wide range of physiological and pathological processes in the human body. Through a lot of research and development on CB1 and CB2 ligands, different synthetic cannabinoid molecules with different affinities have been found. These molecules may be useful for treating a wide range of disorders. However, few of these ligands have found their way into clinical practice. CB1R inverse agonist Rimonabant became the first-in-class molecule approved in the EU as an anti-obesity drug. However, despite its pronounced therapeutic potential, it was withdrawn from the market in 2008 due to its adverse neuropsychiatric side effects. Literature precedent suggests that peripheral blockade of CB1 receptors retains many metabolic benefits without causing CNS side effects and achieves positive benefits like weight loss, less insulin resistance, and better control of glucose. Our main goal is to make CB1R inhibitors with peripheral restrictions. Radioligand binding and GTPγS functional assays were used to investigate a novel series of peripherally limited CB1R antagonists with a diaryl-pyridazine core and a sulfonamide moiety. Several synthesized analogues demonstrated strong CB1R binding affinities (Ki <10 nM, IC50 <15 nM), confirming in silico studies. Based on our preliminary in vitro and in vivo ADME data, we found many chiral antagonists with nanomolar affinity and selectivity for CB1R and functional antagonists at this receptor that may be able to cure fibrosis, diabetes, and obesity.	P Bhattacharjee, S Dvoracsko, N Rutland, B Kundu, L Johnson, R Cinar, MR Iyer	2023	PHARMA

2023-304	Vandita		Bhat	NIEHS	Stem Cell Biology	Post-transcriptional Control of mouse embryonic stem cell maintenance by Ccr4-Not complex	The Ccr4-Not complex regulates mRNA poly(A)-tail length to influence mRNA stability and/or translation in eukaryotic cells. The complex is formed by NOT and deadenylase modules. Several subunits of the complex have been implicated in various development phenotypes and diseases, alluding to its role in post-transcriptional gene regulation and cell fate decisions. We have previously shown that Ccr4-Not is required for mouse Embryonic Stem Cell (ESC) maintenance. To systematically dissect the function of the complex, we generated conditional deletion ESC lines for subunits in the NOT and deadenylase modules using CRISPR/Cas9 mediated genome editing. We found that individual deletion of the NOT module subunits, or simultaneous deletion of the deadenylases led to ESC differentiation. Mechanistically, NOT subunit deletions resulted in decreased complex stability, while deadenylase deletions led to compromised enzymatic activity. We determined the poly(A)-tail length, half-life, and steady-state abundance of mRNAs in wild-type and Ccr4-Not deletion ESCs. Consistent with the cellular phenotypes, the deletion of subunits that are essential for ESC maintenance increases poly(A)-tail length, half-life, and steady-state level in many mRNAs, especially those from genes involved in development and differentiation. Thus, we propose that Ccr4-Not maintains the ESC fate and prevents pre-mature differentiation by repressing differentiation gene expression via mRNA deadenylation. Further, we speculate that Ccr4-Not-mediated poly(A)-tail length regulation may act as a general post-transcriptional switch during cell fate transitions in development and disease. We will test the hypothesis by further analyzing our genomic datasets and examining the function of Ccr4-Not in other stem cell types and biological contexts.	VD Bhat, Q Chen, B Lackford, G Hu	2023	STEMCELL
2023-305	Ammad		Shaukat	NIEHS	Stem Cell Biology	Distinct role of INO80 complex in the Naïve vs Primed pluripotent state	Pluripotent stem cells (PSCs) can self-renew and differentiate into various cell types. Different pluripotent states corresponding to different developmental stages can be recapitulated in-vitro. Among those, the Naïve and Primed pluripotent states represent two consecutive stages in early embryonic development and are most widely studied. The developmental plasticity of PSCs is attributed to the unique epigenetic features. Of particular interest, the pluripotent chromatin contains regions that are occupied by both the active (H3K4me3) and repressive (H3K27me3) histone marks. These bivalent chromatin domains are enriched at the promoters of key developmental genes, and are crucial for cell fate transitions. Our previous work showed that the INO80 chromatin remodeler is selectively required for the maintenance of the Primed but not the Naïve state. It promotes the occupancy of H2AZ histone variant to facilitate the establishment and maintenance of the bivalent promoters during the Naïve to Primed transition. These results identified a state-specific role of INO80. However, the underlying mechanism remained elusive. We hypothesize that additional factors may contribute to the different functions of INO80 in the Naïve and Primed state. To test that, we tagged INO80 with the TurboID biotin ligase and employed proximity labeling strategy to identify novel INO80-interacting factors in the Naïve vs. Primed state. We observed distinct bands in biotin-labeled proteins purified from the two states and are in the process of identifying them via Mass spectrometry. Further characterization of the identified hits will provide new insights to the function of INO80-mediated chromatin regulation in stem cell fate transitions.	A Shaukat	2023	STEMCELL
2023-306	Lita	A	Freeman	NHLBI	Virology	NAPQI, an acetaminophen metabolite, inhibits the SARS-CoV-2 papain-like protease	We show here that NAPQI, a metabolite of acetaminophen, inhibits the SARS-CoV-2 papain-like protease (PL-Pro). Previous reports show that PL-Pro inhibitors prevent viral spread in model organisms. We hypothesize that OTC medications containing acetaminophen taken early in infection may prevent viral spread. Further study may be warranted.	LA Freeman	2023	VIROL
2023-307	Ben		Alleva	NIDDK	Genetics and Genomics	Development of a methodology for analysis of heritable rearrangements: a case study at the human CYP2D6 locus	Meiosis is the reductional cellular division leading to the formation of gametes. At the onset of meiosis, DNA damage in the form of double strand breaks (DSBs) are both purposefully created and necessary for meiotic completion. DSBs cluster at regions in the genome called hotspots which vary in location between human populations. Meiotic DNA repair canonically uses homologous allelic sequences as a template for repair. However, non-allelic homologous sequences can also act as a template which can lead to genomic rearrangements which can be heritable. Whether the location of DSBs predisposes offspring to genomic rearrangements/disorders is relatively unknown. To test this, we designed two methodologies to analyze rearrangements at the repetitive CYP2D6 locus previously shown to harbour hotspots. CYP2D6 is a target of major clinical importance having a vital function in metabolizing ~25% of all prescription drugs and is highly variable with over 400 annotated alleles including large copy number variations. We examined 144 unrelated individuals and 58 parent-offspring trios and found seven different possible rearrangements at this locus including a novel rearrangement. ~23% of individuals were found to have at least one gross rearrangement, higher than what is described in the literature (~5-12%). In addition, we have an ongoing familial analysis with at least one example of a heritable de novo rearrangement. In summary, we have designed a methodology and analysis pipeline to examine variability which can be implemented to further understand the origins of variation in human genomes.	B Alleva, F Pratto, D Dahiya, RD Camerini-Otero	2023	GEN
2023-308	Abhirami	A	Thaivalappil	NHGRI	Cell Biology	Cell-free DNA as a novel biomarker for disease progression and response to treatment in Hutchinson-Gilford Progeria Syndrome.	Hutchinson-Gilford Progeria Syndrome (HGPS) is a premature aging disorder that affects tissues of mesenchymal origin. Most HGPS individuals harbor a de novo c.1824C>T (p.G608G) mutation in the lamin A (LMNA) gene, which activates a cryptic splice donor site resulting in production of a toxic protein termed “progerin”. Clinical manifestations include growth deficiency, lipodystrophy, cardiovascular defects, and bone dysplasia. Currently lonafarnib, a farnesyltransferase inhibitor, is the only FDA-approved treatment. For development of new therapeutics, a reliable biomarker is needed to demonstrate qualitative or quantitative efficacy of disease progression or treatment response. We have developed a novel liquid biopsy approach to characterize phenotypic progression in two HGPS mouse models, as assessed by plasma concentration of cell-free DNA (cfDNA). With a High Sensitivity DNA chip, we observed elevations of cfDNA in heterozygous and homozygous HGPS mice compared to their age-matched counterparts. Digital droplet PCR (ddPCR) amplification targeting short and long interspersed retrotransposable elements (LINEs/SINEs) within cfDNA extracted from small plasma volumes greatly improved assay sensitivity and provided independent validation of cfDNA trends. Validation of cfDNA levels as a clinical biomarker for therapeutic response was achieved by demonstrating quantitative reductions in plasma LINE and SINE copy number up to 56% in 8-week mice treated in vivo with a locus-specific DNA base editor that corrects the mutation and partially rescues the HGPS phenotype. Thus, plasma cfDNA has the right properties to serve as a reliable biomarker for disease progression and treatment response in HGPS mouse models and can now be tested in human trial samples.	AA Thaivalappil, WA Cabral, UL Tavarez, MR Erdos, FS Collins	2023	CELLBIO
2023-309	Isaac	D	Raplee	NIAID	Virology	Effects of alcohol (EtOH) and Δ9-tetrahydrocannabinol (THC) on early monocyte differentiation: implications for HIV-1 replication	Background. Recreational use of marijuana and/or alcohol can modulate host immune networks in response to pathogens. Previously, we found a selective dose-dependent suppression of ex vivo HIV-1 replication in primary macrophages by THC treatment of monocytes during differentiation. In this study, we investigated the molecular consequences of EtOH or THC with EtOH on gene expression profiles during early monocyte differentiation. Methods. Human peripheral blood monocytes from five healthy donors were exposed ex-vivo to EtOH or THC plus EtOH during differentiation for six hours, one day, or three days. Each treatment and time point mRNA profiles were individually compared to untreated monocytes using microarrays. The limma R package was used for Differential Expression Genes (DEG) analyses. Pathway analyses were completed on DEGs using Qiagen’s Ingenuity Pathways Analysis (IPA). Results. EtOH pathways were associated with proinflammation. THC pathways were associated with the regulation of immune activation. Through time EtOH and THC treatments shifted monocyte profiles toward metabolic pathways. By day 3, EtOH treatments no longer perturbed proinflammatory pathways in monocytes, while THC treatments continued to regulate or inhibit the monocyte immune activation pathway profile. Conclusions. EtOH exerts a proinflammatory effect on monocyte gene expression that gradually decreases over time. THC ameliorates the proinflammatory effects of EtOH. Furthermore, THC inhibits immune activation pathways at all time points. Furthermore, THC modifies the immune activation landscape to diminish HIV-1 replication in cells of the monocyte lineage. These ex vivo approaches inform discovery of the complex interactions between substance use, immune function, and HIV-1 replication.	ID Raplee, K Chang, S Appelberg, J Williams, J Salesman, M Goodenow	2023	VIROL
2023-310	Khun Zaw		Latt	NIDDK	Cell Biology	Gene expression profile in an interferon-exposed APOL1 high-risk transgenic mouse resembles expression profiles in urinary podocytes from subjects with APOL1 high-risk genotype	Coding genetic variants in apolipoprotein-L1 (APOL1) include APOL1-G0 (low-risk) and APOL1-G1, APOL1-G2 (high-risk) genotypes. A 13% of African-Americans (estimated six million individuals) carry two APOL1 risk variants and are at substantially increased risk for chronic kidney disease, including focal segmental glomerulosclerosis (FSGS) and arterionephrosclerosis. Although cellular effects of the APOL1 variants have been studied extensively in vitro, their effects on podocytes have not been characterized ex vivo at the single-cell resolution. Bacterial artificial chromosome (BAC)/APOL1 transgenic mice were administered retro-orbitally a single dose of interferon gamma to increase APOL1 expression. Mice were euthanized 24 hours later. Single-nucleus RNA sequencing was performed using isolated glomeruli from wild-type and BAC/APOL1-G0 and -G1 mice. Data from three mouse kidney glomerular samples (one from each genotype) showed three podocyte clusters reflecting healthy, mild injury and severe injury states. The cluster showing severe injury had the highest APOL1 expression. This cluster had high expression of genes related to epithelial-mesenchymal transition. Further, APOL1-G1-specific genes from the severe injury cluster were also more highly expressed in human FSGS APOL1 high-risk urinary podocytes, compared to low-risk urinary podocytes. In conclusion, following interferon gamma administration to BAC/APOL1 mice and prior to the appearance of glomerulosclerosis, we observed a unique gene expression profile in APOL1-G1 risk allele mice compared to APOL1-G0 mice. A similar gene expression profile was observed in APOL1 high-risk human urinary podocytes. This study identified an early signature of APOL1-G1 risk allele-mediated podocyte injury.	K Latt, T Yoshida, S Shrivastav, J Heymann, Y Zhao, AZ Rosenberg, CA Winkler, JB Kopp	2023	CELLBIO
2023-311	Kayla		Amini	NIAID	Immunology	Generation of thymic epithelial progenitor cells from induced pluripotent stem cells obtained from patients with thymic defects	Thymic epithelial cells (TECs) play a critical role in T-cell development as they provide essential cues to hematopoietic progenitors for proliferation and differentiation in the thymus. Patients with genetic mutations affecting TEC functionality present with reduced thymus development and decreased T-cell output in the periphery. We have reported that T-cell development is blocked in patients with hematopoietic-intrinsic genetic defects using an artificial thymic organoid system, but this model does not consider TEC defects. To address this, we have generated multiple induced pluripotent stem cell (iPSC) lines from patients carrying mutations on genes involved in thymic stromal development and/or function, including 22q11.2del (DiGeorge syndrome), CHD7, FOXI3, PAX1, AIRE, EXTL3, and TP63. We aim to differentiate these iPS lines into TECs and assess whether these mutations alter TEC generation. We are currently testing published protocols. However, most of these protocols focused on generating TECs from embryonic stem cells and were not optimized for human iPSCs. To address this, we are utilizing different methods to achieve a high efficiency in inducing definitive endoderm (DE), ventral pharyngeal endoderm (VPE) and finally thymic epithelial progenitors (TEP). We have already successfully reached the DE stage, as gene expression analysis by qPCR shows upregulation of genes associated with the DE and downregulation of iPS genes. Once we successfully generate TECs, we plan to incorporate them into our artificial thymic organoid system to create a model that will be solely based on human cells, obtaining a more accurate in vitro reflection of human thymic T cell development.	K Amini, F Pala, M Bosticardo, S Dinges, L Notarangelo	2023	IMMUNO
2023-312	Nicole	Y	Morgan	NIBIB	Biomedical Engineering and Biophysics	Control and characterization of oxygen concentration in tissue culture	The oxygen concentration experienced by cells plays a crucial role in controlling metabolic pathways and determining culture health, yet delivery of oxygen to cells in culture is often poorly characterized. This can have significant impacts on the relevance of culture models to physiological and pathophysiological environments in vivo; for example, hypoxia in cancer is linked to drug resistance and metastasis. Although the ambient atmosphere in which most tissue culture is performed has an oxygen concentration much higher than physiological levels, the microenvironment of the cells typically experiences substantial depletion due to limits of oxygen transport, primarily diffusive, through the media and, in the case of 3D culture, through the surrounding matrix. The balance between source concentration, transport to the cells, and consumption is what determines the intracellular oxygen concentration, which can therefore depend heavily on the density and location of the cultured cells. We will present work on several aspects of this problem: 1) development of a scalable bioreactor system which controls oxygen delivery to 3D culture in a multiwell plate format, using an oxygen permeable membrane with patterned micropillars to mimic a capillary bed; 2) measurement of oxygen concentrations in vitro in cells transfected to express a novel FLIM-FRET probe, which uses the change in myoglobin absorption spectrum induced by oxygen binding to sense intracellular oxygen levels; 3) finite element modeling aimed at understanding the interplay of delivery, transport, and consumption in determining in vitro oxygen concentrations.	HG Tran, MA Kwarteng, AJH Sedlack, AZ Hawa, KA Link, R Penjweini, JR Knutson, M Garmendia-Cedillos, TJ Pohida, RW Robey, MM Gottesman, NY Morgan	2023	BIOENG
2023-313	Yunlong		He	NCI	Research Support Services	The CCR Sequencing Facility Provides Cutting-Edge NGS Service to NCI Community	The Center for Cancer Research Sequencing Facility (CCR-SF) is committed to utilizing high-throughput sequencing technologies across different Next Generation Sequencing (NGS) platforms and applications. At CCR-SF, we apply the highest quality standards to all projects and communicate project status on a regular basis. We also work closely with each investigator from experimental design through data analysis to ensure that the sequencing experiment delivers high-quality data. Recently, we have seen many new sequencing technologies and applications enter the market. At CCR-SF, we are actively testing the newest sequencing technologies and applications available, to ensure that the NCI community can remain at the leading edge of next-generation sequencing technologies. Here we introduce the new applications and sequencing platforms that were launched at CCR-SF recently, which include PIP-Seq Single-Cell RNA-Seq from Fluent Biosciences, Mission Bio Tapestri single-cell multi-omics (DNA+Protein), PacBio MAS-seq, targeted RNA Iso-seq, and whole genome 5-mC and 5-hmC detection and analysis. We also acquired several new instruments, which include the Chromium X high-throughput single cell RNA-seq platform from 10X Genomics, the Illumina short read sequencer NovaSeq X Plus, the PacBio Revio and Oxford Nanopore P24 PromethION long read sequencing systems, as well as the Xdrop Sort for targeted DNA sequencing from Samplix.	Y He, E Schick, C Fromont, JM Caravaca, S Turan, Y Kriga, TW Shen, S Xie, S Choudhari, Y Wu, B Shrestha, Y Zhao, J Shetty, B Tran	2023	RSCHSUPP

2023-314	Verity	J	Ford	CC	Clinical Research	Sepsis Cardiac Edema Related Reversible Injury (SCERRI)	Effects of sepsis on the heart evaluated by Cardiac Magnetic Resonance (CMRs) in a canine model of Staphylococus aureus pneumonia that reproduces the reversible cardiac dysfunction of human septic shock. For 96h a protocol using fluid boluses maintained normal cardiac filling pressures. No exogenous catecholamines were given. Sepsis within 48h after bacterial challenge resulted in a significant increase in LV wall edema of >2-3% on T2 CMR, which could explain the cardiac dysfunction seen during sepsis. Edema was confirmed on histology to be interstitial, affecting both myocytes and endothelial cells. In the first 24h, as cardiac dysfunction increased in septic animals, ventricular chamber size initially decreased in the presence of normal cardiac filling pressures. This suggests that the observed edema might result in a "restrictive-like" cardiomyopathy. From 24-48h cardiac chamber size increased. During this time the ventricular wall thinned along with a significant loss of dry mass (approximately 1 gram/day of tissue). This loss of mass occurred as cardiac function recovered, suggesting that it may represent a reparative remodeling of the heart. Wall thinning might in part explain the increase in ventricular chamber size. Biochemical and histological data suggest that myocytes are relatively preserved. Endothelial cells are next most common cell type in the LV wall, which like myocytes developed edema as seen by electron microscopy. This pattern of cardiac injury as well as mechanisms underlying the reparative process associated with dry mass loss are being actively investigated.	VJ Ford, WN Applefeld, J Wang, J Sun, J Feng, V Sachev, S Sidenko, Z Yu, RL Danner, SB Solomon, MA Solomon, MY Chen, C Natanson	2023	CLINICAL
2023-315	Yugantar		Gera	NIDA	Neuroscience	In vivo labeling and molecular characterization of cocaine memory-specific active neurons using the photo-convertible calcium integrator CaMPARI2	Background: In abstinent drug users, drug-associated cues can provoke craving and relapse long after cessation of drug use. These maladaptive drug-cue associations are encoded in sparse patterns of strongly activated neurons (ensembles). However previous immediate early gene based labeling approaches lack temporal specificity needed to study short behavioral events (e.g, lever press). To address this gap, we developed procedures to label and characterize active neurons in vivo with sub-second temporal specificity using the green-to-red photo-convertible calcium-based activity marker CaMPARI2, and single-nucleus RNA sequencing (snRNAseq). Methods: We expressed CaMPARI2 in infra-limbic cortex (IL) of male and female Sprague-Dawley rats, implanted optical fibers for photo-conversion and inserted jugular catheters for cocaine self-administration. Following self-administration training and 21 abstinence days, we used green-to-red CaMPARI2-photoconversion to permanently label IL cocaine-memory ensembles during a 1-min cocaine-seeking test. We collected brains either immediately after test (0-min group) or waited 10 minutes for experience-induced gene expression (10-min group). We isolated red (active) and green (inactive) CaMPARI2-labeled nuclei and performed snRNAseq. Results: We observed reliable cocaine self-administration during training and robust cue-induced cocaine seeking during the 1-min test. CaMPARI2-snRNAseq revealed distinct clusters of glutamatergic and GABAergic IL neurons that sub-clustered into expected layer and subtypes. Further, IEGs were selectively induced in red neurons from 10-min, but not 0-min group. Discussion: We will identify unique molecular alterations within IL cocaine-memory ensembles and investigate their distribution across IL cell types. Molecular and cell-type characterization of drug-memory ensembles could identify new targets to selectively weaken persistent drug memories and prevent relapse.	Y Gera, KE Savell, OR Drake, MB Brenner, VA Lennon, DQ Pham, SJ Weber, LE Komer, L Wang, K Schaefer, FJ Rubio, A Lemire, ER Schreiter, V Menon, BT Hope, R Madangopal	2023	NEURO
2023-316	Aleah	L	Eschman	NIAID	Microbiology and Infectious Diseases	Absence of Alpha-gal IgE Response in Humans Exposed to Larval Ixodes scapularis Tick Bites	Alpha-gal syndrome (AGS), also known as red meat allergy, is a delayed onset of an allergic reaction post ingestion of mammalian meat and other mammalian-derived food products. It is associated with IgE antibodies to galactose-alpha-1,3-galactose (alpha-gal). There is strong evidence that Amblyomma mericanum (Lone star) tick bites are a cause of AGS in humans, but it is unknown how tick bites initiate the anti–α-Gal IgE response. Although Ixodes scapularis (Deer) tick bites have not been associated with AGS, its genome was reported to contain three genes involved in alpha-gal synthesis. Our group developed the methodology for using laboratory reared I. scapularis larval ticks in research protocols investigating Lyme disease and tick immunity. The procedure is very well tolerated, and none of the participants have developed AGS. To further corroborate the clinical experience, we tested serum samples from participants for the presence of alpha-gal specific IgE. Of the 29 samples collected, 27 were found negative. Two samples had low positive results, and repeat testing showed a borderline result for one sample and a low positive result for the second. In samples collected over two years before the procedure, the second individual had similarly low levels of alpha-gal specific IgE. Therefore, procedures using I. scapularis larval ticks are not associated with development of significant anti-alpha-gal IgE antibodies and corroborates the clinical experience.	A Eschman, S Turk, Y Yin, A Marques	2023	MICROBIO
2023-317	Wenling		Li	NHLBI	Developmental Biology	Deletion of Von Hippel-Lindau (VHL) in vascular endothelial cells triggers the aberrant activation of HIF-Cxcr4 axis, leading to the disruption of vascular patterning	The VHL gene, a tumor suppressor gene, plays a vital role in cellular oxygen sensing, by targeting the degradation of hypoxia-inducible factors (HIFs) under normoxic conditions. VHL syndrome is an autosomal dominant genetic disorder resulting from germ line mutations in the VHL gene and patients develop highly vascularized tumors in multiple organs due to the activation of HIFs and their downstream targets, such as VEGF, in non-vascular tissues which affects neighboring endothelial cells and stimulates angiogenesis. Whether VHL mutations in endothelial cells affect angiogenesis, however, remains unclear. To address this question, we investigated skin vascular development in the mutants having the endothelial cell-specific VHL deletion. The mutants exhibit vascular abnormalities and embryonic lethal. At the mechanistic level, the deletion of VHL leads to aberrant expression of the chemokine receptor Cxcr4, a well-known target of HIFs, in endothelial cells. Indeed, the upregulation of Cxcr4 expression observed in VHL knockdown is reversed when HIFs are additional knocked down of HIFs in cultured endothelial cells. Moreover, endothelial cell-specific overexpression of Cxcr4 results in similar vascular abnormalities to those observed in endothelial cell-specific VHL deletion. These findings suggest that VHL deletion induces aberrant expression of Cxcr4 through constitutive stabilization of HIFs, leading to vascular abnormalities. AMD3100, a Cxcr4 antagonist, partially restored vascular abnormalities in endothelial cell-specific VHL deletion. Combined, these studies demonstrate that VHL mutations in endothelial cells lead to vascular abnormalities through the aberrant activation of HIF-Cxcr4 axis. AMD3100 can be serve as an additional therapeutic approach for VHL syndrome, complementing anti-VEGF therapy.	WL Li, YS Mukouyama	2023	DEVBIO
2023-318	David		D'Onofrio	NHGRI	Genetics and Genomics	Machine Learning and Misalignment: a Comprehensive Approach	Intro: The Undiagnosed Diseases Program (UDP) enrolls participants with undiagnosed disorders despite past extensive clinical evaluation. The UDP utilizes genomic analysis optimized for detecting variants that may be missed by standard analyses. This high-sensitivity approach generates many false positives. Methodologies for prioritizing results include identifying short read misalignments. We hypothesize that current mapping and genotype scores do not adequately capture alignment quality for individual variants. To address this question, we are developing a machine learning based tool to rank variants based on the quality of the alignment associated with variants. Methods: We are generating a list of alignment characteristics, building on those in existing tools such as the GATK pipelines. These characteristics are being built into a random forest classifier. This model will be trained and tested with a combination of highly characterized genomes (i.e. Genome in a Bottle), synthetic genomes and a set of 7748 hand-curated variants from prior UDP evaluations. Results: Initial assessment of potential model classifiers has demonstrated marked operator bias in hand-curated datasets. Evaluation of a heuristic alignment filtration system from a prior project suggests that some specific alignment patterns, such as >2 haplotypes covering the called variant, provide information that is not captured by traditional quality score filters. Conclusion: We present preliminary data for in progress work on a machine learning classifier designed to assist with the prioritization of results in noisy short read variant data sets. Our hope is that this work will prompt discussion and feedback that will be useful during tool development.	DA D'Onofrio, DR Adams	2023	GEN
2023-319	Ana	D	Armenta Vega	NIDA	Neuroscience	Mouse model of operant oral nicotine self-administration	Nicotine is an active ingredient that leads to addiction to tobacco products. Nicotine binds to the nicotinic acetylcholine receptors (nAChRs) of the brain and has many downstream effects, including positive reinforcement that leads to habit formation and addiction to nicotine. However, there is no established behavioral procedure to examine the reinforcing effects of nicotine in mice. We examine if oral nicotine self-administration can work as an effective model of nicotine reinforcement. We found that mice orally consume nicotine solutions. Using a free choice procedure in which mice had access to nicotine solutions and water daily for 24 hours, mice readily consumed nicotine solutions. As the concentration of the nicotine solutions increased, mice consumed more nicotine per day despite consuming less volume of the solutions. We also found sex differences: female mice consumed more nicotine than males. We were also able to train mice to operantly respond for oral administration of nicotine. Mice were placed in operant chambers where they had access to a nicotine solution upon pressing a lever and they learned to respond for oral nicotine. However, once mice learned to operantly respond for oral nicotine, behavioral responses were not sensitive to manipulations including differential concentrations of nicotine solution and pharmacological challenges with nicotinic receptor agonists and antagonists. These observations suggest that behavior reinforced by oral nicotine is highly habitual. Our operant self-administration of oral nicotine procedure has potential to be an effective model for investigating neural mechanisms of the reinforcing and habitual effects of nicotine.	AD Armenta Vega, Y Arima, S Ikemoto	2023	NEURO
2023-320	F. Graeme		Frost	NHGRI	Genetics and Genomics	Pathogenic tandem splice acceptor variants escape screening by in silico tools	Introduction. Tandem splice acceptor (NAGNAG) sites are a known mechanism of alternative splicing and serve as loci of transcriptional regulation. Previous literature demonstrated that variants modifying existing, or creating novel, NAGNAG sites can cause mendelian disease. Despite advances in in silico splicing prediction tools, predicting the pathogenicity of NAGNAG variants remains difficult and, as a result, are rarely contextualized in clinical reporting. Methods. We characterized NAGNAG variants in reference databases and among 1236 individuals from the NIH Undiagnosed Diseases Program (UDP). We evaluated pathogenicity of each NAGNAG variant in 130 UDP cases with RNA-Seq data. Results. We found a depletion of AG-containing trimers from position -3 to -14, which often overlaps acceptor site enhancer motif. SpliceAI scores of AG-gain variants in that region were similarly high in UDP and reference populations. Evaluation of RNA-Seq data in UDP cases showed that variants with verified usage were more abundant in the -3 to -14 window compared to the rest of the intron. Furthermore, while those variants verified tended to have high SpliceAI acceptor gain scores, they had a PPV of 0.344, demonstrating the incomplete ability of in silico tools to assess AG-gain variants. Conclusions. The pathogenicity of variants affecting splicing are difficult to assess. We show that a subset of those variants, those which create NAGNAG sites, frequently lead to the usage of a novel acceptor site. Predicting the function of those variants using in silico tools is inconsistent. This supports the use of empirical evaluation of AG-gain variants by RNA-Seq.	FG Frost, S Gu, A Elbert, MCV Malicdan, CF Boerkoel, PF Cherukuri	2023	GEN
2023-321	Jaanam		Gopalakrishnan	NEI	Immunology	Single cell sequencing reveals important immune cell features in an Alzheimer's disease model	Alzheimer's disease (AD) is the leading cause of dementia worldwide. Amyloid beta plaques and neurofibrillary tau tangles in the brain result in neurodegeneration and cognitive decline. Microglia, brain-resident macrophages, play a major role in AD progression, but the role of non-microglial immune cells are least understood. In our study, we used a mouse model (5xFAD) with human mutations in the Amyloid Precursor Protein and Presenilin genes to mimic AD pathology. Using high-dimensional flow cytometry, single-cell RNA-seq, and single-cell T-cell receptor-seq (scTCR-seq), we studied innate and adaptive immune cells in neurodegeneration. Our results showed increased alpha-beta T cells in the 5xFAD brains compared to the wild-type B6 (WT) brains at 4 and 12 months of age. Unsupervised clustering revealed a Type I Interferon responsive CD8+ T cells subset, termed disease associated CD8+ T cells (DATs), significantly enriched in 5xFAD brains. scTCR-seq analysis identified unique TCR clonotypes enriched in 5xFAD brains, with one leading clonotype indicating mucosa-associated invariant T cells (MAITs). The TCR alpha CDR3 region of this clonotype was conserved across human and mouse. Further analysis of other TCR repertoire datasets from mouse tauopathy model and cerebrospinal fluid from AD patients confirmed the MAIT cell enrichment in AD. Recent studies have linked MAITs to cognitive function and blood brain barrier integrity. Therefore, understanding the precise role of MAITs and DATs is crucial. In conclusion, our findings suggest the involvement of DATs and MAITs in AD progression. Characterizing their tissue resident location and functions may guide the development of AD therapies.	J Gopalakrishnan, N Fernando, A Behensky, M Bono, V Nagarajan, HY Shih	2023	IMMUNO
2023-322	Diana	M	King	CC	Neuroscience	Efficient removal of naturally occurring lipofuscin-derived autofluorescence in human nervous tissue using high intensity white light	Autofluorescence in human tissue impedes optimal multiplex fluorescence imaging and accurate signal quantification. One pervasive source of autofluorescence is lipofuscin, an age-associated agglomeration of oxidized lipoprotein, which absorbs and emits maximally between 400 and 600 nm which are critical wavelengths for multiplex imaging, preventing full utilization of the technique. When lipofuscin is present alongside target signal, signal detection is occluded, especially for low-expressed targets. Previous experiments done on formalin-fixed paraffin embedded human dorsal root ganglion (DRG) tissue (healthy controls, AnaBios Corp.) showed that prolonged exposure to high intensity white light prior to multiplex staining effectively photobleaches the autofluorescence, substantially reducing lipofuscin intensity. Because the samples were paraffin embedded and remained at 2˚C for the duration of the exposure, the tissue RNA was minimally impacted. This was assessed by measuring fluorescence intensity in DRG using four Opal dyes in a 4-plex TSA-amplified in situ hybridization protocol. Subsequently, we tested the rigor of the technique on brain tissue from patients with Alzheimer's Disease. Because lipofuscin accumulates in direct association with age, samples taken from older individuals tend to be greatly affected. Additionally, Alzheimer's pathogenesis causes especially high levels of autofluorescent plaques, often being so severe as to limit the accuracy of data interpretation. Our preliminary data shows effective photobleaching of the Alzheimer's tissue, thereby validating this technique for both healthy and pathologic human samples. The technique can be used on multiple slides simultaneously which enhances its utility for comparative experiments evaluating multiple disease states, brain regions and treatment conditions.	DM King, MR Sapio, D Maric, AP Manalo, A Ghetti, MJ Iadarola, AJ Mannes	2023	NEURO

2023-323	Erica	R	Lesko	NICHD	Neuroscience	Behavioral difference during aversive states provides insight into medial habenular PKA signaling significance	The protein kinase A regulatory subunit (PKA RIIa) is ubiquitously expressed peripherally, but within the central nervous system is nearly exclusively expressed in the small epithalamic structure of the medial habenula. The habenula-interpeduncular nucleus network is known to modulate intrinsic motivation and aversive behavior as well as addiction and withdrawal. To explore what role PKA signaling has on behavior under aversive states, our lab compared the PKA RIIα knockout (RIIαKO) mouse to its wild-type counterpart in established aversion paradigms such as quinine aversion, lithium-chloride sucrose pairing, and conditioned place aversion. For bitter taste aversion, daily water supply was replaced with increasing concentrations of quinine (max. concentration 2,000uM). Standard error of mean suggested a needed increase in statistical power to draw conclusive results. Lithium-chloride sucrose pairing included a conditioning and testing phase, where 10% sucrose solution was paired with and without an i.p. injection of Li-Cl respectively. Our findings indicate significant differences in KO consumption of 10% sucrose between treatment with Li-Cl and saline compared to wild type. For conditioned place aversion, once morphine dependence was established, mice were confined to one chamber and withdrawal was precipitated with an i.p. injection of naloxone. Preliminary findings suggest a potential difference between average time spent in the aversive room between RIIαKO and control. These findings provide new insight into the influence of medial habenular PKA signaling on behavior during aversive states.	ER Lesko, EC London, CJ McBain	2023	NEURO
2023-324	Maxine	R	Rubin	NCI	Cancer Biology	Amplified LZK is a novel therapeutic target in esophageal squamous cell carcinomas with 3q amplicon	Esophageal Squamous cell carcinoma (ESCC) is the dominant histological type (90%) of esophageal cancers worldwide. The estimated global frequency is 512,000 new cases, with a 5-year survival rate of less than 25%, ranking it as one of the deadliest cancers with an urgent need for new therapies. Copy number alterations are frequently observed in ESCCs. Distal amplification of chromosome 3 (3q26-3q29, the 3q amplicon) occurs in 35% of ESCC patients. One of the most frequently amplified genes residing on chromosome 3 is MAP3K13, which encodes the Leucine Zipper-bearing Kinase (LZK). The focus of our research is to examine whether amplified LZK can serve as a therapeutic target in ESCC cells harboring the 3q amplicon. Through dox-inducible shRNA knockdown of LZK, we validated MAP3K13 as a novel oncogenic driver required to maintain the proliferation and cell survival of ESCC cells with 3q amplicon. We then tested pharmacological inhibitors of LZK and established several lead LZK inhibitors that abolish LZK kinase activity and reduce tumorigenic phenotypes of ESCC cell lines harboring amplification compared to control cell lines. Furthermore, these effects were rescued by a drug-resistant mutant form of LZK, confirming the specificity of LZK inhibitors. Importantly, LZK inhibitors suppressed in vivo tumor growth in PDX models with amplified LZK. Finally, we identified LZK as an upstream regulator of the oncogene Akt, where catalytic inhibition of LZK suppresses Akt expression in ESCCs with the 3q amplicon. This research has far-reaching implications as it identifies LZK is a new pharmacological target in ESCCs.	MR Rubin, M Katerji, CC Woodroofe, E Lindberg, RE Swenson, J Brognard	2023	CANCER
2023-325	Joy		Mojumder	CC	Biomedical Engineering and Biophysics	Novel MRI Phantoms for Investigating Skull-Brain Mechanics	Traumatic brain injury (TBI) is a serious health condition that affects both military and civilian populations. However, the mechanisms linking mechanical insult and neurological injury, more specifically how skull motion is transmitted to brain motion during TBI, are not well understood. Here, we developed two skull-brain phantom (SBP) models to evaluate MRI investigations of skull-brain mechanics. The SBP models were developed using two identical cylindrical molds with attached boundary (SBPa) and unattached boundary (SBPu). The inside of the mold represents the brain region whereas the cavities inside the wall represent marrow within the skull. Polyacrylamide gel is used as a brain tissue simulant. We performed neck rotation (32° rotation within the axial plane) experiment using a custom MRI-compatible device. The tagged MRI study was performed using a 1.5 T Siemens Aera MR scanner. Data was acquired using a 1–1 SPAMM tagging pulse followed by 2D cine gradient echo acquisition using two axial acquisitions with orthogonal tag directions and the following acquisition parameters: FOV = 240×240 mm, matrix = 24×160, slice thickness = 8 mm, TR/TE = 3.18/1.68 ms, tag spacing = 8 mm. Harmonic phase (HARP) analysis was performed to measure the displacement vectors and calculate maximum principal strain (MPS, largest eigenvalue of strain tensor). The results suggest that at the point of impact, the MPS is larger with a fixed boundary (SBPa: 0.014 vs SBPu: 0.010). However, after impact, strains were increased in SBPu model due to torsional wave. These models can be developed further by incorporating fat-water emulsion.	J Mojumder, S Vidhate, YC Lu, A Alshareef, A Diano, CL Johnson, DL Pham, JA Butman	2023	BIOENG
2023-326	Debangan		Dey	NIMH	Epidemiology	Investigating the relationship of overnight change in salivary cortisol with daily emotional states using mobile technologies	Introduction: This study aims to explore the relationship between emotional states and a larger overnight change in cortisol (ONC), indicating a healthy circadian rhythm of the HPA axis. However, research on this topic is scarce. The primary objective is to investigate the bidirectional associations between real-time emotional states and ONC, considering potential variations among mood disorder subtypes. Methods: The study included 154 participants, comprising 58 adolescents/young adults (<30 years) and 96 adults (>30 years). Salivary cortisol and self-reported ratings of emotional states were collected four times daily for two weeks. Linear mixed effects models were employed, incorporating the average anxiety level and day-specific changes. This approach enabled the examination of both between-person and within-person effects of anxiety. Additionally, the diverse population in the NIMH family study data facilitated exploration of potential differences among different mood or anxiety disorders. Results: Higher average anxiety and lower current-day deviation from average anxiety were associated with higher ONC values. The negative effect of current-day deviation from average anxiety was significantly greater in individuals with Bipolar II compared to controls. Average sad mood was associated with a greater decline in ONC, unaffected by within-day mood shifts. No significant associations were found between ONC and next-day average or deviations of sad mood, energy, or anxiety in the overall sample. Conclusions: The findings suggest that daily emotional states and/or stressors likely drive changes in cortisol levels, rather than cortisol influencing emotional states. This highlights the potential influence of daily emotional experiences on physiological responses.	D Dey, A Swaminathan, A Leroux, K Merikangas	2023	EPIG
2023-327	Mary	E	Hackbarth	NHGRI	Genetics and Genomics	Generation and characterization of a novel mouse model for Free Sialic Acid Storage Disorder	Free sialic acid storage disorder (FSASD) is an autosomal recessive lysosomal storage disorder characterized by mutations in SLC17A5, resulting in sialin transporter deficiency and subsequent accumulation of free sialic acid in tissues and biological fluids. FSASD exists as a clinical spectrum, ranging from mild developmental delay with progressive neurodegeneration, to severe disease with infantile fatality. Given the lack of approved therapies, the development of a reliable animal model is crucial for advancing preclinical translational studies. Utilizing CRISPR/Cpf1 genome editing, we generated the Slc17a5-R39C mouse model carrying the most prevalent SLC17A5 variant observed in FSASD patients. Extensive phenotyping was performed through biochemical, molecular, behavioral, and histological assays. Homozygous Slc17a5-R39C animals exhibited increased perinatal lethality, with 25% dying within four weeks. Progressive neurodegeneration was evident, characterized by gait abnormalities, tremors, and discoordination. Neurological evaluation revealed significant ataxia and impaired motor performance. A significant proportion of mutant mice exhibited seizures. Urinary analysis demonstrated a five-fold increase in free sialic acid levels, establishing that the Slc17a5-R39C mouse faithfully replicates the biochemical hallmark of disease. Histological examination revealed hypomyelination in the corpus callosum, cerebellum, and spinal cord tracts, along with a reduction in Purkinje neurons in the cerebellum. Ongoing investigations aim to elucidate the spatiotemporal progression of these findings. The Slc17a5-R39C mouse represents a valuable tool for investigating molecular mechanisms, particularly regarding neurodevelopmental aspects of FSASD. This model holds promise for identifying longitudinal biomarkers and determining optimal treatment windows, thus enabling the development of molecular and pharmacological interventions to slow or halt disease progression.	ME Hackbarth, JD Burke, G Elliott, L Garrett, P Leoyklang, P Zerfas, D Springer, MS Sabir, L Pollard, M Huizing, WA Gahl, MCV Malicdan	2023	GEN
2023-328	Asuka		Ishihara	NIDDK	Clinical Research	Effects of daytime cold and warm ambient temperatures on sleep in men with and without obesity	Thermal environment plays a crucial role in regulating energy metabolism and sleep in humans. Deviation from thermoneutral ambient temperatures increases metabolic demand and may lead to sleep disturbances. Here we examined the effects of daytime ambient temperature on sleep in adult men with and without obesity. Twelve lean men (23.2 ± 4.9 yrs; 23.4 ± 1.6 kg/m2) and nine men with obesity (29.6 ± 4.9 yrs; 34.4 ± 3.4 kg/m2) were exposed to a single temperature between 16-31°C, randomly assigned each day for 5h (0800-1300) during a 14-day inpatient study (NCT01568671). Nighttime sleep (at 23-25°C) was assessed using wrist actigraphy. Sleep parameters, including total sleep time (TST), time in bed (TIB), wake after sleep onset (WASO), and sleep efficiency, were not significantly different between the groups after exposure to a thermoneutral baseline temperature (24.2 ± 0.3°C). There was a significant interaction between the ambient temperatures (coldest at 19.1 ± 1.5°C and warmest at 30.8 ± 0.5°C) and BMI groups for TST, TIB, and WASO (p's ≤ 0.05), with greater TST (430.7 ± 35.6 vs. 357.0 ± 67.4 min; p=0.02), TIB (488.9 ± 38.0 vs. 383.3 ± 76.0 min; p=0.003), and WASO (57.2 ± 27.1 vs. 26.3 ± 20.3 min; p=0.02) in men with obesity compared to lean men after cold exposure. No significant differences were observed after warm ambient temperatures. Future studies assessing sleep architecture and core temperature may provide further insights into metabolic and sleep physiology in response to ambient temperatures in individuals with and without obesity.	A Ishihara, RJ Brychta, SR LaMunion, KY Chen	2023	CLINICAL
2023-329	Elizabeth		Ottinger	NCATS	Computational Biology	Rare Diseases Literature Mining using Large Language Models	Rare diseases affect millions globally, but information and resources are often scarce. NCATS has formed a collaboration with the Frederick National Lab to create a user-friendly platform for rare disease information. The main objective for the project, named RARe-SourceTM, is to provide an innovative application and searchable interface for data mining, by integrating various bioinformatics databases and enabling users to navigate the wealth of information quickly and efficiently. Biomedical literature is largely unstructured, extracting relevant details is still challenging, and mining for contextual information such as variant pathogenicity, clinical and phenotypic details, and their relations to the genome are not yet resolved. Developing a scalable and agnostic literature mining workflow is especially important for the rare disease field. Diagnoses of the more than 3000 rare diseases with a known genetic etiology is still challenging and many causative genetic variants are still languishing in published articles without easy access. We initiated development on the literature AI feature in RARe-SourceTM with the goal of mining relevant rare disease details and making the information accessible to researchers, clinicians, and patient caregivers. Customized implementation of novel natural language processing models will help assess the fit of the models to rare disease research. Development on the literature AI feature is split into several phases to enable access to results at multiple stages of implementation. The first phase of the project was successfully completed and the results on finding rare disease related articles along with information on associated genes is available through RARe-SourceTM.	M Alodadi, E Lyons, A Che, D Watson, S Roy, GJ Tawa, F Porter, SJ Haugabook, E Ottinger, US Mudunuri	2023	COMPBIO
2023-330	Angela	E	Lee	NHGRI	Genetics and Genomics	Optimizing generation of human isogenic iPSC lines via CRISPR prime editing	CRISPR prime editing (PE) enables precise and versatile genomic modification without inducing double-stranded breaks. PE requires multiple components, including a prime editor enzyme complex, pegRNA (finds the target and provides the new sequence), and sgRNA (directs prime editor complex to nick non-edited strand). Optimization of PE components is essential for most genomic targets. Here, we use PE to introduce type 2 diabetes (T2D) candidate risk variants into human induced pluripotent stem cells (iPSCs), a cell type which can be differentiated into numerous disease-relevant cell types. We tested various PE component systems and developed a highly efficient pipeline that generated isogenic lines carrying heterozygous or homozygous risk or non-risk alleles for six T2D loci. We found that PE can support editing in iPSCs, but optimization of all components is critical to achieve high efficiency. PE systems utilizing PEmax, epegRNA modifications, and MLH1dn provide significant benefit, with maximal editing efficiency ranging from 36-73%. Editing success for each variant differs considerably depending on the sequence at the target site. pegRNA design also plays a critical role, as slight variations in sequence guide parameters can have significant effects. Established guidelines for pegRNA design should be followed during the initial optimization for each target before making small changes to pegRNA lengths and/or shifting its position to enhance editing rate. Although considerable effort is required to achieve acceptable efficiencies for PE, it is a promising approach to generate isogenic iPSC lines, enabling the study of specific genetic changes in a common genetic background.	AE Lee, AJ Swift, EC Mansell, E Winnicki, E Li, CC Robertson, T Huynh, N Narisu, C Krilow, MR Erdos, FS Collins, LL Bonnycastle	2023	GEN
2023-331	Lauren	M	Herr	NIA	Molecular Biology and Biochemistry	RECON syndrome helicase RECQL1 trapped by a mono-ribonucleotide suppresses RNase H2 incision	Ribonucleotides are frequently mis-incorporated into the genome during cellular DNA replication, resulting in genomic instability and mutations. Although DNA repair mechanisms that replace mono-ribonucleotides are known to involve nucleolytic incision by RNaseH1/2 or Topoisomerase I, it is unclear if other DNA binding proteins affect recognition/incision of the lesion. This prompted us to assess the effects of a site- and strand-specific uridylate (rU) or cytidylate (rC) harbored within forked duplex DNA substrate on unwinding catalyzed by disease relevant helicases implicated in replication or DNA repair. The ring-like replicative DNA helicases MCM and Twinkle are tolerant of a rU or rC lesion. In contrast, the repair helicase RECQL1, mutated in the premature aging disorder RECON syndrome, is strongly inhibited by a rU or rC positioned in the helicase-translocating strand. To probe the mechanism further, we tested the clinically relevant and catalytically compromised RECQL1-A459S mutant and found exacerbated inhibition by the translocating strand rU. RECQL1 was sequestered by the rU in the translocating strand of the helicase substrate, suggesting that the helicase is trapped by the ribonucleotide upon encountering it. Moreover, RECQL1 trapped at the translocating rU protects the duplex from both HaeIII endonuclease cleavage at a restriction site adjacent to the ribonucleotide and nucleolytic incision by the ribonucleotide excision repair endoribonuclease RNase H2. These results suggest that a single ribonucleotide can affect genomic transactions of RECQL1 by inducing trapping at the damage site, which may serve to signal DNA repair machinery for localization, or possibly interfere with normal DNA transactions.	LM Herr, KF Fuchs, S Awate, S Waghmare, S Dhar, T Kulikowicz, JA Sommers, RM Brosh, Jr.	2023	MOLBIO

2023-332	Maya	E	Goldberg	NIEHS	Clinical Research	Stressful Life Events in the Year Prior to Diagnosis are Associated with Adult and Pediatric Systemic Rheumatic Diseases	Background. Systemic rheumatic diseases (SRDs) are thought to result from multiple genetic and environmental risk factors, among which is psychosocial stress, although evidence is inconclusive. Methods. Life events data from the NIEHS Study of Twins/Siblings Discordant for SRDs was examined in 96 Adults, 129 Young Children (YC), and 41 Teen Probands within 5 years of diagnosis of SRDs, and in unaffected same-gender, close-in-age Siblings (SIBs) and Healthy Controls (HCs). Life events within 12 months of SRD diagnosis were queried using Paykel's Recent Life Events scale for adults and the Adolescent Perceived Event Scale for pediatric subjects. The same reference period was used for SIBs/HCs. Logistic regression analysis, adjusting for demographics, disease duration and smoking, was performed to identify predictors of SRD diagnosis. Results. In adults, the number of Total, Uncontrollable, Undesirable, and Highly Stressful life events was higher in Probands compared to HCs (P≤0.001–0.05). From logistic regression, the number of Total, Major, Uncontrollable, Undesirable, and Highly Stressful life events and their stress ratings were associated with an increased odds of SRD diagnosis in adult Probands vs. HCs (OR 1.22–2.03, P≤0.05). The number of Total, Major Negative, and Major Total events were protective for SRD diagnosis in YC/Teens combined (OR 0.69–0.96, P≤0.05), while higher undesirable ratings for Major Negative life events were associated with SRD (OR 2.25, P=0.04). Conclusion. This study suggests negative life events and their stress perceptions are associated with greater odds for SRD in adults, with a more nuanced relationship in pediatrics.	ME Goldberg, I Bauer Ventura, A Schiffenbauer, M Shi, R Volochayev, SH Jackson, A Jansen, N Bayat, P Noroozi Farhadi, CG Parks, CR Weinberg, A Picardi, FW Miller, LG Rider	2023	CLINICAL
2023-333	Abhinav		Parashar	NIDCR	Stem Cell Biology	Searching for the physiological functions of Copeptin	Arginine vasopressin (AVP) secreted by hypothalamic neurons controls water resorption and blood pressure via its receptors in the kidneys and in vasculature, respectively. Our group has found that AVP receptors are present in hematopoietic progenitor cells. We have shown a novel physiological role for AVP in stimulating red blood cell precursors in mice. We also showed that the lack or decrease of AVP in patients results in anemia. While many functions of vasopressin have been described, so far no physiological function has been found for AVP's C-terminal glycopeptide, Copeptin (CP). CP is well preserved through many species suggests an important physiological function. Because of the novel effects of AVP on bone marrow (BM) cells, we decided to study a potential role of CP modifying hematopoiesis. We performed in vivo studies by injecting CP in mice. Our preliminary data suggest that CP is also involved in regulating hematopoietic progenitors. Following i.p injection we observed effects in peripheral blood on the number of platelets. Next, we studied platelet aggregation upon CP treatment. Our results indicate that like vasopressin, CP receptor/s are also present on platelets. To identify the specific receptor/s responsible for these responses we performed receptor-ligand binding assays using a biotinylated CP. Using a pull-down approach we identified different bands corresponding to the proteins binding to labelled CP. Next, we will use mass spectrometry, to identify these potential targets as CP receptor/s. Once we find the putative receptor, we hope to start to understand the interaction between CP and its receptor/s.	A Parashar, VD Myneni, E Mezey	2023	STEMCELL
2023-334	William		Thompson	NINR	Social and Behavioral Sciences	Eye Tracking in an Immersive Virtual Study Environment	At the Advanced Visualization Branch of the National Institute of Nursing Research, we use immersive virtual reality (IVR) as a technical platform to study how people carry out instrumental activities of daily living, such as grocery shopping. We performed a pilot test to evaluate the performance of eye-tracking technology within our IVR grocery store to validate what study participants are viewing on the nutrition label. Our eye-tracking system was developed using commercial software that was modified for the purpose of our test. Lab staff and associates (n=8) acted as testers, and entered a custom IVR experience where they viewed a virtual nutrition label; We created digital boundaries around each nutrient value on the label so that the eye-tracker system could detect eye-gaze locations. Participants then looked at different nutrients, and the performance of the eye-tracker was assessed based on rate of detection of the expected nutrient value. Overall, eye-tracking was able to detect the true eye-gaze location in 98.5% of observations, but the average duration of detection varied based on nutrient. Our preliminary test results indicate that our eye-tracking system is capable of detecting the location of eye-gaze, but whether this detection is consistent or accurate enough to be reliable for our future study remains to be seen. The difference in performance between testers with and without prescription eyewear also warrants further exploration. Our preliminary data provides us with enough information to refine the design process and further explore the performance of eye-tracking in our IVR environments.	WE Thompson, R Tredinnick, DM Goldsmith, K Kevorkian, T Nelson, PF Brennan	2023	SOCIAL
2023-335	Richard	V	Remigio	NCI	Epidemiology	Geographic patterns in wildfire exposures and county-level lung cancer mortality in the United States	Emissions from wildland fire plumes are composed of modified biomass combustion by-products, including carcinogens. However, studies of the association between wildland fire exposures and lung cancer are scant. We evaluated geographic patterns in these exposures and lung cancer mortality to explore possible associations. We extracted historical fire (wildfires and prescribed burns) information and satellite imagery for the conterminous U.S. from the Monitoring Trends in Burn Severity program (1984-2001). Age-adjusted, sex-specific lung cancer mortality rates at the county level for two 5-year periods (2011-2015 and 2016-2020) were obtained from the National Center for Health Statistics. Lee's L statistic for bivariate spatial association was used to identify geographic patterns with significant associations between fire exposures and lung cancer mortality rates. There were over 6,100 wildland fires (67% were wildfires) and 7,650,000 km2 burned area during the exposure period. Among females, we observed clusters of counties where area burned ratios and lung cancer mortality rates (2011-2015) were both high across eastern Kentucky (n=17 counties, p-values: 0.009-0.03), southwestern West Virginia (n=9, p-values: 0.009-0.01), and Florida (n=17, p-values: 0.009-0.03). Among western counties, greater fire exposure was associated with lower lung cancer mortality (n=47, p-values: 0.009-0.03). These patterns were consistent among men and by time period. Our findings differed from recently published lung cancer mortality clusters associated with smoking prevalence. Our novel analysis identified U.S. counties where wildfires might contribute to lung cancer mortality; the inverse association in some Western counties requires additional investigation. Studies with individual-level exposure-response assessments are needed to evaluate this relationship further.	RV Remigio, ID Bueller, M Bogle, M Kamenetsky, J Fisher, S Ammons, JE Bell, ND Freedman, RR Jones	2023	EPIG
2023-336	Karli	R	LeFort	NIAAA	Molecular Biology and Biochemistry	PROTECTIVE ROLE OF MITOCHONDRIAL ALDEHYDE DEHYDROGENASE 2 (ALDH2) AGAINST BINGE ALCOHOL-INDUCED ACUTE KIDNEY INJURY THROUGH THE GUT-KIDNEY AXIS	Introduction: Aldehyde dehydrogenase 2 (ALDH2) participates in the oxidative metabolism of alcohol. Studies have shown that Aldh2-knockout (KO) mice are susceptible to alcohol-mediated organ damage, but the mechanisms of binge alcohol induced-acute kidney injury (AKI) in Aldh2-KO mice are poorly understood. We hypothesized that exposure to three doses of alcohol may cause AKI due to increased gut barrier dysfunction (GBD) in Aldh2-KO mice compared to the corresponding WT mice. Methods: WT and Aldh2-KO mice were exposed to three doses of alcohol (4 g/kg/dose via oral gavage) in 12-h intervals. Blood plasma, gut enterocytes, and kidney tissues were collected from each mouse at 1 hour and 24 hours after treatment. Serum creatinine levels, lipopolysaccharide (LPS) levels, expression of intestinal junction proteins (TJs/AJs), oxidative/nitrative stress markers (ROS/RNS), apoptosis-related proteins, and markers of kidney injury were measured. Results: Aldh2-KO mice exposed to 3 doses of 4 g/kg ethanol showed elevated GBD, serum LPS, and serum creatinine, expression of kidney tissue proteins involved in apoptosis, ROS/RNS, and inflammation, gut enterocyte proteins involved in apoptosis and ROS/RNS, and less expression of TJs/AJs compared to the corresponding WT counterparts or dextrose-exposed Aldh2-KO, all suggesting that binge alcohol-mediated ROS/RNS may promote AKI through GBD and endotoxemia. Conclusion: These mechanistic results are the first to report the critical role of GBD in the mechanism of alcohol-mediated AKI, exacerbated in an Aldh2-KO animal model. Furthermore, these results also suggest that ALDH2 is an important target for clinical intervention against alcohol-mediated tissue injury, including AKI.	KR LeFort, B Ray, W Rungratanawanich, BJ Song	2023	MOLBIO
2023-337	Vaishnavi	J	Purandare	NCI	ACI/IRS	Tooth loss and risk of colorectal, pancreatic and liver cancers in the Golestan cohort study	The oral microbiome is involved with the development of poor oral health conditions such as tooth decay/loss, and periodontal disease. Poor oral health has been associated with various cancers. Here, we assessed the association between tooth loss and risk of colorectal, liver and pancreatic cancers in the Golestan Cohort Study (GCS). GCS, a large prospective cohort from Golestan Province, Iran, includes 50045 individuals within 40 to 75 years of age at baseline. Cox proportional hazards models were used to estimate hazard ratios (HRs) and corresponding 95% confidence intervals (CIs). During a median follow-up of 15 years, there were 171, 82 and 98 incident colorectal, liver and pancreatic cancer cases, respectively. The preliminary models, adjusted for demographic and lifestyle variables, did not find any statistically significant associations for colorectal cancer. For liver cancer, the first two tertiles of tooth loss had a nonsignificant increased HR of 1.56 (95% CI: 0.89 - 2.74) and 1.44 (95% CI: 0.79 – 2.63), respectively and dropped to 0.93 (95% CI: 0.46 – 1.89) for the highest tertile. For pancreatic cancer, the HRs showed an increasing trend with HRs of 0.98 (95% CI: 0.55 - 1.76), 1.03 (95% CI: 0.59 - 1.78) and 1.53 (95% CI: 0.87 - 2.68) respectively, across the tooth loss tertile categories. In this population with low general oral hygiene, we did not find significant associations between tooth loss and colorectal, pancreatic and liver cancers, but we plan to evaluate other measures of oral health and the risk of these cancers.	V Purandare, Y Yano, C C Abnet, H Poustchi, G Roshandel, F Kamangar, P Boffetta, P Brennan, S M Dawsey, E Vogtmann, R Malekzadeh, A Etemadi	2023	ACI/IRS
2023-338	Joanna	R	Thomas	NCI	Cancer Biology	Development of a high-throughput zebrafish model of blood-brain barrier disruption	The blood-brain barrier (BBB) excludes most drugs, including chemotherapeutics, from the brain. Transient disruption of the BBB is an effective strategy to increase drug delivery to the brain. Assessment of the BBB in vitro is technically challenging, and mammalian models are low throughput. Zebrafish, which have a remarkably conserved BBB, are an ideal model for high-throughput BBB disruption studies. We have created a zebrafish model of BBB disruption, by expressing the luciferase NanoLuc under the control of the glial-specific promoter GFAP (glial fibrillary acidic protein) in the brain parenchyma, behind the BBB. The NanoLuc substrate furimazine is BBB impermeable as it is a substrate of the multi-drug efflux transporter ABCG2, which is expressed on the lumenal surface of BBB endothelial cells, and effluxes drugs back into the blood, preventing brain entry. Zebrafish have 4 homologs of ABCG2 (abcg2a, -b, -c, -d). We identified abcg2a as the only paralog expressed at the BBB in larvae and adults, and it also shares the most substrates with human ABCG2, including furimazine. Treatment of zebrafish larvae with the ABCG2 inhibitor Ko 143 blocks Abcg2a from effluxing furimazine, allowing it to cross the BBB, producing a dose-dependent increase in bioluminescent light. Younger larvae (3 vs 7 days old) have higher baseline bioluminescence, indicating a less restrictive developing BBB. Our future goal is to adapt this assay for high-throughput screening of BBB disruptors, and eventually combine these methods with brain tumor xenografts to assess the delivery of chemotherapeutics to brain tumors.	JR Thomas, WE Frye, CT Inglut, RW Robey, AC Warner, D Butcher, J Matta, EF Edmondson, AY Mitrophanov, B Carrington, R Sood, MM Gottesman	2023	CANCER
2023-339	Sazzad		Mahmood	NIAID	Cell Biology	The "sialome switch" of Ixodes scapularis at the single-cell resolution	Tick salivary glands (SGs) secrete a complex saliva, assisting the blood feeding. Transcriptomic studies revealed salivary transcription profile switches at intervals, characterizing the phenomenon of "sialome switch". Here, using a transcriptomic approach, we explored the sialome of Ixodes scapularis adult female ticks fed on rabbits for different periods. Ticks were sorted in seven groups based on their weight. Groups categorized here represent the unfed, slow-feeding, and the rapid-feeding phases of tick feeding. Transcriptomic analysis showed dynamic expression with remarkable signatures for each phase, confirming the "sialome switch". As a SG is composed of different types of acini which differ both morphologically and functionally, we performed a transcriptome at the single-cell level as well and validated the "sialome switch". Interestingly, the analysis of scRNA-seq data revealed a substantial upregulation of mitochondrial genes in the fed groups, which can be attributed to the cellular hypertrophy observed when feeding progresses. A total of ten cellular clusters was observed and its distribution was influenced by the feeding. Notably, one cluster consisting of undifferentiated cells was found to be enriched in the SGs of unfed ticks. As feeding progresses, this cluster diminished, giving rise to different cell populations that expressed classical salivary genes. This cluster was identified as the trajectory root and the origin of all other clusters. Nuclei counting and PH3 staining indicated absence of cellular proliferation, supporting the idea that these undifferentiated cells differentiate into specialized cells when feeding starts. These findings offer a potential explanation for the plasticity observed in SG expression.	S Mahmood, ABB Ferreira, CS Lewis, O Oluwayiose, S Lu, J Leung, J Lack, LA Martins, J Kotal, JM Ribeiro, L Tirloni	2023	CELLBIO
2023-340	William	F	Heinz	NCI	Cancer Biology	Hypoxic gradients direct the spatial organization of epithelial-to-mesenchymal transition in an in-vitro breast cancer tumor microenvironment	Poor prognosis in ER- breast cancer is predicted by high cyclooxygenase-2 (COX2) and inducible nitric oxide synthase (NOS2) expression. In hypoxic gradients of the tumor microenvironment (TME) these proteins promote epithelial-to-mesenchymal transition (EMT), initiating metastasis. We define epithelial (E) and mesenchymal (M) phenotypes by E-cadherin (ECAD) and vimentin (VIM) expression, respectively. We hypothesize that hybrid (E/M) phenotypes, which are implicated in metastatic disease, (1) organize along hypoxic gradients and (2) correlate spatially COX2 and NOS2 expression. Restricted exchange environment chambers (REECs) mimic the cell-generated hypoxic gradients of solid tumors in 2D live cell culture. We cultured 4T1 cells – a murine model of human triple-negative breast cancer – in REECs, and at 0, 48, 96, and 168 h, fixed and imaged them with multiplexed immunofluorescent microscopy. The proportion of VIM+ cells in the REECs increased over 7 days, with a maximum in normoxic regions, as observed in 4T1 mouse tumors. Across all oxygen concentrations in the REEC, VIM+ expression was greater than in a monolayer of cells cultured under hypoxic conditions. E/M cells increased in all regions over time. In hypoxic regions, discrete VIM+ clusters emerged in spoke-like patterns aligned along the gradient. COX2 and NOS2 expression also increased significantly in response to hypoxic gradients. Neighborhoods around clustered VIM+ cells are dominated by VIM+/ECAD+/COX2+ cells, but solitary VIM+ cells inhabit primarily VIM-/ECAD+/COX2- neighborhoods. These results support the hypothesis that COX2 and NOS2 contribute to the organization of E/M phenotypes in a hypoxic gradient. Supported in part by NCI contract:75N91019D00024.	S Anmalsetty, SJ Silva, G Vitale, AJ Walke, DA Scheiblin, LA Ridnour, DA Wink, SJ Lockett, WF Heinz	2023	CANCER

2023-341	Xiwen		Cui	NCI	Cancer Biology	Deciphering Melanoma Evolution: Insights into Phylogeny and Structural Variants for Precision Medicine	Melanoma exhibits extensive intratumoral heterogeneity and complex evolutionary dynamics. To investigate subclonal dynamics, we established a novel model system comprised of 24 single cell-derived clonal sublines (C1-C24) from a melanoma model, M4, which was created from the genetically engineered HGF-transgenic mouse. We used Trisicell, a computational toolkit for intratumor heterogeneity evaluation from single-cell RNA mutations, to build the phylogeny tree. The result revealed the evolutionary patterns of melanoma, with ancestral clones giving rise to genetically distinct subclones. Using long-read sequencing, we identified the structural variants (SVs), including deletion/insertion, amplification, translocation, fusion gene, etc. Through the pattern of gene disruption by the structural variants specific to individual sublines or shared between/among sublines, we can understand the roles of different during melanoma's progression. The preliminary data from four sublines showed that the SVs shared by all sublines, representing ancestral events, were significantly more than the subline-specific SVs, representing the later events. Interestingly, the individual sublines exhibited a higher ratio of disrupted genes by SVs, suggesting the possibility of functional selection. In chromosomes, the SVs shared among all the sublines are associated with genes enriched in the cell growth pathways, such as Kras, Myc, Pik3r1, etc. Interestingly, genes disrupted by SVs are enriched in pathways of tissue differentiation, especially neural developmental genes. These results shed light on the genetic conditions that can predispose individual melanocytes to melanomagenesis and could uncover relationships between progression and resistance to therapy. Further analysis is ongoing to delineate SVs on the whole mutation-based phylogeny of all sublines.	X Cui, AG Keskus, FR Mehrabadi, S Malikic, G Merlino, M Kolmogorov, CS Sahinalp, C Day	2023	CANCER
2023-342	Adaira	J	Dumm	NIA	Molecular Biology and Biochemistry	SARS-CoV-2 Nsp13 helicase catalyzes RNA-protein remodeling to facilitate proofreading and bimodally modulates RNA synthesis by the Replication-Transcription Complex dictated by ATP-dependent catalytic function or protein interaction with Nsp12/7/8	SARS-CoV-2, a single-stranded, positive-sense RNA virus responsible for COVID-19, requires a set of virally encoded nonstructural proteins that compose a replication-transcription complex (RTC) to replicate its 30 kilobase genome. One such nonstructural protein within the RTC is Nsp13, a highly conserved molecular motor ATPase/helicase. We biochemically characterized the enzyme by examining its catalytic functions, nucleic acid substrate specificity, and putative protein-nucleic acid remodeling activity. We determined that Nsp13 preferentially interacts with single-stranded (ss) DNA compared to ssRNA, demonstrating strand-specific interactions. Furthermore, we demonstrated for the first time the ability of the coronavirus Nsp13 to disrupt a high-affinity nucleic acid-protein interaction, in a uni-directional manner and with a preferential displacement of streptavidin complex from biotinylated ssDNA versus ssRNA. Our studies demonstrate that this displacement is dependent on its intrinsic ATP hydrolysis function, building upon structural studies of the RTC in which it was suggested that Nsp13 pushes the RNA polymerase (Nsp12) backward on the template RNA strand. We propose that this novel biochemical activity implicates a catalytic role of Nsp13 in protein-RNA remodeling during genome replication beyond its duplex strand separation or structural stabilization of the RTC, yielding new insight into coronavirus proofreading. In further studies, we have examined the ability of Nsp13 to resolve SARS-CoV-2 derived RNA secondary structures to enable the polymerase complex (Nsp12/7/8) during synthesis. Our results show that wild-type Nsp13 inhibited polymerase extension whereas the ATPase-dead mutant stimulated activity, implicating an ATP-dependent catalytic function or protein interaction of Nsp13 that modulates RNA synthesis by Nsp12/7/8 during replication.	AJ Dumm, JA Sommers, LN Loftus, MP Jones 3rd, RA Lee, CE Haren, T Kulikowicz, KM Wicker, RM Brosh Jr.	2023	MOLBIO
2023-343	Gang		Cheng	NIDDK	Genetics and Genomics	Coordinated loading and unloading of cohesins define the mitotic-to-meiotic chromatin reorganization	During meiotic prophase I (MPI), chromosomal reorganization enables complex events like DNA double-strand break formation and homologous recombination. The most overt change as cells transition from germ cells through MPI is that chromosomes condense into an array of chromatin loops. However, the conversion from interphase chromatin folding to meiotic loops is poorly understood. Using fluorescence-activated nuclei sorting, we isolated precise stages of mouse spermatogenesis and applied in-situ Hi-C to examine genome structure transitions from mitotic to meiotic states and during pre-meiotic homologous pairing. We found cohesin density decreases as spermatogonia differentiate, hitting a minimum at the onset of the mitotic-to-meiotic transition and resulting in the loss of most chromatin loops. Notably, a comparable chromatin folding intermediate was identified at telophase during mitotic exit. As cells transitioned further towards meiosis, we observed a progressive elevation in cohesin density, accompanied by an increase in loop length. Levels of RAD21, a mitotic cohesin kleisin, declined, while levels of REC8, a meiotic kleisin, escalated during the same period. This suggests an orchestrated cohesin exchange mediates chromatin reorganization during the mitotic-to-meiotic transition, potentially setting the stage for the axis-loop array reconfiguration in MPI. By conducting Hi-C in hybrid mice, we discovered inter-homolog interactions in all pre-meiotic stages. Interestingly, these interactions were disrupted during meiotic replication and early leptonema. This is consistent with yeast findings, indicating extensive pre-meiotic pairing in male mouse meiosis preceding DSB formation.	G Cheng, F Pratto, K Brick, M Huang, G Lam, R D Camerini-Otero	2023	GEN
2023-344	Dharmendra	N	Bhatt	NIAID	Cancer Biology	CTCFL/BORIS loss in ovarian cancer cells unleashes massive deregulation in transcriptional clusters	The CCCTC-binding factor (CTCF) protein, a conserved architectural protein, shares its multivalent 11 ZnF DNA-binding domain with a paralogous counterpart named BORIS (a.k.a. CTCFL for "CTCF-like"). Although both proteins recognize the same variety of highly diverged target DNA sequences, they possess distinct N- and C-terminal domains interacting with specific protein partners to cause different functional outcomes. Recent studies have proposed testis-specific BORIS as a prognostic and therapeutic marker for ovarian cancers. Despite the high incidence of aberrant BORIS activation in ovarian cancers, its precise functional role remains elusive. In this study, we analyzed the impact of BORIS knockdown in ovarian cancer cells on chromatin status and transcriptional regulation, and observed extensive changes caused by BORIS K/O in genome-wide chromatin accessibility surrounding CTCF and BORIS co-binding sites. Transcriptome analysis revealed significant dysregulation of critical cancer-promoting transcription factors and signaling pathways. Intriguingly, we discovered that these changes in gene transcription occur in clusters, resulting in the simultaneous upregulation or downregulation of multiple adjacent genes. This suggests that the loss of BORIS impacts the 3D genome organization mediated by CTCF. Our findings begun to shed light on the involvement of BORIS in ovarian cancer and its potential role in modulating chromatin regulation, transcriptional dysregulation, and 3D genome organization. Further investigation into the contribution of BORIS to 3D genome organization will provide valuable insights into the underlying mechanisms and may uncover novel therapeutic targets for ovarian cancer.	D N Bhatt, E M Pugacheva, L M Fedida, E Price, Y J Ji, D Loukinov, A Vostrov, V V Lobanenkov	2023	CANCER
2023-345	Christopher		Shults	NIDCD	Genetics and Genomics	The Helios Transcription Factor is Necessary for Both Outer Hair Cell Development and Maintenance	In 2018, our laboratories demonstrated that the transcription factor helios is essential for OHC maturation. We showed that a mutation in the Ikzf2 gene, which encodes helios, resulted in a reduction in prestin-dependent electromotility and early-onset hearing loss. Moreover, ectopic expression of helios in inner hair cells (IHCs) led to the downregulation of markers specific to IHCs and a transcriptional shift towards an OHC-like state. In this study, we tested whether helios also plays a role in maintaining OHC function after the onset of hearing. Ikzf2 was conditionally deleted by crossing Ikzf2 floxed mice with either Gfi1-Cre (depletion beginning at ~E16.5) or Prestin-CreERT2 (tamoxifen-induced at P12/13/14) mice. Auditory function of these Ikzf2 cKO mice was evaluated at 6-weeks of age by distortion product otoacoustic emission (DPOAE) and auditory brainstem response (ABR) measurements. To evaluate OHC loss, cytocochleaograms were performed on whole mount cochlear preparations from 6-week-old mice, stained with phalloidin, DAPI and an anti-prestin antibody. To define the regulatory transcriptional cascade downstream of helios, OHCs from P8 Ikzf2fl/fl;Gfi1Cre mice and their littermate controls were isolated by flow cytometry, and analyzed by bulk and scRNA-seq. Both mouse lines with conditionally deleted Ikzf2 exhibited elevated ABR hearing thresholds and increased DPOAE thresholds across all frequencies tested. Aberrant OHC morphology and OHC loss is observed in both mouse models, with the fewest OHCs remaining in the Ikzf2fl/fl;Gfi1Cre mice. Lastly, transcriptional changes were recorded in the helios-deficient OHCs. Our data reveal that in addition to OHC development helios is also critical for their maintenance.	CL Shults, R Aminapour, B Milon, K Gwilliam, E Chrysostomou, MR Bowl, R Hertzano	2023	GEN
2023-346	Richard	V	Remigio	NCI	Epidemiology	Chlorpyrifos use and human cancer risk: An Agricultural Health Study update	Chlorpyrifos is an organophosphate insecticide recently banned in the US for use on food and animal feed crops due to associations with neurodevelopmental effects in children. Its relationship with cancer risk is unclear. Here we incorporate more than 13 additional years of follow-up, updated exposure information, and >6700 additional cancer cases in the AHS to more comprehensively evaluate cancer risk associated with chlorpyrifos. We included 52,848 AHS applicators with follow-up from enrollment (1993-1997) through 2014 (North Carolina) or 2017 (Iowa). We determined cumulative intensity-weighted lifetime days of chlorpyrifos use using self-reported data at enrollment and follow-up (1999-2005). Poisson regression was used to calculate rate ratios (RR) and 95% confidence intervals (CI) for combined cancers and specific sites/subsites, adjusting for potential confounders. A total of 22,080 AHS applicators (41.8%) reported applying chlorpyrifos. We observed an increased risk of brain cancer (RRQ4 vs. no chlorpyrifos use=1.74, CI: 1.00-3.02; p-trend=0.38). Our findings also suggested an elevated risk of leukemia (RR Q4=1.64, CI: 0.96-2.78; p-trend=0.13), which appeared to be driven by acute myeloid leukemia (AML) (RR Q4=2.71, CI: 1.46-5.05; p-trend=0.005). We did not observe an association for non-Hodgkin lymphoma overall but found a positive association for follicular lymphoma (RR Q4=1.95, CI: 1.07-3.56; p-trend=0.38). Our results provide evidence of positive associations with brain cancer, AML, and follicular lymphoma. These findings are important in understanding cancer risk among individuals historically exposed to chlorpyrifos in the US and in regions of the world where chlorpyrifos remains widely used.	KH Berry, RV Remigio, MCR Alvanja, G Andreotti, P Albert, WJ Lee, DP Sandler, JN Hofmann, LE Beane Freeman	2023	EPIG
2023-347	Mahin	S	Hossain	NHGRI	Neuroscience	Dysmyelination or demyelination: Investigating the role of SLC17A5 in myelination in a murine model of Free Sialic Acid Storage Disorder	Free Sialic Acid Storage Disorder (FSASD) is a rare lysosomal storage disorder resulting from bi-allelic variants in SLC17A5. Patients with FSASD display significant hypomyelination, neurodegeneration, and altered lysosomal transport of sialic acid to the cytosol. To better understand the link between SCL17A5 function and neurodegeneration, we generated Slc17a5R39C knock-in mice with the prevalent p.Arg39Cys mutation. These mice exhibit features of FSASD, including progressive ataxia, neurodegeneration, and hypomyelination. We examined the cortex, cerebellum, and cervical spinal cord of Slc17a5R39C mice and control littermates at developmental stages critical for neuronal development using immunofluorescence staining of Myelin basic protein (MBP), Purkinje cell protein 4 (PCP4) and glial fibrillary acidic protein (GFAP). Slc17a5R39C mice had decreased MBP expression, significant white matter astrogliosis, and decreased PCP4 expression over time, indicative of progressive Purkinje cell loss throughout development. Luxol Fast Blue staining, which highlights myelinated regions, revealed prominent hypomyelination in the corpus callosum, cerebellar white matter, and all major spinal white matter tracts as early as P14. Surprisingly, Nissl staining did not show differences in neuronal body numbers, suggesting myelin density changes are independent of neuronal loss. Our findings suggest dysmyelination or hypomyelination has occurred prior to P14, during the biological window for myelination, resulting in myelination deficits in Slc17a5R39C mice. This is consistent with progressive neurodegeneration having occurred alongside myelination abnormalities. These results align with clinical presentation in FSASD patients and provide insights into the pathophysiology of FSASD and the role of SLC17A5 in myelin production, composition, and maintenance	MS Hossain, P Leoyklang, MS Sabir, ME Hackbarth, H Dorward, M Huizing, WA Gahl, MCV Malicdan	2023	NEURO
2023-348	Ezazul		Haque	NIEHS	Genetics and Genomics	Epigenetic signatures of cigarette smoke exposure in a murine model	The epigenetic signatures of cigarette smoke exposure have been studied in human populations. These population-based studies are limited by confounding factors and can be difficult to establish causality and their downstream biological effects. Animal models provide an opportunity to causally study the epigenetic signatures of cigarette smoke and their downstream impacts on the transcriptome, metabolome and proteome. Furthermore, they allow investigations within tissues difficult to study in human studies such as lung and bone marrow. Here, female C57BL/6 mice were exposed to cigarette smoke (n=32) or room air (n=32) using two 50 minute exposure session per day, 5 days per week for 6 weeks. Blood, lung, and bone marrow samples were collected after the last day of exposure. Efforts are currently underway to study the DNA methylation signatures of cigarette smoke exposure in lung, whole blood and bone marrow, RNAseq analysis will be done in lung and whole blood. Metabolomics analysis is being conducted in lung and plasma samples. Lastly, proteomics will be used to evaluate lungs.	E Haque, J Oladosu, H Li, D Zeldin, SJ London	2023	GEN
2023-350	Ethan	D	Schaffer	NIA	Cell Biology	Synthetic Lethality during Replication Stress Induced by the Loss of RECQ1 and BLM DNA Helicases	Nephrotoxicity is a major cause of kidney disease, a reason for drug development failure, and a challenge for chemical risk assessment in humans. Historically, tools for nephrotoxicity assessment consisted of 2D monocultures of undifferentiated cells and mammalian animal models. However, due to a limited ability to recapitulate fundamental aspects of human kidney physiology, these systems often fail to predict nephrotoxicity. Proximal tubule (PT) cells are the most frequent site of damage as they transport and metabolize xenobiotics, leading to intracellular accumulation of reactive metabolites, which can impair PT solute reabsorption and disrupt essential nutrient homeostasis, causing negative health effects. In vitro systems that mimic key aspects of human PT physiology hold the potential to better model and predict nephrotoxicity. Here, we introduce two advanced in vitro systems that we have developed to address unique aspects of nephrotoxicity assessment: (1) screening level system – designed to create interpretive context for decision making by efficient survey of chemicals – consisting of self-organizing, lumen-forming, free-floating 3D microtissues of human PT cells that develop tubular structures, express transporters, and demonstrate enhanced differentiated longevity and sensitivity to nephrotoxic compounds compared to 2D cultures. (2) Microphysiological system integrating microfluidics with co-cultures of human-derived cells and tissue engineering to create 3D microenvironments that mimic in vivo functions and dynamics. Biologically relevant flow rates promote barrier function and transporter activity. Both screening level systems and microphysiological systems are integral to address contemporary challenges of new approach methodologies (NAMs)-based risk assessments.	ED Schaffer, LM Herr, S Dhar, L Johnson, GL Moldovan, RM Brosh Jr.	2023	CELLBIO

2023-351	Alondra	A	Martinez Osorno	NCI	Cancer Biology	Development of multiplex panels to examine changes in the tumor microenvironment	The tumor microenvironment (TME) consists of the surrounding blood vessels, immune cells, fibroblasts, signaling molecules, and the extracellular matrix. It is important to investigate multiple aspects of the TME including identifying populations and cell-function interactions for prognosis and treatment of cancer. We hypothesize that using a multiple multiplex immunofluorescence panel we can characterize cells in normal and tumor in murine formalin-fixed paraffin-embedded tissues. We use multiplex immunofluorescence (IF) analysis to quantifying immune cell subsets, their functional state, and especially their spatial arrangement in the tumor microenvironment. In conclusion, several markers in our tumor microenvironment marker panel allowed for visualizing the spatial organization of the TME.	AA Martinez Osorno, A Browne, R Kaplan	2023	CANCER
2023-352	Kathleen	F	Fuchs	NIA	Molecular Biology and Biochemistry	Molecular Characterization of the DEAH-box Helicase DHX37 and Implication in RNA Processing and Human Disease	DEAH-box helicase, DHX37, is a multidomain protein that contains two RecA-like domains (RecA1 and RecA2), a helicase-associated domain (HA2), and an oligosaccharide-binding fold domain (OB). DHX37 is an ATP-binding RNA helicase crucial in maturation of the small ribosomal subunit in ribosome biogenesis and is required for the release of the U3 snoRNP from pre-ribosomal particles. The ATP-dependent 3'-5' RNA translocation stimulates ATPase activity and enhanced RNA binding. In the presence of clinically relevant DHX37 mutations, R490G and A898T, patients with juvenile dermatomyositis (JDM) and anti-MDA5 autoantibodies experience endothelial dysfunction. Evidence suggests types I and II IFN play a role in JDM, leading to Janus kinase (JAK) inhibitor being used to target the IFN pathway in these patients. Targeting the IFN pathway through inhibitor treatments may allow insight into reduction of disease activity in JDM and anti-MDA4 positive patients. Post-treatment assessment indicated down-regulation of symptoms associated with phenotype of MDA5 and functional impact of these mutations. Initial molecular characterization experiments analyzed wild-type DHX37 for the functionality of ATPase activity through kcat determination (the hydrolysis of ATP to ADP per time unit by DHX37, represented by per second units). The biochemical characterization of the A898T mutation indicated a more modest effect on any conformational changes than the R490G mutation. Additionally, the clinically associated DHX37 missense mutants display a robust molecular defect in comparison to wild-type DHX37 and indicate the inactivation of catalytic ATPase function.	KF Fuchs, JA Sommers, M Neog, F Miller, L Rider, R Goldbach-Mansky, A de Jesus Rasheed, RM Brosh Jr.	2023	MOLBIO
2023-353	Sonali		Das	NHLBI	Immunology	A new pipeline SPICE identifies novel JUN-IKZF1 composite elements	Transcription factor partners can cooperatively bind to DNA composite elements to augment gene transcription. Here, we report a novel protein-DNA binding screening pipeline, termed Spacing Preference Identification of Composite Elements (SPICE), that can systematically predict novel protein binding partners and their DNA motif spacing preferences. SPICE not only successfully de novo predicted known composite elements, including AP1-IRF composite elements (AICE) and STAT5 tetramers, but also predicted a range of potential novel binding partners, including JUN-IKZF1 composite elements throughout the genome. We showed cooperative binding of JUN and IKZF1 to an upstream conserved noncoding region, CNS9, in the human IL10 gene. Furthermore, the activity of an IL10 luciferase reporter construct depended on both AP1 and IKZF1 binding sites within this composite element in primary mouse B cells and T cells. These data provide new insights into the biological actions of IKZF1 and AP1 and moreover establish SPICE as a valuable new pipeline for predicting novel transcription binding complexes that regulate gene transcription.	P Li, S H Pulugulla, S Das, J Oh, R Spolski, J X Lin, K Georgopoulos, W J Leonard	2023	IMMUNO
2023-354	Michael	J	Iadarola	CC	Clinical Research	Shaping a new interventional drug treatment for peripheral neuropathic pain	Peripheral neuropathic pain (PNP) affects 10 to 30 million people in the general population and results from a broad array of causes including direct nerve injury, viral infection, metabolic problems such as diabetes, and chemical insults. The shear variety of etiologies and sites of nerve damage make effective treatment difficult, and currently available agents do not provide complete pain relief. We have developed a new interventional approach to peripheral neuropathic pain treatment that can be adapted to the varied sites of pain generation. The treatment involves instillation of the potent and highly selective TRPV1 agonist resiniferatoxin (RTX), to inactivate pain fibers in affected peripheral nerve. Morton's neuroma (MN) is a chronic pain condition characterized by burning, stabbing, or shooting pain upon weight-bearing in the ball of the foot due to nerve damage. Its localized nature makes MN an optimal model for testing neuropathic pain symptomatology and the proposed treatment. We report on our initial pain phenotyping of MN patients and controls using comprehensive quantitative sensory testing (QST) to subjectively assess responses to innocuous and noxious thermal, mechanical, and deep tissue pressure stimuli. Patients with MN had lower pressure pain thresholds and reported higher pressure pain ratings in comparison to healthy participants and an extended area of heat hyperalgesia in the MN affected foot. We are about to commence a Phase I clinical trial to treat refractory MN pain using perineural injection of RTX. We hypothesize this compound, and this route will provide effective pain relief in MN patients.	ES Staedtler, MJ Iadarola, MR Sapio, TS Williams, E Frangos, M Bačkonja, AJ Mannes	2023	CLINICAL
2023-355	Md Shakir	U	Ahmed	NCI	Health Disparities	Single cell analysis of circulating peripheral blood mononuclear cells in African American men with prostate cancer and their association with lethal disease	Prostate cancer is a leading cause of cancer-related deaths among men in the US and affects African American (AA) men more so than other men. We and others previously described a distinct tumor immunobiology in AA, which is associated with lethal prostate cancer. In this study, we sought to investigate the composition of circulating peripheral blood mononuclear cells (PBMCs) in AA and European American (EA) prostate cancer patients and their association with race and lethal prostate cancer. We obtained high-quality RNA-sequencing data for 277642 single cells representing circulating PBMCs from 59 AA and EA men. In the analysis, being AA patients associated with increased abundance of exhausted CD8+T cells and higher numbers of tumor-associated macrophages, whereas metallothionine-expressing macrophages were decreased in these men. Gene signatures indicative of T cell exhaustion were generally elevated in AA PBMCs while T cell effector function features were decreased. Within the myeloid cell population, cytokine and NFKB signatures were more prevalent in AA than EA. This gene signature pattern that we observed in AA patients also associated with lethal prostate cancer, namely the T cell exhaustion and elevated cytokine gene signatures, pointing to potential clinical implications. Lastly, the interferon-induced transmembrane protein (IFITM3), interferon alpha inducible protein (IFI6), cysteine rich protein-1 (CRIP1), and the RAC family small GTPase2 (RAC2) were notably upregulated in AA patients. In summary, we show that circulating immune cell populations and associated gene signatures differ between men of African and European descent. Those elevated in AA patients correlated with lethal prostate cancer.	MU Ahmed, T Dorsey, S Ambs	2023	HEALTH
2023-356	Natalia	I	Dmitrieva	NHLBI	Epidemiology	Middle age high normal serum sodium as a risk factor for accelerated biological aging, chronic diseases, and premature mortality: targeting hydration as preventive lifestyle intervention	It is known that some people age faster than others, some people live into old age disease-free, while others develop age-related chronic diseases. With a rapidly aging population and an emerging chronic diseases epidemic, identifying and implementing preventive measures that could slow down the aging process has become a new challenge for biomedical research and public health. In mice, lifelong water restriction shortens the lifespan and promotes degenerative changes. By analyzing data from the Atherosclerosis Risk in Communities study (middle-age enrollment (45-66 years, n=15752) and 25 years follow-up), we tested the hypothesis that optimal hydration may slow down the aging process in humans. We used serum sodium as a proxy for hydration habits. The analysis showed that middle age serum sodium >142 mmol/l was associated with a 39% increased risk to develop chronic diseases (hazard ratio [HR]=1.39, 95% confidence interval [CI]:1.18-1.63) and >144 mmol/l with 21% elevated risk of premature mortality (HR=1.21,95%CI:1.02-1.45). People with serum sodium >142 mmol/l had up to 50% higher odds to be older than their chronological age (OR=1.50, 95%CI:1.14-1.96). The results indicate that serum sodium exceeding 142 mmol/l increases the risk to be biologically older, develop chronic diseases and die at younger age. Although intervention studies are needed to confirm the link between hydration and aging, the data justifies the goal of paying closer attention to good hydration habits and development of more straightforward recommendations for optimal fluid intake that has a potential to delay or prevent chronic diseases in a safe and widely available way.	NI Dmitrieva, D Liu, CO Wu, DR Rosing, M Boehm	2023	EPIG
2023-358	Kevin	P	Rose	NIDCD	Developmental Biology	A jack of all trades: POU3F4 orchestrates diverse transcriptional programs in the developing cochlea.	During inner ear development, otic mesenchyme cells (OMCs) surround and influence the development of many key cochlear structures, including the organ of Corti, spiral ganglion neurons (SGNs), and stria vascularis. We have recently shown that OMCs are not homogenous, but are transcriptionally, spatially, and functionally distinct. Mutations of the OMC-specific transcription factor Pou3f4 are associated with DFNX2, the most common form of X-linked deafness. Loss of Pou3f4 results in numerous cochlear defects, seemingly affecting each of the OMC subpopulations differentially. Here, we hypothesized that the transcriptional changes downstream of POU3F4 in each of the four OMC subpopulations are unique, resulting in the multifaceted cochlear phenotype observed in Pou3f4-KO mice. Indeed, using scRNA-seq and scATAC-seq at embryonic day 15 and postnatal day 7, we show that loss of Pou3f4 leads to an OMC subtype-specific response, with each OMC subtype displaying a unique chromatin landscape and sharing only a few differentially expressed genes. Finally, using cell-cell communication analyses, we describe potential mis-regulated signaling cascades in Pou3f4-KO mice responsible for the defects observed in the surrounding cell types such as the SGNs and stria vascularis. In conclusion, the otic mesenchyme specific transcription factor POU3f4 supports four distinct transcriptional cascades in the regionally and molecularly distinct mesenchymal domains during cochlear development.	KP Rose, G Manilla, B Milon, Y Song, TM Thomas, R Hertzano	2023	DEVBIO
2023-359	Pooja		Varma	NINR	Molecular Biology and Biochemistry	Quantitative Analysis of Ryanodine Receptor (RyR) Protein Levels in Muscle Biopsy Samples using RT-PCR	Background: Rare diseases present significant health inequities and economic burden on affected individuals. RYR1-related myopathies are congenital myopathies caused by pathogenic variations in ryanodine receptor-type 1 gene (RYR1). Ryanodine receptors are homotetrameric channels responsible for excitation-contraction coupling, linking action potentials and contraction of the striated muscle by releasing calcium ions required to activate contractile proteins. There is currently no approved treatment for RYR1-RM. Objective: The aim of the study was to quantify RyR1 protein levels in RYR1-RM patients using skeletal muscle biopsy samples. Method: Four muscle samples from affected individuals with different pathogenic variants were analyzed (1 recessive and 3 dominant). The protein levels were quantified using real-time polymerase chain reaction (RT-PCR) using the Custom Applied Biosystems TaqMan Gene Expression (by Thermofisher) assays. These assays were designed to measure RNA expression in the regions in which the variants are located within RYR1. Results: Based on a visual observation of the data, abundant RYR1 expression could be amplified and detected in the region of variants, c.6721C>T and c.325C>T, in Patient 1. Variant c.7354C>T could not be analyzed in the patient control or patient 4. Possible reasons for these overly high and low CT values include low abundance of RNAs/expression in this region and/or low RNA sample integrity. We have designed and ordered custom TaqMan gene expression assays to target variants identified in two other RYR1-RM patients within this cohort that were not included in this experiment and look forward to updating our findings with the RYR1 expression data from these additional variants.	Pooja Varma BS[1], Eunice Chukwunyere[1], Claudia Colina Prisco PhD[2], Joshua J. Todd PhD[3], Tokunbor A. Lawal PhD[1]	2023	MOLBIO

PosterCatNum
13
8
22
7
14

23

5

5

16

16

16

17

16

21

15

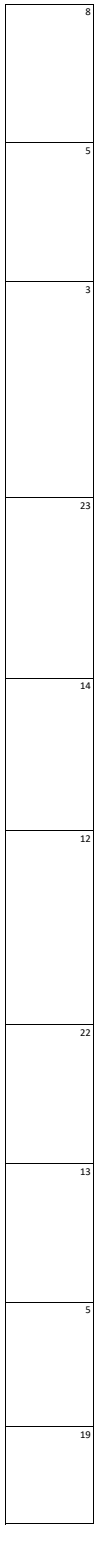
8
5
3
23
14
12
22
13
5
19

19

11

10

22

16

7

14

22

14

14

15

9

10

1

14

3

1

11

16

22

4

3

18

11

24

11

16

6

3

17

18

16

17

5

2

20

1

4

1

1

4

20

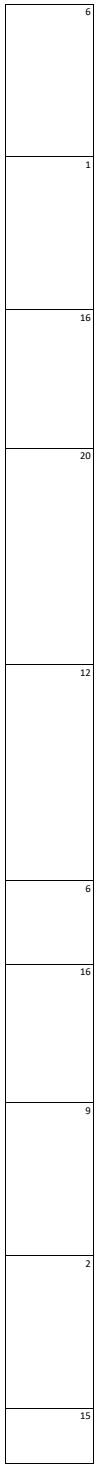
6
1
16
20
12
6
16
9
2
15

14

16

23

2

14

24

5

11

4

24

4

2

14

20

16

16

24

2

7

1

6

5

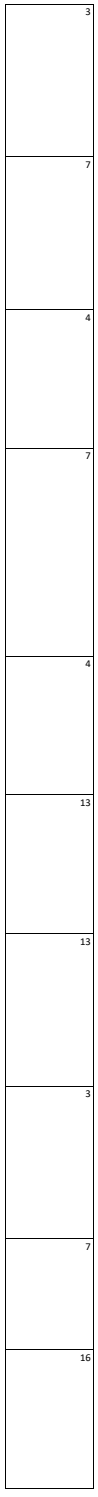
3
7
4
7
4
13
13
3
7
16

19

2

3

16

16

19

4

13

11

16

2

10

9

13

4

9

21

16

2

8

16

11

10

13

15

8

17

8

10

1

11

14

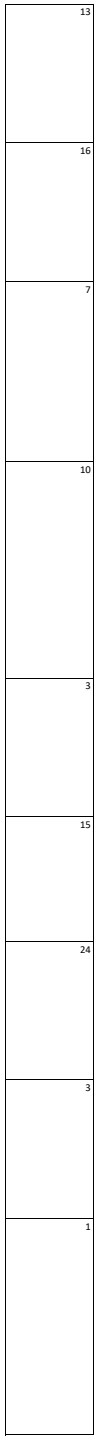
13
16
7
10
3
15
24
3
1

5

3

4

15

12

12

10

12

5

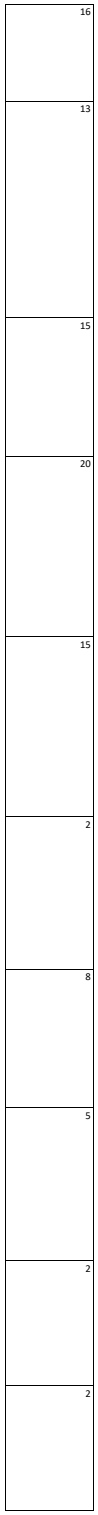
16
13
15
20
15
2
8
5
2
2

7

3

24

7

13

19

24

10

7

15	1	16	13	11	8	1	7	6	4

14

19

1

16

3

12

1

20

5

17

3

7

6

24

17

3

14

16

2

3

20

20

8

17

8

15

3

16

11

22

15

1

2

8

13

5

15

3

7

15

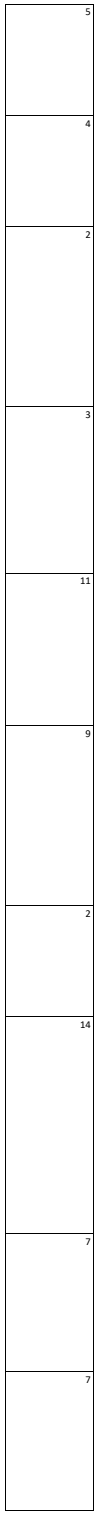
5
4
2
3
11
9
2
14
7
7

11

11

9

11

15

13

13

16

13

7

17

13

11

8

19

15

14

2

24

24

20

3

6

5

10

3

13

4

22

7

2

1

22

10

18

7

13

14

7

13

1

16

7

10

18

24

24

17

21

21

24

11

4

24

4

13

2

19

16	13	11	16	11	9	14	16	7

16

3

2

10

11

7

8

11

15

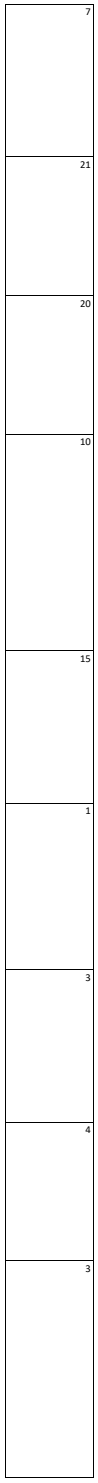
7
21
20
10
15
1
3
4
3

3

15

11

3

11

10

16

4

4

3

15

13

7

12

10

9

15